

Aus dem Institut für Toxikologie und Pharmakologie für Naturwissenschaftler
Universitätsklinikum Schleswig-Holstein Campus Kiel

Identification of microRNAs as potential novel regulators of
HSD11B1 expression

Dissertation
zur Erlangung des Doktorgrades
der Agrar- und Ernährungswissenschaftlichen Fakultät
der Christian-Albrechts-Universität zu Kiel

vorgelegt von
M.Sc. Yanyan Han
aus Heilongjiang, P. R. China

Kiel, 2011

Dekanin: Prof. Dr. Karin Schwarz

1. Berichterstatter: Prof. Dr. Edmund Maser

2. Berichterstatter: Prof. Dr. Gerald Rimbach

Tag der mündlichen Prüfung: 09.02.2012

Gedruckt mit der Genehmigung der Agrar- und Ernährungswissenschaftlichen Fakultät der
Christian-Albrechts-Universität zu Kiel

Contents

Summary	IV
Zusammenfassung	V
Abbreviations	VI
1 Introduction	1
1.1 11β-Hydroxysteroid dehydrogenase type 1 (11β-HSD1)	1
1.1.1 The 11 β -Hydroxysteroid dehydrogenase (11 β -HSD) system	1
1.1.2 Human <i>HSD11B1</i> gene and alternative promoter usage.....	3
1.1.3 11 β -HSD1 and glucocorticoid action	5
1.1.4 Localization of 11 β -HSD1.....	6
1.1.5 Regulation of <i>HSD11B1</i> expression	8
1.1.6 11 β -HSD1 and obesity/type 2 diabetes	13
1.1.7 Inhibition of 11 β -HSD1 as a therapeutic target	15
1.2 MicroRNAs	17
1.2.1 Discovery of miRNAs	17
1.2.2 Biogenesis of miRNAs	18
1.2.3 Mechanisms of miRNA-mediated gene silencing	19
1.2.4 MiRNAs and diseases.....	23
2 Aim of this study.....	29
3 Materials and Methods	30
3.1 Materials	30
3.1.1 Chemicals	30
3.1.2 Enzymes.....	32
3.1.3 Molecular weight markers.....	32
3.1.4 Kits.....	32
3.1.5 Plasmids.....	33
3.1.6 MicroRNAs	33
3.1.7 Primers	34
3.1.8 Oligonucleotides	36
3.1.9 Cell lines	36
3.1.10 Cell culture media, solution and materials	36
3.1.11 Hepatocyte Total RNAs	37
3.1.12 Frozen Hepatocytes	37

3.1.13 Antibodies	37
3.1.14 Bacterial media	37
3.1.15 Radiochemical.....	38
3.1.16 Buffers and solutions.....	38
3.1.17 Equipments	42
3.2 Methods	43
3.2.1 Molecular biology.....	43
3.2.2 Cell culture and cell-based assays.....	49
3.2.3 Protein biochemical methods	52
3.2.4 Web-based tools.....	54
3.2.5 Statistical analysis	55
4 Results.....	56
4.1 miRNA prediction	56
4.2 Construction of pmir-HSD11B1-3'UTR plasmid (dual-luciferase assay system)	59
4.3 Optimizing plasmid DNA (pmir-HSD11B1-3'UTR) transfection	60
4.4 MiRNAs bind to 3'UTR of <i>HSD11B1</i> mRNA.....	64
4.5 Deletion/mutation of the corresponding miRNA response elements (MREs) in the HSD11B1-3'UTR.....	66
4.6 Deletion/mutation of the corresponding miRNA response elements (MREs) in the 3'UTR of <i>HSD11B1</i> mRNA abolished the effect for hsa-miR-561 and hsa-miR- 579, but not completely for hsa-miR-340	68
4.7 Target mRNA levels were unchanged by hsa-miR-561 and hsa-miR-579	72
4.8 Glucocorticoids induction of <i>HSD11B1</i> expression in A549 cells	75
4.9 Cloning of <i>HSD11B1</i> -Promoter 1 or <i>HSD11B1</i> -Promoter 2 into pmir-HSD11B1- 3'UTR.....	76
4.10 Assessment of regulation of <i>HSD11B1</i> expression by glucocorticoids using the pmir-Promoter constructs	78
4.11 Hsa-miR-579, but not hsa-miR-561, represses <i>HSD11B1</i> expression after induction with glucocorticoids	79
4.12 Analysis of <i>HSD11B1</i> promoter activity	81
4.13 Detection of endogenous 11 β -HSD1 expression.....	84
4.14 Detection of miR-579 and miR-561 in HepG2 cells using the dual-luciferase assay system	85

4.15 Detection of miR-561 and miR-579 in human hepatocytes and HepG2 cells by Northern Blot.....	87
4.16 Detection of miR-561 and miR-579 in human hepatocytes and HepG2 cells by RT-PCR.....	88
4.17 Potential transcription of miRNAs in hepatocytes with different BMI	90
4.18 Pathway enrichment analysis.....	91
5 Discussion	96
5.1 miRNA prediction tools	96
5.2 Dual-luciferase assay system	97
5.3 Mechanism of miRNA-mediated suppression: mRNA degradation or translational repression	100
5.4 Glucocorticoids versus miRNAs for regulation of <i>HSD11B1</i> expression.....	101
5.5 The regulation of <i>HSD11B1</i> expression	103
5.6 The presence of the studied miRNAs in human liver cells	106
5.7 Regulatory role of microRNAs in liver	108
5.8 Pathway Enrichment Analysis	109
5.9 Outlook.....	112
6 References	113
7 Appendix	133
7.1 Plasmid maps	133
7.2 Sequences	135
7.3 Supplement data.....	139
Acknowledgements.....	164
Curriculum vitae	165
Erklärung.....	166

Summary

11 β -Hydroxysteroid dehydrogenase type 1 (11 β -HSD1, gene name *HSD11B1*) is a ubiquitously expressed enzyme that converts glucocorticoid receptor-inert cortisone to receptor-active cortisol. *HSD11B1* expression is regulated in a highly tissue-specific manner by immunomodulatory and metabolic regulators. Multiple evidences support a causal role for 11 β -HSD1 in the current obesity epidemic. In obese people, *HSD11B1* expression is increased in adipose tissue, but typically decreased in liver, and the underlying tissue-specific mechanisms are largely unknown.

In this context, a potential role of microRNAs (miRNAs) was investigated. Four different miRNA target prediction tools were used to choose possible candidates and a publicly available miRNA expression atlas to further select candidates expressed in hepatocytes. Using a luciferase reporter assay, where the complete 3'UTR of *HSD11B1* mRNA was inserted downstream of the gene for firefly luciferase, three potential miRNAs, hsa-miR-561, -579 and -340 were identified as potential negative regulators of *HSD11B1* expression. Moreover, disruption of the corresponding microRNA response elements (MREs) abolished repression of luciferase activity for hsa-miR-561 and -579, but not completely for hsa-miR-340. Therefore, hsa-miR-561 and hsa-miR-579-mediated downregulation of *HSD11B1* expression are strictly dependent on the binding of miR-561- and miR-579-MRE in the 3'UTR of *HSD11B1* mRNA. Levels of firefly luciferase mRNA were not changed by miR-561 and -579; and levels of endogenous *HSD11B1* mRNA were as well unchanged by miR-561 and -579, indicating a mechanism based on translational repression rather than on mRNA degradation. Interestingly, hsa-miR-579 was still performing downregulation of *HSD11B1* expression after treatment with glucocorticoids to induce *HSD11B1* expression, due to different regulatory mechanisms for *HSD11B1* expression by glucocorticoids and miRNAs in a dual luciferase assay system. The function of miR-561 and -579 could be blocked by anti-microRNA oligonucleotides (AMOs). MiR-561 and -579 were amplified by specific stem-loop reverse transcription primers and specific PCR primers from human hepatocytes and HepG2 cells. Although their relative contribution to *HSD11B1* expression remains unclear, literature findings and a pathway enrichment analysis of miR-561 and -579 target mRNAs support a role of these miRNAs in glucocorticoid metabolism/signalling and associated diseases.

Zusammenfassung

Die 11 β -Hydroxysteroid-Dehydrogenase Typ 1 (11 β -HSD1, Gen *HSD11B1*) ist ein ubiquitäres Enzym, welches Glucocorticoidrezeptor-inaktives Cortison in Rezeptor-aktives Cortisol umwandelt. Die Expression von *HSD11B1* wird höchst gewebespezifisch von immunomodulatorischen und metabolischen Regulatoren beeinflusst. Zahlreiche Befunde sprechen für eine kausale Rolle der 11 β -HSD1 in der aktuellen Übergewichtsepidemie. Übergewichtige Patienten weisen erhöhte *HSD11B1*-Expression in Fettgewebe auf, die typischerweise mit erniedrigten Levels in der Leber einhergeht. Die diesem Phänomen zugrundeliegenden gewebespezifischen Mechanismen sind weitgehend unverstanden.

In diesem Zusammenhang wurde in der vorliegenden Arbeit eine potentielle Rolle von microRNAs (miRNAs) untersucht. Vier unterschiedliche miRNA-Vorhersageprogramme wurden verwendet, um mögliche Kandidaten zu identifizieren sowie ein öffentlich zugänglicher miRNA-Expressionsatlas, um die Auswahl auf in der Leber exprimierte Kandidaten einzuschränken. Mit Hilfe eines Luciferase-Reporter-Assays, in dem die komplette 3'-UTR der *HSD11B1* mRNA an das Gen für Glühwürmchen-Luciferase gekoppelt war, identifizierten wir schließlich drei miRNAs, nämlich hsa-miR-561, -579 und -340, als potentielle negative Regulatoren der *HSD11B1*-Expression. Mutation oder Deletion der entsprechenden miRNA-Response-Elemente (MRE) hob die Repression der Luciferase-Aktivität für hsa-miR-561 and -579 vollständig auf, aber nicht für hsa-miR-340. Daraus folgt, dass die hsa-miR-561- und hsa-miR-579-vermittelte Herunterregulation der *HSD11B1*-Expression streng abhängig von der Bindung an die entsprechenden MREs in der 3'-UTR der *HSD11B1*-mRNA ist. Hsa-miR-561 und hsa-miR-579 veränderten dabei aber weder die Glühwürmchen-Luciferase-Transkriptspiegel noch die Levels der endogenen *HSD11B1*-mRNA, was auf translationelle Repression statt mRNA-Abbau als Mechanismus hinweist. Außerdem wurde beobachtet, dass im Luciferase-Assay-System hsa-miR-579 auch nach glucocorticoid-induzierter *HSD11B1*-Expression noch in der Lage ist, die selbige herunterzuregulieren, aufgrund der Regulation auf unterschiedlichen Ebenen der Proteinbiosynthese. Weiterhin konnten miRNA-561 und -579 unter Verwendung von spezifischen Haarnadelstruktur-Primern für die Reverse Transkription und spezifischen Primern für die PCR aus normalen und malignen humanen Hepatozyten amplifiziert werden. Obwohl ihr relativer Beitrag zur Regulation der *HSD11B1*-Expression unklar bleibt, sprechen sowohl Literaturbefunde als auch eine Stoffwechselweg-Enrichment-Analyse ihrer Zielgene für eine Rolle dieser miRNAs in Glucocorticoid-Metabolismus/Signaltransduktion und damit assoziierten Krankheiten.

Abbreviations

11 β -HSD1	11 β -Hydroxysteroid dehydrogenase type 1
μ g	microgram
μ l	microliter
aa	amino acid
Ab	Antibody
ACTH	Adrenocorticotropin Hormone
AMOs	anti-microRNA oligonucleotides
Amp	Ampicillin
APS	Ammonium Persulfate
ASOs	antisense oligonucleotides
bp	base pairs
BMI	Body Mass Index
BSA	Bovine Serum Albumine
cDNA	complementary DNA
C/EBP	CCATT/enhancer binding protein
dNTP	deoxynucleotide triphosphate
DMEM	Dulbecco's Modified Eagle Medium
DNA	Deoxyribonucleic Acid
<i>E.coli</i>	<i>Escherichia coli</i>
EDTA	Ethylenediaminetetraacetic Acid
FBS	Foetal Bovine Serum
g	gram or gravity
GADPH	Glyceraldehyde Phosphate dehydrogenase
GC	Glucocorticoid
GR	Glucocorticoid Receptor
HPA	Hypothalamic-Pituitary-Adrenal
HRP	Horseradish Peroxidase
IL	Interleukin
kb	kilobase pairs
kD	kilodalton
kg	kilogram
K _m	Michaelis constant
L	Liter

mg	milligram
min	minute
ml	milliliter
miRNA	microRNA
miRNP	microRNA ribonucleoprotein
mRNA	messenger RNA
MRE	miRNA Response Element
ng	nanogram
nM	nanomolar
nt	nucleotide
NAD	Nicotinamide Adenine Dinucleotide
NADP	Nicotinamide Adenine Dinucleotide Phosphate
PBS	Phosphate Buffered Saline
PCR	Polymerase Chain Reaction
PPAR	Peroxisome proliferator-activated receptor
PVDF	Polyvinylidene Difluoride
rpm	revolutions per minute
RNA	Ribonucleic Acid
RLU	Relative luminescence unit
RT	Reverse Transcription
RT-PCR	Reverse Transcription-Polymerase Chain Reaction
SD	Standard Deviation
SDR	Short-chain Dehydrogenase/Reductase
SDS	Sodium Dodecyl Sulfate
SDS-PAGE	SDS-Polyacrylamide Gel Electrophoresis
SNP	Single Nucleotide Polymorphism
<i>Taq</i>	<i>Thermophilus aquaticus</i>
TAE	Tris Acetic Acid EDTA
TEMED	N,N,N',N'-Tetramethylethylenediamine
TFBS	transcription factor binding sites
TNF α	Tumor Necrosis Factor α
U	Unit
UTR	Untranslated Region
UV	Ultraviolet

v/v	Volume per Volume
V	Voltage
w/v	Weight per Volume
WT	Wild Type

1 Introduction

1.1 11 β -Hydroxysteroid dehydrogenase type 1 (11 β -HSD1)

11 β -Hydroxysteroid dehydrogenase type 1 (11 β -HSD1, gene name *HSD11B1*) belongs to the short-chain dehydrogenase/reductase (SDR) superfamily. 11 β -HSD1 is a microsomal enzyme responsible for the reversible interconversion of active 11 β -hydroxyglucocorticoids into inactive 11-ketosteroids and, by this mechanism, regulates access of glucocorticoids to the glucocorticoid receptor (Blum *et al.*, 2000). Although bidirectional *in vitro*, *in vivo* it is believed to function as a reductase generating active glucocorticoid at a prereceptor level, enhancing glucocorticoid receptor activation (Tomlinson *et al.*, 2004). 11 β -HSD1 is a ubiquitously expressed enzyme, but occurs at highest levels in glucocorticoid target tissues. Moreover, *HSD11B1* expression is regulated in a highly tissue-specific manner by immunomodulatory and metabolic regulators. 11 β -HSD1 is responsible for intracellular glucocorticoid activation and appears to play a central role in obesity (Rask *et al.*, 2001; Tiosano *et al.*, 2003) and the associated metabolic syndrome (Tomlinson *et al.*, 2001a; Andrews *et al.*, 2003; Duplomb *et al.*, 2004; Bays *et al.*, 2007). Over the past ten years, 11 β -HSD1 has emerged as a major potential drug target in the prevention of obesity (Livingstone *et al.*, 2003), type 2 diabetes (Andrews *et al.*, 2003) or other metabolic syndrome symptoms (Nuotio-Antar *et al.*, 2007).

1.1.1 The 11 β -Hydroxysteroid dehydrogenase (11 β -HSD) system

11 β -Hydroxysteroid dehydrogenase (11 β -HSD) was designated the number EC1.1.1.146 by the Nomenclature Committee of the International Union of Biochemistry. Two isozymes of 11 β -HSD, 11 β -HSD1 and 11 β -HSD2, catalyse the interconversion of hormonally active cortisol and inactive cortisone in human (Figure 1.1). The type 1 or 'liver' isozyme was the first to be characterized (Amelung *et al.*, 1953) about 50 years ago, whereas the type 2 or 'kidney' isozyme was discovered in the late 1980s to mid-1990s (Edwards *et al.*, 1988; Castello *et al.*, 1989; Rundle *et al.*, 1989). Both isozymes belong to the short-chain dehydrogenase/reductase (SDR) superfamily. The identity of 11 β -HSD1 and 11 β -HSD2 on the amino acid level is approximately 25%, and both enzymes are anchored in the endoplasmic reticulum (ER) with hydrophobic domains (Tsigelny *et al.*, 1995). The tissue-specific expression of the isozymes plays a crucial role in regulating glucocorticoid and mineralocorticoid receptor activation. 11 β -HSD1 was shown to act as a low-affinity NADP(H)-dependent enzyme. 11 β -HSD1 displays reductase and dehydrogenase activities *in vitro*, but the dominant reaction direction *in vivo* is reduction, thus generating receptor-active

Introduction

cortisol from inactive cortisone. Hence, in glucocorticoid target tissues, such as liver, lung, and adipose tissue, 11β -HSD1 regulates the exposure of active glucocorticoids to the glucocorticoid receptor. In contrast, 11β -HSD2 is a high-affinity NAD-dependent enzyme which shows almost no reductase activity (Walker *et al.*, 1992), suggesting that the enzyme is a unidirectional dehydrogenase. 11β -HSD2 is found principally in mineralocorticoid target tissues, such as kidney, colon, and placenta, where it protects the mineralocorticoid receptor from cortisol excess. The characteristics of 11β -HSD1 and 11β -HSD2 isozymes are summarized in Table 1.1. However, the work in this thesis focuses on 11β -HSD1.

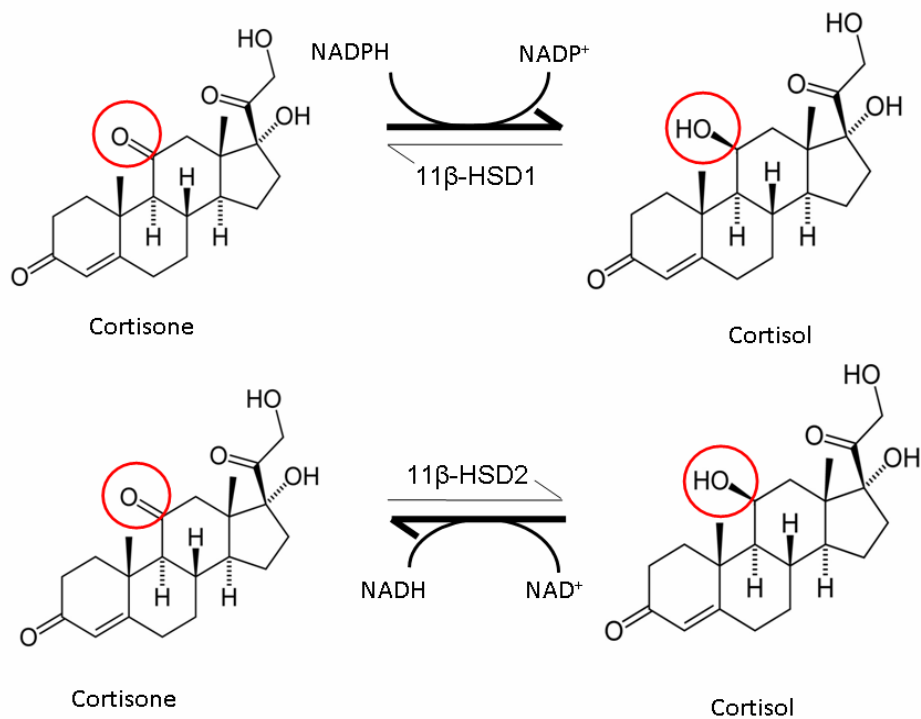


Figure 1.1 Predominant reaction directions of 11β -HSD1 and 11β -HSD2 *in vivo*.

Table 1.1 Direct comparisons between the characteristics of 11 β -HSD1 and 11 β -HSD2 isozymes. (Blum *et al.*, 2003; Draper *et al.*, 2005)

	11β-HSD1	11β-HSD2
Chromosomal location	1q32.2	16q22
Size	Gene: 30 kb, 6 exons Protein: 292 aa, 34 kD	6.2 kb, 5 exons 405 aa, 44 kD
Enzyme family	SDR superfamily	SDR superfamily
Distribution	Ubiquitous (liver, adipose tissue, lung, brain)	Aldosterone target tissue (kidney, colon, placenta)
Cofactor	NADP(H)	NAD
Enzyme kinetics	<i>In vitro</i> bidirectional <i>In vivo</i> mainly reductase, Low affinity ($K_m \sim \mu\text{M}$)	Only dehydrogenase High affinity ($K_m \sim \text{nM}$)
Physiological role	Regulates cortisol to glucocorticoid receptor	Protects mineralocorticoid receptor from cortisol

1.1.2 Human *HSD11B1* gene and alternative promoter usage

1.1.2.1 Human *HSD11B1* gene

The human *HSD11B1* gene was firstly cloned and isolated from a human testis cDNA library by hybridization with a previously isolated rat 11 β -HSD1 cDNA clone (Tannin *et al.*, 1991). Hybridization of the human 11 β -HSD1 cDNA to a human-hamster hybrid cell panel localized the single corresponding *HSD11B1* gene to chromosome 1 (1q32-41). Human *HSD11B1* gene consists of six exons (182 bp, 130 bp, 111 bp, 185 bp, 143 bp and 617 bp, respectively) and five introns (776 bp, 767 bp, 120 bp, 25,300 bp and 1,700 bp, respectively) (Figure 1.2). The human 11 β -HSD1 cDNA predicted a protein of 292 amino acids and was 77% identical at the amino acid level to the rat 11 β -HSD1 cDNA (Tannin *et al.*, 1991). Originally, the human *HSD11B1* gene was thought to be approximately 9 kb in size; however, subsequent studies revealed a much larger than previously recognized intron 4 of approximately 25 kb, expanding the size of the *HSD11B1* gene to approximately 30 kb (Draper *et al.*, 2002).

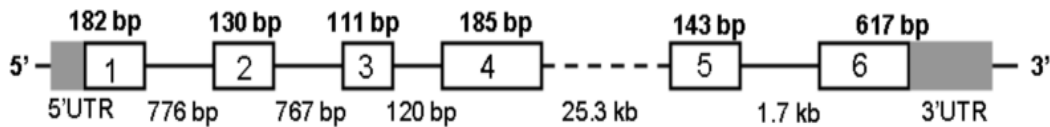


Figure 1.2 Organization of the human *HSD11B1* gene. Gray boxes indicate the 5'- and 3'-UTR, Open boxes indicate coding exons (1-6), and intervening solid lines indicate introns (the dashed line of intron 4, corresponding to 25.3 kb, is not to scale).

There are few reports describing polymorphisms in and around the *HSD11B1* gene locus and few polymorphisms have been identified in the *HSD11B1* gene. To date, 39 polymorphisms are documented in the GenBank single nucleotide polymorphisms (SNP) database (dbSNP at <http://www.ncbi.nlm.nih.gov/SNP/>). All but one polymorphism is located in non-coding regions of the gene; 31 SNPs are within intron 4, one SNP is located in the 3'-untranslated region, and seven SNPs are located within 2 kb of the mRNA transcript (three in 5' regions of the gene and four in 3' regions of the gene).

1.1.2.2 Alternative promoter usage

Expression of human *HSD11B1* is highly tissue-specific and controlled by two distinct promoters, an aspect which to date has been studied very little. However, studies in the mouse have shown that both promoters are active in liver, lung, adipose tissue and brain (Bruley *et al.*, 2006). Alternative promoter usage in expression of murine *Hsd11b1* and human *HSD11B1*, as transcription from the distal promoter P1 or the proximal promoter P2, results in distinct transcript variants differing in the 5'-untranslated region (UTR), which are translated to the same protein. A schematic illustration depicting the two distinct transcript variants is shown in Figure 1.3. Little work on alternative promoter usage has been published for the human *HSD11B1* gene, but the evidence for corresponding alternative transcripts can be found in public databases (NCBI, <http://www.ncbi.nlm.nih.gov/>; Ensembl Genome Browser, <http://www.ensembl.org/>). In our lab, Staab *et al.* (2011) used 5'UTR-specific primers for their detection by semi-quantitative PCR and also established a quantitative real-time PCR method using 5'UTR-specific fluorescent probes in combination with 5'-UTR-specific primers for absolute quantification of the two human transcripts in a duplex approach. The combined results demonstrated that transcription from P1 (transcript from the distal promoter P1) predominated in the human tumor cell lines A431 and HT-29 and contributed significantly to overall *HSD11B1* expression in human lung (Staab *et al.*, 2011). Transcription

from P2 (transcript from the proximal promoter P2) predominated in most tissues and cell lines assessed, including human liver, human lung, human subcutaneous adipose tissue, and the cell lines A549, Caco-2, C2C12 and 3T3-L1 (Staab *et al.*, 2011).

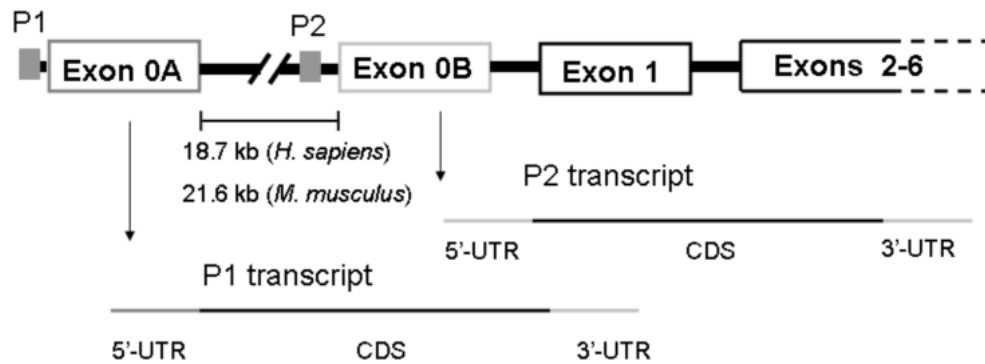


Figure 1.3 Schematic illustration of the two distinct transcripts of human *HSD11B1*. The *HSD11B1* is regulated by two different promoters, leading to two distinct transcript variants that differ in the 5'-UTR. Both transcripts have the same coding sequence and 3'-UTR. Hence both transcripts code for the same 11 β -HSD1 protein.

1.1.3 11 β -HSD1 and glucocorticoid action

Glucocorticoids (GCs) are a vital class of steroid hormones that are secreted by the adrenal cortex. The secretion is regulated by adrenocorticotrophic hormone (ACTH) under the control of the hypothalamic-pituitary-adrenal axis (HPA). Glucocorticoids play a key role in the modulation of immune and inflammatory processes, in the regulation of energy metabolism, in cardiovascular homeostasis, and in the body's response to stress. Multiple factors regulate glucocorticoid secretion, such as the abundance of plasma binding proteins and glucocorticoid receptor (GR). 11 β -HSD1 has been identified as tissue-specific glucocorticoid activating enzyme and thus as an additional intracellular determinant in the glucocorticoid signaling pathways. Within the cell, 11 β -HSD1 functions as an important pre-receptor regulator by converting the inert 11-ketoforms 11-dehydrocorticosterone in rodents and cortisone in human to the receptor-active hydroxyforms corticosterone and cortisol, respectively. When not activated by ligand, the GR is retained in the cytoplasm by the association with chaperones (Yudt *et al.*, 2002). Once activated by the ligand, the GR-chaperone complex dissociates and the GR is translocated rapidly into the nucleus where it binds to the promoter region of glucocorticoid-responsive genes and leads to induction or repression of gene transcription. Hence, 11 β -HSD1 regulates glucocorticoid access to the glucocorticoid receptor

and can thus be considered an enzymatic pre-receptor regulator in the signaling pathway of glucocorticoid hormones.

1.1.4 Localization of 11 β -HSD1

Numerous studies have assessed *HSD11B1* expression using different methodologies that include PCR, RNase protection assays, Western blotting, immunohistochemistry, immunocytochemistry, Northern blotting and specific enzyme assays. Table 1.2 gives a comprehensive list of the tissue-specific distribution of 11 β -HSD1 in different species. It seems that 11 β -HSD1 is expressed in many tissues throughout the body. 11 β -HSD1 is highly expressed in glucocorticoid target tissues including liver and lung, at modest levels expressed in adipose tissue and brain, and also found in a number of other tissues, including heart, eye, bone and ovary.

Table 1.2 Tissue- and species-specific expression of 11 β -HSD1 (Tomlinson *et al.*, 2004).

Tissue (11 β -HSD1)	References
Hepatobiliary system	
Human liver (centripetal distribution)	Ricketts <i>et al.</i> , 1998; Brereton <i>et al.</i> , 2001
Human pancreatic islets	Brereton <i>et al.</i> , 2001
Rodent pancreatic islets	Davani <i>et al.</i> , 2000
Rat liver	Nwe <i>et al.</i> , 2000
Adrenal	
Human adrenal cortex	Ricketts <i>et al.</i> , 1998; Brereton <i>et al.</i> , 2001
Lung	
Lung (rodent)	Bruley <i>et al.</i> , 2006
Heart	
Rat cardiac myocytes	Sheppard <i>et al.</i> , 2002
Rat cardiac fibroblasts	Sheppard <i>et al.</i> , 2002
Kidney	
Human kidney medulla	Whorwood <i>et al.</i> , 1995
Central nervous system	
Human cerebellum	Whorwood <i>et al.</i> , 1995

Introduction

Rodent hippocampus, brain stem	Jellinck <i>et al.</i> , 1999
Rat spinal cord	Moisan <i>et al.</i> , 1990
Human microglia	Gorrfried-Blackmore <i>et al.</i> , 2010
Gonad	
Rat epididymis	Waddell <i>et al.</i> , 2003
Human granulosa-lutein cells	Michael <i>et al.</i> , 1993
Human testis	Tannin <i>et al.</i> , 1991
Rat Leydig cells	Leckie <i>et al.</i> , 1998
Rat testis	Nwe <i>et al.</i> , 2000
Bone	
Human osteoblasts	Cooper <i>et al.</i> , 2000
Human osteoclasts	Cooper <i>et al.</i> , 2000
Connective tissues	
Human adipose tissue	Bujalska <i>et al.</i> , 1997
Human skeletal myoblasts	Whorwood <i>et al.</i> , 2002
Human skin fibroblasts	Hammami and Siiteri, 1991
Lymphoid tissue	
Human spleen	Hennebold <i>et al.</i> , 1996
Human macrophage	Thieringer <i>et al.</i> , 2001
Human thymus	Whorwood <i>et al.</i> , 1995
Human lymph nodes	Whorwood <i>et al.</i> , 1995
Colon	
Human lamina propria and the surface epithelium	Whorwood <i>et al.</i> , 1994
Eye	
Rat nonpigmented ciliary epithelium	Stokes <i>et al.</i> , 2000
Rat trabecular meshwork	Stokes <i>et al.</i> , 2000
Rat corneal epithelium	Stokes <i>et al.</i> , 2000
Human corneal epithelium	Rauz <i>et al.</i> , 2001
Human nonpigmented epithelium	Rauz <i>et al.</i> , 2001
Uterus	
Human ovary	Smith <i>et al.</i> , 1997

Introduction

Rat endometrial stroma and myometrium	Burton <i>et al.</i> , 1998
Murine uterus	Thompson <i>et al.</i> , 2002
Pituitary	
Rat anterior pituitary	Moisan <i>et al.</i> , 1990
Human lactotrophs	Korbonits <i>et al.</i> , 2001
Placenta	
Human placenta and fetal membranes	Sun <i>et al.</i> , 1997
Murine placenta	Thompson <i>et al.</i> , 2002
Human syncytiotrophoblast	Pepe <i>et al.</i> , 1999
Ear	
Rat inner ear	Terakado <i>et al.</i> , 2011
Skin	
Human skin	Tiganescu <i>et al.</i> , 2011

1.1.5 Regulation of *HSD11B1* expression

Expression of *HSD11B1* is regulated by many regulatory factors including some proinflammatory cytokines (TNF- α and IL-1 β), glucocorticoids (cortisol and dexamethasone), insulin, growth hormone, CCATT/enhancer binding proteins (C/EBPs), peroxisome proliferator-activated receptor (PPAR) agonists, leptin, sex hormones, thyroid hormone and other nuclear receptors. The regulation of *HSD11B1* expression is highly tissue-specific manner (Tomlinson *et al.*, 2004). For instance, the proinflammatory cytokines, TNF- α and IL-1 β induce *HSD11B1* expression in smooth muscle cells and adipocytes, but not in human monocytes and primary hepatocytes (Cai *et al.*, 2001; Tsuqita *et al.*, 2008; Tomlinson *et al.*, 2001; Friedberg *et al.*, 2003; Handoko *et al.*, 2000; Thieringer *et al.*, 2001). A comprehensive list of to date published studies on regulation of *HSD11B1* expression in different tissues after induction and species is given in Table 1.3.

Table 1.3 Regulation of *HSD11B1* expression by regulatory factors in different tissues and cell types. Upward arrows, downward arrows and horizontal arrows depict upregulated, downregulated and unchanged *HSD11B1* expression and/or activity, respectively (Tomlinson *et al.*, 2004; Wamil *et al.*, 2007; Staab *et al.*, 2010).

Regulatory factor	Tissue/cell type	<i>HSD11B1</i> expression and/or activity	References
Glucocorticoid receptor (GR) agonists			
Cortisol	Human skeletal muscle cells	↑	Whorwood <i>et al.</i> , 2002
	Human omental adipose cells	↑	Bujaska <i>et al.</i> , 1997
	Human osteoblasts	↑	Cooper <i>et al.</i> , 2002
	Human fetal lung	↑	Yang <i>et al.</i> , 2009
	Fetal ovine liver	↑	Gupta <i>et al.</i> , 2003
Corticosterone	Rat liver	←	Nwe <i>et al.</i> , 2000
	Rat testis	↑	Nwe <i>et al.</i> , 2000
	Rat Leydig cells	↓	Sankar <i>et al.</i> , 2000
Dexamethasone	Rat hepatocytes	↑	Liu <i>et al.</i> , 1996
	Rat hippocampus	↑	Moisan <i>et al.</i> , 1990
	Human skin fibroblasts	↑	Hammami <i>et al.</i> , 1991
	Rat liver	↓	Jamieson <i>et al.</i> , 1999
	Rat 2S FAZA hepatoma cells	↑	Voice <i>et al.</i> , 1996
Betamethasone	Baboon placenta	←	Ma <i>et al.</i> , 2003
Cytokines			
Interleukin (IL)			
IL-1β	Human smooth muscle cells	↑	Cai <i>et al.</i> , 2001
	Human osteoblasts	↑	Cooper <i>et al.</i> , 2001
	Human adipose stromal cells	↑	Tomlinson <i>et al.</i> , 2001
	Rat glomerular mesangial cells	↑	Escher <i>et al.</i> , 1997
	Human adipocytes	↑	Friedberg <i>et al.</i> , 2003
	Human HuH7 cells	↑	Iwasaki <i>et al.</i> , 2008

Introduction

	Human fibroblasts	↑	Hardy <i>et al.</i> , 2006
IL-2	Human granulosa-lutein cells	←	Evagelatou <i>et al.</i> , 1997
IL-4	Human monocytes	↑	Thieringer <i>et al.</i> , 2001
	Human granulosa-lutein cells (leukocyte depleted)	↑	Evagelatou <i>et al.</i> , 1997
	Human ASM cells	↑	Hu <i>et al.</i> , 2009
IL-5	Human granulosa-lutein cells	↑	Evagelatou <i>et al.</i> , 1997
IL-6	Human adipose stromal cells	↑	Tomlinson <i>et al.</i> , 2001
	Human granulosa-lutein cells	↑	Evagelatou <i>et al.</i> , 1997
IL-13	Human monocytes	↑	Thieringer <i>et al.</i> , 2001
	Human ASM cells	↑	Hu <i>et al.</i> , 2009
Tumor Necrosis Factor α (TNF α)	Rat glomerular mesangial cells	↑	Escher <i>et al.</i> , 1997
	Human adipocytes	↑	Friedberg <i>et al.</i> , 2003
	Human HuH7 cells	↑	Iwasaki <i>et al.</i> , 2008
	Human fibroblasts	↑	Hardy <i>et al.</i> , 2006
	Human adipose stromal cells	↑	Tomlinson <i>et al.</i> , 2001
	Human osteoblasts	↑	Cooper <i>et al.</i> , 2001
	Human monocytes	←	Thieringer <i>et al.</i> , 2001
Interferon γ (IFN γ)	Human granulosa-lutein cells (leukocyte depleted)	↑	Evagelatou <i>et al.</i> , 1997
Insulin-like growth factor I (IGF-I)	Human adipose stromal cells	↓	Tomlinson <i>et al.</i> , 2001
	HEK 293 cells	↓	Moore <i>et al.</i> , 1999
	Human hepatocytes	←	Tomlinson <i>et al.</i> , 2001

Introduction

	3T3-L1 cells	↓	Moore <i>et al.</i> , 1999
	Rat 2S FAZA hepatoma cells	↓	Voice <i>et al.</i> , 1996
	Mouse liver	↓	Huang <i>et al.</i> , 2010
Growth hormone (GH)	HEK 293 cells	←	Moore <i>et al.</i> , 1999
	Rat hepatocytes	↓	Liu <i>et al.</i> , 1996
	Human adipocytes	←	Friedberg <i>et al.</i> , 2003
	Rat liver	↓	Low <i>et al.</i> , 1994
Insulin	3T3-F442A and 3T3-L1	↓	Napolitano <i>et al.</i> , 1998
	Human adipose stromal cell	←	Bujaska <i>et al.</i> , 1999
	Rat hepatocytes	↓	Liu <i>et al.</i> , 1996
	Rat 2S FAZA hepatoma cells	↓	Voice <i>et al.</i> , 1996
Leptin	Mouse hepatocytes	↑	Liu <i>et al.</i> , 2003
	Mouse liver	↑	Liu <i>et al.</i> , 2003
	Human hepatocytes	←	Tomlinson <i>et al.</i> , 2001
Liver X receptor (LXR) agonist	Mouse 3T3-L1 cells	↓	Stulnig <i>et al.</i> , 2002
	Mouse embryonic fibroblasts	↓	Stulnig <i>et al.</i> , 2002
Adrenergic receptor agonists			
Salbutamol	Human subcutaneous adipocytes	↑	Friedberg <i>et al.</i> , 2003
Clonidine	Human subcutaneous adipocytes	↓	Friedberg <i>et al.</i> , 2003
PPAR α agonists			
Fenofibrate	KKAy mice (hepatic and adipose)	↓	Srivastava, 2009
Bezafibrate	Murine adipose tissue	↓	Nakano <i>et al.</i> , 2007
	3T3-L1 adipocytes	↓	Nakano <i>et al.</i> , 2007
WY14643	Murine liver	↓	Hermanowski-Vosatka <i>et al.</i> , 2000

Introduction

PPAR γ agonists			
Rosiglitazone	3T3-L1 adipocytes	↓	Berger <i>et al.</i> , 2001
TZD2	3T3-L1 adipocytes	↓	Berger <i>et al.</i> , 2001
COOH	Rat adipose	↑	Laplante <i>et al.</i> , 2003
Protein kinase A (PKA) activators			
Forskolin	Rat 2S FAZA hepatoma cells	↓	Voice <i>et al.</i> , 1996
	Rat granulosa cells	↑	Tetsuka <i>et al.</i> , 1999
8-bromo-cAMP			
8-bromo-cAMP	Human skin fibroblasts	↓	Hammami <i>et al.</i> , 1991
Dibutyryl-cAMP			
Dibutyryl-cAMP	Rat granulosa cells	↑	Tetsuka <i>et al.</i> , 1999
Protein kinase C (PKC) activators			
Phorbol ester	Rat granulosa cells	↑	Tetsuka <i>et al.</i> , 1999
	Human skin fibroblasts	↓	Hammami <i>et al.</i> , 1991
Retinoic acid			
Retinoic acid	Mouse 3T3-L1 cells	↓	Stulnig <i>et al.</i> , 2002
	Mouse C2C12 myotubes	↓	Aubry <i>et al.</i> , 2009
(1, 25-Dihydroxy-) Vitamin D3			
(1, 25-Dihydroxy-) Vitamin D3	Human monocytes	↑	Thieringer <i>et al.</i> , 2001
	Human adipocytes	↑	Morris <i>et al.</i> , 2005
	THP-1 cells	↑	Thieringer <i>et al.</i> , 2001
Vitamin A			
Vitamin A	Rat liver	↓	Sakamuri <i>et al.</i> , 2011
Eicosanoids			
15-Deoxy12,14- prostaglandin J2			
Prostaglandin F2 α	Human chorionic trophoblast cells	↑	Alfaidy <i>et al.</i> , 2001
	Bovine endometrial stromal cells	↑	Lee <i>et al.</i> , 2009

Introduction

Sex steroids			
Estradiol	Rat uterus	↑	Ho <i>et al.</i> , 1999
	Rat kidney	↓	Low <i>et al.</i> , 1993
	Human endometrial decidual cell	↑	Arcuri <i>et al.</i> , 1997
	Rat liver	↓	Nwe <i>et al.</i> , 2000
	Rat testis	↓	Nwe <i>et al.</i> , 2000
Testosterone	Rat liver	←	Nwe <i>et al.</i> , 2000
	Rat testis	↓	Nwe <i>et al.</i> , 2000
CCATT/enhancer binding			
Protein (C/EBP)			
C/EBP α	Human HepG2 cells	↑	Williams <i>et al.</i> , 2000
C/EBP β	Human HepG2 cells	↑	Williams <i>et al.</i> , 2000
Protease inhibitor	Human omental and subcutaneous preadipocytes	↓	Moore <i>et al.</i> , 1999
Thyroid hormone (T ₃)	Rat liver	↓	Whorwood <i>et al.</i> , 1993
	Rat pituitary	↓	Whorwood <i>et al.</i> , 1993
	Rat kidney	←	Whorwood <i>et al.</i> , 1993

1.1.6 11 β -HSD1 and obesity/type 2 diabetes

1.1.6.1 11 β -HSD1 and obesity

Obesity has become an epidemic in the western world and is tightly associated with type 2 diabetes and other symptoms of the metabolic syndrome (DeFronzo *et al.*, 1991; Stulnig *et al.*, 2004). Excess glucocorticoids produce visceral obesity and diabetes, but circulating glucocorticoid levels are normal in typical obesity. The enzyme 11 β -HSD1 plays a pivotal role in determining intracellular glucocorticoid concentrations by regenerating the active glucocorticoids cortisol in human and corticosterone in mice from inert glucocorticoids cortisone in human and 11-dehydrocorticosterone in mice, hence amplifying active glucocorticoids in key metabolic tissues including adipose tissue and liver. Transgenic mice overexpressed 11 β -HSD1 selectively in adipose tissue and increased adipose levels of

corticosterone, thus developing visceral obesity (Masuzaki *et al.*, 2001). Other data provide evidence for a role of 11 β -HSD1 in the development of visceral obesity. In leptin-resistant fatty ‘Zucker’ rats, obesity comes along with decreased 11 β -HSD1 activity in liver, but increased 11 β -HSD1 activity in adipose tissue, notably in visceral fat (Livingstone *et al.*, 2000). Similar changes have been reported in leptin-deficient ob/ob mice (Liu *et al.*, 2003; Wamil *et al.*, 2007). Furthermore, several research groups have reported that obese patients show selective downregulation of 11 β -HSD1 in liver and upregulation in adipose tissue, but the underlying tissue-specific mechanisms are still unknown (Stewart *et al.*, 1999; Rask *et al.*, 2001; Tiosano *et al.*, 2003).

1.1.6.2 11 β -HSD1 and type 2 diabetes

Type 2 diabetes is a metabolic disorder characterized by insulin resistance, hyperglycemia and relative insulin deficiency. National health surveys estimated that more than 80% of patients with type 2 diabetes are either obese or overweight in the USA (Bays *et al.*, 2007), but that does not mean that everyone with obesity is equally at risk to develop type 2 diabetes (Brochu *et al.*, 2001). Indeed, the majority of patients with obesity do not develop diabetes (Felber *et al.*, 2002). Type 2 diabetes is mainly characterized by disturbed insulin secretion in addition to decreased insulin sensitivity. 11 β -HSD1 is expressed in islets of Langerhans isolated from ob/ob mice and also from human pancreas (Davani *et al.*, 2000). 11 β -HSD1 is increased in islets of diabetes but not pre-diabetes ‘Zucker’ rats (Duplomb *et al.*, 2004). High levels of *HSD11B1* mRNA and enzyme activity have been correlated with the appearance of diabetes (Duplomb *et al.*, 2004). Moreover, treatment with glucocorticoids decreases insulin sensitivity and accelerates to the development of diabetes (Stunlnig *et al.*, 2004). Fewer studies of 11 β -HSD1 have been conducted in type 2 diabetes (Valsamakis *et al.*, 2004). Although hepatic 11 β -HSD1 activity is mild impaired, adipose tissue 11 β -HSD1 activity appears to be normal in lean patients with type 2 diabetes (Andrews *et al.*, 2002). However, in obese type 2 diabetes patients, 11 β -HSD1 expression is increased in skeletal muscle myotubes (Abdallah *et al.*, 2005), which may contribute to the pathogenesis of insulin resistance (Abdallah *et al.*, 2005).

1.1.7 Inhibition of 11 β -HSD1 as a therapeutic target

Glucocorticoids such as cortisol are important regulators of fuel metabolism during stress and starvation. Chronic glucocorticoids excess induce all features of the metabolic syndrome including obesity, type 2 diabetes and hypertension as well as neurological disorders such as memory impairments and mood disorders. 11 β -Hydroxysteroid dehydrogenase type 1 (11 β -HSD1) amplifies glucocorticoid concentrations in key metabolic tissues including liver and adipose tissue (Seckl *et al.*, 2001). Inhibition of 11 β -HSD1 shows considerable promise as a therapeutic target for the treatment of obesity, type 2 diabetes and other aspects of the metabolic syndrome (Stulnig *et al.*, 2004; Hughes *et al.*, 2008). Two principal therapeutic strategies to diminish the exaggerated activation of a receptor are thinkable: antagonism of the receptor and /or its signaling pathway or reducing ligand availability, systemically or locally.

In current therapies available for treatment of Cushing's syndrome, obesity and type 2 diabetes, cortisol antagonism might be a therapeutic target for all of the major features of the metabolic syndrome. Several approaches have been proposed (Hughes *et al.*, 2008). One example is inhibition of steroid biosynthesis in the adrenal to decrease glucocorticoid activity (Hughes *et al.*, 2008). For instance, metyrapone and ketoconazole are traditionally used for the treatment of Cushing's syndrome, as they reduce the cortisol level in plasma by inhibiting key enzymes in adrenal steroidogenesis (Wolkowitz *et al.*, 1999). Other studies have focused on GR antagonists such as RU38484, which is known as a glucocorticoid and progestin receptor antagonist. In Cushing's syndrome, administration of RU38484 shows such marked improvements in glycemic control, demonstrating the beneficial metabolic effects of reducing glucocorticoid activity (Chu *et al.*, 2001). Administration of RU38484 also improved plasma glucose level in diabetic mice (Gettys *et al.*, 1997).

Inhibition of 11 β -HSD1 is used as a therapeutic target for obesity and type 2 diabetes. Up to date, more than twenty-five companies have involved in the development of 11 β -HSD1 inhibitor drugs, several 11 β -HSD1 inhibitors are in late preclinical or early clinical development as therapeutic target for obesity or type 2 diabetes, for instance, carbenoxolone (Livingstone *et al.*, 2003; Andrews *et al.*, 2003; Nuotio-Antar *et al.*, 2007; Tomlinson *et al.*, 2007), derivatives of 18 β -glycyrrhetic acid (Su *et al.*, 2007), adamantane sulfone (Sorensen *et al.*, 2007), and beta-keto sulfones (Xiang *et al.*, 2007). Recently, several new 11 β -HSD1 inhibitors have been reported as therapeutic target for obesity or type 2 diabetes, like BVT.2733 (Liu *et al.*, 2011), HSD-016 (Wan *et al.*, 2011), dipeptidyl peptidase-IV inhibitors

Introduction

(DPP-IV, Sun *et al.*, 2011), MK-0916 (Feig *et al.*, 2011) and INCB-13739 (Tiwair, 2010). However, advances in the treatment of obesity and the metabolic syndrome have been limited with the availability of very few drugs on the market (Kolonin *et al.*, 2004). Moreover, known drugs have many limitations and side effects, for instance, thiazolidinediones may cause an increase in the risk of death from cardiovascular events (Nissen *et al.*, 2007), insulin and many other antidiabetic treatments are associated with weight gain (Verspohl *et al.*, 2009). Therefore, it will be a more promising perspective to explore less toxic and side effect 11 β -HSD1 inhibitors for the treatment of obesity and type 2 diabetes in the future.

1.2 MicroRNAs

MicroRNAs (miRNAs) are short, single-stranded, evolutionarily conserved noncoding RNAs with an average length of 22 nucleotides (Ambros, 2003). MiRNAs regulate gene expression by translational repression or degradation of target mRNAs, depending on the level of complementarity between the miRNAs and the target mRNAs. In plants, miRNAs-target mRNAs complementarity is perfect or near perfect and the target mRNA is degraded (Rhades *et al.*, 2002). In animals, in general, miRNAs-target mRNAs complementarity is imperfect (Lai, 2004), but partial complementarity is sufficient to trigger target mRNA degradation (Bagga *et al.*, 2005; Du *et al.*, 2005; Lim *et al.*, 2005) or translational repression, while in mammals translational repression seems to be the key approach (Bartel, 2004). The interaction of miRNAs and target genes is intricately regulated, in that one miRNA may modulate multiple target genes whereas one target gene may be regulated by various miRNAs. Although the first miRNA was identified over 10 years, it is only recently that people began to understand the scope and the diversity of these regulatory molecules. MiRNAs comprise one of more abundant classes of gene regulatory molecules in multicellular organisms and likely influence the output of many protein-coding genes. Computational analyses predict the presence of up to 50,000 different miRNAs in a mammalian cell, each with hundreds to thousands of potential mRNA targets regulating approximately 30% of protein-coding genes (Berezikov *et al.*, 2005).

1.2.1 Discovery of miRNAs

In 1993, Lee *et al.* discovered that *lin-4* in *C.elegans* did not code for a protein but instead produced a pair of short RNA transcripts that regulate the timing of larval development by translational repression of *lin-14*. *Lin-4* acts by negatively regulating the level of *lin-14* protein, creating a temporal decrease in *lin-14* protein starting in the first larval stage. They postulated that the regulation was due to in part sequence complementarity between *lin-4* and unique repeats within the 3' untranslated region (UTR) of the *lin-14* mRNA (Lee *et al.*, 1993). For seven years after the discovery of the *lin-4* RNA, Reinhart *et al.* (2000) discovered the second miRNA, *let-7*. The *let-7* miRNA, similarly to *lin-4*, regulates developmental timing in *C. elegans* and acts to promote the transition from late-larval to adult cell fates in the same way that the *lin-4* RNA acts earlier in development to promote the progression from the first larval stage to the second (Reinhart *et al.*, 2000). Up to date, thousands of miRNAs have been identified in organisms as diverse as human, rat, mouse, worm, and *Drosophila*. The

identified miRNAs are currently annotated at miRBase, as a publicly available repository (<http://microrna.sanger.ac.uk/>).

1.2.2 Biogenesis of miRNAs

Most miRNAs reside in intergenic or intronic regions, which are transcribed as a part of a long transcript through RNA polymerase II (Esquela-Kerscher *et al.*, 2006). The current model for maturation of the mammalian miRNAs is shown in Figure 1.4. In mammalian cells, the miRNA pathway begins with the transcription of a primary miRNA from a miRNA gene. The primary miRNA is processed in the nucleus by the microprocessor machinery, which contains the Drosha RNase and the double-stranded RNA binding protein DGCR8 (Han *et al.*, 2006). The nuclear cleavage of the primary miRNA by the Drosha RNase III endonucleases liberates a 60-70 nt stem-loop intermediate, termed precursor miRNA. Precursor miRNA is actively transported from the nucleus to the cytoplasm by the export receptor Exportin-5 (Lund *et al.*, 2004; Yi *et al.*, 2003), where it is further processed by a protein complex that includes DICER, AGO1, AGO2 and TRBP, leading to the production of ~21 bp miRNA duplexes (Yue, 2006; Chendrimada *et al.*, 2005). Generally, the strand with the 5' terminus located at the thermodynamically less-stable end of the duplex is selected to function as a mature miRNA, while the other strand is degraded (Du *et al.*, 2005; Kim *et al.*, 2006). Following processing, to perform regulatory functions, miRNAs are assembled into ribonucleoprotein (RNP) complexes called micro-RNPs (miRNPs) or miRNA-induced silencing complexes (miRISCs) or RNA-induced silencing complexes (RISCs). The key components of miRNPs are proteins of the Argonaute (AGO) family. In mammals, four AGO proteins (AGO 1 to AGO4) function in the miRNAs repression. With these complexes, miRNAs lead Argonaute proteins to fully or partially complementary mRNA targets, which are then silenced posttranscriptionally (Bushati and Cohen, 2007).

Introduction

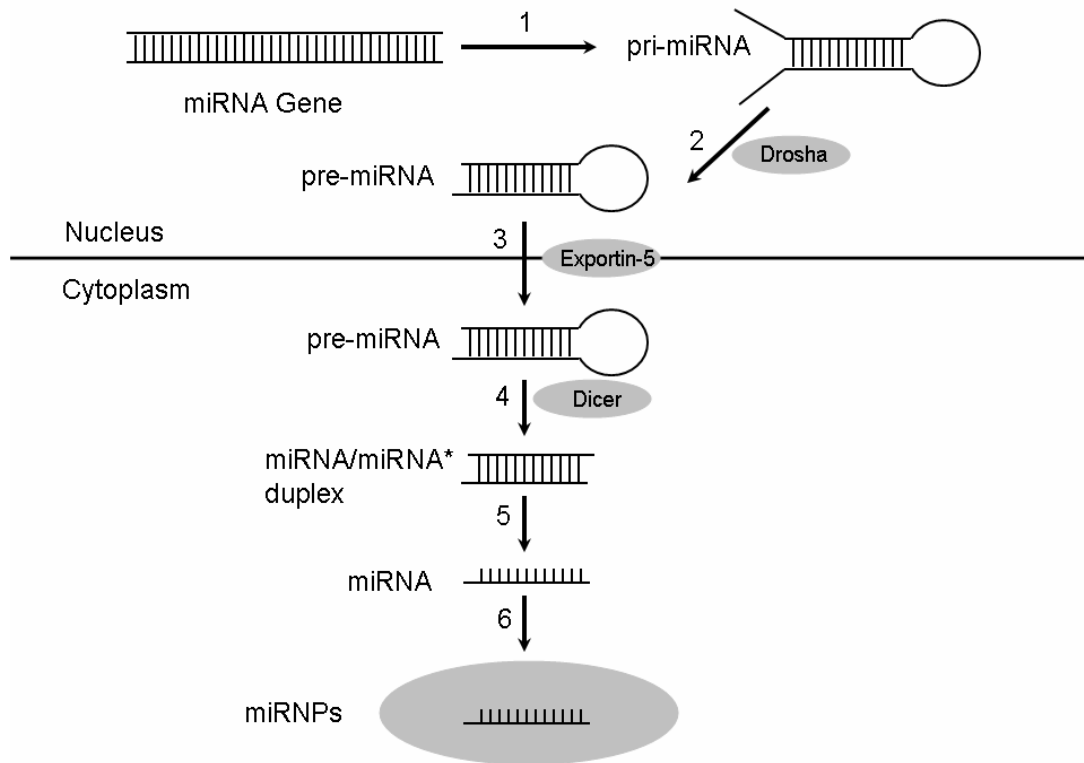


Figure 1.4 Biogenesis of miRNAs. 1: miRNA gene is transcribed into a primary miRNA (pri-miRNA). 2: Pri-miRNA is cleaved by Drosha to a pre-miRNA. 3: Pre-miRNA is transported out of the nucleus by exportin-5. 4: Pre-miRNA is cleaved by Dicer to form a short double-stranded miRNA duplex. 5: miRNA duplex separates into single-stranded mature miRNA. 6: miRNAs are assembled into ribonucleoprotein (RNP) complexes called micro-RNPs (miRNPs).

1.2.3 Mechanisms of miRNA-mediated gene silencing

According to our current understanding, the mature miRNAs are assembled into ribonucleoprotein (RNP) complexes called micro-RNPs (miRNPs). Subsequently, miRNAs could lead the miRNPs to downregulate gene expression by one of two posttranscriptional mechanisms: mRNA cleavage or translational repression.

1.2.3.1 Mechanism: mRNA cleavage

MiRNAs interact with their target mRNAs by base pairing. In plants, miRNAs generally bind to mRNAs with almost perfect complementarity and trigger endonucleolytic mRNA cleavage by an RNAi-like mechanism (Jones-Rhoades *et al.*, 2006). The mRNA is cleaved endonucleolytically in the middle of the miRNA-mRNA duplex by miRNPs (Figure 1.5A).

Introduction

After cleavage of the mRNA, the miRNA remains intact and can guide the recognition and destruction of additional messages (Tang *et al.*, 2003). In contrast, with few exceptions, metazoan miRNA is imperfect base pairing with their target mRNAs. The most stringent requirement is a contiguous and perfect base pairing of the miRNA nucleotides 2-8, representing the ‘seed’ region, which is mainly binding sites for the miRNA-mRNA association. Usually, miRNA-binding sites in metazoan mRNAs lie in the 3’UTR, but partial complementarity is sufficient to trigger target mRNA cleavage (Figure 1.5B, Lewis *et al.*, 2005; Grimson *et al.*, 2007; Nielsen *et al.*, 2007). For example, in zebrafish embryos at the onset of zygotic transcription, the dramatic increase of miR-430 expression correlates with the degradation of a large number of maternal mRNAs containing miR-430 binding sites in their 3’UTRs (Giraldez *et al.*, 2006).

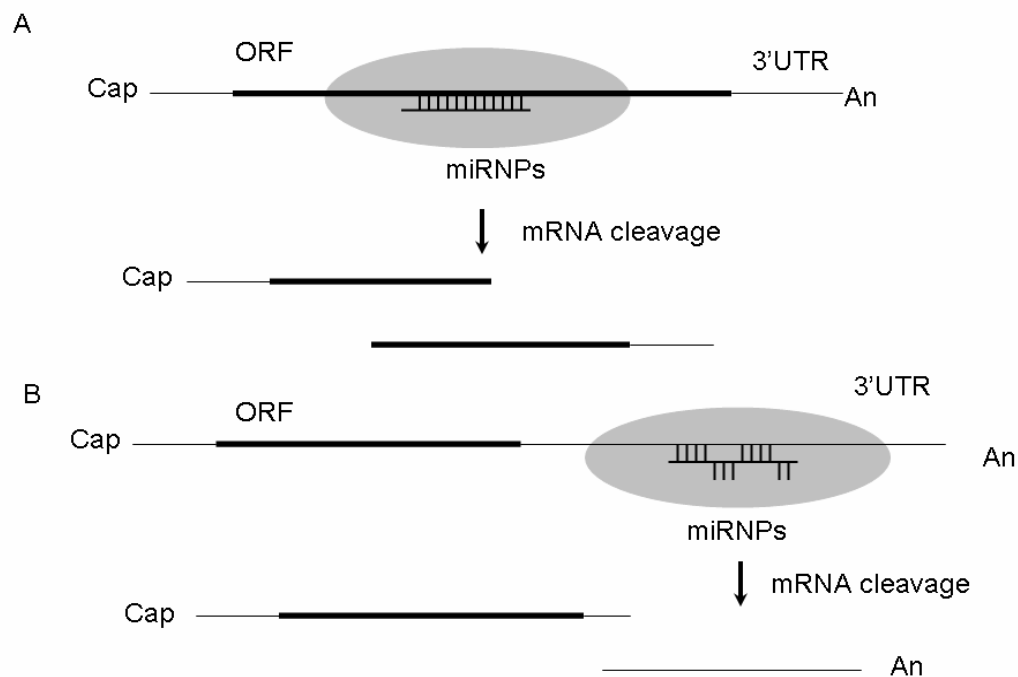


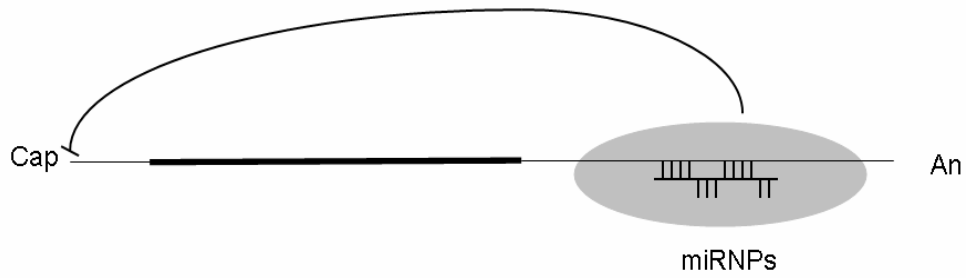
Figure 1.5 Modes of mRNA cleavage by miRNA. A: In plants B: In metazoans (Filipowicz *et al.*, 2008).

1.2.3.2 Mechanism: translational repression

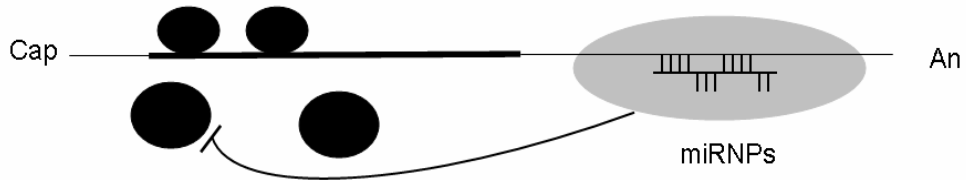
In animals, miRNAs regulate gene expression by imperfect base pairing with the 3'-untranslated region (3'UTR) of target mRNAs, and repressing protein synthesis. According to the published studies, miRNAs can repress protein expression in all steps of mRNA translation, namely by inhibition of translational initiation, by inhibition of translational elongation, by premature termination of translation (like ribosome drop-off) or by proteolysis (degradation of nascent peptide) (Figure 1.6; Eulalio *et al.*, 2008; Filipowicz *et al.*, 2008). The key components of miRNPs are proteins of the Argonaute (AGO) family. Kiriakidou *et al.* (2007) reported an unexpected observation, the central domain of Argonaute proteins exhibits sequence similarities to the cytoplasmic cap-binding protein eIF4E (eukaryotic translation initiation factor 4E), which is essential for cap-dependent translation initiation. MiRNAs inhibit translation at cap-recognition step by displacing eIF4E from the cap structure (Figure 1.6A; Kiriakidou *et al.*, 2007). Chendrimada *et al.* (2007) showed that human Argonaute 2 (AGO2) associates with both eukaryotic translation initiation factor 6 (eIF6) and large ribosomal subunit in human cells. EIF6 prevents the large ribosomal subunit from binding to the small ribosomal subunit. Therefore, if AGO2 recruits eIF6, then the large and small ribosomal subunits might not be associated, leading to translational repression (Figure 1.6B; Chendrimada *et al.*, 2007). Studies by Petersen *et al.* have identified that repression by miRNA mimics increased rate of termination at the stop codon, leading the authors to propose that miRNAs promote premature termination and ribosome drop-off (Figure 1.6C; Petersen *et al.*, 2006). The paradoxical observation that the targets of mRNAs appear to be actively translated while the corresponding protein product remains undetectable prompted the proposal that the nascent polypeptide chain might be degraded (Figure 1.6D; Nottrott *et al.*, 2006). However, this proposal is based on negative rather than direct positive evidence. In summary, translational repression by miRNAs probably occurs via multiple mechanisms in all different steps of mRNA translation.

Introduction

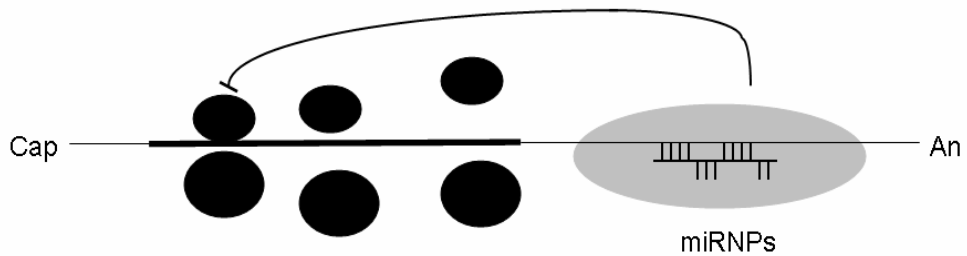
A: Inhibition of translational initiation (competition for the cap structure)



B: Inhibition of ribosomal subunit joining



C: Premature termination of translation (like ribosome drop-off)



D: Proteolysis (degradation of nascent peptide)

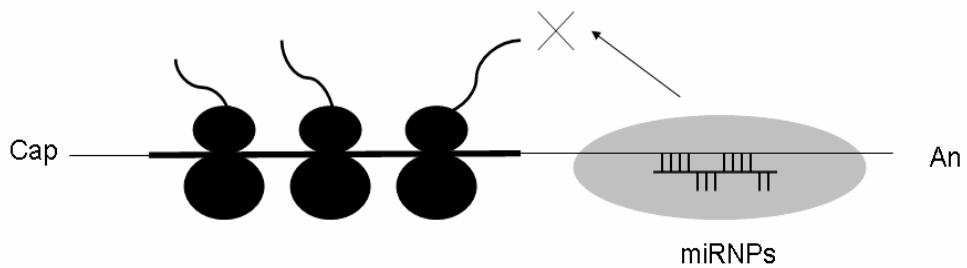


Figure 1.6 Possible mechanisms of the miRNA-mediated translational repression in animals.
(Eulatio *et al.*, 2008; Filipowicz *et al.*, 2008).

1.2.4 MiRNAs and diseases

MiRNAs have been implicated in a wide diversity of basic cellular functions, such as insulin secretion (Poy *et al.*, 2004), cardiac regulation (Care *et al.*, 2007), organ development (Schratt *et al.*, 2006), immune response (Li *et al.*, 2007), and muscle differentiation (Chen *et al.*, 2006). Therefore, mutation of miRNAs, dysfunction of miRNAs biogenesis and dysregulation of miRNAs and their targets may result in various diseases. Currently, approximately 150 different diseases including obesity and type 2 diabetes which are associated with miRNAs have been reported (Esau *et al.*, 2004; He *et al.*, 2007; Herrera *et al.*, 2009; Herrera *et al.*, 2010; Lovis *et al.*, 2008; Takanabe *et al.*, 2008). In 2008, Lu *et al.* performed a comprehensive analysis of the literature on human microRNA-disease associations and built the human microRNA disease database (HMDD) (Lu *et al.*, 2008; see database <http://cmbi.bjmu.edu.cn/hmdd>). Recently, it has been reported that miRNAs are used for rapid and accurate diagnosis of cancers (Martens-Uzunova *et al.*, 2011) and as novel epigenetic biomarkers for human cancers (Cortes-Sempere *et al.*, 2011). Moreover, miRNAs are special because they are stable, tissue-specific, and dysregulated in the diseased organs and cancers. These characteristics make them potential biomarkers in prognostic and predictive purposes (Lin *et al.*, 2011).

1.2.4.1 MiRNAs and obesity

Obesity is characterized by increased fat mass and energy storage in adipose tissues (Lean *et al.*, 1998). Fat mass can be grown by increasing in the size of adipocytes, or expanding the numbers of adipocytes (Rosen and MacDougald, 2006). Recently, evidences of miRNA dysregulation have been reported in human obesity (Martinelli *et al.*, 2010). Several miRNA profiling studies have identified miRNAs associated with obesity in adipose tissues from obese mouse models and obese people (Klötting *et al.*, 2009; Xie *et al.*, 2009; Martinelli *et al.*, 2010; Ortega *et al.*, 2010). The findings of these studies are summarized in Table 1.4. Two miRNAs, miR-21 and miR-143, were profiled in subcutaneous adipose tissues from healthy humans with varying degrees of obesity. MiR-21 showed higher expression in persons with a BMI >30, while miR-143 showed lower expression in human adipose tissue with BMI >30 (Keller *et al.*, 2011). In the ob/ob mouse, which develops obesity and type 2 diabetes-like symptoms, expression of miR-21 is downregulated in liver suggesting that miR-21 may have different roles depending on the cell types (Keller *et al.*, 2011). Increased miR-143 expression in adipose tissue of obese mice is associated with parallel alterations in PPAR γ and aP24 which are markers of adipocyte differentiation (Takanabe *et al.*, 2008). MiR-27 gene family is

Introduction

downregulated during adipogenic differentiation (Lin *et al.*, 2009). Overexpression of miR-27 specifically inhibited adipocyte formation, without affecting myogenic differentiation (Lin *et al.*, 2009). Expression of miR-27 resulted in blockade of expression of PPAR γ and C/EBP α , the two master regulators of adipogenesis (Lin *et al.*, 2009; Table 1.4). The levels of miR-335 expression in liver and white adipose tissue were upregulated in murine models of obesity, including KKAY44 mice, leptin deficient ob/ob mice, leptin receptor deficient db/db mice (Nakanishi *et al.*, 2009). Increased miR-335 expression was associated with an elevated body, liver and white adipose tissue weight, and hepatic triglyceride and cholesterol (Nakanishi *et al.*, 2009). In 3T3-L1 adipocyte, the induction of miR-335 expression was accompanied by that of the adipogenic genes including PPAR γ and aP24 after induction of differentiation. These results indicated that miR-335 might be involved in the adipocyte differentiation and lipid accumulation (Nakanishi *et al.*, 2009). Overexpression of miR-519d was reported to be associated with severe obesity in human subcutaneous adipose tissue (Martinelli *et al.*, 2010). MiR-519d has been identified to bind to the 3'UTR of PPAR α . The level of PPAR α mRNA was highly expressed in obese subjects, while PPAR α protein was undetectable compared to the controls (Martinelli *et al.*, 2010). It indicated that a post-transcriptional mechanism may be involved to downregulate PPAR α protein. Several studies have reported that miR-519d is differentially expressed in obesity or during adipogenic differentiation (Table 1.4).

Table 1.4 MiRNAs associated with adipogenesis and obesity

(<http://cmbi.bjmu.edu.cn/hmdd>; McGregor and Choi, 2011)

MiRNA	Species	Function	Targets	References
miR-15a	Mouse	Adipogenesis $\uparrow\downarrow$	DLK1	Kajimoto <i>et al.</i> , 2006; Andersen <i>et al.</i> , 2010
	Human	Adipose tissue \uparrow		Martinell <i>et al.</i> , 2010
miR-17/92	Mouse	Adipogenesis \uparrow	RB2; p130	Lin <i>et al.</i> , 2009
				Wang <i>et al.</i> , 2008
miR-21	Human/Mouse	Adipogenesis $\uparrow\downarrow$	TGFB2	Gerin <i>et al.</i> , 2010
				Kim <i>et al.</i> , 2009
				Sun <i>et al.</i> , 2009
miR-24	Mouse	Adipogenesis \uparrow		Sun F <i>et al.</i> , 2009
miR-27	Human/Mouse	Adipogenesis \downarrow	PPAR γ	Lin <i>et al.</i> , 2009
				Karbiener <i>et al.</i> , 2009
				Qin <i>et al.</i> , 2010

Introduction

	Human/Mouse	Adipose tissue ↓		Kim SY <i>et al.</i> , 2010 Lin <i>et al.</i> , 2009 Karbiener <i>et al.</i> , 2009
miR-31	Human/Mouse	Adipogenesis ↑↓	CEBPA	Gerin <i>et al.</i> , 2010 Sun <i>et al.</i> , 2009 Tang <i>et al.</i> , 2009 Ortega <i>et al.</i> , 2010
		Adipose tissue ↓		
miR-103	Human/Mouse	Adipogenesis ↑ ↓	PDK1	Esau <i>et al.</i> , 2004 Kajimoto <i>et al.</i> , 2006 Oskowitz <i>et al.</i> , 2008 Qin <i>et al.</i> , 2010 Sun <i>et al.</i> , 2009
	Mouse	Adipose tissue ↓	WNT3A	Xie <i>et al.</i> , 2009
miR-107	Human/Mouse	Adipogenesis ↑		Esau <i>et al.</i> , 2004 Oskowitz <i>et al.</i> , 2008 Gerin <i>et al.</i> , 2010 Qin <i>et al.</i> , 2010 Xie <i>et al.</i> , 2009
	Mouse	Adipose tissue ↓		
miR-125b	Human/Mouse	Adipogenesis ↑ ↓		Gerin <i>et al.</i> , 2010 Ortega <i>et al.</i> , 2010
	Human/Mouse	Adipose tissue ↑ ↓		Xie <i>et al.</i> , 2009 Ortega <i>et al.</i> , 2010
miR-132	Human	Adipose tissue ↑		Heneghan <i>et al.</i> , 2011
miR-138	Human	Adipogenesis ↓	EID1	Yang <i>et al.</i> , 2011
miR-143	Human/Mouse	Adipogenesis ↑	ERK5	Esau <i>et al.</i> , 2004 Kajimoto <i>et al.</i> , 2006 Sun <i>et al.</i> , 2009 Oskowitz <i>et al.</i> , 2008 Xie <i>et al.</i> , 2009 Takanabe <i>et al.</i> , 2008
	Human/Mouse	Adipose tissue ↑ ↓		
miR-150	Mouse	Adipogenesis ↓		Gerin <i>et al.</i> , 2010
	Human	Adipose tissue ↑		Martinell <i>et al.</i> , 2010
miR-200	Mouse	Adipogenesis ↑		Kennell <i>et al.</i> , 2008
miR-210	Mouse	Adipogenesis ↑	TCF7L2	Gerin <i>et al.</i> , 2010

				Qin <i>et al.</i> , 2010
				Sun <i>et al.</i> , 2009
	Human	Adipose tissue ↑		Ortega <i>et al.</i> , 2010
miR-221	Mouse	Adipogenesis ↓		Xie <i>et al.</i> , 2009
	Human/Mouse	Adipose tissue ↑		Ortega <i>et al.</i> , 2010
				Xie <i>et al.</i> , 2009
miR-222	Mouse	Adipogenesis ↓		Xie <i>et al.</i> , 2009
	Mouse	Adipose tissue ↑		Xie <i>et al.</i> , 2009
miR-326	Human	Adipose tissue ↑		Ortega <i>et al.</i> , 2010
miR-335	Human/Mouse	Adipogenesis ↑		Oskowitz <i>et al.</i> , 2008
				Nakanishi <i>et al.</i> , 2009
				Qin <i>et al.</i> , 2010
	Mouse	Adipose tissue ↑		Nakanishi <i>et al.</i> , 2009
miR-378	Mouse	Adipogenesis ↑		Gerin <i>et al.</i> , 2010
miR-448	Mouse	Adipogenesis ↓	KLF5	Kinoshita <i>et al.</i> , 2010
miR-519d	Human	Adipose tissue ↑	PPAR α	Martinell <i>et al.</i> , 2010

1.2.4.2 MiRNAs and type 2 diabetes

Type 2 diabetes is a progressive metabolic disorder characterized by reduced insulin sensitivity, insulin resistance in tissues such as adipose tissue, liver and skeletal muscle, and combined with pancreatic β -cell dysfunction. However, the major mechanisms underlying the pathogenesis of diabetes remain obscure. The various miRNAs have been identified as being potentially involved in type 2 diabetes, which are mainly expressed in adipose tissue, liver, skeletal muscle and pancreatic β -cells, shown in Table 1.5. MiR-24 is downregulated in the diabetic rat skeletal muscle and is shown to target directly p38 mitogen-activated protein kinase (MAPK) (Huang *et al.*, 2009). Based on microarray technology, miR-27b and miR-335 have been identified to contribute to fatty liver and associated pathologies. Furthermore, miR-27b expression is downregulated in the liver of type 2 diabetes rats (Herrera *et al.*, 2010). MiR-27b can bind to 3'UTR of PPAR γ mRNA and induce its degradation (Jennewein *et al.*, 2010; Table 1.5). The destabilization of PPAR γ in 3T3-L1 adipocytes by miR-27b blocks their differentiation into lipid-storing adipocytes (Karbiener *et al.*, 2009). As mentioned above, miR-335 is involved in lipid metabolism and upregulated not only in the liver of type 2 diabetes (Table 1.5), but also in the liver of obese mice (Nakanishi *et al.*, 2009). MiR-125a is

Introduction

up-regulated in the white adipose tissue of type 2 diabetes rats as well as in insulin-resistant 3T3-L1 adipocytes (Ling *et al.*, 2009; Table 1.5). *In vivo* or *in vitro*, although none of the miR-125a target has been identified, bioinformatics analysis revealed that several predicted target mRNAs were involved in glucose metabolism (Herrera *et al.*, 2009). MiR-375 is essential for pancreatic β -cell development and function. MiR-375 knock-out mice show a lowered pancreatic α - and β -cell mass and reduced insulin secretion (Poy *et al.*, 2009). The level of miR-375 in pancreatic islets has been found to be decreased in diabetic rats as well as in obese mice (Zhao *et al.*, 2009), suggesting that miR-375 down-regulation plays a major role in the pathogenesis of type 2 diabetes in islet (El Ouaamari *et al.*, 2008).

Table 1.5 The involvement of miRNAs in type 2 diabetes

(<http://cmbi.bjmu.edu.cn/hmdd>; Ferland-McCollough *et al.*, 2010)

MiRNA	Species	Tissue/Cell	Expression	References
miR-15a	Human	Skeletal muscle	down	Gallagher <i>et al.</i> , 2010
	Human	Plasma	down	Zampetaki <i>et al.</i> , 2010
miR-15b	Human	Skeletal muscle	up	Gallagher <i>et al.</i> , 2010
miR-21	Rat	Adipose tissue	up	Herrera <i>et al.</i> , 2010
miR-24	Rat	Skeletal muscle	down	Huang <i>et al.</i> , 2009
miR-27b	Rat	Liver	down	Herrera <i>et al.</i> , 2010
miR-29a	Rat	Adipose tissue	up	Karolina <i>et al.</i> , 2011
miR-30a*	Human	Adipose tissue	down	Ortega <i>et al.</i> , 2010
miR-103	Rat	Liver	up	Herrera <i>et al.</i> , 2010
	Mouse	Liver	up	Trajkovski <i>et al.</i> , 2011
miR-107	Mouse	Liver	up	Trajkovski <i>et al.</i> , 2011
miR-125a	Rat	Adipose tissue	up	Ling <i>et al.</i> , 2009
				Herrera <i>et al.</i> , 2009
miR-126	Human	Plasma	down	Zampetaki <i>et al.</i> , 2010
miR-140*	Rat	Liver	up	Herrera <i>et al.</i> , 2010
miR-143	Human	Skeletal muscle	up	Gallagher <i>et al.</i> , 2010
miR-144	Rat	Pancreas	down	Karolina <i>et al.</i> , 2011
miR-146	Mouse	Pancreatic β -cell	up	Lovis <i>et al.</i> , 2008
miR-146a	Human	Peripheral blood mononuclear cell	down	Balasubramanyam M <i>et al.</i> , 2011
miR-150	Rat	Liver	up	Karolina <i>et al.</i> , 2011

Introduction

miR-182	Rat	Skeletal muscle	down	Karolina <i>et al.</i> , 2011
miR-190	Human	Skeletal muscle	up	Gallagher <i>et al.</i> , 2010
miR-191	Rat	Liver	up	Herrera <i>et al.</i> , 2010
	Human	Plasma	down	Zampetaki <i>et al.</i> , 2010
miR-197	Human	Plasma	down	Zampetaki <i>et al.</i> , 2010
miR-223	Rat	Liver	up	Herrera <i>et al.</i> , 2009
	Human	Plasma	down	Zampetaki <i>et al.</i> , 2010
miR-320a	Human	Plasma	down	Zampetaki <i>et al.</i> , 2010
miR-335	Rat	Liver	up	Herrera <i>et al.</i> , 2010
miR-375	Mouse	Pancreatic β -cell	down	EI Ouaamari <i>et al.</i> , 2008
miR-486	Human	Plasma	down	Zampetaki <i>et al.</i> , 2010

2 Aim of this study

11 β -Hydroxysteroid dehydrogenase type 1 (11 β -HSD1, gene name *HSD11B1*) is responsible for intracellular glucocorticoid activation and plays an important role in obesity and the associated metabolic syndrome. During the last ten years, 11 β -HSD1 has emerged as a major potential drug target in the prevention of obesity, type 2 diabetes and other symptoms of the metabolic syndrome. Regulation of *HSD11B1* expression is multifactorial and highly tissue-specific manner. Interestingly, increased 11 β -HSD1 levels in adipose tissue typically parallel unchanged or decreased 11 β -HSD1 levels in liver of obese patients, and the underlying tissue-specific mechanisms remain obscure.

The aim of the present study is to investigate the potential impact of miRNAs in *HSD11B1* expression.

- to identify potential miRNA candidates by bioinformatic miRNA prediction tools
- to perform functional analysis in human cell culture with interesting candidates
- to assess the mechanism of the miRNA-mediated suppression
- to investigate promoter and miRNAs in regulation of *HSD11B1* expression
- to explore alternative promoter usages by induction with regulatory factors
- to detect potential miRNAs that are present in human liver cells
- to evaluate potential miRNAs expression in hepatocytes of normal, overweight and obese people
- to analyze potential miRNAs that are involved in regulation of *HSD11B1* expression in obesity, type 2 diabetes or other symptoms of the metabolic syndrome

3 Materials and Methods

3.1 Materials

3.1.1 Chemicals

β-mercaptoethanol	BIOMOL, Germany
Acetic acid	Carl Roth GmbH, Karlsruhe, Germany
Adiponectin	Alexis Biochemicals, United States
Agarose	Carl Roth GmbH, Karlsruhe, Germany
Ammonium persulfate (APS)	SERVA, Germany
Ampicillin	AppliChem, Germany
Blocking reagent	Carl Roth GmbH, Karlsruhe, Germany
Bovine serum albumin (BSA)	Behringwerke AG, Germany
Bradford reagent	Sigma-Aldrich Chemie GmbH, Germany
Bromophenol blue	Sigma-Aldrich Chemie GmbH, Germany
Chloroform	Carl Roth GmbH, Karlsruhe, Germany
Ciglitazone	Enzo Life Sciences, Germany
Cortisol	Sigma-Aldrich Chemie GmbH, Germany
dNTPs	Fermentas GmbH, Germany
Dexamethasone	Sigma-Aldrich Chemie GmbH, Germany
EDTA	Sigma-Aldrich Chemie GmbH, Germany
Estradiol	Sigma-Aldrich Chemie GmbH, Germany
Ethanol	Carl Roth GmbH, Karlsruhe, Germany
Ethidium bromide	Sigma-Aldrich Chemie GmbH, Germany
Formaldehyde	Merck KGaA, Germany
Formamide	Sigma-Aldrich Chemie GmbH, Germany
Gel 40	Carl Roth GmbH, Karlsruhe, Germany
GelRed	Biotium, Inc., Germany
Glycerin	Merck KGaA, Germany
Glycine	Carl Roth GmbH, Karlsruhe, Germany
Hydrochloric acid (HCl)	Carl Roth GmbH, Karlsruhe, Germany
Insulin	Sigma-Aldrich Chemie GmbH, Germany
Isopropanol	Merck KGaA, Germany
Kanamycin	CALBIOCHEM, Germany
KAc	Merck KGaA, Germany
KCl	Merck KGaA, Germany

Materials and Methods

KH ₂ PO ₄	Merck KGaA, Germany
Leptin	Enzo Life Sciences, Germany
Loading dye solution 6×	Fermentas GmbH, Germany
Maleic acid	Merck KGaA, Germany
Methanol	Merck KGaA, Germany
MgCl ₂ (25mM)	Fermentas GmbH, Germany
Milk powder Blotting grade	Carl Roth GmbH, Karlsruhe, Germany
MOPS	Sigma-Aldrich Chemie GmbH, Germany
NaCl	Merck KGaA, Germany
NaOH	Merck KGaA, Germany
Na ₂ HPO ₄	Merck KGaA, Germany
N-lauroylsarcosine	Merck KGaA, Germany
NuPage MES SDS Transfer buffer 10×	Invitrogen Co., Germany
NuPage Running buffer 20×	Invitrogen Co., Germany
Oligo (dT) 15 primer	Promega GmbH, Germany
Oligo (dT) 18 primer	Fermentas GmbH, Germany
Phenol	Carl Roth GmbH, Karlsruhe, Germany
Protease Inhibitor Cocktail Tablet	Roche GmbH, Germany
Reducing Agent	Invitrogen Co., Germany
Resistin	Alexis Biochemicals, United States
Retinoic acid	Sigma-Aldrich Chemie GmbH, Germany
RNase A	Carl Roth GmbH, Karlsruhe, Germany
Salmon sperm DNA	Invitrogen Co., Germany
Sodium dodecyl sulfate (SDS)	Carl Roth GmbH, Karlsruhe, Germany
Sodium acetate	Sigma-Aldrich Chemie GmbH, Germany
Sodium citrate	Sigma-Aldrich Chemie GmbH, Germany
Sucrose	Sigma-Aldrich Chemie GmbH, Germany
T4 Polynucleotide Kinase buffer	BioLabs, Frankfurt, Germany
TEMED	Sigma-Aldrich Chemie GmbH, Germany
TNF α	Enzo Life Sciences, Germany
Trichostatin A	Enzo Life Sciences, Germany
Tris base	Merck KGaA, Germany
Tween-20	Sigma-Aldrich Chemie GmbH, Germany
Vitamin D ₃	Sigma-Aldrich Chemie GmbH, Germany

WY14643	Sigma-Aldrich Chemie GmbH, Germany
Xylene cyanol	Sigma-Aldrich Chemie GmbH, Germany

3.1.2 Enzymes

Restriction enzymes, *Taq*-polymerase, Revert Aid M-MuLV Reverse Transcriptase, T4-DNA Ligase, and Shrimp Alkaline Phosphatase (SAP) were obtained from Fermentas (St. Leon-Rot, Germany). Phire Hotstart DNA polymerase was from Finnzymes (Keilaranta, Finland). T4 Polynucleotide Kinase was purchased from BioLabs (Frankfurt, Germany).

3.1.3 Molecular weight markers

For DNA analysis, GeneRuler™ 1 kb DNA ladder (250-10000 bp) and GeneRuler™ 100 bp plus DNA ladder (100-3000 bp) were used. For protein analysis, PageRuler™ prestained protein ladder (10-170 kDa) was used. All molecular weight markers were obtained from Fermentas (St. Leon-Rot, Germany).

3.1.4 Kits

All kits used are listed in the table 3.1 below including their applications and suppliers.

Table 3.1 List of all kits used in this work

Kit name	Application	Supplier
QIAGEN Plasmid Midi Kit	Plamid midi preparation	QIAGEN, Hilden, Germany
QIAEX II Gel Extraction Kit	Purification of DNA fragments from gels	QIAGEN, Hilden, Germany
TOPO TA Cloning Kits	PCR fragments Cloning	Invitrogen GmbH, Karlsruhe, Germany
Master Pure RNA Purification Kit	RNA preparation	Epicentre Biotechnologies, Madison, USA
Amersham ECL and Amersham ECL Advance Western Blotting Detection Reagents	Western Blotting Detection	GE Healthcare, Munich, Germany
Lipofectamine™ 2000	Transfection Reagent (Mammalian cells)	Invitrogen GmbH, Darmstadt, Germany
Dual-Glo™ Luciferase	Measuring firefly and <i>Renilla</i>	Promega, Mannheim,

Materials and Methods

Assay System	luciferase activities	Germany
TaqMan [®] MicroRNA Assays	miRNA-specific primers for RT-PCR	Applied Biosystems, Darmstadt, Germany
TaqMan [®] MicroRNA Reverse Transcription Kit	Reverse transcription	Applied Biosystems, Darmstadt, Germany
TaqMan [®] Universal PCR Master Mix II, with UNG	Polymerase Chain Reaction	Applied Biosystems, Darmstadt, Germany
Bis-Tris Gel: NuPAGE Novex 4-12% Bis-Tris Gel 1.0 mm, 10 well	Protein analysis	Invitrogen GmbH, Darmstadt, Germany
Cortisol Assay	Cortisol measurement	R&D, Administration and Europe Office, Cisbio Bioassay, France

3.1.5 Plasmids

pCR2.1-TOPO Cloning of *Taq* polymerase-amplified PCR products; ampicillin/kanamycin resistance (Invitrogen GmbH, Karlsruhe, Germany); plasmid map in Appendix 7.1.1

pmir-GLO pmir-GLO Dual-luciferase miRNA target expression vector, mammalian expression vector for transient transfection; ampicillin-resistance (Promega, Mannheim, Germany); plasmid map in Appendix 7.1.2

3.1.6 MicroRNAs

All microRNA precursors were purchased from Applied Biosystems/Ambion (Darmstadt, Germany). All microRNAs used are listed in Table 3.2.

Table 3.2 List of all miRNA precursors used in this work. Also two negative control precursors (Negative control miRNA#1 and #2) were purchased. Their sequences are not disclosed by the manufacturer, but they are supposed not to bind to any mRNA.

MiRNA name	Sequence of the mature miRNA
hsa-miR-561	5'-CAAAGUUUAAGAUCUUGAAGU-3'
hsa-miR-579	5'-UUCAUUUGGUUAUAAACCGCGAUU-3'
hsa-miR-340	5'-UUAUAAAGCAAUGAGACUGAUU-3'
hsa-miR-181b	5'-AACAUUCAUUGCUGUCGGUGGGU-3'
Negative control#1	
Negative control#2	

3.1.7 Primers

All primers were purchased from Eurofins MWG Operon (Ebersberg, Germany) and are listed in Table 3.3. Forward primers are named fd, reverse primers are named re. Bold letters indicate restriction enzyme sites; Lowercases indicate mismatch mutations.

Table 3.3 List of all primers used in this work

Name	Type	Sequence
HSD11B1-3'UTR-fd	PCR forward primer	5'- CTCGAGG AACTCCCTGAGGGC TGGGCATGCTGAGGGATTTTG-3'
HSD11B1-3'UTR-re	PCR reverse primer	5'- GTCGACT AAGAAACAAATATT GAAAAATTTTCATTTGTACAG-3'
HSD11B1-3'UTR- 561-del-fd	Mutagenesis primer	5'-CAATATTAATTATAAATTCATAA CTGGTAGCTATAACT-3'
HSD11B1-3'UTR- 561-del-re	Mutagenesis primer	5'-CTACCAGTTATGAATTTATAAT TAATATTGTATTAATC-3'
HSD11B1-3'UTR- 561-mut-fd	Mutagenesis primer	5'-AAGGT CACATA tAgTcTATAAA TTCATAACTGGTAG-3'
HSD11B1-3'UTR- 561-mut-re	Mutagenesis primer	5'-TATGAATTTATA gAcTa TATGTGA CCTTTATTATAAT-3'
HSD11B1-3'UTR- 579-del-fd	Mutagenesis primer	5'- CTCGAGG AACTCCCTGAGGGCT GGGCATGCTGAGGGATTTTG-3'
HSD11B1-3'UTR- 579-del-re	Mutagenesis primer	5'- GTCGACT AAGAAACAAATATTG AAAAATTAAGAAACCATCCTG-3'
HSD11B1-3'UTR- 579-mut-fd	Mutagenesis primer	5'- CTCGAGG AACTCCCTGAGGGCT GGGCATGCTGAGGGATTTTG-3'

Materials and Methods

HSD11B1-3'UTR-579-mut-re	Mutagenesis primer	5'- GTCGACTAAGAAACAAATATTG AAAAATTTgAcTaGTACAGTTTA-3'
HSD11B1-3'UTR-340-del-fd	Mutagenesis primer	5'-CAATATTAATTATAAATTCATAA CTGGTAG-3'
HSD11B1-3'UTR-340-mut-fd	Mutagenesis primer	5'-GGTCACATAAACgTgAgAAATTC ATAACTGG-3'
HSD11B1-P1-fd	PCR forward primer	5'-CAGATTTGTTTCGAAATC TTGAGG-3'
HSD11B1-P2-fd	PCR forward primer	5'-CTGCCTGCTTAGGAGGTTGT-3'
HSD11B1-all-fd	PCR forward primer	5'-ACCAGAGATGCTCCAAGGAA-3'
HSD11B1-all-re	PCR reverse primer	5'-CAAGGCAGCTACAGTCAGGA-3'
GAPDH-fd	PCR forward primer	5'-TGGAAGGCTCATGACCACA-3'
GAPDH-re	PCR reverse primer	5'-TTCTAGACGGCAGGTCAGGT-3'
Firefly-fd	PCR forward primer	5'-CACCTTCGTGACTTCCCATT-3'
Firefly-re	PCR reverse primer	5'-CCTCACCTACCTCCTTGCTG-3'
Renilla-fd	PCR forward primer	5'-CCGAGTTCGTGAAGGTGAAG-3'
Renilla-re	PCR reverse primer	5'-ACAACGTCGAGCACAGCTGC-3'
P-deletion PGk-fd	PCR forward primer	5'- AGATCTCCCGGGAAGCTTGG CAATCCGGTA-3'
P-deletion PGk-re	PCR reverse primer	5'- CTCGAGGCTAGCGAGCTCGTT TAA-3'
HSD11B1-P1-fd	PCR forward primer (cloning)	5'- CCCGGGGCCAGAAAAATTAG GAG-3'
HSD11B1-P1-re	PCR reverse primer (cloning)	5'- CCCGGGAGATTCGAACAAA TCTG-3'
HSD11B1-P2-fd	PCR forward primer (cloning)	5'- CCCGGGGAGAACCAGC CATG TAAA-3'
HSD11B1-P2-re	PCR reverse primer (cloning)	5'- CCCGGGCCGACAGGGAGCTG GCCT-3'

3.1.8 Oligonucleotides

All oligonucleotides were purchased from Eurofins MWG Operon (Ebersberg, Germany). All oligonucleotides used are listed in Table 3.4.

Table 3.4 List of all oligonucleotides used in this work

Name	Sequence
DNA-579	5'-TTCATTTGGTATAAACCGCGATT-3'
AMO-579	5'-AATCGCGGTTTATACCAAATGAA-3'
DNA-561	5'-CAAAGTTTAAGATCCTTGAAGT-3'
AMO-561	5'-ACTTCAAGGATCTTAAACTTTG-3'

3.1.9 Cell lines

A549 cells (passages 3-9)
(human lung adenocarcinoma cell line) DSMZ-Deutsche Sammlung von Mikroorganismen und Zellkulturen GmbH, Germany

HepG2 (passages 19-21)
(human hepatoma cell line) CLS-Cell Line Service, Germany

3T3-L1 (passages 23-24)
(Mouse embryonic fibroblast
-adipose like cell line) Health Protection Agency's Culture Collection, Salisbury, UK

3.1.10 Cell culture media, solution and materials

Dulbecco's Modified Eagle Medium
(DMEM): high glucose PAA laboratories GmbH, Gölbe, Germany

Dulbecco's Modified Eagle Medium
(DMEM) Ham's F-12 PAA laboratories GmbH, Gölbe, Germany

Foetal bovine serum PAA laboratories GmbH, Gölbe, Germany

OPTI-MEM I Reduced Serum Medium
modification of MEM (Eagle's) Invitrogen GmbH, Karlsruhe, Germany

Trypsin/EDTA PAA laboratories GmbH, Gölbe, Germany

Penicillin/Streptomycin (100×) PAA laboratories GmbH, Gölbe, Germany

L-Glutamine 200 mM (100×) PAA laboratories GmbH, Gölbe, Germany

Materials and Methods

Cell culture materials were obtained from Sarstedt AG & Co (Nümbrecht, Germany).

3.1.11 Hepatocyte Total RNAs

Human Hepatocyte Total RNA, BMI 14.9	BioCat GmbH, Heidelberg, Germany
Human Hepatocyte Total RNA, BMI 29.9	BioCat GmbH, Heidelberg, Germany
Human Hepatocyte Total RNA, BMI 35.4	BioCat GmbH, Heidelberg, Germany

3.1.12 Frozen Hepatocytes

Human Hepatocyte, BMI 23.5	BioCat GmbH, Heidelberg, Germany
Human Hepatocyte, BMI 23.8	BioCat GmbH, Heidelberg, Germany
Human Hepatocyte, BMI 26.1	BioCat GmbH, Heidelberg, Germany
Human Hepatocyte, BMI 38	BioCat GmbH, Heidelberg, Germany
Human Hepatocyte, BMI 38.2	BioCat GmbH, Heidelberg, Germany

3.1.13 Antibodies

Primary Antibodies:

11 β -HSD1 antibody

(Raised in: Rabbit; Polyclonal antibody) Abcam GmbH, Cambridge, UK

β -Actin

(Raised in: Rabbit; Polyclonal antibody) Neomarkers Inc, Fremont, CA

Secondary antibody:

ECL peroxidase labelled anti-rabbit antibody GE Healthcare, Munich, Germany

3.1.14 Bacterial media

Standard I Nutrient Broth
(SIN) 25 g Standard I Nutrient Broth/liter,
autoclave (15 min at 121 °C)

Standard I Nutrient Broth plate 25 g Standard I Nutrient Broth/liter,
20 g agar, autoclave (15 min at 121 °C)

Media were autoclaved, and 100 mg/l ampicillin or 25 mg/l kanamycin was supplemented prior to use.

3.1.15 Radiochemical

ATP, [$\gamma^{32}\text{P}$]-3000Ci/mmol PerkinElmer, Rodgau, Germany

3.1.16 Buffers and solutions

DNA loading dye (6×) (Agarose gel)	0.1% bromophenol blue 0.1% xylene cyanol 10 mM EDTA 40% glycerol
TAE (50×)	242 g Tris base 57.1 ml Acetic Acid 100 ml 0.5 M EDTA Add deionized water to 1 liter and adjust pH to 8.0 using NaOH
TAE (1×) (Agarose gels)	20 ml TAE (50×) in 980 ml deionized water
SDS running buffer (SDS-PAGE)	25 mM Tris-HCl, pH 8.3 192 mM glycine 0.1% (w/v) SDS
15% Resolving gel (SDS-PAGE)	5.5 ml 40% gel (the molar ratio of acrylamide: bisacrylamide is 37.5: 1) 3.8 ml 1.5 M Tris-HCl (pH 8.8) 150 μl 10% SDS 150 μl 10% APS 6 μl TEMED 5.5 ml deionized water
5% Stacking gel (SDS-PAGE)	1.25 ml 40% gel (the molar ratio of acrylamide: bisacrylamide is 37.5: 1) 1.25 ml 1 M Tris-HCl (pH 6.8) 100 μl 10% SDS

Materials and Methods

	100 μ l 10% APS
	10 μ l TEMED
	2.3 ml deionized water
Protein loading buffer (5 \times) (SDS-PAGE)	10% (w/v) SDS 5% (w/v) β -mercaptoethanol 50% (w/v) glycerol 0.13% (w/v) bromophenol blue 312 mM Tris-HCl (pH 6.8)
Coomassie brilliant blue solution	0.1% (w/v) coomassie brilliant blue R250 40% (v/v) ethanol 10% (v/v) acetic acid
Destaining solution	40% (v/v) methanol 10% (v/v) acetic acid
P1 Buffer (Miniprep plasmid)	50 mM Tris-HCl, pH 8.0 10 mM EDTA 100 μ g/ml RNase A
P2 Buffer (Miniprep plasmid)	200 mM NaOH 1% SDS
P3 Buffer (Miniprep plasmid)	2.8 M KAc, pH 5.1
Cell lysis buffer	10 mM Tris-HCl pH 8.0 1 mM EDTA 0.1% (w/v) SDS
Homogenization buffer (Microsomal preparation)	20 mM Tris-HCl pH 7.4 0.25 M sucrose 1 mM EDTA

Materials and Methods

Protease-inhibitors	Resuspending 1 pill in 2 ml PBS results in a 25× stock solution (COMPLETE™ pills, Roche Mannheim, Germany).
Phosphate buffered saline (PBS 1×)	137 mM NaCl 2.7 mM KCl 4.3 mM Na ₂ HPO ₄ 1.47 mM KH ₂ PO ₄ pH 7.6
PBS-T	0.1% (v/v) Tween-20 in PBS
Blocking buffer (Western blot)	5% milk powder in PBS-T
Transfer buffer (Western blot)	25 mM Tris base 0.2 M glycine 20% methanol pH 8.5
Stripping buffer	100 mM glycine pH 2.5
RNA loading buffer (5×)	16 µl saturated aqueous bromophenol blue solution 80 µl 500 mM EDTA, pH 8.0 720 µl 37% (12.3M) formaldehyde 2 ml 100% glycerol 3.084 ml formamide 4 ml 10 × Formaldehyde agarose gel buffer
10 × Formaldehyde agarose gel buffer	200 mM MOPS

Materials and Methods

	50 mM sodium acetate 10 mM EDTA pH 7.0
SSC (20×)	175.3 g NaCl 88.2 g sodium citrate Add deionized water to 1 liter and adjust to pH 7.0
10% SDS solution	10 g SDS Dissolve in 100 ml deionized water
Blocking stock solution (Northern blot)	10% (w/v) Blocking reagent dissolve in 0.1 M Maleic acid 0.15 M NaCl pH 7.5
Prehybridization buffer (Northern blot)	5 × SSC 0.1% N-lauroylsarcosine 0.02% SDS 1% Blocking reagent 100 µg/ml Salmon sperm DNA
Hybridization buffer (Northern blot)	10 ml prehybridization buffer 150 µl γ - ³² P-labelled DNA probe
Washing solution I 2× SSC buffer, 0.1% SDS (Northern blot)	100 ml 20×SSC 10 ml 10% SDS solution Add deionized water to 1 liter
Washing solution II 0.2× SSC buffer, 0.1% SDS (Northern blot)	10 ml 20×SSC 10 ml 10% SDS solution Add deionized water to 1 liter

Materials and Methods

TE buffer 10 mM Tris-Cl, pH 7.5
1 mM EDTA

3.1.17 Equipments

Centrifuge Biofuge	Schnakenberg GmbH, Germany
GeneQuant II Photometer	Pharmacia Biotech, Germany
Gel iX Imager	Intas GmbH, Germany
Homogenizator	Corlora Messtechnik GmbH, Germany
Optima L90k Ultracentrifuge	Beckman Coulter, Germany
Scanner PowerLook III	Umax Digital, Germany
SDS-PAGE electrophoresis apparatus	Roche Diagnostics, Germany
T Profession Thermocycler	Biometra GmbH, Germany
T1 Thermocycler	Biometra GmbH, Germany
Tecan Photometer	Tecan Trading AG, Switzerland
Thermal Imaging System FTI-500	Pharmacia Biotech, Germany
XCell II Blot Module	Invitrogen Co., Germany

3.2 Methods

3.2.1 Molecular biology

3.2.1.1 Polymerase chain reaction (PCR)

To amplify DNA fragments for cloning or detection, PCR was used. *Taq* polymerase was used for amplification of DNA fragments for subsequent cloning, while Phire Hotstart DNA polymerase was used for detection of specific DNA sequences. The following reaction mixture was used for the different applications:

Reaction mixture for a PCR with *Taq* polymerase

MgCl ₂ (25 mM)	10 µl
PCR buffer (10×)	5 µl
dNTPs (10 mM)	1 µl
Template	10-100 ng plasmid or 1 µl of cDNA
Forward primer	10 µM
Reverse primer	10 µM
<i>Taq</i> polymerase	1 U
ddH ₂ O	add to 50 µl

Reaction mixture for a PCR with Phire Hotstart DNA polymerase

Phire Reaction buffer (5×)	4 µl
dNTPs (10 mM)	0.4 µl
Forward primer	10 µM
Reverse primer	10 µM
cDNA template	2 µl
Phire Hotstart DNA polymerase	0.4 U
ddH ₂ O	add to 20 µl

The PCR was performed with the following step gradient:

95 °C	3 min		initial denaturation step
95 °C	30 sec	} × 30-40	denaturation
45 °C	30 sec		annealing
72 °C	30 sec		elongation (1 min/1kb)
72 °C	10 min		final elongation step

Materials and Methods

4 °C		hold	
(<i>Taq</i> polymerase)			
98 °C	30 sec	initial denaturation step	
98 °C	10 sec	denaturation	
60 °C	15 sec	} × 30-40	annealing
72 °C	15 sec		elongation (20 sec/1kb)
72 °C	1 min	final elongation step	
4 °C		hold	
(Phire Hotstart DNA polymerase)			

3.2.1.2 Reverse transcription polymerase chain reaction (RT-PCR)

RT-PCR is a PCR amplification of a product from the reverse transcription (RT) reaction, where all messenger RNAs (mRNAs) are reverse transcribed into single-stranded complementary DNA (cDNA). This is followed by a PCR reaction for amplification of a specific cDNA using Phire Hotstart DNA polymerase as specified above. Reverse transcriptase was used according to the manufacturer's instructions. Reverse transcription was performed using oligo (dT) primer targeting the 3' poly (A) mRNA tail. The following RT reaction mixture was used:

RevertAid™ buffer (5×)	6.9 µl
RNA	2 µg
dNTPs (10 mM)	3 µl
Oligo(dT) 15 primer	1 µl
RvertAid M-MuLV (Reverse Transcriptase)	1 µl
RNase inhibitor	1 µl
ddH ₂ O	add to 34.4 µl

The reaction mixture was incubated at 42 °C for 60 min and then the enzyme was inactivated at 70 °C for 10 min. 2 µl of the cDNA was used directly for the subsequent PCR or cDNA samples were stored at -80 °C until use.

3.2.1.3 DNA Gel-electrophoresis

DNA fragments were separated in horizontal electrophoresis chambers using agarose gels. Agarose gels were prepared by heating 0.8-2% (w/v) agarose in 1× TAE buffer, depending on

the size of the DNA fragments. The samples were mixed with an appropriate amount of 6 × DNA loading dye and loaded on the agarose gel. The gels were run at constant current (100 mA). The gels were stained in ethidium bromide (EB) solution (5 min, room temperature) with constant agitation. The gels were then placed in water for 5 min. Finally, the gels were documented using the Gel UV-light documentation system. For semi-quantitative RT-PCR, gel electrophoresis of PCR samples was performed using 1% agarose gels. 0.5 g of agarose was suspended in 50 ml of 1× TAE buffer and melted in a microwave. After cooling to approximately 50 °C, 5 µl of GelRed was added and the solution was poured into a casting tray. After half an hour the gel was solidified and then submerged into 1× TAE running buffer. The 20 µl of PCR sample was mixed with 6× DNA loading dye and loaded on the agarose gel. DNA fragments were separated at 100 V for 40 min. The DNA fragments were visualized under UV-light (Gel iX Imager).

3.2.1.4 Digestion of plasmid

The plasmid was incubated with an appropriate amount of restriction enzymes in the recommended buffer in a final volume of 20 µl in a 1.5 ml Eppendorf tube for 1-2 hours at 37 °C. The digestion was terminated by heating 80 °C for 20 min. Then, the tube was placed on ice for 5 min. Finally, the digested DNA was applied to an agarose gel.

3.2.1.5 Dephosphorylation of plasmid DNA

After digestion, the plasmid DNA was dephosphorylated by direct addition 1 U of Shrimp Alkaline Phosphatase (SAP) and 4 µl of SAP buffer (Fermentas, St. Leon-Rot, Germany) to the restriction reaction in a final volume of 60 µl. The dephosphorylation was carried out at 37 °C for 15-20 min.

3.2.1.6 Extraction of DNA fragments

For isolation and purification of DNA fragments from agarose gels, ethidium bromide stained gels were illuminated with UV-light and the appropriate DNA band was excised from the gel with a clean scalpel and transferred into an Eppendorf tube. The fragment was mostly isolated using QIAEX II Gel Extraction Kit (QIAGEN, Hilden, Germany) following the manufacturer's instructions. In some cases, isolation and purification of DNA fragments were used by phenol/chloroform: After digestion of DNA, ddH₂O was added up to 200 µl, followed by 100 µl of phenol. The reaction mixture was shaken and incubated at room temperature for 5 min, followed by centrifugation at 13,000 rpm for 5 min. Then, the upper phase was

Materials and Methods

transferred to a new tube, 100 μ l of chloroform was added and after vortexing, the mixture was again centrifuged at 13,000 rpm for 1 min (twice). The upper phase was transferred to a new tube and two volumes of 100% ethanol and 1/20 volume of 5 M NaCl were added, followed by centrifugation at 13,000 rpm for 10 min. The DNA pellet was washed with 200 μ l of 70% ethanol, and then centrifuged at 13,000 rpm for 10 min. Finally, the pellet was dried at room temperature for 5 min and dissolved in 10 μ l ddH₂O.

3.2.1.7 Ligation of DNA fragment

Ligation of DNA fragment was performed by mixing 10-100 ng of plasmid DNA with the insert DNA. The reaction mixture was supplemented with 1 U of T4-DNA Ligase (Fermentas, St. Leon-Rot, Germany), 1 μ l of ligation buffer (10 \times) and filled up to a final volume of 10 μ l ddH₂O. The reaction was incubated at room temperature for 1-2 hours or at 4 °C overnight, which was used directly for transformation in competent *E.coli* bacteria.

3.2.1.8 Transformation of bacteria

To 100 μ l of competent *E.coli* HB101 either 50-100 ng of plasmid DNA or 10 μ l of ligation mixture were added and incubated for 30 min on ice. After a heat shock at 42 °C for 90 sec and successive incubation on ice for 5 min, 400 μ l of SIN medium was added to the bacteria and the bacterial suspension was shaken at 37 °C and 110 rpm for 60 min. After that, bacteria were spreaded on SIN-agar plates containing the appropriate antibiotics. Plates were incubated at 37 °C overnight.

3.2.1.9 Plasmid isolation from 1 ml of bacterial cultures (Minipreps)

A single colony was inoculated into 0.5-1 ml of SIN medium supplemented with the appropriate antibiotic and incubated at 37 °C with constant agitation for 5 hours. Bacterial cultures were pelleted by centrifugation (13,000 rpm, 20 sec.) and the bacterial pellet was resuspended in 50 μ l of P1 buffer. For bacterial lysis, 50 μ l of P2 buffer was added to the suspension which was then mixed thoroughly by vigorously inverting 4-6 times and incubated at room temperature for 5 min. Then, 50 μ l of P3 buffer was added and the mixture was inverted until a homogenous suspension containing a white flocculate was formed. The bacterial lysate was cleared by centrifugation (13,000 rpm, 10 min) and the supernatant was transferred to a new eppendorf tube and two times the supernatant volume of 100% ethanol was added. The plasmid DNA was precipitated by centrifugation (13,000 rpm, 10 min).

Finally, the pellet was dried at room temperature for 5 min and dissolved in 10 μ l of TE buffer.

3.2.1.10 Plasmid isolation from 50 ml of bacterial cultures (Midipreps)

For preparation of large quantities of high- or low-copy plasmid DNA, the QIAGEN Plasmid MIDI Kit was used. First, the bacterial cells were harvested by centrifugation at $6000\times g$ for 10 min at 4 °C. The bacterial pellet was resuspended in 4 ml of P1 buffer, then 4 ml of P2 buffer was added, and the suspension was thoroughly mixed by vigorously inverting the sealed tube 4-6 times and incubated at room temperature for 5 min. 4 ml of chilled P3 buffer was added, and the suspension was thoroughly mixed by vigorously inverting 4-6 times and incubated on ice for 15 min, followed by centrifugation at $13,000\times g$ for 10 min at 4 °C. The QIAGEN-tip was equilibrated by applying 3 ml of QBT buffer, and the column was allowed to empty by gravity flow. The supernatant was applied from last centrifugation to the QIAGEN-tip with filter paper and allowed to enter the resin by gravity flow. The QIAGEN-tip was washed with 2×10 ml of wash buffer. The DNA was eluted with 5 ml of elution buffer and precipitated by adding 5 ml of room temperature isopropanol to the eluted DNA, followed by centrifugation immediately at $13,000\times g$ for 10 min at 4 °C. The supernatant was carefully decanted. The DNA pellet was washed with 2 ml of room temperature 70% ethanol, followed by centrifugation at $13,000\times g$ for 5 min. The supernatant was carefully decanted without disturbing the pellet. The pellet was dried for 5-10 min. Finally, the plasmid pellet was dissolved in 500 μ l of TE buffer and the plasmid concentration was determined by UV-spectrophotometry.

3.2.1.11 DNA sequencing

DNA sequencing was performed by the company Eurofins MWG Operon (Ebersberg, Germany). For sequencing 0.7 μ g of plasmid DNA was diluted in 15 μ l of TE buffer.

3.2.1.12 Isolation of genomic DNA from A549 cells

A549 cells were harvested from the flask surface by mechanical scraping with cell scraper. After that, A549 cells were resuspended in 1 ml of cell lysis buffer and transferred into a new tube. Isolation of genomic DNA was used by phenol/chloroform: The suspension was added 1 ml of phenol and mixed by vortexing for 1 min. Then the suspension was incubated at room temperature for 5 min, followed by centrifugation at 13,000 rpm for 5 min. Then, the upper phase was transferred to a new tube, 1 ml of chloroform was added and after vortexing, the

Materials and Methods

mixture was again centrifuged at 13,000 rpm for 1 min (twice). The upper phase was transferred to a new tube and two volumes of 100% ethanol were added, followed by centrifugation at 13,000 rpm for 10 min. The DNA pellet was washed with 2 ml of 70% ethanol, and then centrifuged at 13,000 rpm for 5 min. Finally, the pellet was dried at room temperature for 5 min and dissolved in 500 µl of TE buffer.

3.2.1.13 Determination of DNA or RNA concentration

DNA or RNA concentration was determined using GeneQuant II Photometer (Pharmacia, Germany). The DNA or RNA samples were normally diluted in ratio of 1: 10, 10 µl of sample was used for every determination.

3.2.1.14 RNA Isolation

The cells were harvested from the flask surface by mechanical scraping with cell scraper. After that, total RNA was isolated from the A549 or HepG2 cells using the Master Pure RNA Purification Kit according to the manufacturer's instructions. RNA concentration was determined by UV-spectrophotometry. 2 µg of isolated total RNA was used as template for RT-PCR reaction, as described in 3.2.1.2.

3.2.1.15 Northern blot

3.2.1.15.1 Preparation of RNA samples

First, the HepG2 cells were harvested from the flask surface by mechanical scraping with cell scraper. After that, total RNA was isolated from HepG2 cells with RNA Purification Kit according to the manufacturer's instructions. The human hepatocyte total RNA samples were obtained from BioCat GmbH (Heidelberg, Germany).

3.2.1.15.2 RNA electrophoresis

Total RNA was separated by electrophoresis under denaturing conditions on a 2% agarose gel containing 2.2 M formaldehyde. 10 µg of RNA mixed with 6 µl of 5× RNA loading buffer was loaded. The gel was run in RNA electrophoresis buffer at 80 mA constant current.

3.2.1.15.3 Transfer and fixation of RNA to membrane

Capillary transfer of RNA from an agarose gel to nylon membrane (Amershen Biosciences, Germany) was carried out at neutral pH in 20× SSC buffer (pH 7.0) overnight. For fixation of

RNA to the membrane, the membrane was placed between two dry filter papers (Whatman, Germany) and baked at 100 °C for 1 hour.

3.2.1.15.4 Preparation of γ -³²P-labelled DNA probe

1 μ l of DNA oligonucleotide probe (100 pmol/ μ l), 2 μ l of 10 \times T4 Polynucleotide Kinase buffer, 1 μ l of γ -³²P-ATP, 1 μ l of T4 Polynucleotide Kinase, and 15 μ l of distilled water were mixed and incubated at 37 °C for 1 hour. The labelled DNA probe was extracted with phenol/chloroform and precipitated with ethanol. Finally, the labelled DNA probe was dissolved in 150 μ l of TE buffer.

3.2.1.15.5 Hybridization, washing and exposure to X-ray film

The membrane was put into a hybridization bottle and incubated in prehybridization buffer at 37 °C for 30 min under rotation. Hybridization buffer with labelled DNA probe was boiled at 95 °C for 10 min and chilled on ice for 10 min. The membrane was put into hybridization buffer and incubated at 37 °C overnight in the hybridization bottle under rotation. The membrane was washed twice with 2 \times SSC, 0.1% SDS for 5 min at room temperature and then washed twice with 0.2 \times SSC, 0.1% SDS for 15 min at 37 °C. The membrane was baked at 80 °C for 10 min, then wrapped in plastic and exposed to X-ray film.

3.2.2 Cell culture and cell-based assays

3.2.2.1 Cell cultivation

All human cells were cultured at 37 °C with 5% CO₂ in a 90% humidified atmosphere. A549 cells (human lung adenocarcinoma cell line) were usually grown in 75 cm² flasks or 96-well plates in DMEM High Glucose (4.5 g/l) Medium with L-Glutamine supplemented with 10% FBS and 1% penicillin/streptomycin. HepG2 cells (human hepatoma cell line) were normally grown in 75 cm² flasks or 96-well plates in DMEM Ham's F-12 Medium with L-Glutamine supplemented with 10% FBS and 1% penicillin/streptomycin. For maintenance, medium was refreshed at least three times weekly. Cells were passaged at around 90% confluency. Adherent cells were detached by 2 ml of trypsin/EDTA for 3 min at 37 °C. After centrifugation (1000 rpm, 5 min), the cell pellet was gently resuspended in fresh medium. The split ratio was 1: 5 – 1: 10.

3.2.2.2 Transfection of mammalian cells

3.2.2.2.1 Plasmid DNA Transfection

Materials and Methods

To transfect mammalian cells with plasmid DNA in a 96-well plate, one day before transfection, the cells were changed with 200 μ l of fresh growth medium without antibiotics so that cells will be 90-95% confluent at the time of transfection. For each transfection sample, complexes were prepared as follows: Plasmid DNA (10-50 ng) was diluted in 25 μ l of Opti-MEM I Reduced Serum Medium without serum. After gently mixing the transfection reagent (LipofectamineTM 2000) before use, 0.3-0.6 μ l (depending on different cell lines) of transfection reagent was diluted in 25 μ l of Opti-MEM I Reduced Serum Medium and incubated at room temperature for 5 min. After 5 min of incubation, the diluted DNA and the diluted transfection reagent were combined and incubated at room temperature for 20 min. Before addition of complexes, the growth medium was removed from the cells and the cells were covered with 100 μ l of fresh growth medium without antibiotics. Then, 50 μ l of complexes were added to each well. The plate was gently rocked back and forth and incubated at 37 °C in a CO₂ incubator for 48 hours.

3.2.2.2.2 MicroRNA Transfection

To transfect mammalian cells with microRNAs in a 6-well plate or 75 cm² flask, one day before transfection, the cells were changed with 3 ml or 22 ml (6-well plate, 75 cm² flask) of fresh growth medium without antibiotics so that cells will be 80-90% confluent at the time of transfection. For each transfection sample, complexes were prepared as follows: microRNA (150 pmol, 6-well plate; 600 pmol, 75 cm² flask) was diluted in 250 μ l or 1.5 ml (6-well plate, 75 cm² flask) of Opti-MEM I Reduced Serum Medium without serum. After gently mixing the transfection reagent (LipofectamineTM 2000) before use, 5 μ l or 35 μ l (6-well plate, 75 cm² flask) of transfection reagent was diluted in 250 μ l or 1.5 ml (6-well plate, 75 cm² flask) Opti-MEM I Reduced Serum Medium and incubated at room temperature for 5 min. After 5 min of incubation, the diluted microRNA and the diluted transfection reagent were combined and incubated at room temperature for 20 min. Before addition of complexes, the cells were changed with 2 ml or 19 ml (6-well plate, 75 cm² flask) of fresh growth medium without antibiotics. Then, complexes were added to cells. The plate or flask were gently rocked back and forth and incubated at 37 °C in a CO₂ incubator for 48 hours.

3.2.2.2.3 Cotransfection of mammalian cells with plasmid DNA and microRNA

To cotransfect mammalian cells with plasmid DNA and microRNA in a 96-well plate, one day before cotransfection, the cells were changed with 200 μ l of fresh growth medium without antibiotics such that cells will be 80-90% confluent at the time of transfection. For

Materials and Methods

each transfection sample, DNA-miRNA molecule-Lipofectamine™ 2000 complexes were prepared as follows. The DNA (10 ng) and miRNA (3 pmol) were diluted in 25 µl of Opti-MEM I Reduced Serum Medium without serum. The transfection reagent was diluted in 25 µl of Opti-MEM I Reduced Serum Medium without serum and incubated for 5 min at room temperature. After 5 min of incubation, the diluted DNA and miRNA molecule and the diluted transfection reagent were combined and incubated for 20 min at room temperature. Before addition of complexes, the growth medium was removed from the cells and the cells were covered with 100 µl of fresh growth medium without antibiotics. Then, 50 µl of complexes were added to each well. The plate was gently rocked back and forth and incubated at 37 °C in a CO₂ incubator for 48 hours.

3.2.2.2.4 Cotransfection of HepG2 cells with plasmid DNA and microRNA/AMOs

To cotransfect HepG2 cells with plasmid DNA and microRNA/AMOs in a 96-well plate, one day before cotransfection, the cells were changed with 200 µl of fresh growth medium without antibiotics such that cells will be 80-90% confluent at the time of transfection. For each transfection sample, DNA-microRNA/AMOs-Lipofectamine™ 2000 complexes were prepared as follows. The plasmid DNA (50 ng) and miRNA (3 pmol)/AMOs (15 pmol) were diluted in 25 µl of Opti-MEM I Reduced Serum Medium without serum. Then, the complexes were incubated at 70 °C for 3 min and cooled down around 30 °C. The transfection reagent was diluted in 25 µl of Opti-MEM I Reduced Serum Medium without serum and incubated for 5 min at room temperature. After 5 min of incubation, the diluted DNA and miRNA/AMOs and the diluted transfection reagent were combined and incubated for 20 min at room temperature. Before addition of complexes, the growth medium was removed from the cells and the cells were covered with 100 µl of fresh growth medium without antibiotics. Then, 50 µl of complexes were added to each well. The plate was gently rocked back and forth and incubated at 37 °C in a CO₂ incubator for 48 hours.

3.2.2.3 Luciferase reporter assay

After transfection of plasmid DNA or cotransfection of plasmid DNA and miRNA for 48 hours, a 96-well plate was removed from the incubator. The medium on the cells was removed and 75 µl of fresh growth medium was added to each well. For measuring firefly luciferase activity, 75 µl of Dual-Glo™ Luciferase Reagent was added to each well. The plate was gently rocked back and forth for 10 min. Then, the cell lysates were transferred to a 96-well white microplate (Greiner bio-one, BioScience, Germany). The firefly luminescence was

measured using GENios Pro microplate reader (Tecan GmbH, Crailsheim, Germany). For measuring *Renilla* luciferase activity, 75 µl of Dual-Glo™ Stop & Glo Reagent was added to each well and mixed gently. After 10 min, the *Renilla* luminescence was measured using GENios Pro microplate reader (Tecan GmbH, Crailsheim, Germany). *Renilla* luminescence should be measured in the same plate order as the firefly luminescence was measured using GENios Pro microplate reader (Tecan GmbH, Crailsheim, Germany).

3.2.2.4 Calculation of relative luciferase activity

After measurement of the firefly luciferase luminescence and *Renilla* luciferase luminescence, the ratio of luminescence from the experimental reporter (firefly luciferase) to luminescence from the control reporter (*Renilla* luciferase) was calculated as followed.

$$\text{Relative luciferase activity (\%)} = \text{RLU}_{\text{firefly}} / \text{RLU}_{\text{Renilla}} (\%)$$

3.2.2.5 Induction cells with regulatory factors

Cells were maintained and transfected as described above. One day before induction, the cells (96-well plate) were changed with 200 µl of fresh growth medium. The regulatory factor was diluted with fresh medium. After 4 hours of transfection, the resulting solution was directly added onto the cells. The plate was gently rocked back and forth and incubated at 37 °C in a CO₂ incubator for 48 hours.

3.2.3 Protein biochemical methods

3.2.3.1 Preparation of microsomes from human liver tissue (Maser *et al.*, 2002)

The homogenization buffer was supplemented with protease inhibitor solution before use. The complete procedure was performed on ice or at 4 °C. Human liver samples were obtained following routine surgical procedures and in accordance with German legislation. Samples were rinsed in an ice-cold isotonic solution of NaCl and homogenized in four volume of ice-cold homogenization buffer with a homogenizer (Corlora Messtechnik GmbH, Germany). The homogenate was centrifuged at 600× *g* for 10 min and 10,000× *g* for 10 min to sediment nuclei, cell debris, and mitochondria. The supernatant at this stage was centrifuged at 100,000× *g* for 1 h to sediment the microsomes. The microsomal pellet was resuspended and washed with 150 mM KCl to remove glycogen, then centrifuged at 100,000× *g* for 45 min. Finally, the pellet was resuspended in the homogenization buffer without protease inhibitor and stored at -80 °C.

3.2.3.2 Preparation of cell total protein

The cells were harvested from the flask surface by mechanical scraping with cell scraper and washed with PBS buffer and centrifuged at 1000 rpm for 5 min. The homogenization buffer was supplemented with protease inhibitor solution before use. The cell pellets were resuspended in 1 ml of ice-cold homogenization buffer. Then, cells were repeatedly frozen and thawed for 10 times. The cell lysates were centrifuged at 13,000× g for 30 min. The supernatant containing total protein was transferred to a new tube and stored at -80 °C.

3.2.3.3 Bradford assay for determination of protein concentration

The concentration of protein sample was determined using the Bradford protein assay. Five standard solutions of BSA with concentration ranging from 0.1 to 1.4 mg/ml were prepared to generate a standard curve using the corresponding sample buffer. Protein sample was diluted 1: 10 to get a concentration within the linear range of the standard protein. 5 µl of blank (buffer only), 5 µl of each standard solution and 5 µl of each sample were distributed in a 96-well plate. Each measurement was performed at least in duplicates. 250 µl of Bradford reagent was added to each well, followed by 5 min of incubation at room temperature. Finally, absorbance at 595 nm was measured with GENios Pro microplate reader (Tecan GmbH, Crailsheim, Germany).

3.2.3.4 SDS-polyacrylamid gel electrophoresis (SDS-PAGE)

Separation of protein was performed with a discontinuous SDS-PAGE using the Mini-Protean III system (Bio-Rad Laboratories GmbH, Munich, Germany). The resolving and stacking gels were prepared as described in 3.1.16. After complete polymerization of the gel, the chamber was assembled as described by the manufacturer's protocol. SDS running buffer was added. Protein sample was supplemented with protein loading buffer and heated at 95 °C for 5 min before loading to the gel. Up to 30 µl sample was loaded into the pockets and the gel was run at constant voltage at 80 V for 15 min and then at 140 V for the remainder. The gel run was stopped when the bromophenol blue line reached the end of the gel. After electrophoresis, the proteins were visualized by staining with Coomassie brilliant blue solution at room temperature for half an hour and destaining with destaining solution at room temperature for an hour.

3.2.3.5 NuPAGE and Western blotting

Materials and Methods

The proteins were separated with a NuPAGE Novex Bis-Tris Mini Gels (Invitrogen GmbH, Darmstadt, Germany) using XCell SureLock Mini-Gel (Invitrogen GmbH, Darmstadt, Germany) according to manufacturer's protocol. The proteins were transferred from the NuPAGE mini gel on a polyvinylidene difluoride (PVDF) membrane using the XCell II™ Blot Module (Invitrogen GmbH, Darmstadt, Germany). First the PVDF membrane was activated by methanol for 30 sec, and subsequently soaked with transfer buffer. Also the blotting pads and 2 pieces of Whatman filter papers were soaked with transfer buffer. The blotting sandwich was assembled according to manufacturer's instructions. Proteins were transferred at 30 V constant for 1 hour. Afterwards the membrane was blocked in 5% milk powder in PBS-T for 1 hour at room temperature or overnight at 4 °C. The membrane was rinsed shortly two times with PBS-T. The membrane was incubated with primary antibody at room temperature for 1 hour with constant agitation. The membrane was washed three times with PBS-T for 10 min and the appropriate secondary antibody was probed at room temperature for 1 hour with constant agitation. After three washing steps, the membrane was incubated with ECL and Amersham ECL Advance Western Blotting Detection Reagents (GE Healthcare, Munich, Germany) according to manufacturer's instructions. The membrane was exposed to X-ray film (GE Healthcare, Munich, Germany).

3.2.3.6 Stripping of membrane

After detection, the membrane was incubated in stripping buffer two times for 25 min. The membrane was washed 3× with PBS-T for 10 min. Then, the membrane was reactivated by dipping into methanol for 5 sec. After that, the membrane was washed 3× with PBS-T for 5 min and then redone by Western blot analysis from blocking procedure.

3.2.4 Web-based tools

3.2.4.1 Prediction of miRNAs and web-based tissue profiling

Four different miRNA target prediction tools were applied to search for microRNA response elements (MREs) in the 3'UTR of human *HSD11B1* mRNA, namely Diana micro-T-ANN (http://diana.cslab.ece.ntua.gr/microT_ANN/, Maragkakis *et al.*, 2009a; Maragkakis *et al.*, 2009b), TargetScan (<http://www.targetscan.org>, Lewis *et al.*, 2005; Liu *et al.*, 2003; Grimson *et al.*, 2007; Lewis *et al.*, 2003), microRNA (<http://www.microrna.org>, Betel *et al.*, 2008), and MicroCosm Targets (<http://www.ebi.ac.uk/enright-srv/microcosm/htdocs/targets/v5/>, Griffiths-Jones *et al.*, 2006; Griffiths-Jones *et al.*, 2008). Non-human miRNAs were removed from the results obtained by MicroCosm Targets. The miRNAs identified by at least three

prediction tools were pre-selected for web-based tissue profiling using the smiRNAdb miRNA expression atlas (www.mirz.unibas.ch, Landgraf *et al.*, 2007; Hausser *et al.*, 2009), choosing liver as target tissue including all subsamples, *e.g.* hepatoma samples and cell lines. The smiRNAdb miRNA expression atlas is based on relative cloning frequencies which represents a measure of miRNA expression (Landgraf *et al.*, 2007). The relative cloning frequencies are expressed as log₂ values, *i.e.* a value of *e.g.* -2 signifies a relative cloning frequency of $2^{-2} \times 100\% = 25\%$.

3.2.4.2 Pathway Enrichment Analysis using DIANA mirPATH

Two miRNAs, hsa-miR-561 and hsa-miR-579 were subjected to a pathway enrichment analysis by DIANA-mirPATH (<http://diana.cslab.ece.ntua.gr/pathways/>, Papadopoulos *et al.*, 2009), using the online tool for multiple miRNAs analysis and the beta-version of the prediction software DIANA-microT-4.0. The enrichment analysis compares the set of predicted target genes for each miRNA with all biological pathways in the Kyoto Encyclopedia of Genes and Genomes (KEGG) database (Papadopoulos *et al.*, 2009; Kanehisa *et al.*, 2000). Results are ranked by negative natural logarithm of the p-value. P-values < 0.01 and < 0.05 correspond to $-\ln(\text{p-value}) > 4.6$ and > 3.0 , respectively.

3.2.5 Statistical analysis

Data are expressed as average \pm SD (standard deviation). Statistical analysis was performed by using a Student's *t* test. A p-value below 0.05 was considered statistically significant (* P < 0.05; ** P < 0.01; *** P < 0.001).

4 Results

4.1 miRNA prediction

To investigate the potential impact of miRNAs in *HSD11B1* expression, four different miRNA target prediction tools were applied to predict miRNA response elements (MREs) in the 3'UTR of human *HSD11B1* mRNA, yielding four different lists of miRNAs (Table 4.1). Diana microT suggested in total four miRNAs while the other three prediction tools proposed considerably more miRNAs, namely 50 (TargetScan), 46 (microRNA), 57 (MicroCosm Targets). Two miRNAs (hsa-miR-561 and hsa-miR-579) were predicted by all four different tools and thus directly selected for functional analysis. Twenty additional miRNAs were predicted by three of four tools (Table 4.1). Subjecting all twenty-two miRNA candidates to web-based tissue profiling using the smiRNadb miRNA expression atlas (www.mirz.unibas.ch, Hausser *et al.*, 2009; Landgraf *et al.*, 2007) revealed that at least five miRNAs are expressed in hepatocytes including the above mentioned hsa-miR-579, but also hsa-miR-142-5p, hsa-miR-181a, hsa-miR-181b, and hsa-miR-340 (Figure 4.1). From the latter four miRNAs, two of them were selected with higher ranking in the various predictions, namely hsa-miR-181b and hsa-miR-340, as additional candidates for functional analysis.

Table 4.1 MiRNA candidates for regulation of *HSD11B1* expression. Four different miRNA target gene prediction tools (head row) were used to identify miRNA candidates for binding to the 3'UTR of *HSD11B1* mRNA. Only candidates identified independently by at least three different tools are shown with the ranks from the corresponding hit lists. For TargetScan, double ranks indicate two potential binding sites with different scores; for all other tools, the number of binding sites contributes to the score and thus to the ranking. All displayed miRNAs were selected for visualisation of miRNA profiles (<http://www.mirz.unibas.ch>, Figure 4.1).

Results

prediction tool hsa-miR-	Rank in DIANA microT ¹	Rank in TargetScan ²	Rank in microRNA ³	Rank in MicroCosm Targets ^{4,5}
132	-	6	26	25
142-5p	-	45	41	35
181a	-	30	31	23
181b	-	28	4	4
181c	-	29	42	40
181d	-	27	2	1
212	-	5	11	14
330-5p	-	11,15	3	2
340	-	46	9	9
376a	-	10	17	7
376b	-	9	18	10
410	-	37,40	33	36
450b-5p	-	21	5	6
513a-3p	1	39, 50	16	-
561	2	1	8	16
577	-	7,8	22	18
579	4	2	20	29
593	-	16	24	8
605	-	4	14	3
637	-	13	29	17
647	-	32	25	19
889	3	38	40	-

¹ <http://diana.cslab.ece.ntua.gr/microT> (Maragkakis *et al.*, 2009a; Maragkakis *et al.*, 2009b)

² <http://www.targetscan.org> (Lewis *et al.*, 2005; Liu *et al.*, 2003; Grimson *et al.*, 2007; Lewis *et al.*, 2003); the list includes miRNAs binding to poorly conserved sites. ³ <http://www.microrna.org> (Betel *et al.*, 2008)

⁴ <http://www.ebi.ac.uk/enright-srv/microcosm/htdocs/targets/v5/> (Griffiths-Jones *et al.*, 2006; Griffiths-Jones *et al.*, 2008); non-human miRNAs and miRNA* species were not considered

⁵ Results for 3'-UTR of transcript ENST00000367028

Results

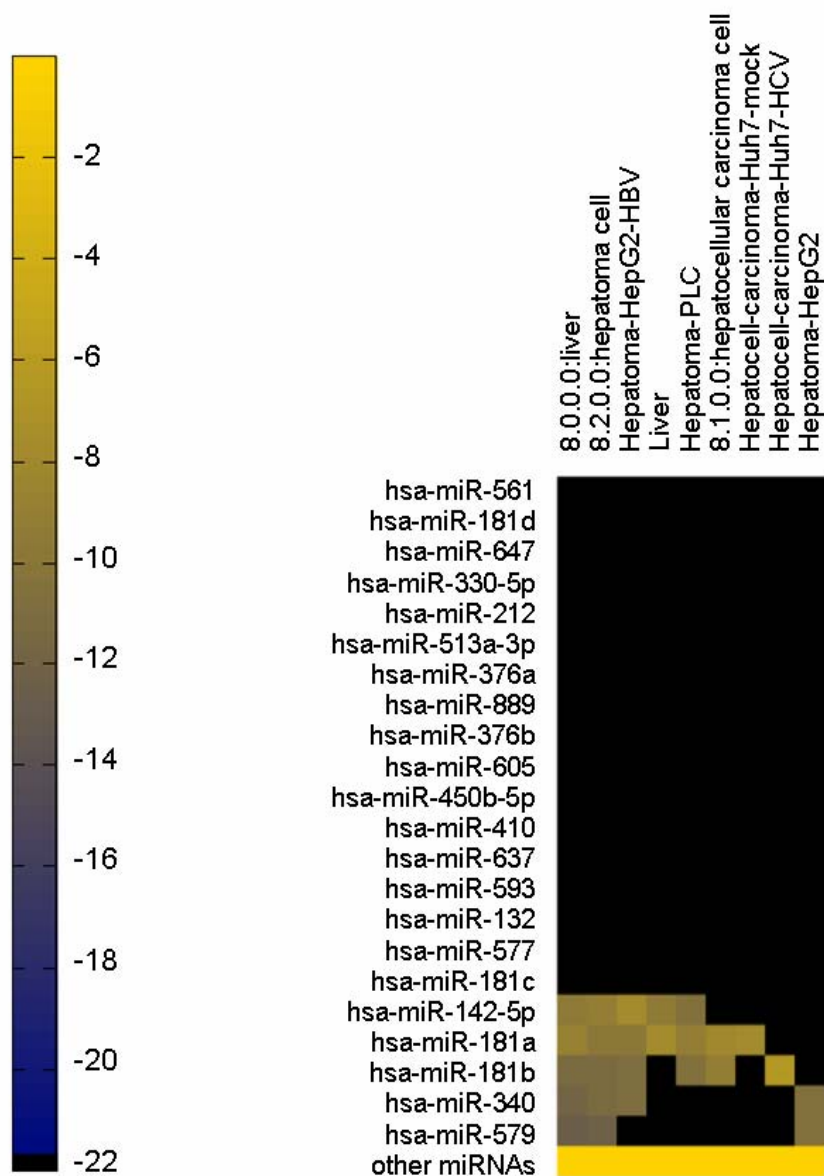


Figure 4.1 Results of the web-based tissue profiling. Twenty-two miRNAs were suggested as potential regulators of *HSD11B1* expression by at least three of four miRNA target prediction tools (see Table 4.1) and subjected to tissue profiling using the publicly available smiRNadb miRNA expression atlas (<http://www.mirz.unibas.ch/>). Expression levels of miRNAs (rows) are estimated by relative cloning frequencies which are expressed as log₂ values and displayed with a colour code according to the left panel. Yellow colour indicates high cloning frequency, blue colour indicates low cloning frequency and black colour indicates no detection. The columns represent different hierarchical categories and samples of the smiRNadb miRNA expression atlas: 8.0.0.0: Liver represents all hepatocyte samples; 8.2.0.0: hepatoma cell represents the human HepG2 and PLC hepatoma cell lines; 8.1.0.0: hepatocellular carcinoma represents the HuH7 hepatoma cell line. ‘Liver’ is a normal liver from a 43-year old female (Landgraf *et al.*, 2007).

4.2 Construction of pmir-HSD11B1-3'UTR plasmid (dual-luciferase assay system)

The pmir-GLO, dual-luciferase miRNA target expression vector, is designed to quantitatively evaluate miRNAs activity by the insertion of miRNA target sites on the downstream of the firefly luciferase gene. Firefly luciferase is the primary reporter gene; reduced firefly luciferase expression indicates the binding of endogenous or introduced miRNAs to the cloned miRNA target sequence. The map of pmir-GLO vector is shown in Appendix 7.1.2, firefly luciferase is used as the primary reporter to monitor mRNA regulation, and *Renilla* luciferase is acting as a control reporter for normalization and selection. Therefore, the pmir-GLO vector was used to study miRNA function. The complete 3'UTR sequence of the *HSD11B1* mRNA was cloned into pmir-GLO vector between the *XhoI* and *SalI* sites, immediately 3' downstream in the firefly luciferase gene as follows: First, the complete 3'UTR sequence of the *HSD11B1* mRNA was amplified from a human liver cDNA library (UniZAP XR, Stratagene) using HSD11B1-3'UTR-primers (see Table 3.3). The desired 3'UTR sequence of the *HSD11B1* mRNA was designed 429 bp in length, the PCR product was visualized by agarose gel (Figure 4.2). Then, the fragment was inserted into the pCR2.1-TOPO vector (Appendix 7.1.1). The sequencing result corresponded to the published one (http://www.ncbi.nlm.nih.gov/nuccore/NM_005525.3, http://www.ncbi.nlm.nih.gov/nuccore/NM_181755.2, see Appendix 7.2.1). Subsequently, the 3'UTR sequence was released from the pCR2.1-TOPO vector by *XhoI* and *SalI* and ligated into pmir-GLO. The resulting plasmid was named pmir-HSD11B1-3'UTR (Figure 4.3).

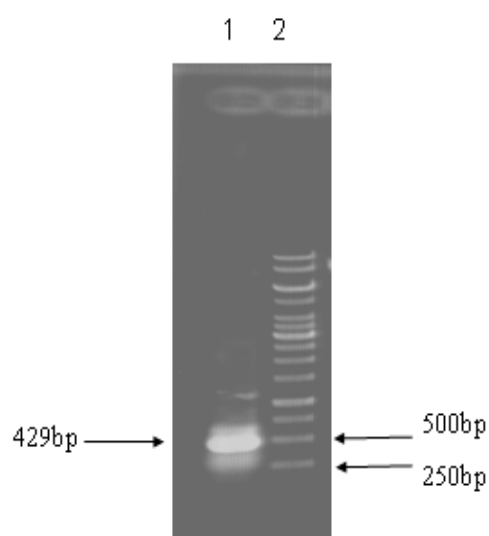


Figure 4.2 The PCR product from a human liver cDNA library.

Lane 1: HSD11B1-3'UTR Lane 2: 1 kb DNA ladder

Results

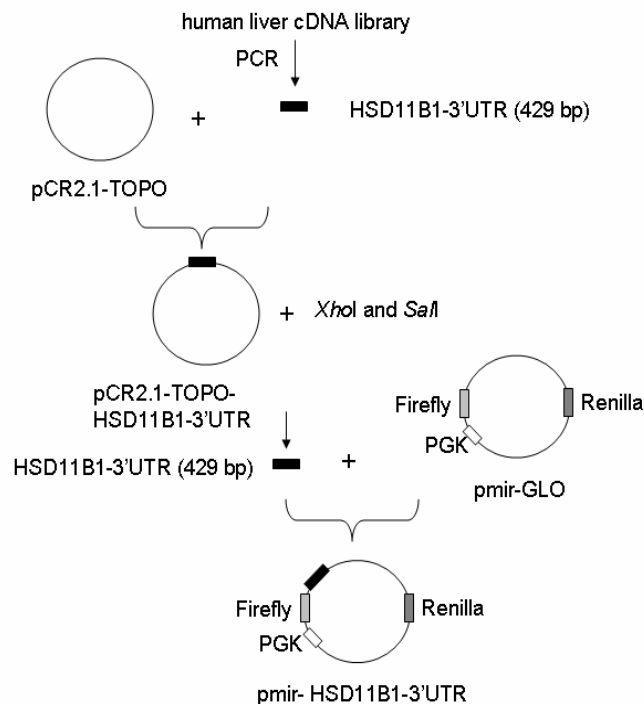


Figure 4.3 Schematic overview of cloning of HSD11B1-3'UTR into pmir-GLO.

See text for details

4.3 Optimizing plasmid DNA (pmir-HSD11B1-3'UTR) transfection

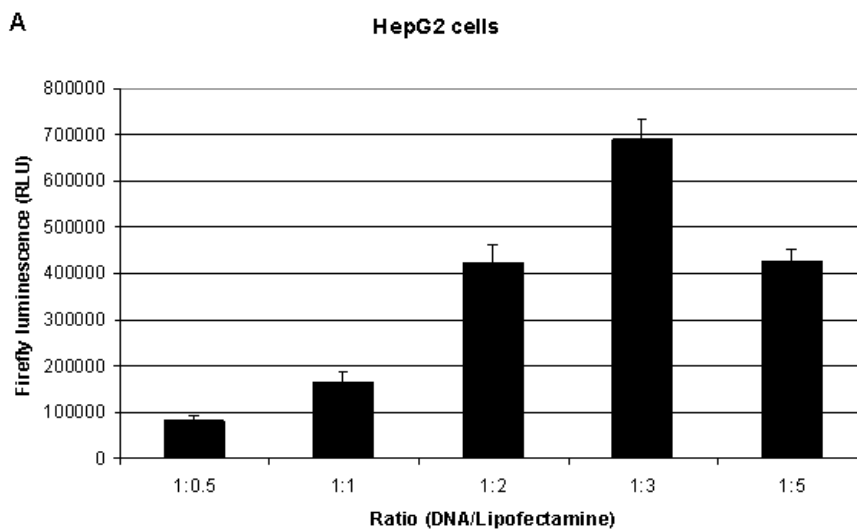
To obtain the highest transfection efficiency and low cytotoxicity, transfection conditions were optimized by DNA and LipofectamineTM 2000 (transfection reagent) concentrations in different cell lines, which are A549 (human lung adenocarcinoma cell line), HepG2 (human hepatoma cell line) and 3T3-L1 (Mouse embryonic fibroblast adipose like cell line) cell lines, respectively. One day before transfection, each well (96-well plate) was plated with $0.6-2 \times 10^4$ cells (depending on different cell lines) in 200 μ l of growth medium without antibiotics so that cells would be greater than 90% confluent at the time of transfection and DNA (μ g): LipofectamineTM 2000 (μ l) ratios varied from 1: 0.5 to 1: 5 (Table 4.2). After 48 hours of transfection, the firefly luciferase and *Renilla* luciferase activities were measured using Dual-GloTM Luciferase Reagent (see Method 3.2.2.3).

Results

Table 4.2 The ratio of DNA (μg): LipofectamineTM 2000 (μl)

Ratio	Plasmid DNA [$\mu\text{g}/\text{well}$]	Lipofectamin 2000 [$\mu\text{l}/\text{well}$]
DNA (μg): Lipofectamine 2000 (μl)		
1 : 0.5	0.2	0.1
1 : 1	0.2	0.2
1 : 2	0.2	0.4
1 : 3	0.2	0.6
1 : 5	0.2	1.0

For transfection of HepG2 cells, the value of firefly luminescence was gradually enhancing due to increased transfection reagent and the maximum value of firefly luminescence was DNA (μg): LipofectamineTM 2000 (μl) = 1: 3 (Figure 4.4A). Meanwhile, the value of *Renilla* luminescence got the maximum value as well as DNA (μg): LipofectamineTM 2000 (μl) = 1: 3 (Figure 4.4B). However, when DNA (μg): LipofectamineTM 2000 (μl) ratio was 1: 5, the values of firefly luminescence and *Renilla* luminescence were decreased, because increased transfection reagent was toxic to cells and part of cells were dead. The result showed that the ratio of Firefly/*Renilla* luminescence was unchanged (Figure 4.4C), even DNA (μg): LipofectamineTM 2000 (μl) ratios varied from 1: 0.5 to 1: 5. Therefore, when the DNA (μg): LipofectamineTM 2000 (μl) ratio was 1: 3 in HepG2 cells, the transfection efficiency got the highest level and the values of firefly luminescence and *Renilla* luminescence reached the maximum at the same time.



Results

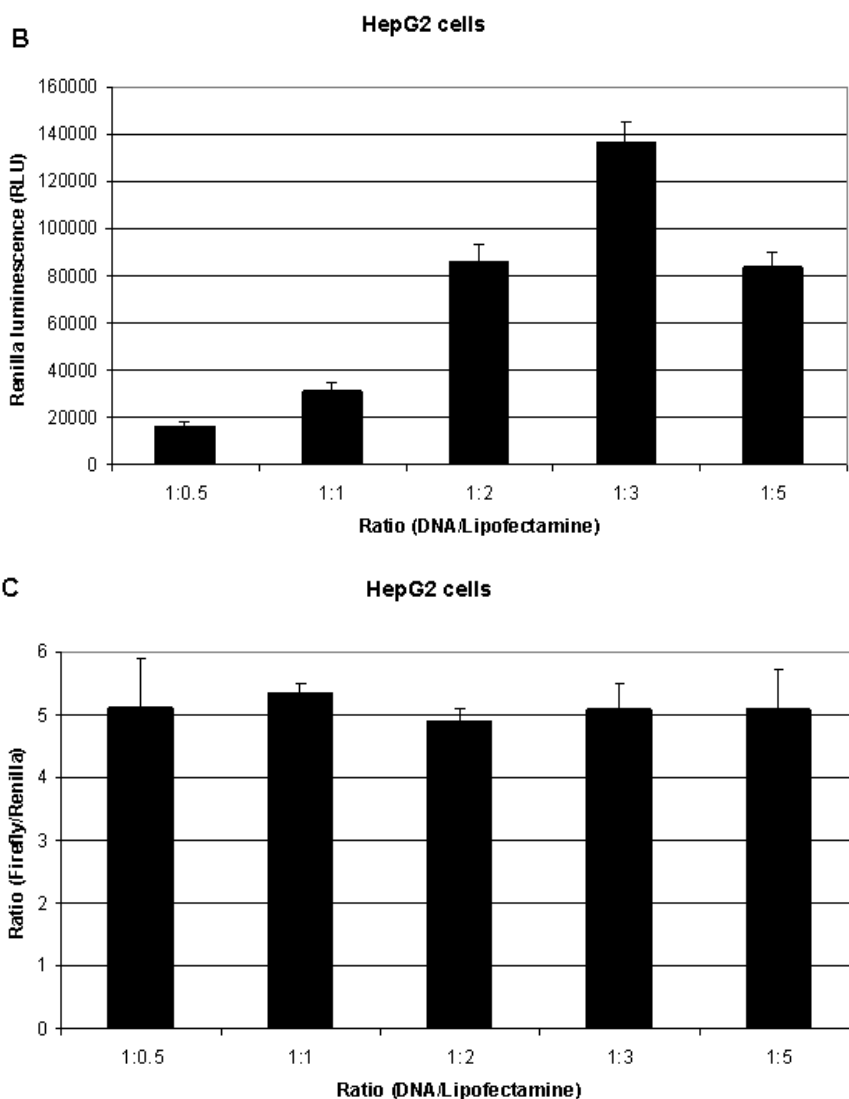


Figure 4.4 Measurement of firefly and *Renilla* luciferase activities in HepG2 cells. (A) Firefly luciferase activity. (B) *Renilla* luciferase activity. (C) Ratio (Firefly/*Renilla*). (Supplement data see Appendix 7.3 Table 1)

For transfection of A549 cells, the value of firefly luminescence was gradually enhancing, when DNA (μg): LipofectamineTM 2000 (μl) ratio was 1: 2, the value of firefly luminescence reached the maximum (Figure 4.5A). Then, the value of firefly luminescence was gradually decreasing, because increased transfection reagent was toxic to cells and part of cells were dead. Meanwhile, the value of *Renilla* luminescence was also gradually enhancing, the maximum value of *Renilla* luminescence also appeared that DNA (μg): LipofectamineTM 2000 (μl) ratio was 1: 2 (Figure 4.5B). The result showed that the ratio of Firefly/*Renilla* luminescence was unchanged (Figure 4.5C), even DNA (μg): LipofectamineTM 2000 (μl)

Results

ratios varied from 1: 0.5 to 1: 5. Therefore, when the DNA (μg): LipofectamineTM 2000 (μl) ratio was 1: 2 in A549 cells, the transfection efficiency got the highest level and the values of firefly luminescence and *Renilla* luminescence reached the maximum at the same time.

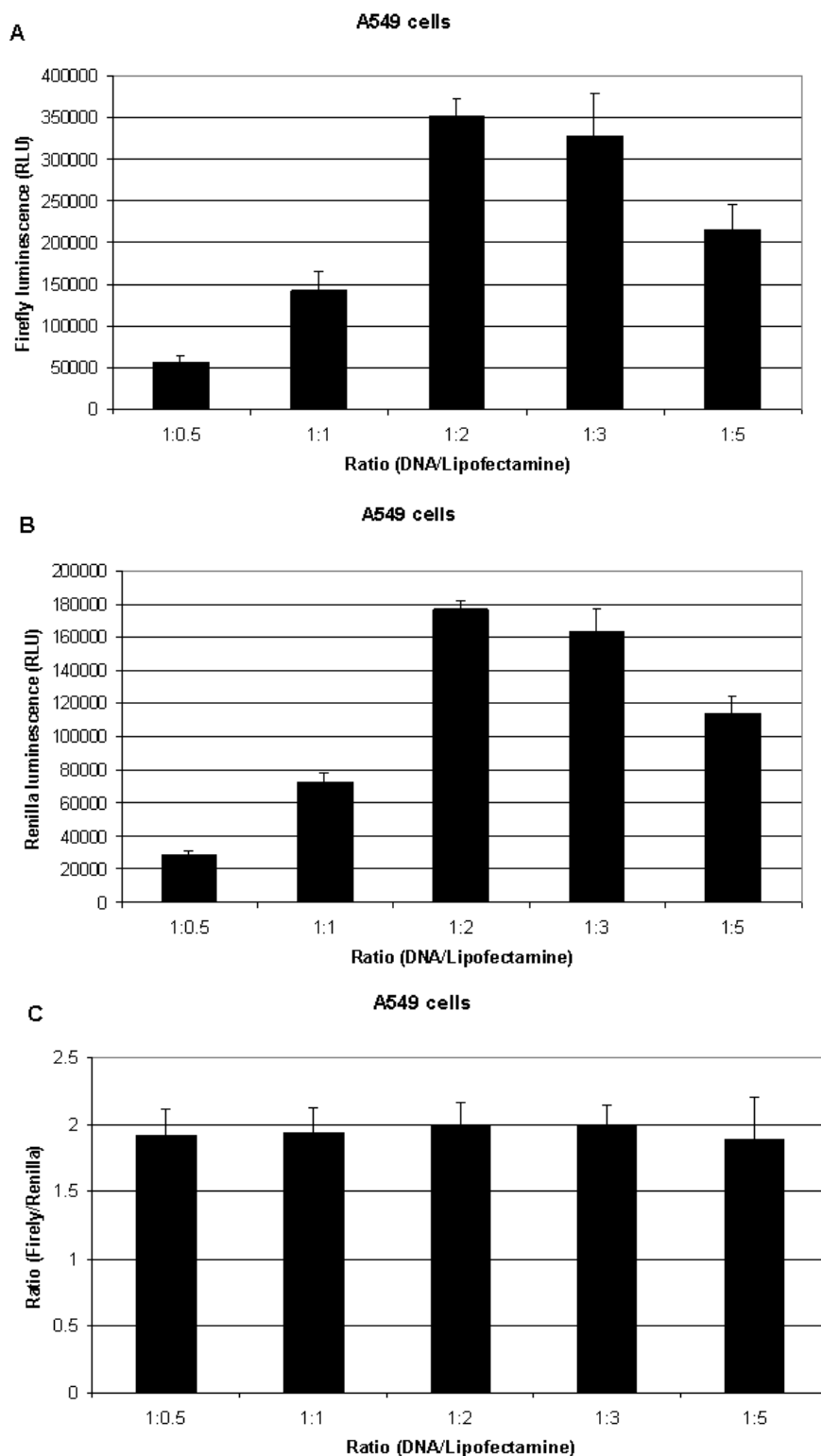


Figure 4.5 Measurement of firefly and *Renilla* luciferase activities in A549 cells.

(A) Firefly luciferase activity. (B) *Renilla* luciferase activity. (C) Ratio (Firefly/*Renilla*).

(Supplement data see Appendix 7.3 Table 2)

Results

However, for transfection of 3T3-L1 cells, transfection efficiency was pretty low. The values of firefly luminescence and *Renilla* luminescence were very low and close to background values (blank control). Therefore, the 3T3-L1 cell line was not used in the following experiments.

4.4 MiRNAs bind to 3'UTR of *HSD11B1* mRNA

To examine the possibility of *HSD11B1* regulation by miRNAs, four different miRNAs, namely hsa-miR-561, hsa-miR-579, hsa-miR-181b and hsa-miR-340, were selected as candidates for functional analysis. The plasmid, pmir-HSD11B1-3'UTR was transfected alone or cotransfected with negative control miRNA#2 and candidate miRNAs, hsa-miR-561, hsa-miR-579, hsa-miR-181b and hsa-miR-340 into HepG2 cells. Relative luciferase activity was significantly suppressed by about 30% by hsa-miR-561 and about 40% by hsa-miR-579 and hsa-miR-340, but unchanged by hsa-miR-181b compared with cotransfection with negative control miRNA#2 (Figure 4.6A). Here, I must mention that negative control miRNA#1 was used as negative control miRNA at the beginning, but negative control miRNA#1 suppressed the firefly luciferase expression in HepG2 cells, thus another negative control miRNA#2 was selected as negative control miRNA in HepG2 cells.

Similar experiments were carried out with A549 cells. The same plasmid, pmir-HSD11B1-3'UTR, was transfected alone or cotransfected with negative control miRNA#1, hsa-miR-561, hsa-miR-579, hsa-miR-181b and hsa-miR-340 into A549 cells. Similar results were also obtained. Relative luciferase activity was significantly suppressed by about 20% by hsa-miR-561 and about 40% by hsa-miR-579 and hsa-miR-340, but not significantly changed by hsa-miR-181b compared with cotransfection with negative control miRNA#1 (Figure 4.6B). These results suggested that three of the selected miRNA candidates, namely hsa-miR-561, hsa-miR-579, and hsa-miR-340, but not hsa-miR-181b, bound to the 3'UTR of the *HSD11B1* mRNA. Therefore, to validate these results, several follow-up experiments were carried out with hsa-miR-561, hsa-miR-579, and hsa-miR-340.

Results

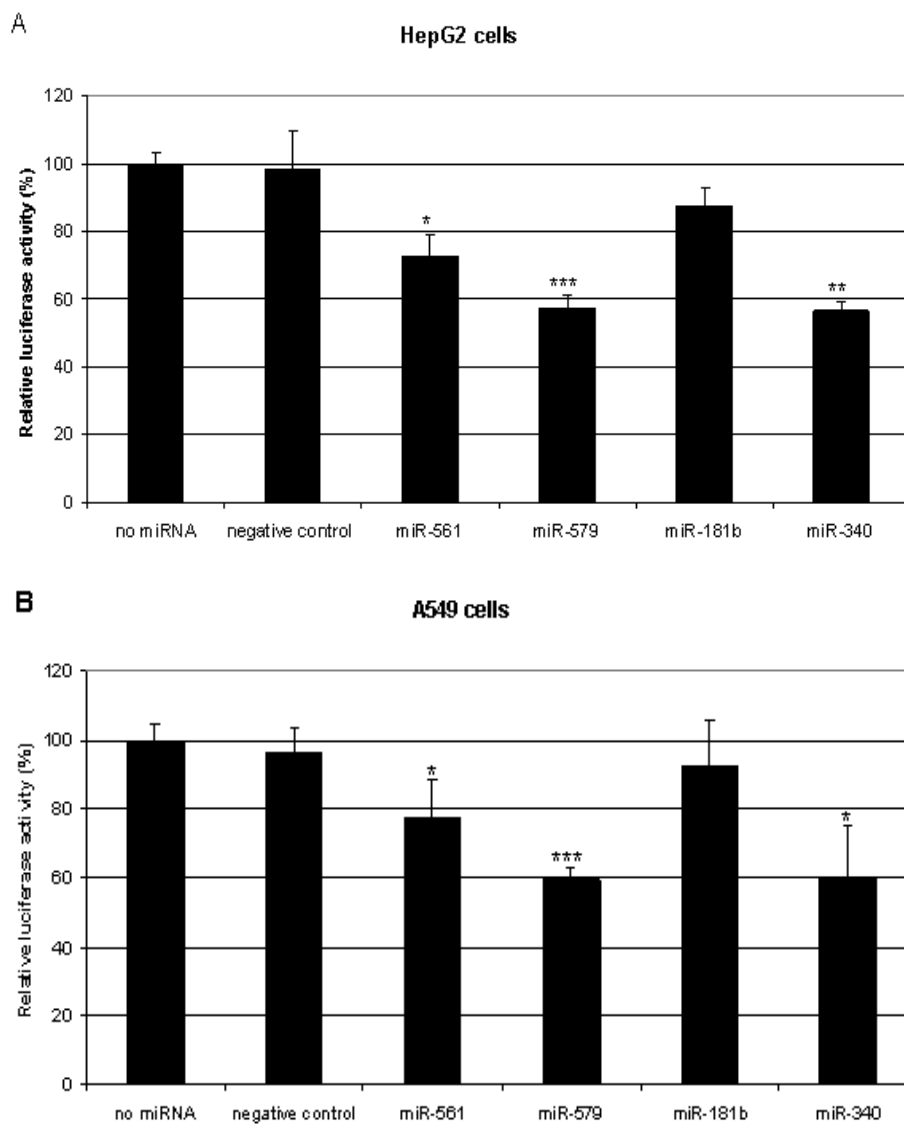
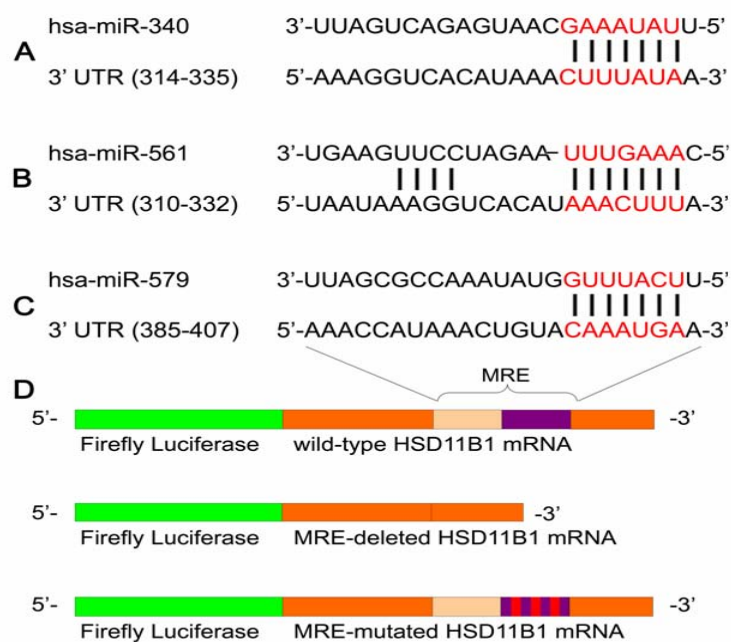


Figure 4.6 Results of luciferase reporter assay for four miRNA candidates interaction with the 3'UTR of human *HSD11B1* mRNA. (A) Results of cotransfection experiments in HepG2 cells with the pmir-GLO vector carrying the HSD11B1-3'UTR and various miRNA precursors: negative control miRNA#2, hsa-miR-561, -579, -181b, and -340. (B) Results of cotransfection experiments in A549 cells with the pmir-GLO vector carrying the HSD11B1-3'UTR and various miRNA precursors: negative control miRNA#1, hsa-miR-561, -579, -181b, and -340. Luciferase activities were measured 48 hours after transfection. All results were normalized to luciferase activity in the absence of miRNA which was set to 100%. Results are based on three independent experiments and shown as average \pm SD. Statistical analysis was by student's *t*-test: *, $p < 0.05$; **, $p < 0.01$; ***, $p < 0.001$ (Supplement data see Appendix 7.3 Table 3).

4.5 Deletion/mutation of the corresponding miRNA response elements (MREs) in the HSD11B1-3'UTR

Two prediction tools, TargetScan Human (<http://www.targetscan.org/>) and MicroCosm Targets (<http://www.ebi.ac.uk/enright-srv/microcosm/htdocs/targets/v5/>) were used to predict the corresponding miRNA response elements in the 3'UTR of *HSD11B1* mRNA. The predicted miRNA response elements (MREs) of the three positive miRNAs, hsa-miR-340, hsa-miR-561, and hsa-miR-579, in the 3'UTR of human *HSD11B1* mRNA are shown in Figure 4.7 (A, B and C). The prediction results indicated that miRNAs-target *HSD11B1* mRNA are imperfect complementarity. To further verify whether repression by hsa-miR-561, hsa-miR-579, and hsa-miR-340 was due to binding to the predicted MREs, particularly in 'seed region' main miRNA binding sites (red letters; Figure 4.7), luciferase reporter constructs were generated where the corresponding MREs were either deleted or mutated (3 points mutation) in the seed region (Figure 4.7D). The sequences of deletion/mutation of the hsa-miR-561, hsa-miR-579 and hsa-miR-340 MREs in the HSD11B1-3'UTR were shown in Figure 4.7E. Deletion/mutation of the hsa-miR-561, hsa-miR-579 and hsa-miR-340 MREs in the HSD11B1-3'UTR construct were performed using splicing by overlapping extension PCR (Vallejo *et al.*, 1994). The resulting PCR fragment was purified and inserted into the pCR2.1-TOPO vector. After sequencing, the expected fragment was subcloned into the pmir-GLO vector. The resulting plasmids were named pmir-561-del, pmir-561-mut, pmir-579-del, pmir-579-mut, pmir-340-del and pmir-340-mut, respectively, for deletion/mutation of the hsa-miR-561, hsa-miR-579 and hsa-miR-340 MREs in the HSD11B1-3'UTR.



E

```

                                     340-mut
                                     G G C
301 UAUUAAUUAU AAUAAAGGUC ACAUAAACUU UAUAAATTCA UAACUGGUAG
                                     340-del
351 CUAUAACUUG AGCUUAUUCA GGAUGGUUUC UUUAAAACCA UAAACUGUAC

401 AAAUGAAAUU UUUCAUAUUA UGUUUCUUA

                                     561-mut
                                     U G C
301 UAUUAAUUAU AAUAAAGGUC ACAUAAACUU UAUAAAUUCA UAACUGGUAG
                                     561-del
351 CUAUAACUUG AGCUUAUUCA GGAUGGUUUC UUUAAAACCA UAAACUGUAC

401 AAAUGAAAUU UUUCAUAUUA UGUUUCUUA

301 UAUUAAUUAU AAUAAAGGUC ACAUAAACUU UAUAAAUUCA UAACUGGUAG
351 CUAUAACUUG AGCUUAUUCA GGAUGGUUUC UUUAAAACCA UAAACUGUAC
                                     579-del

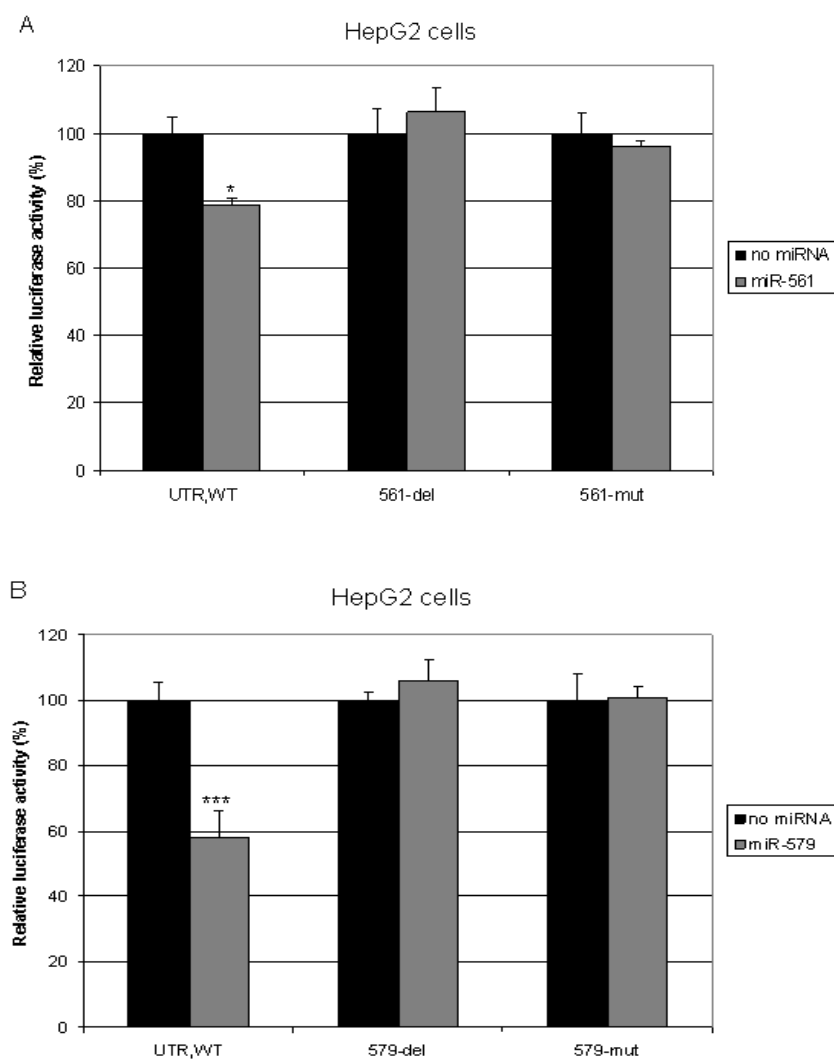
579-mut
U G C
401 AAAUGAAAUU UUUCAUAUUA UGUUUCUUA

```

Figure 4.7 Outline of luciferase reporter assay for validating the interaction of hsa-miR-340, hsa-miR-561, and hsa-miR-579 with the 3'UTR of human *HSD11B1* mRNA: The miRNA response elements (MREs) of (A) hsa-miR-340, (B) hsa-miR-561, and (C) hsa-miR-579 in the 3'UTR of human *HSD11B1* mRNA are shown as predicted by TargetScan (<http://www.targetscan.org>). Red letters indicate the 'seed' (S) region. (D) The complete 3'UTR sequence (depicted in orange) of the *HSD11B1* mRNA was inserted into the pmir-GLO vector, immediately downstream of the firefly luciferase gene (depicted in green). In mutant reporter constructs, the MRE (depicted in beige, seed region in purple) was deleted or a three-mismatch mutation (red boxes) was introduced into the seed region. (E) Sequences of deletion or mutation for miR-340-MRE, miR-561-MRE and miR-579-MRE in the 3'UTR of *HSD11B1* mRNA.

4.6 Deletion/mutation of the corresponding miRNA response elements (MREs) in the 3'UTR of *HSD11B1* mRNA abolished the effect for hsa-miR-561 and hsa-miR-579, but not completely for hsa-miR-340

To further verify whether repression by hsa-miR-561, hsa-miR-579, and hsa-miR-340 was due to binding to the predicted MREs, the plasmid pmir-HSD11B1-3'UTR (wild type), or the above mentioned MRE-deleted/mutated variants, namely pmir-561-del, pmir-561-mut, pmir-579-del, pmir-579-mut, pmir-340-del and pmir-340-mut, were transfected alone or cotransfected with the corresponding miRNA into HepG2 cells. Suppression of luciferase activity by hsa-miR-561 and hsa-miR-579 was completely abolished when the miR-561-MREs and miR-579-MREs, respectively, were deleted from the HSD11B1-3'UTR, as well as when a 3-base mismatch mutation was introduced into the MREs seed region (Figure 4.8A and B). However, for hsa-miR-340, suppression of luciferase activity was not completely abolished in these experiments (Figure 4.8C).



Results

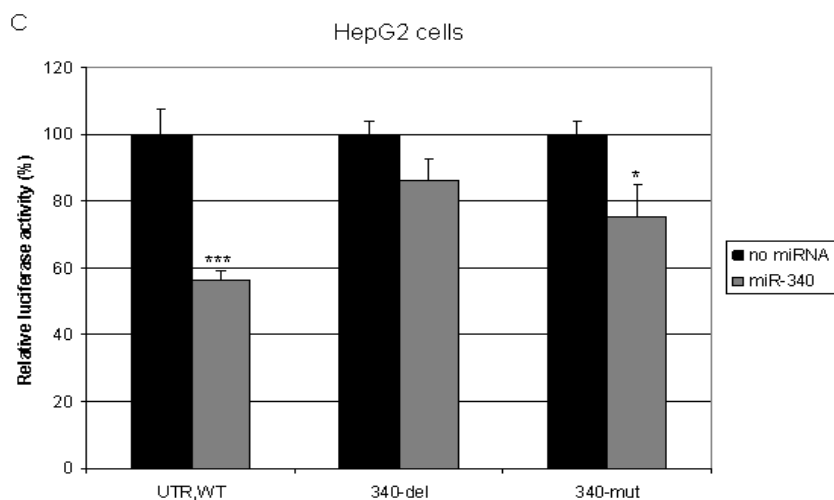
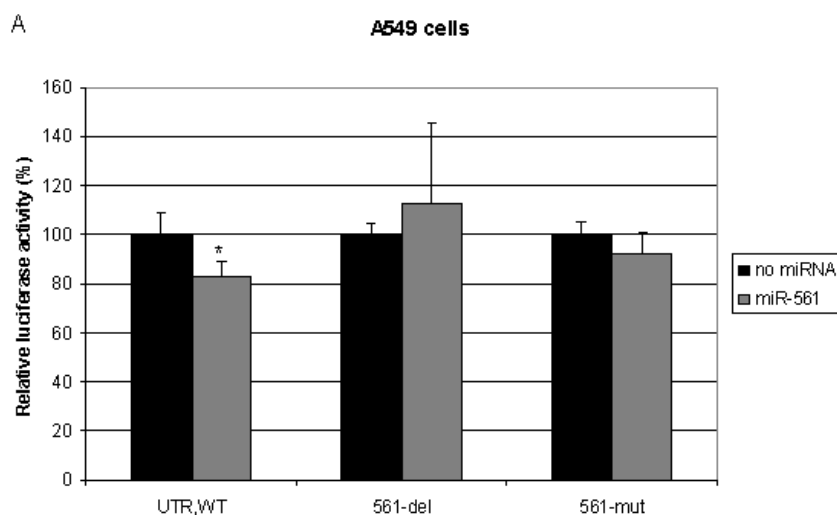


Figure 4.8 Deletion (3'UTR XXX del) as well as mutation (3'UTR XXX mut) of the corresponding MREs abolished the repression by hsa-miR-561 (A) and hsa-miR-579 (B), but did not completely abolish repression by hsa-miR-340 (C). The pmir-GLO vector carrying the HSD11B1-3'UTR (UTR, WT) or the MRE-deleted/mutated constructs were cotransfected with hsa-miR-561, hsa-miR-579, or hsa-miR-340 into HepG2 cells, respectively. Luciferase activities were measured 48 hours after transfection. All results were normalized to luciferase activity in the absence of miRNA which was set to 100%. Results are based on three independent experiments and shown as average \pm SD. Statistical analysis was by student's *t*-test: *, $p < 0.05$; ***, $p < 0.001$ (Supplement data see Appendix 7.3 Table 4).

The same experiments were carried out in A549 cells, similar results were obtained. Suppression of luciferase activity by hsa-miR-561 and hsa-miR-579 was completely abolished, but not completely abolished by hsa-miR-340 (Figure 4.9). These results indicated that deletion/mutation of the corresponding miRNA response elements (MREs) in the HSD11B1-3'UTR abolished the effect for hsa-miR-561 and hsa-miR-579, but did not completely abolish for hsa-miR-340. Mutated luciferase constructs results showed that the 'seed region' is main and valid miRNA binding sites in the 3'UTR of *HSD11B1* mRNA.



Results

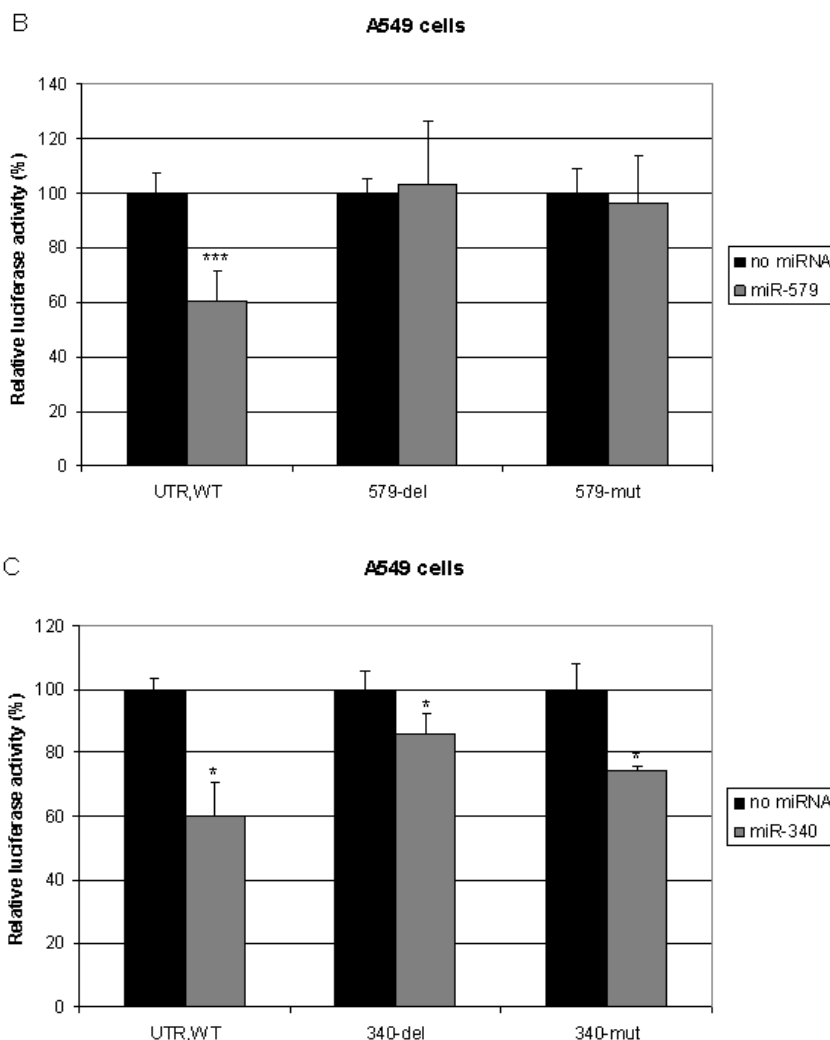
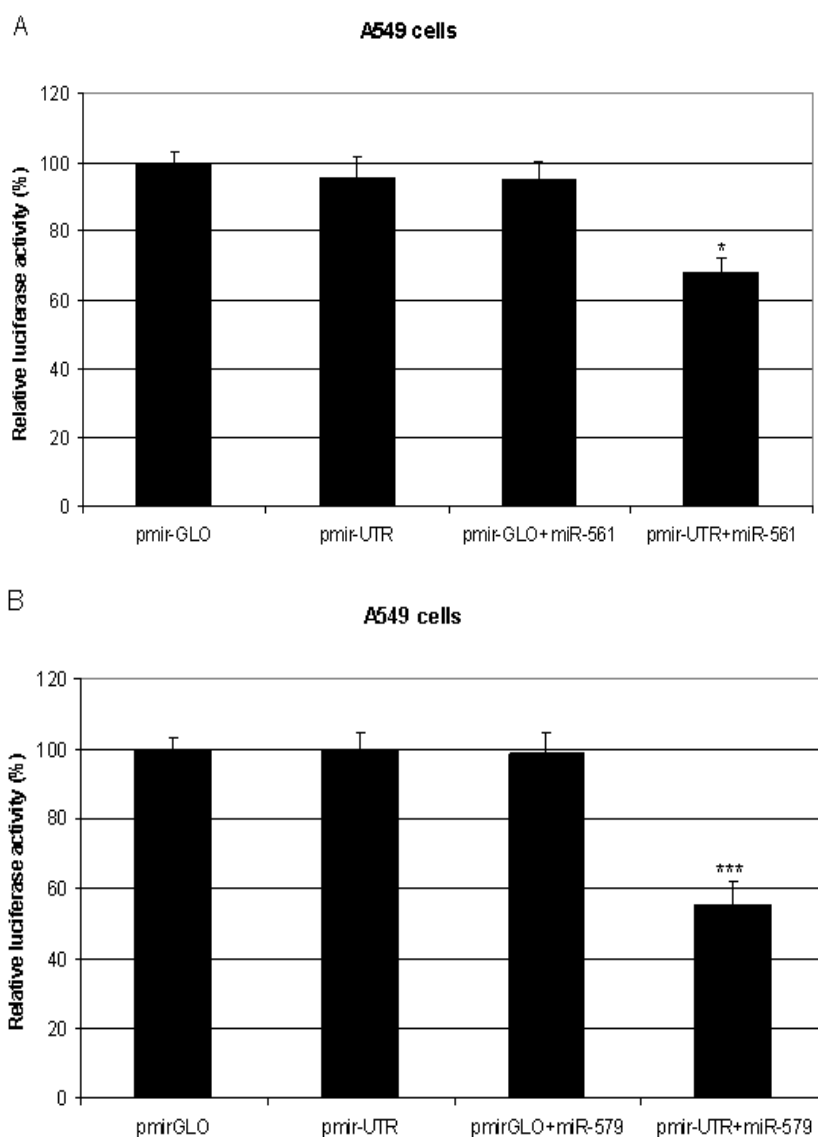


Figure 4.9 Deletion (3'UTR XXX del) as well as mutation (3'UTR XXX mut) of the corresponding MREs abolished the repression by hsa-miR-561 (A) and hsa-miR-579 (B), but did not completely abolish repression by hsa-miR-340 (C). The pmir-GLO vector carrying the HSD11B1-3'UTR (UTR, WT) or the MRE-deleted/mutated constructs were cotransfected with hsa-miR-561, hsa-miR-579, or hsa-miR-340 into A549 cells, respectively. Luciferase activities were measured 48 hours after transfection. All results were normalized to luciferase activity in the absence of miRNA which was set to 100%. Results are based on three independent experiments and shown as average \pm SD. Statistical analysis was by student's *t*-test: *, $p < 0.05$; ***, $p < 0.001$ (Supplement data see Appendix 7.3 Table 5).

To further make sure that suppression of luciferase activity is due to miRNA binding to 3'UTR of *HSD11B1* mRNA, the plasmid pmir-GLO (absence of HSD11B1-3'UTR) and pmir-HSD11B1-3'UTR (pmir-UTR) were transfected alone or cotransfected with miRNAs into A549 cells, respectively. For the plasmid pmir-GLO, the results showed that relative luciferase activity was unchanged by hsa-miR-561 and hsa-miR-579 compared to that without

Results

miRNAs (Figure 4.10A and B). For the plasmid pmir-HSD11B1-3'UTR, in agreement with previous results, relative luciferase activity was significantly suppressed by about 30% by hsa-miR-561 and about 40% by hsa-miR-579 compared to that without miRNAs (Figure 4.10A and B). However, for the plasmid pmir-GLO (absence of HSD11B1-3'UTR) and pmir-HSD11B1-3'UTR, relative luciferase activity was significantly suppressed by about 20% and about 40% by hsa-miR-340 compared to that without miRNAs (Figure 4.10C), respectively. These results showed that suppression of luciferase activity by hsa-miR-340 was not due to specific binding to the predicted MREs in the 3'UTR of *HSD11B1* mRNA. Therefore, hsa-miR-561 and hsa-miR-579 were used in the following experiments, but not including hsa-miR-340.



Results

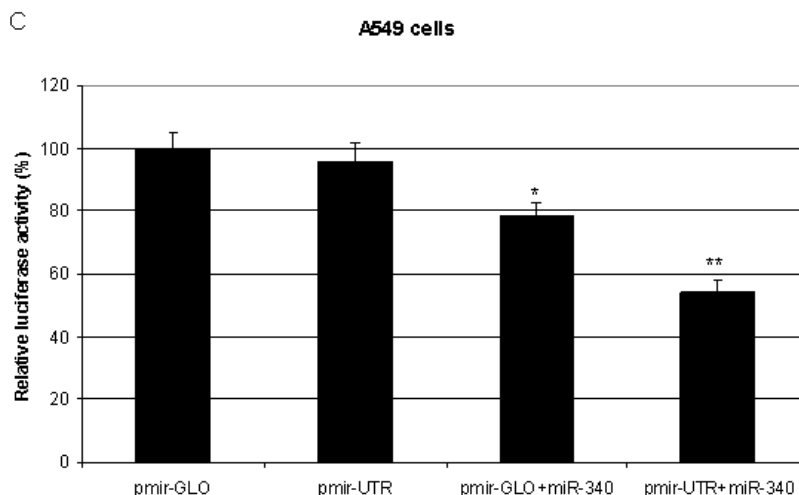


Figure 4.10 Results of luciferase reporter assay for hsa-miR-561, hsa-miR-579, and hsa-miR-340 binding to the 3'UTR of human *HSD11B1* mRNA. Results of transfection experiments in A549 cells with the pmir-GLO or pmir-GLO vector carrying the *HSD11B1*-3'UTR (pmir-UTR) and various miRNA precursors: hsa-miR-561(A), hsa-miR-579 (B), and hsa-miR-340 (C). Luciferase activities were measured 48 hours after transfection. All results were normalized to luciferase activity in the absence of miRNA (pmir-GLO) which was set to 100%. Results are based on three independent experiments and shown as average \pm SD. Statistical analysis was by student's *t*-test: *, $p < 0.05$; **, $p < 0.01$; ***, $p < 0.001$ (Supplement data see Appendix 7.3 Table 6).

4.7 Target mRNA levels were unchanged by hsa-miR-561 and hsa-miR-579

In efforts to explore the underlying mechanism of miRNA-mediated suppression (either mRNA degradation or translational repression), levels of firefly (reporter) and *Renilla* (control) luciferase mRNA were semi-quantified after cotransfection experiments with the luciferase construct containing the 3'UTR of *HSD11B1* mRNA and negative control miRNA#1, hsa-miR-561 or hsa-miR-579. The result showed that none of the miRNAs significantly changed the ratio of firefly/*Renilla* luciferase mRNAs (Figure 4.11). In fact, levels of both mRNAs decreased in the cotransfection experiment compared to the experiment where miRNA was not used (Figure 4.11).

Results

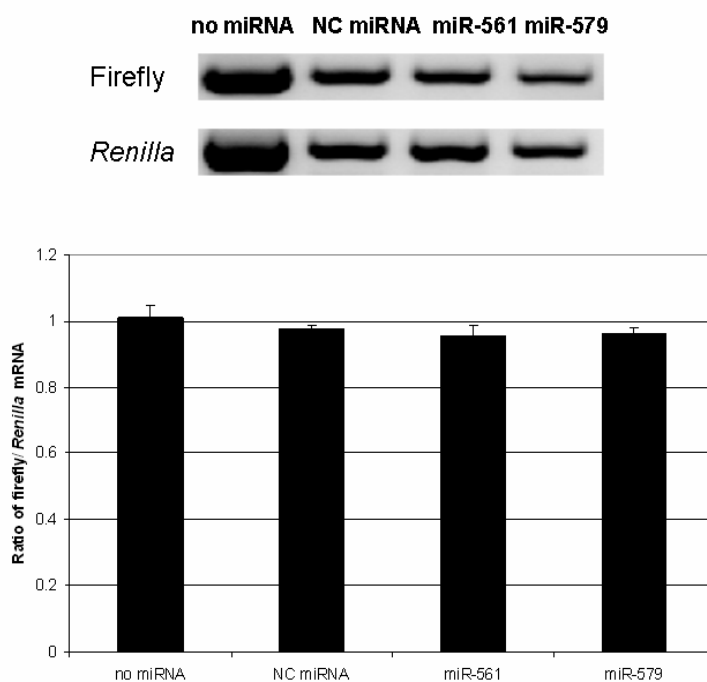


Figure 4.11 Results of luciferase reporter assay on mRNA level. A549 cells were cotransfected with the pmir-GLO vector carrying the HSD11B1-3'UTR and various miRNA precursors: negative control (NC) miRNA#1, hsa-miR-561, and -579. Cotransfection was followed by RNA isolation (treatment with DNase), cDNA synthesis and finally semi-quantitative RT-PCR. Results are based on three independent experiments (Appendix 7.3 Figure 1). Results were semi-quantified by determination of band intensity using GIMP 2.6 (GNU Image Manipulation Program) and shown as average \pm SD.

Moreover, the levels of endogenous *HSD11B1* mRNA were semi-quantified after transfection experiments with negative control miRNA, hsa-miR-561 or hsa-miR-579 into HepG2 cells and A549 cells. GAPDH (glyceraldehyde 3-phosphate dehydrogenase) was used as loading control in semi-quantitative RT-PCR. The results showed that the ratios of *HSD11B1* mRNA/GAPDH mRNA were unchanged after transfection with negative control miRNA, hsa-miR-561 and hsa-miR-579 in HepG2 cells (Figure 4.12A) and A549 cells (Figure 4.12 B).

Results

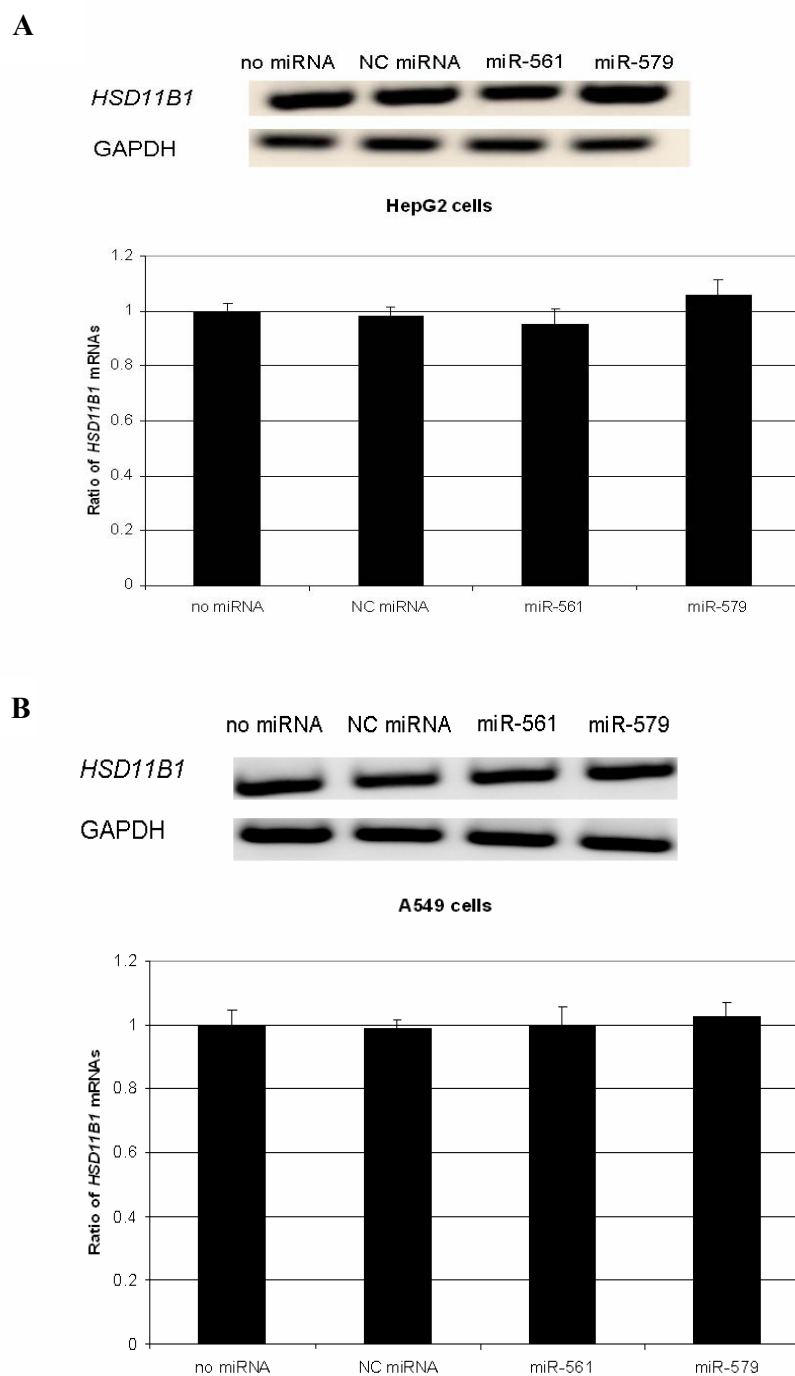


Figure 4.12 The levels of endogenous *HSD11B1* mRNA were analyzed by semi-quantitative RT-PCR. (A) HepG2 cells were transfected with the various miRNA precursors: negative control (NC) miRNA#2, hsa-miR-561, and -579. (B) A549 cells were transfected with the various miRNA precursors: negative control (NC) miRNA#1, hsa-miR-561, and -579. Transfection was followed by RNA isolation, cDNA synthesis and finally semi-quantitative RT-PCR. GAPDH was used as a loading control in semi-quantitative RT-PCR. Results are based on three independent experiments (Appendix 7.3 Figure 2). Results were semi-quantified by determination of band intensity using GIMP 2.6 (GNU Image Manipulation Program) and shown as average \pm SD.

4.8 Glucocorticoids induction of *HSD11B1* expression in A549 cells

Glucocorticoids such as dexamethasone and cortisol are important regulators of *HSD11B1* expression in human liver, lung, and many cells. To assess the relative contribution of the two alternative promoter usage after glucocorticoids induction of *HSD11B1* expression in A549 cells, primers were designed for specifically amplifying the two distinct *HSD11B1* transcripts (Figure 4.13).

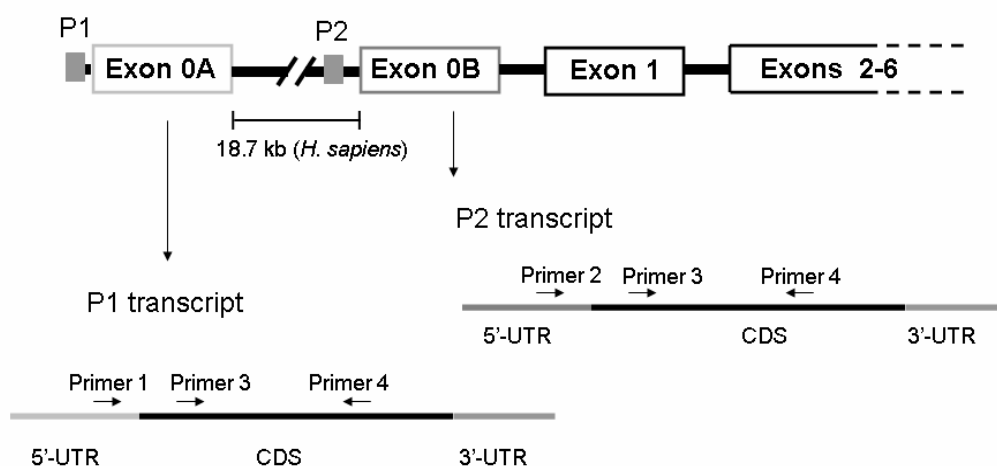


Figure 4.13 Human *HSD11B1* transcripts for assessment of alternative promoter usage. The forward primers (primer 1 and primer 2) were designed that bind specifically to the 5'UTRs of transcript 1 and 2, respectively. Total transcript levels can be captured by a common forward primer (primer 3) which binds to the coding sequence (CDS). One common reverse primer (primer 4) was used in all RT-PCR preparations.

After A549 cells were induced with dexamethasone and cortisol, levels of *HSD11B1* mRNA from P1-, P2-, and total transcript were assessed with semi-quantitative RT-PCR. The results showed that *HSD11B1* mRNA from P1-, P2-, and total transcript were significantly increased by induction with dexamethasone and cortisol (Figure 4.14). *HSD11B1* expression from Promoter 2 was much stronger than from Promoter 1 (Figure 4.14). Therefore, dexamethasone and cortisol induce *HSD11B1* transcription in A549 cells mostly via P2 promoter.

Results

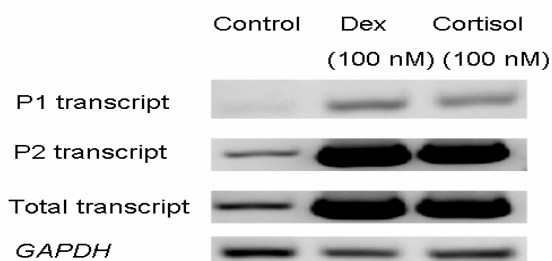


Figure 4.14 *HSD11B1* expression from P1-, P2-, and total transcript were semi-quantified by RT-PCR. *HSD11B1* transcription can be assessed in A549 cells. A549 cells were induced with dexamethasone (Dex) and cortisol for 48 hours, total RNA was isolated and *HSD11B1* mRNA from P1-, P2-, and total transcript were detected by semi-quantitative RT-PCR. Results are based on three independent experiments (Appendix 7.3 Figure 3).

4.9 Cloning of *HSD11B1*-Promoter 1 or *HSD11B1*-Promoter 2 into pmir-*HSD11B1*-3'UTR

To explore the relative influence of 5'-regulatory elements as *e.g.* transcription factors versus 3'-regulatory elements as miRNAs in *HSD11B1* expression or analyze *HSD11B1* promoter activity, the *HSD11B1*-Promoter 1 and the *HSD11B1*-Promoter 2 were cloned into the dual-luciferase assay system. The DNA fragment of *HSD11B1*-Promoter 1 on upstream about 2 kb of transcription start sites was amplified, which contains all evolutionarily conserved regions as estimated by the ECR browser (<http://ecrbrowser.dcode.org/>) and a part of the 5'-untranslated region (UTR). The fragment of *HSD11B1*-Promoter 2 was amplified the region designated as promoter in NCBI (<http://www.ncbi.nlm.nih.gov/>), which contains all evolutionarily conserved regions as estimated by the ECR browser and the 5'-untranslated region (UTR). The PGK promoter of pmir-*HSD11B1*-3'UTR was replaced by the Promoter 1 or 2 fragment of *HSD11B1* as follows. First, the fragment of *HSD11B1*-Promoter 1 and *HSD11B1*-Promoter 2 were successfully amplified from genomic DNA of A549 cells. The desired DNA fragments of Promoter 1 and 2 were 2.173 kb and 2.506 kb, respectively, which were shown correct molecular weight in an agarose gel (Figure 4.15). Then, these fragments were cloned into the pCR2.1-TOPO vector. The sequencing results showed that the correct sequences of Promoter 1 and 2 were obtained (Identical to the database entry NCBI, <http://www.ncbi.nlm.nih.gov/>; Ensembl Genome Browser, <http://www.ensembl.org/>, sequences see Appendix 7.2.2 and 7.2.3). The PGK promoter of pmir-*HSD11B1*-3'UTR was deleted and a new *Xma* I restriction site was introduced. Subsequently, the fragment of

Results

HSD11B1-Promoter 1 or *HSD11B1*-Promoter 2 was digested by *Xma* I and subcloned into the deleted and modified pmir-HSD11B1-3'UTR vector (Figure 4.16). The resulting plasmids were named pmir-Promoter 1 and pmir-Promoter 2, respectively.

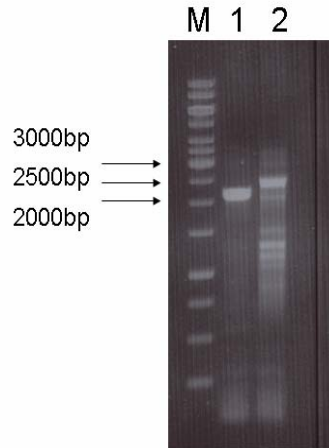


Figure 4.15 PCR products of *HSD11B1*-Promoter 1 and -Promoter 2.

M: 1kb DNA ladder 1: Promoter 1 (2.173kb) 2: Promoter 2 (2.506kb)

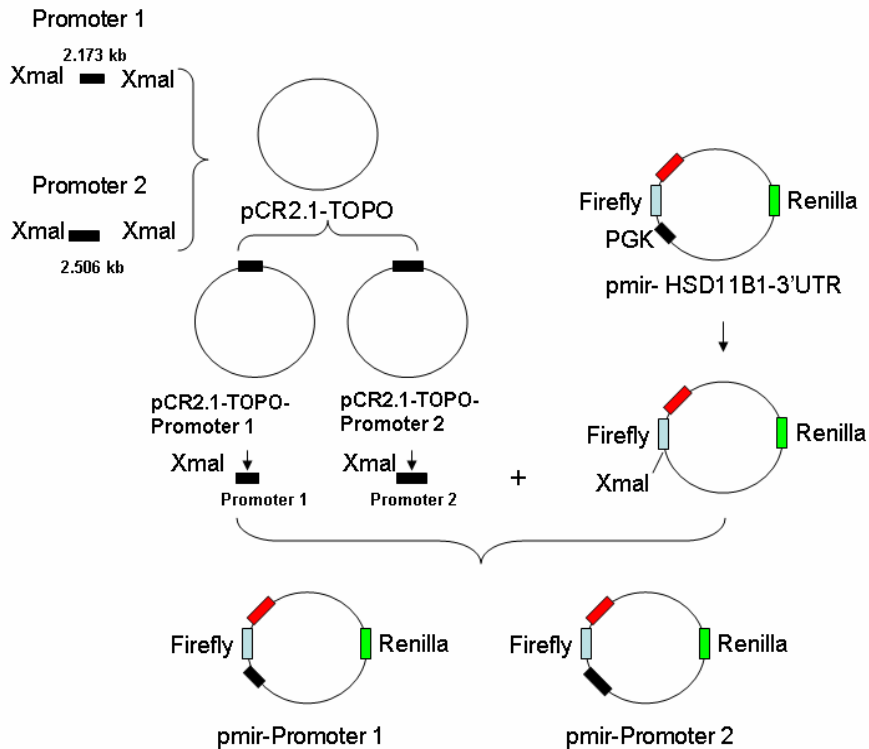


Figure 4.16 Schematic overview of the cloning of *HSD11B1*-Promoter 1 or *HSD11B1*-Promoter 2 into the dual-luciferase assay system. See text for details

4.10 Assessment of regulation of *HSD11B1* expression by glucocorticoids using the pmir-Promoter constructs

To investigate regulation of *HSD11B1* expression by glucocorticoids in the dual-luciferase assay system, the pmir-Promoter 1 or pmir-Promoter 2 was transfected into A549 cells, followed by induction with dexamethasone and cortisol 4 hours after transfection. Luciferase activities were measured 48 hours after transfection. Relative luciferase activity of the Promoter 2 reporter construct was significantly increased after induction with dexamethasone and cortisol in A549 cells, while luciferase activity of the Promoter 1 reporter construct was unchanged (Figure 4.17). Therefore, the pmir-Promoter 2 plasmid was used in subsequent experiments.

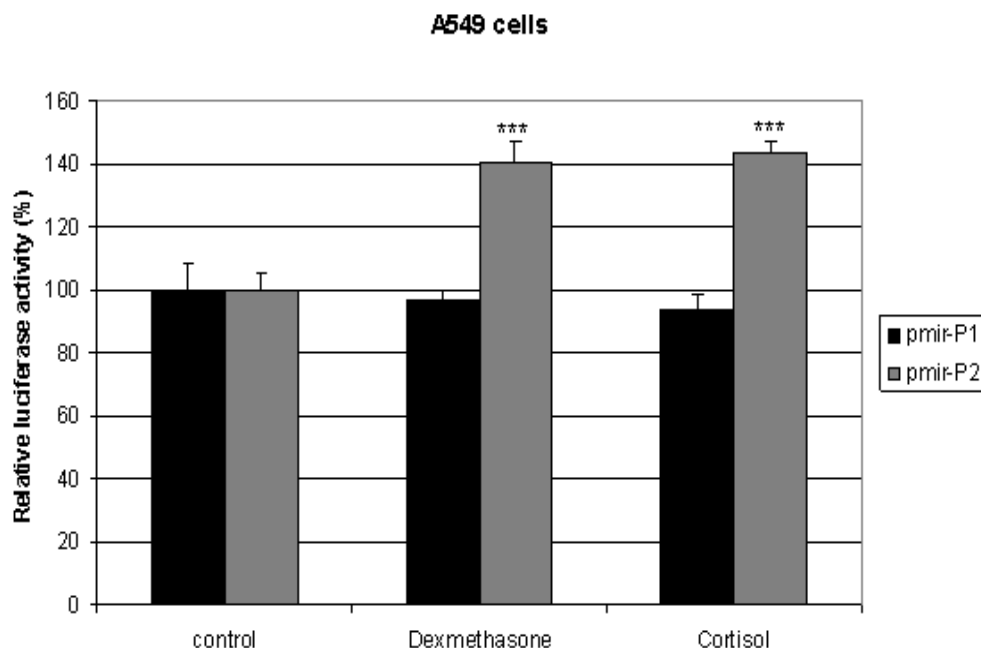
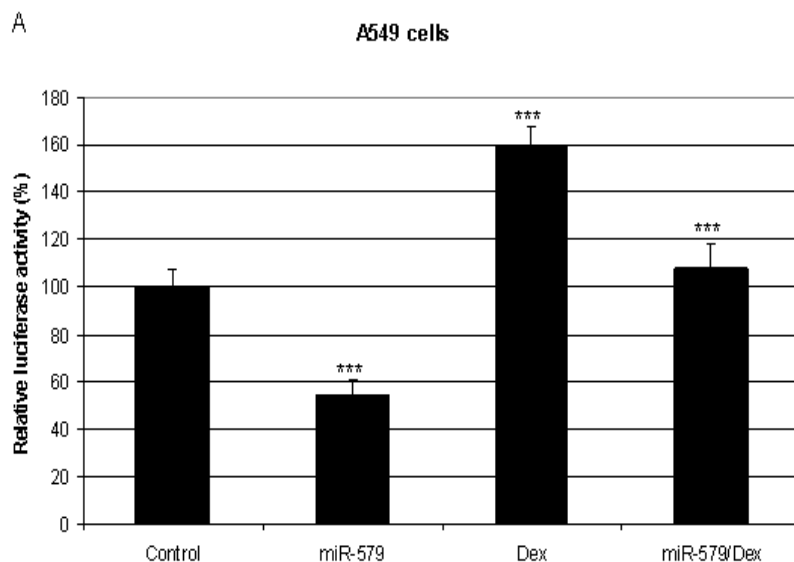


Figure 4.17 Glucocorticoids regulation of *HSD11B1*-Promoter 1 or 2 expression in the dual-luciferase assay system. All results were normalized to luciferase activity in the absence of glucocorticoids which was set to 100%. Results are based on three independent experiments and shown as average \pm SD. Statistical analysis was by student's *t*-test: ***, $p < 0.001$ (Supplement data see Appendix 7.3 Table 7).

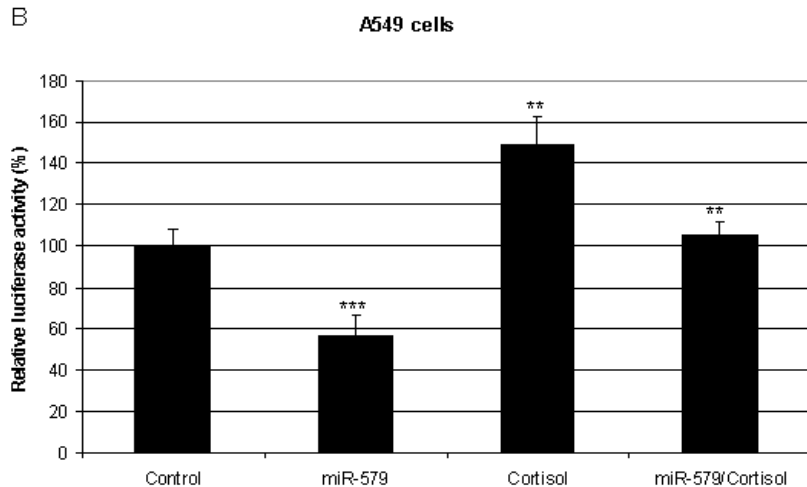
4.11 Hsa-miR-579, but not hsa-miR-561, represses *HSD11B1* expression after induction with glucocorticoids

To investigate the relative influence of glucocorticoids in *HSD11B1* expression versus miRNAs, the pmir-Promoter 2 was transfected alone or cotransfected with hsa-miR-579 or hsa-miR-561 into A549 cells. 4 hours after transfection, the cells were induced with dexamethasone or cortisol and luciferase activities were measured 48 hours after transfection. Relative luciferase activity was significantly decreased by transfection with hsa-miR-579 and increased by induction with dexamethasone or cortisol compared to the control (Figure 4.18A and B). After induction with dexamethasone or cortisol, the relative luciferase activity was still inhibited by hsa-miR-579 compared to induction with dexamethasone or cortisol and absence of miRNAs (Figure 4.18A and B). For hsa-miR-561, the relative luciferase activity was decreased by transfection with hsa-miR-561 and increased by induction with dexamethasone or cortisol compared to the control (Figure 4.18C and D). However, after induction with dexamethasone or cortisol, the relative luciferase activity could not be significantly repressed by hsa-miR-561 compared to induction with dexamethasone or cortisol and absence of miRNAs (Figure 4.18C and D). Therefore, hsa-miR-579 is a more potent repressor than hsa-miR-561. To some extent, hsa-miR-579 could resist the effect of glucocorticoids induction of *HSD11B1* expression.

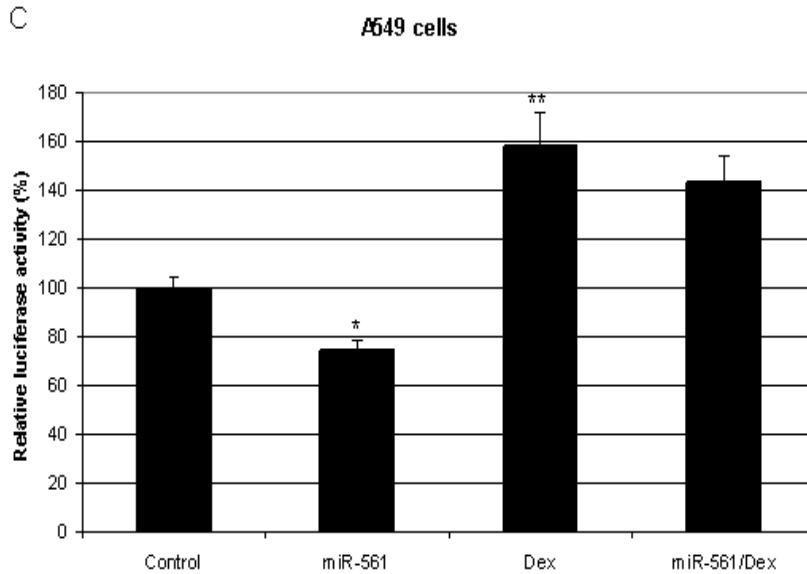


Results

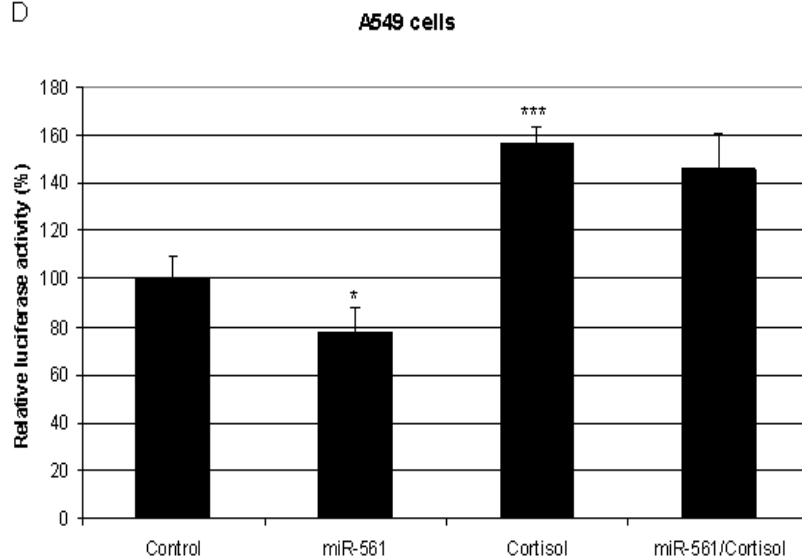
B



C



D



Results

Figure 4.18 Hsa-miR-579, but not hsa-miR-561, represses *HSD11B1* expression after induction with glucocorticoids. (A) The pmir-Promoter 2 was transfected alone or cotransfected with hsa-miR-579 into A549 cells, 4 hours after transfection, the cells were induced with dexamethasone. (B) The pmir-Promoter 2 was transfected alone or cotransfected with hsa-miR-579 into A549 cells, 4 hours after transfection, the cells were induced with cortisol. (C) The pmir-Promoter 2 was transfected alone or cotransfected with hsa-miR-561 into A549 cells, 4 hours after transfection, the cells were induced with dexamethasone. (D) The pmir-Promoter 2 was transfected alone or cotransfected with hsa-miR-561 into A549 cells, 4 hours after transfection, the cells were induced with cortisol. All results were normalized to luciferase activity in the absence of miRNA and glucocorticoids which was set to 100%. Results are based on three independent experiments and shown as average \pm SD. Statistical analysis was by student's *t*-test: *, $p < 0.05$; **, $p < 0.01$; ***, $p < 0.001$ (Supplement data see Appendix 7.3 Table 8).

4.12 Analysis of *HSD11B1* promoter activity

As mentioned previously, *HSD11B1* expression is controlled by two distinct promoters, and *HSD11B1* expression is regulated by many regulatory factors including some proinflammatory cytokines (TNF- α), glucocorticoids (cortisol and dexamethasone), insulin and so on. To explore alternative promoter usages, luciferase constructs containing fragments of *HSD11B1*-Promoter 1 or -Promoter 2, namely the plasmid pmir-Promoter 1 and pmir-Promoter 2 (Figure 4.16) were used in the following experiments. The pmir-Promoter 1 or pmir-Promoter 2 was transfected into A549 cells, 4 hours after transfection, the cells were induced with regulatory factors and detected regulatory factors are listed in Table 4.3. Luciferase activities were measured after 48 hours.

Table 4.3 List of regulatory factors used

Regulatory factors	Concentration
TNF α	50 ng/ml
Insulin	1 μ g/ml
Leptin	50 ng/ml
Resistin	50 ng/ml
Adiponectin	30 ng/ml
Retinoic acid	30 ng/ml
WY14643	300 ng/ml
Vitamin D ₃	500 ng/ml
Ciglitazone	30 ng/ml

Results

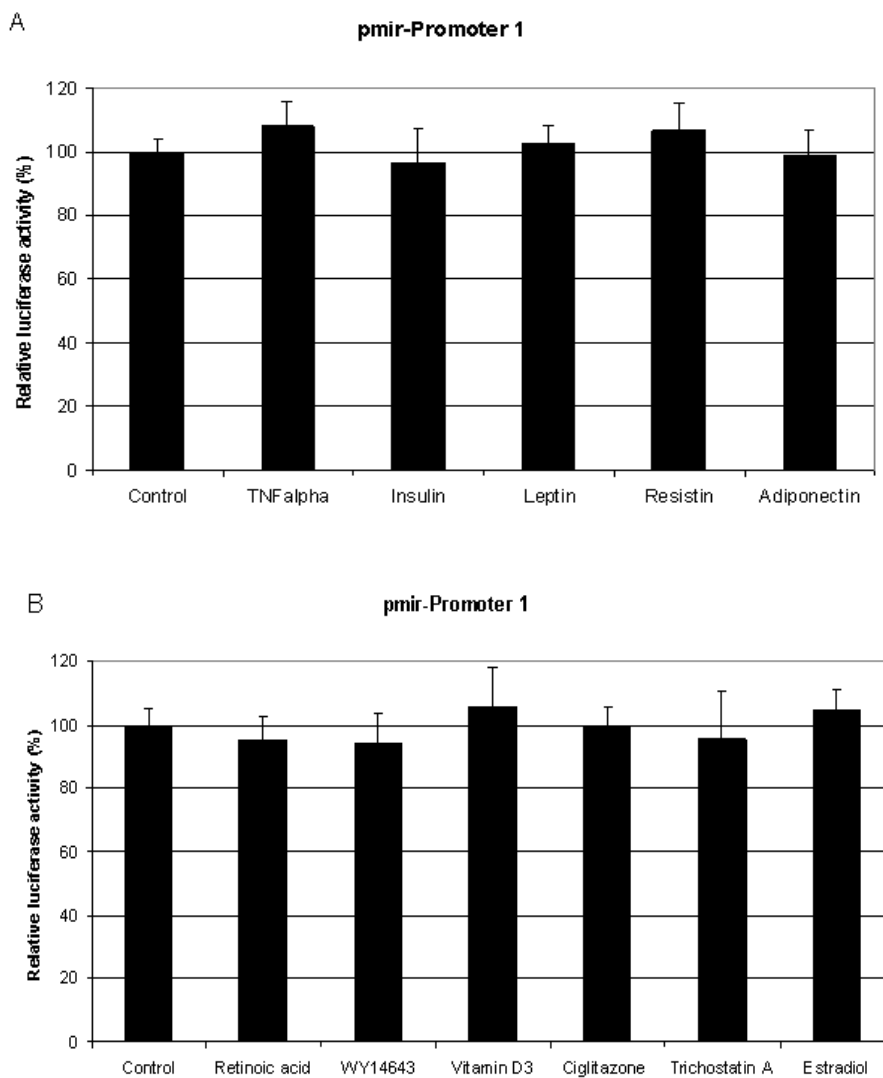
Trichostatin A

30 ng/ml

Estradiol

50 ng/ml

The results show that relative luciferase activities of pmir-Promoter 1 and pmir-Promoter 2 were not changed after induction with TNF α , Insulin, Leptin, Resistin and Adiponectin (Figure 4.19A and C) and Retinoic acid, WY14643, Vitamin D3, Ciglitazone, Trichostatin A, Estradiol (Figure 4.19B and D) compared to the control without induction. In other words, in A549 cells both Promoter 1 and Promoter 2 of *HSD11B1* are not activated by regulatory factors. It is possible that the fragments of Promoter 1 and Promoter 2 do not contain related binding sites of the regulatory factors. Another possibility is that *HSD11B1* expression is not influenced by absence of relative factors which react with regulatory factors in lung cells (A549).



Results

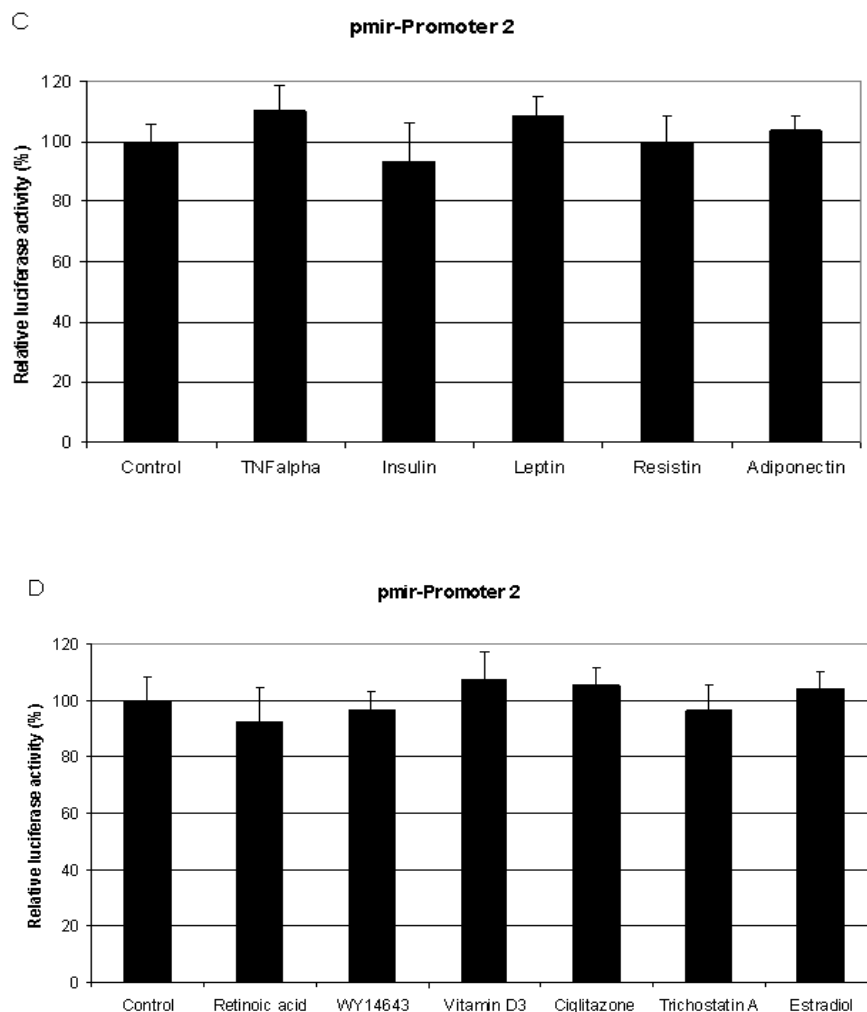


Figure 4.19 Results of luciferase reporter assay for pmir-Promoter 1 and pmir-Promoter 2.

(A) After transfection of pmir-Promoter 1 and induction with $\text{TNF}\alpha$, Insulin, Leptin, Resistin and Adiponectin. (B) After transfection of pmir-Promoter 1 and induction with Retinoic acid, WY14643, Vitamin D₃, Ciglitazone, Trichostatin A and Estradiol. (C) After transfection of pmir-Promoter 2 and induction with $\text{TNF}\alpha$, Insulin, Leptin, Resistin and Adiponectin. (D) After transfection of pmir-Promoter 2 and induction with Retinoic acid, WY14643, Vitamin D₃, Ciglitazone, Trichostatin A and Estradiol. The pmir-Promoter 1 or pmir-Promoter 2 was transfected into A549 cells. 4 hours after transfection, the cells were induced with regulatory factors. All results were normalized to luciferase activity in the absence of regulatory factor which was set to 100%. Results are based on three independent experiments and shown as average \pm SD. (Supplement data see Appendix 7.3 Table 9).

4.13 Detection of endogenous 11 β -HSD1 expression

To investigate the regulation of endogenous human 11 β -HSD1 by hsa-miR-561 and hsa-miR-579, A549 cells (human lung adenocarcinoma cell line) and HepG2 cells (human hepatoma cell line) were used, which are known to express wild-type 11 β -HSD1. The levels of endogenous 11 β -HSD1 expression in A549 cells and HepG2 cells are very low, so 11 β -HSD1 protein was detected after induction with dexamethasone by Western blot analysis. Hsa-miR-579 or hsa-miR-561 was transfected into A549 cells or HepG2 cells. 4 hours after transfection, A549 cells or HepG2 cells were induced with dexamethasone. The cells were harvested 48 hours after transfection. Microsomes and total proteins were isolated from A549 and HepG2 cells, which were used for Western blot analysis. 11 β -HSD1 was detected using microsomes from A549 and HepG2 cells, the results showed that no band was visualized (Figure 4.20A and B). One possibility is that it's difficult to completely extract 11 β -HSD1 from microsomes of the cells. Therefore, the total proteins were used for detection of 11 β -HSD1. The results showed that no band was observed (Figure 4.20C and D). All of Western blot results indicated that 11 β -HSD1 protein is hardly detectable, even A549 and HepG2 cells were induced with dexamethasone (Figure 4.20). However, human liver microsomes (HLM) were used to purify 11 β -HSD1 and large amount of hepatic 11 β -HSD1 was obtained. The purified protein was applied on Western blot and showed a strong signal in Figure 4.20.

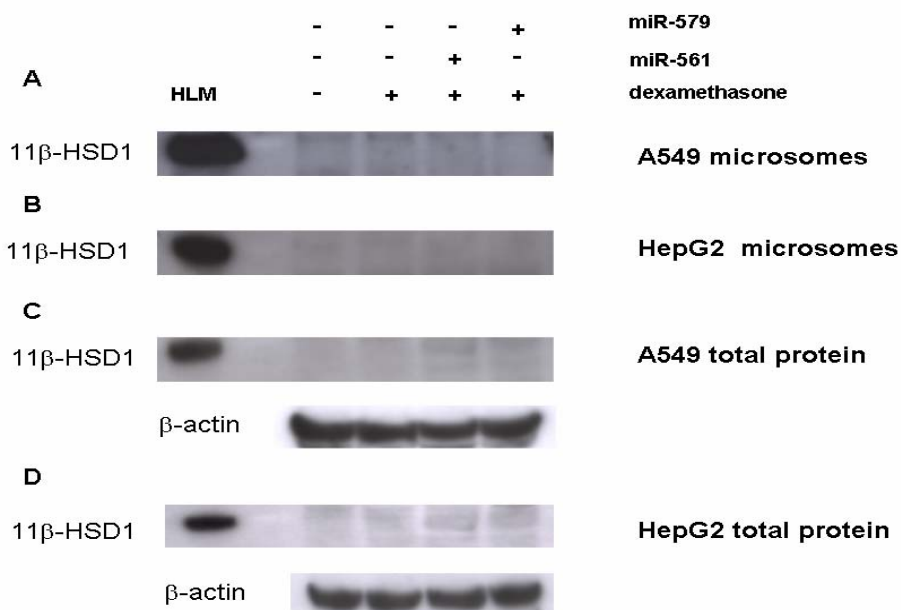


Figure 4.20 Western Blot for detection of 11 β -HSD1 in A549 cells and HepG2 cells. 11 β -HSD1 was detected with microsomes or total proteins using an anti-11 β -HSD1 antibody. β -actin was used as a loading control for detection of total protein. HLM: human liver microsomes were used as positive control. Results are based on three independent experiments (Appendix 7.3 Figure 4).

4.14 Detection of miR-579 and miR-561 in HepG2 cells using the dual-luciferase assay system

Anti-microRNA oligonucleotides (AMOs) were used to determine the presence of miR-579 and miR-561 in HepG2 cells and block endogenous or exogenous miRNAs function. The natural miR-579 and miR-561 sequences can be found in miRBase database (<http://www.mirbase.org/>). The sequences of AMOs used in the study were exactly the same as the antisense sequences of the natural miR-579 and miR-561. These oligonucleotide sequences are listed in Table 4.4.

Table 4.4 The sequences of mature miR-579, AMO-579 and DNA-579 and mature miR-561, AMO-561 and DNA-561

Name	Sequence
miR-579	5'-UUCAUUUGGUAUAAACCGCGAUU-3'
AMO-579	5'-AATCGCGGTTTATAACCAAATGAA-3'
DNA-579	5'-TTCATTTGGTATAAACCGCGATT-3'
miR-561	5'-CAAAGUUUAAGAUCUUGAAGU-3'
AMO-561	5'-ACTTCAAGGATCTTAACTTTG-3'
DNA-561	5'-CAAAGTTTAAGATCCTTGAAGT-3'

The experiment was performed as follows: the plasmid pmir-HSD11B1-3'UTR was transfected alone or cotransfected with miR-579, miR-579/AMO-579, AMO-579 and DNA-579, respectively. The sequence of mature miR-579, AMO-579 and DNA-579 are listed in Table 4.4. In agreement with previous results, relative luciferase activity was significantly suppressed by about 40% by miR-579 compared with absence of miRNA (Figure 4.21A). AMO-579 could block the repression by miR-579 due to hybridization with miR-579 (Figure 4.21A). Moreover, the luciferase activity was significantly increased about 20% by AMO-579. Obviously, this was due to blocking endogenous miR-579 function (Figure 4.21A). The luciferase activity was unchanged by DNA-579 (Figure 4.21A).

The same experiments were carried out by miR-561, and a similar result was obtained. Relative luciferase activity was significantly suppressed by about 20% by miR-561 compared with absence of miRNA (Figure 4.21B). AMO-561 could block the repression by miR-561 (Figure 4.21B). Moreover, the luciferase activity was significantly increased about 20% by

Results

AMO-561 (Figure 4.21B). The luciferase activity was unchanged by DNA-561 (Figure 4.21B). These results indicated that miR-579 and miR-561 are present in HepG2 cells indirectly.

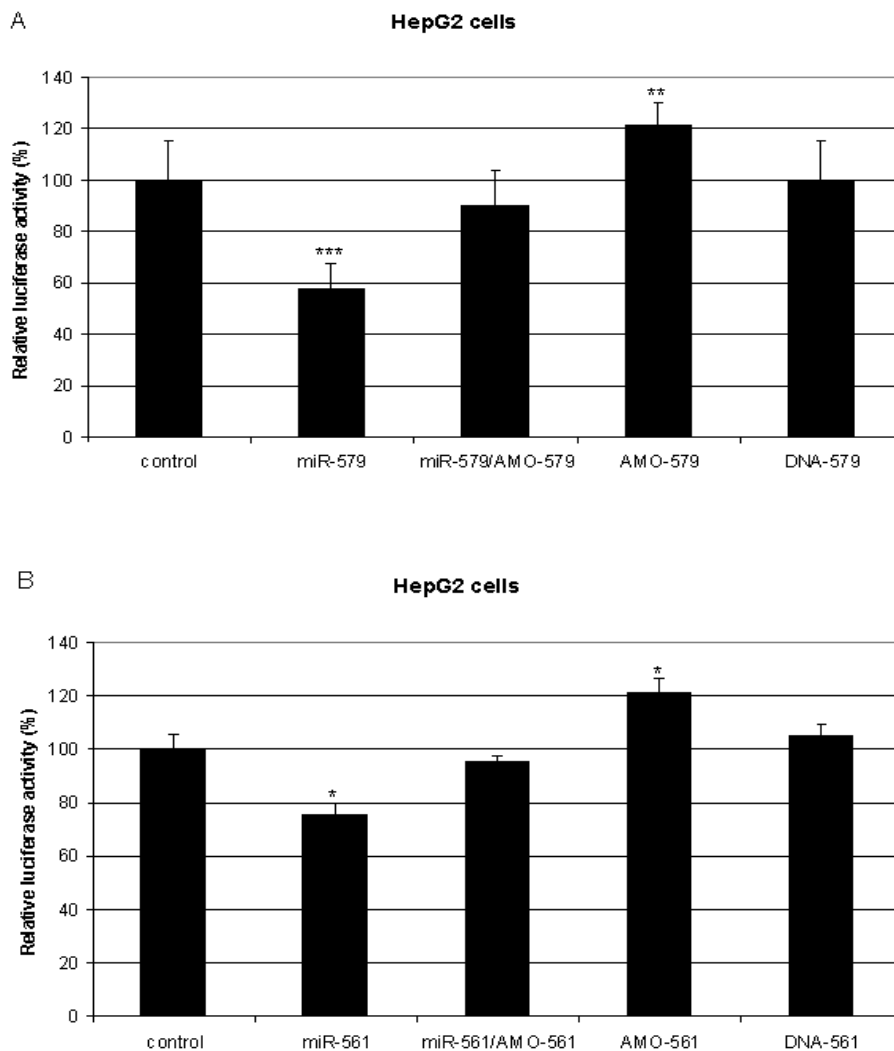


Figure 4.21 Results of luciferase reporter assay with AMOs in HepG2 cells.

(A) The plasmid pmir-HSD11B1-3'UTR was transfected alone or cotransfected with miR-579, miR-579/AMO-579, AMO-579 and DNA-579, respectively. (B) The plasmid pmir-HSD11B1-3'UTR was transfected alone or cotransfected with miR-561, miR-561/AMO-561, AMO-561 and DNA-561, respectively. Luciferase activities were measured 48 hours after transfection. All results were normalized to luciferase activity in the absence of miRNA which was set to 100%. Results are based on three independent experiments and shown as average \pm SD. Statistical analysis was by student's *t*-test: *, $p < 0.05$; **, $p < 0.01$; ***, $p < 0.001$ (Supplement data see Appendix 7.3 Table 10).

4.15 Detection of miR-561 and miR-579 in human hepatocytes and HepG2 cells by Northern Blot

To detect hsa-miR-561 or hsa-miR-579 in human hepatocytes and HepG2 cells, Northern blot analysis was carried out using a radioactive-labeled (γ - ^{32}P -ATP) DNA oligonucleotides as probe. DNA-561 and DNA-579 were used as positive controls. The sequences of DNA oligonucleotides used in this work are listed in the Material Table 3.4. When 10 μg of total RNA was loaded for each sample, both hsa-miR-561 and hsa-miR-579 remained undetected in human hepatocytes and HepG2 cells by Northern blot analysis (Figure 4.22). However, 20 ng of both positive controls, DNA-561 and DNA-579, showed strong signals (Figure 4.22).

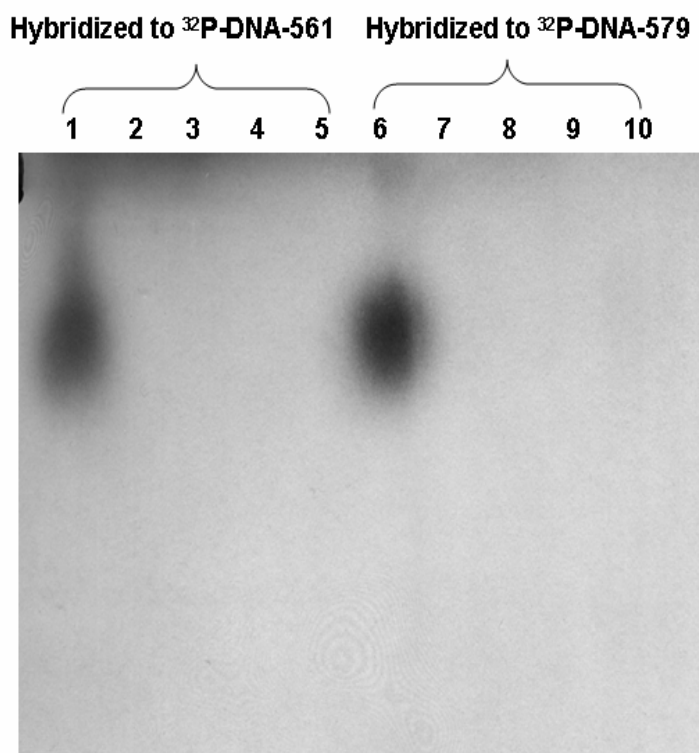


Figure 4.22 Detection of miRNAs expression by Northern blot. 10 μg of total RNA of human hepatocytes and HepG2 cells were separated on 2% agarose/formaldehyde gel, transferred onto a nylon membrane and hybridized with γ - ^{32}P -ATP-radioactive-labelled probe. 1: DNA-561 (20 ng) as positive control; 2:- ; 3: Human hepatocytes RNA (BMI: 35.4); 4: Human hepatocytes RNA (BMI: 29.4); 5: HepG2 cells RNA; 6: DNA-579 (20 ng) as positive control; 7:- ; 8: Human hepatocytes RNA (BMI: 35.4); 9: Human hepatocytes RNA (BMI: 29.4); 10: HepG2 cells RNA; Results are based on three independent experiments (Appendix 7.3 Figure 5).

4.16 Detection of miR-561 and miR-579 in human hepatocytes and HepG2 cells by RT-PCR

RT-PCR was used to assess the presence of hsa-miR-561 or hsa-miR-579 in human hepatocytes and HepG2 cells. For the detection of miRNAs by RT-PCR, a stem-loop primer specific to the interest miRNA for reverse transcription (RT) and a miRNA-specific forward primer and a specific reverse primer were used for PCR amplification (Figure 4.23). The RT-PCR results showed that specific bands were obtained for amplifying miR-561 and miR-579 from total RNA of human hepatocytes and HepG2 compared with negative control, no genomic amplification (Figure 4.24A) or no template control (Figure 4.24B). Sequences of all the primers are confidential in Ambion (Applied Biosystems, Germany). Therefore, the exact size of the expected amplicons upon RT-PCR amplification can only roughly be determined as being lower than 97 or 98 base pairs, which corresponds to the precursor miRNAs size of miR-561 and miR-579, respectively.

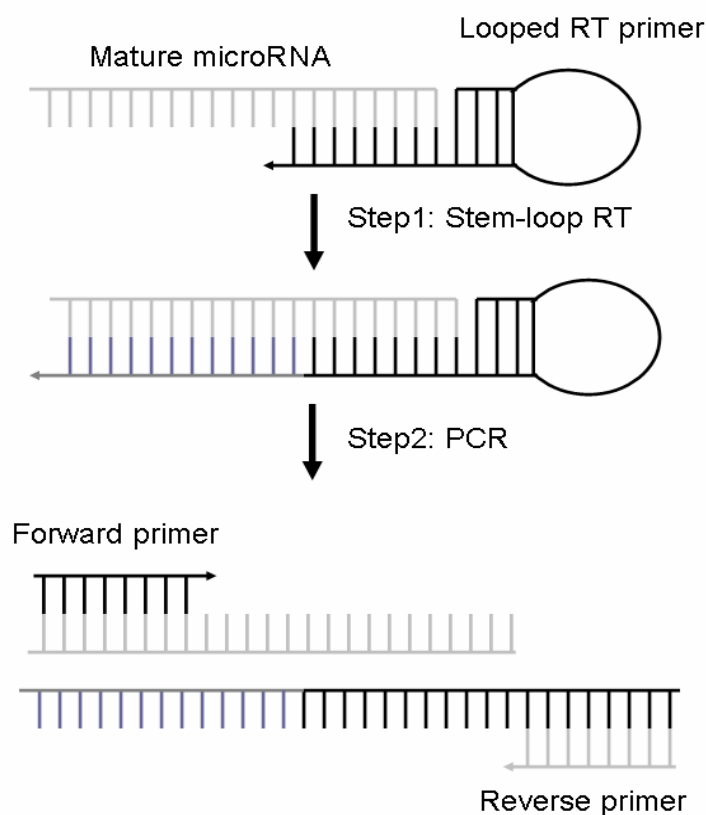


Figure 4.23 Schematic of RT-PCR primers design (from Ambion).

Results

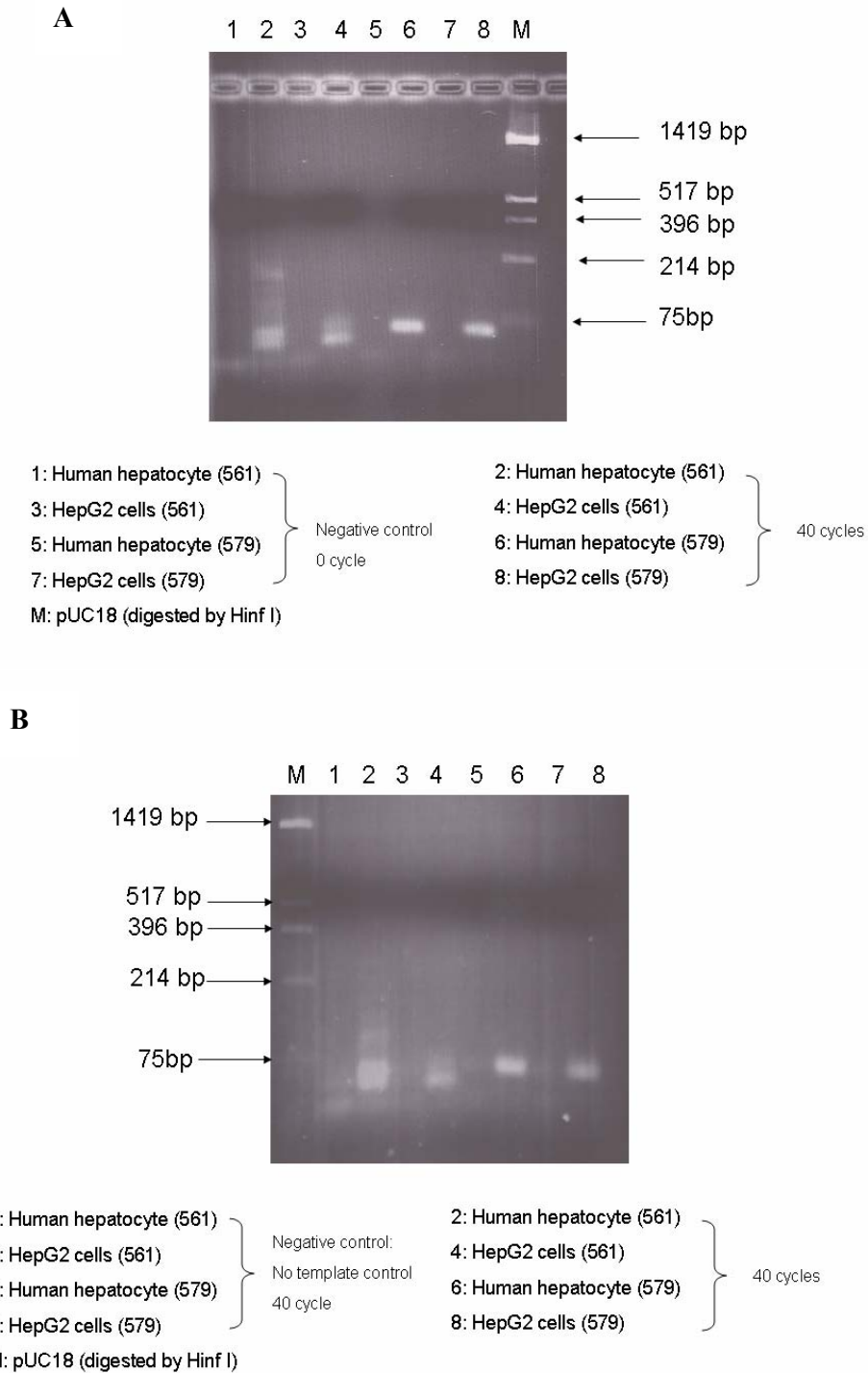
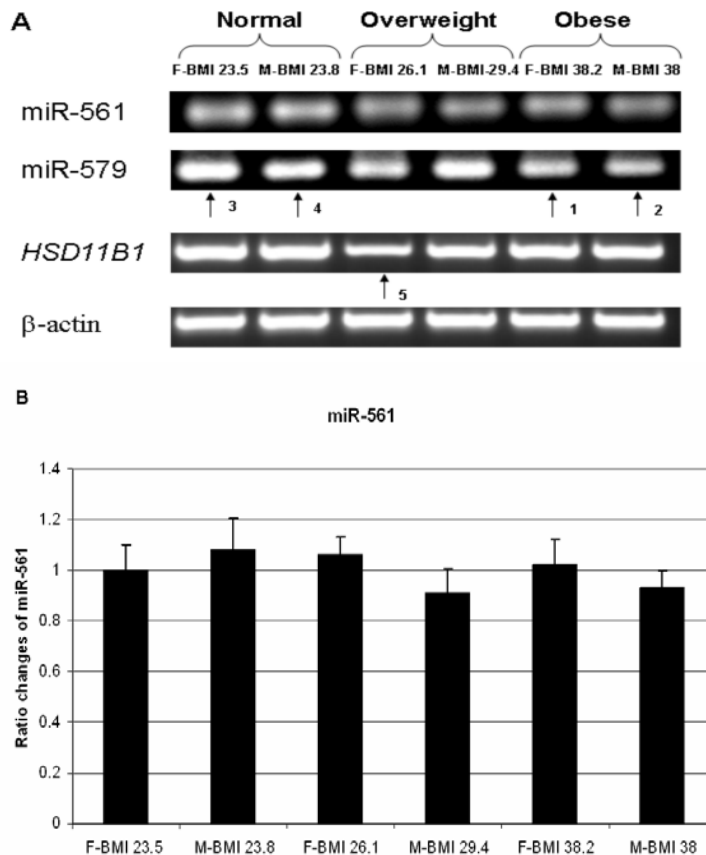


Figure 4.24 RT-PCR results. RT-PCR was carried out by cDNA synthesis and PCR. Results are based on three independent experiments (Appendix 7.3 Figure 6). The bands were obtained in the 75 bp region correspond to the expected miR-561 (lanes 2 and 4) and miR-579 (lanes 6 and 8).

4.17 Potential transcription of miRNAs in hepatocytes with different BMI

Body Mass Index (BMI) is a simple index of weight-for-height that is commonly used to classify underweight, normal, overweight and obesity in adults. It is defined as the weight in kilograms divided by the square of the height in metres (kg/m^2). The world health organization (WHO) regards a BMI range from 18.5 to 24.99 as normal weight, while a BMI between 25 and 30 is considered overweight and above 30 is considered obese. To test the potential transcription of miR-561 and miR-579 in hepatocytes, six different BMI hepatocyte samples were used, they are Female BMI 23.5 (normal weight, age 27), Male BMI 23.8 (normal weight, age 48), Female BMI 26.1 (overweight, age 25), Male BMI 29.4 (overweight, age 48), Female BMI 38.2 (obese, age 37) and Male BMI 38 (obese, age 54), respectively. Transcriptions of miR-561, miR-579 and *HSD11B1* mRNA were generated by semi-quantitative RT-PCR. The results showed that miR-561 transcriptions were in the similar levels in hepatocytes with different BMI (Figure 4.25A and B). However, miR-579 transcriptions were significantly lower in both female and male obese people (Figure 4.25A, arrow 1 and 2) than in the corresponding female and male of normal weight people (Figure 4.25A and C, arrow 3 and 4). Furthermore, in five BMI hepatocyte samples, *HSD11B1* mRNA transcriptions were at the same levels, whereas the sample of female BMI 26.1 showed a low level (Figure 4.25A and D, arrow 5).



Results

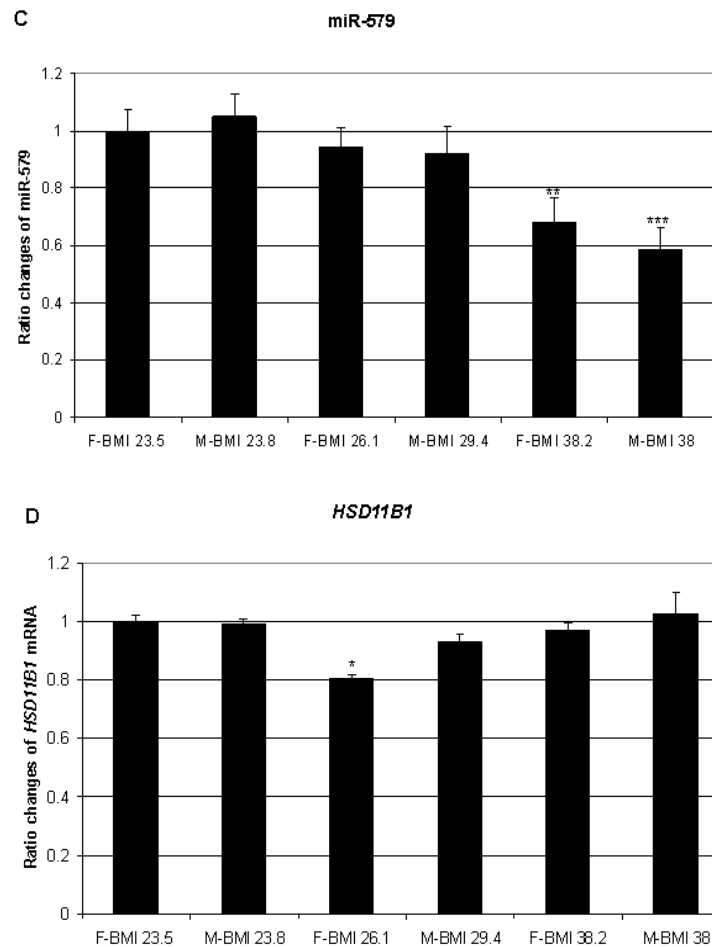


Figure 4.25 The levels of miR-561, miR-579 and *HSD11B1* mRNA transcription were semi-quantified by RT-PCR. (A) RT-PCR results. (B), (C) and (D) Results were semi-quantified by determination of band intensity using GIMP 2.6 (GNU Image Manipulation Program) and shown as average \pm SD. β -actin was used as a loading control in semi-quantitative RT-PCR. Results are based on three independent experiments (Appendix 7.3 Figure 7)

4.18 Pathway enrichment analysis

MiRNAs are characterized by considerable target multiplicity, *i.e.* each miRNA might regulate the expression of up to 100 different target mRNAs. Here, DIANA-mirPATH (<http://diana.cslab.ece.ntua.gr/pathways/>, Papadopoulos *et al.*, 2009) was used for miRNA target gene-based pathway enrichment analysis. Six Kyoto Encyclopedia of Genes and Genomes (KEGG) pathways were statistically overrepresented for both hsa-miR-561 and hsa-miR-579, namely Ubiquitin-mediated proteolysis, Long-term potentiation, Insulin signalling pathway, Melanogenesis, Tight junction and Axon guidance (Table 4.5). The enrichment of twelve KEGG pathways were found for hsa-miR-561 alone, namely Prion disease, Colorectal

Results

cancer, Long-term depression, ErbB signalling pathway, mTOR signalling pathway, Prostate cancer, TGF-beta signalling pathway, Renal cell carcinoma, Focal adhesion, Nicotinate and nicotinamide metabolism, Neurodegenerative Disease, and finally Wnt signalling pathway (Table 4.5). The three enriched KEGG pathways were only found for hsa-miR-579, including Dorso-ventral axis formation, Calcium signalling pathway, and Methane metabolism (Table 4.5). Mostly, at least four genes contributed to the enrichments, with the exception of Methane metabolism, where only two genes contributed to the enrichment (Table 4.5). Furthermore, *HSD11B1* itself did not contribute to any enrichment.

Table 4.5 Pathway Enrichment Analysis of predicted target genes of hsa-miR-561 and hsa-miR-579. The Pathway Enrichment Analysis was carried out using analysis of multiple miRNAs in DIANA-mirPATH with DIANA-microT-4.0 as target prediction software. Only results with a $-\ln(p\text{-value}) > 3$ are shown (corresponding to $p < 0.05$).

KEGG pathway (ID)	Found genes	$-\ln(p\text{-value})$	Gene names
hsa-miR-561			
Ubiquitin mediated proteolysis (hsa04120)	18	14.3	SOCS1, UBE2G1, UBE1, MAP3K1, UBE2Q2, BIRC6, UBE2E3, UBE2E4P, UBE2I, UBE2W, CUL4A, CUL2, SOCS3, UBE1L2, CBLB, HUWE1, UBE2D3, CUL4B, UBE2A
Prion disease (hsa05060)	4	8.8	BCL2, PRNP, LAMC1, NFE2L2
Colorectal cancer (hsa05210)	11	7.45	MSH6, BCL2, PIK3CA, PDGFRA, KRAS, CASP9, FZD1, FZD4, AKT3, CTNNB1, SMAD3
Long-term depression (hsa04730)	10	7.34	GNAI2, PPP2R2B, KRAS, GNAS, PRKG1, GRIA2, NOS1, GRID2, IGF1, PPP2CB
Long-term potentiation (hsa04720)	9	7.31	RPS6KA1, KRAS, PRKX, ENSG00000143933, GRIA2,

Results

			RAP1B, PPP3CA, RPS6KA3, EP300
ErbB signaling pathway (hsa04012)	11	7.13	CDKN1B, PIK3CA, KRAS, PAK2, CBLB, NRG1, ERBB4, PAK7, RPS6KB1, ENSG00000109321, AKT3
Insulin signaling pathway (hsa04910)	14	5.97	IRS2, PIK3CA, SOCS1, ENSG00000143933, PFKP, KRAS, SORBS1, PRKX, PRKAA1, SOCS3, RHOQ, CBLB, RPS6KB1, AKT3
mTOR signaling pathway (hsa04150)	7	5.9	PIK3CA, RPS6KA1, PRKAA1, RPS6KA3, IGF1, RPS6KB1, AKT3
Prostate cancer (hsa05215)	10	5.26	BCL2, CDKN1B, PIK3CA, PDGFRA, KRAS, CASP9, IGF1, EP300, AKT3, CTNNB1
TGF-beta signaling pathway (hsa04350)	10	5.14	PPP2R2B, ID2, RHOA, ID3, ACVR1, ACVR2A, EP300, RPS6KB1, PPP2CB, SMAD3
Renal cell carcinoma (hsa05211)	8	4.41	PIK3CA, KRAS, CUL2, PAK2, RAP1B, PAK7, EP300, AKT3
Focal adhesion (hsa04510)	16	4.25	BCL2, COL6A3, PIK3CA, PDGFRA, RHOA, KDR, PAK2, RAP1B, COL5A2, ENSG00000101608, ARHGAP5, LAMC1, IGF1, PAK7, AKT3, CTNNB1
Melanogenesis (hsa04916)	10	4.17	GNAI2, KRAS, GNAS, ENSG00000143933, PRKX, KITLG, FZD1, FZD4, EP300, CTNNB1

Results

Nicotinate and nicotinamide metabolism (hsa00760)	4	4.12	NADK, PBEF1, C9orf95, NNT
Tight junction (hsa04530)	12	3.83	MYH3, GNAI2, MAGI2, PPP2R2B, RHOA, KRAS, ASH1L, CASK, AKT3, CTNNB1, PPP2CB, ENSG00000101608
Axon guidance (hsa04360)	11	3.46	GNAI2, NTN4, SLIT1, ABLIM1, UNC5C, RHOA, KRAS, NRP1, PAK2, PPP3CA, PAK7
Neurodegenerative Diseases (hsa01510)	5	3.34	BCL2, NR4A2, PRNP, UCHL1, EP300
Wnt signaling pathway (hsa04310)	12	3.09	NKD1, PPP2R2B, RHOA, PRKX, SFRP2, PPP3CA, FZD1, FZD4, EP300, PPP2CB, CTNNB1, SMAD3

KEGG pathway (ID)	Found genes	$-\ln(p\text{-value})$	Gene names
hsa-miR-579			
Melanogenesis (hsa04916)	15	9.66	CSDE1, FZD5, EDNRB, EDN1, ENSG00000143933, ENSG00000198668, MITF, KITLG, PLCB1, PLCB4, FZD4, CREB1, GNAI1, PRKACB, FZD10
Long-term potentiation (hsa04720)	11	9.1	CSDE1, GRIA1, GRIN2A, ENSG00000143933, ENSG00000198668, PPP1CC, RAP1A, PLCB1, PLCB4, RPS6KA3,

Results

			PRKACB
Insulin signaling pathway (hsa04910)	16	5.92	IRS2, CSDE1, PFKP, RHEB, FRAP1, ENSG00000143933, SREBF1, SORBS1, ENSG00000198668, RHOQ, PPP1CC, PPP1R3A, PRKAA1, PRKAB2, RPS6KB1, PRKACB
Tight junction (hsa04530)	15	5.11	MAGI3, OCLN, CSDE1, YES1, PPP2R3A, CLDN11, PTEN, PTENP1, CLDN18, CLDN8, CDC42, PARD6B, INADL, GNAI1, EPB41, MAGI1
Dorso-ventral axis formation (hsa04320)	5	4.6	FMN2, NOTCH2, SPIRE1, ETV6, ERBB4
Axon guidance (hsa04360)	13	3.79	EFNB2, SEMA3G, CSDE1, ITGB1, LRRC4C, SEMA6D, SRGAP2, SEMA3D, NRP1, CDC42, NFAT5, EPHB1, GNAI1
Calcium signaling pathway (hsa04020)	16	3.76	PDE1C, PLN, PDGFRA, EDNRB, ATP2B1, HTR7, ENSG00000143933, PLCB1, PTGER3, NTSR1, PLCB4, GRIN2A, PRKACB, ENSG00000198668, ERBB4, VDAC3
Ubiquitin mediated proteolysis (hsa04120)	13	3.32	UBE2D1, UBE2M, UBE4A, UBE3A, UBE2Z, BIRC6, UBE1C, FBXW7, TRIM37, CUL5, ITCH, BIRC4, CUL4B
Methane metabolism (hsa00680)	2	3.2	PRDX6, SHMT2

5 Discussion

5.1 miRNA prediction tools

Tissue-specific regulation of *HSD11B1* expression is not fully understood. Particularly the mechanisms underlying hepatic downregulation of *HSD11B1* expression in obese patients displaying increased 11 β -HSD1 in adipose tissue remain an enigma. As miRNA expression is highly tissue-specific manner and regulation by miRNAs is predominantly negative, miRNAs targeting *HSD11B1* are clearly interesting candidates in this context, but have till now not been assessed. Four different web-based tools were used for miRNA target prediction, searching for miRNA response elements (MREs) in the 3'UTR of human *HSD11B1* mRNA. Finally, four candidate miRNAs, hsa-miR-561, hsa-miR-579, hsa-miR-340 and hsa-miR-181b, were selected for functional analysis.

The selection for functional analysis was based on two mains: First, every miRNA predicted by all four tools was included and additionally, two miRNAs predicted by three of four tools were included because they had been shown to be expressed in hepatocytes (Hausser *et al.*, 2009; Landgraf *et al.*, 2007), a major site of *HSD11B1* expression *in vivo*. Functional analysis based on a dual luciferase assay system identified two miRNAs as potential novel regulators of *HSD11B1* expression, namely hsa-miR-561, and hsa-miR-579. Experiments using MRE-deleted and MRE-mutated vector constructs showed that the binding of both miRNAs to the predicted MREs was specific. Of note, both these miRNAs had been identified initially by all four predicted tools used in this study (Table 4.1). In contrast, hsa-miR-181b, which was identified by three of four prediction tools, did not bind to the 3'UTR of *HSD11B1* mRNA at all. Another candidate miRNA, hsa-miR-340, was also identified by three of four prediction tools, and suppressed luciferase activity significantly (Figure 4.6). However, experiments with mutant luciferase constructs showed that suppression of luciferase activity by hsa-miR-340 was not due to specific binding to the predicted MREs in the 3'UTR of *HSD11B1* mRNA (Figure 4.8C and 4.9C). Supplementary experiments with the original, *HSD11B1*-3'UTR-deficient vector, showed that hsa-miR-340, but neither hsa-miR-561 nor hsa-miR-579, already leads to suppression of luciferase activity when the 3'UTR of *HSD11B1* mRNA is absent in the vector (Figure 4.10).

In summary, hsa-miR-561 and hsa-miR-579 inhibited luciferase activity due to specific binding to the 3'UTR of *HSD11B1* mRNA, but none of the miRNAs identified by three of

four prediction tools only showed specific binding to the corresponding MRE in the 3' UTR of *HSD11B1* mRNA.

Of the two miRNAs identified, hsa-miR-579 was the more potent regulator, resulting in repression by about 40% in the luciferase reporter assay. This is furthermore emphasized by the fact that, in contrast to hsa-miR-561, hsa-miR-579 is also capable of significantly downregulating *HSD11B1* expression after induction with glucocorticoids (Figure 4.18). It is worth mentioning at this point that two prediction tools, namely DIANA micro-T and MicroCosm Targets, predicted each an additional, albeit not identical, binding site for hsa-miR-579. By deleting as well as mutating only the best-ranked binding site here, we observed complete abolishment of the repression, implying that only this binding site is valid. Hsa-miR-579 has to date been mentioned very little in the literature. One study showed downregulation of hsa-miR-579 and simultaneous upregulation of predicted target genes in fibroblasts in response to high dose X-ray radiation (Maes *et al.*, 2008). A more recent study has identified hsa-miR-579 as a negative regulator of TNF- α in a monocyte line model of endotoxin tolerance, which provides a link between expression of hsa-miR-579 and inflammatory disease, where expression of *HSD11B1* often is deregulated (Staab *et al.*, 2010; El Gazzar *et al.*, 2010).

It is striking that only the two miRNAs identified by all four prediction tools truly bound to the predicted 3'UTR MREs of the *HSD11B1* transcript, and none of the two additionally tested, both identified by only three of four tools. This validates the overall approach of applying several prediction tools in parallel which differ considerably in the applied search algorithms and criteria for ranking (Bartel, 2009). The obtained results also emphasize the usefulness of integrating the conservation profile of the corresponding 3'UTR into the scoring, as both hsa-miR-561 and -579 ranked highest in the applications DIANA-microT-ANN and Target Scan, where conservation of the 3'UTR is a main criterion for scoring (Maragkakis *et al.*, 2009; Lewis *et al.*, 2003).

5.2 Dual-luciferase assay system

In this study, the pmir-GLO, dual-luciferase miRNA target expression vector, is used to quantitatively evaluate miRNA activity by the insertion of miRNA target sequence on the downstream of the firefly luciferase gene. Firefly luciferase is the primary reporter gene; decrease of firefly luciferase expression indicates that miRNAs bind to the cloned miRNA

Discussion

target sequence. Another reporter gene, *Renilla* luciferase is acting as a control reporter for normalization. The map of pmir-GLO vector is shown in Appendix 7.1.2. Normalizing the expression of firefly luciferase (experimental reporter) to the expression of *Renilla* luciferase (control reporter) can differentiate between specific and non-specific cellular responses. This dual-luciferase assay system is mainly applied for miRNA binding site analysis, 3'UTR analysis, miRNA detection and miRNA function analysis through monitoring luciferase gene expression. The feature of this dual-luciferase assay system is quick, easy and sensitive to measure the function of miRNA and miRNA binding sites.

How does the dual-luciferase assay system work? In this assay system, firefly and *Renilla* luciferases contain distinct evolutionary origins and have very different enzyme structures and need different substrates. According to these differences, two luciferases can be measured in succession, with firefly luciferase luminescence elicited by one reagent, while the second reagent simultaneously quenches the firefly luciferase and elicits *Renilla* luciferase luminescence. Luminescence of firefly luciferase requires beetle luciferin, magnesium, ATP and molecular oxygen, while *Renilla* luciferase requires only coelenterate luciferin and molecular oxygen (Figure 5.1; <http://www.promega.com>).

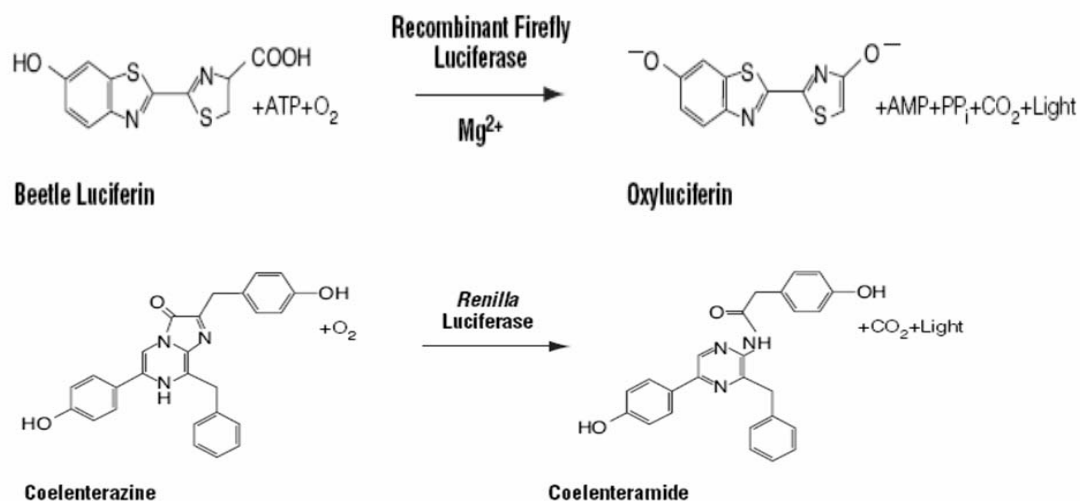


Figure 5.1 Bioluminescent reactions catalyzed by firefly and *Renilla* luciferases.

Mono-oxygenation of beetle luciferin is catalyzed by firefly luciferase in the presence of ATP, Mg²⁺ and molecular oxygen. Unlike beetle luciferin, mono-oxygenation of coelenterazine is catalyzed by *Renilla* luciferase only requires molecular oxygen.

Discussion

Recently, dual-luciferase assay system is extensively used to study miRNA functions. For example, studies by Le *et al.* (2009) demonstrated that miR-125b-mediated down-regulation of p53 in both human and zebrafish is strictly dependent on the binding of miR-125b to microRNA response elements (MREs), which are in the 3'UTR of p53 mRNA. Rogler *et al.* (2009) reported that miR-23b target 3'UTR of Smad (mothers against decapentaplegic homolog) 3, 4 and 5. Dual luciferase reporter assays confirmed down-regulation of constructs containing Smad 3, 4, or 5, 3' UTRs by a mixture of miR-23b cluster mimics. Another study showed that miR-196 directly acts on the 3'UTR of Bach1 mRNA and translationally represses the expression of this protein (Hou *et al.*, 2010). Dual-luciferase reporter assay demonstrated that transfection of miR-196 mimic resulted in a significant decrease in Bach1 3'UTR-dependent luciferase activity, but not in mutant Bach1 3'UTR-dependent luciferase activity. Moreover, there was no detectable effect of mutant miR-196 on Bach 3'UTR-dependent luciferase activity (Hou *et al.*, 2010).

In the present study, dual-luciferase reporter assay demonstrated that in HepG2 and A549 cells miR-579 and miR-561 down-regulate 11 β -HSD1 expression due to binding to 3'UTR of *HSD11B1* mRNA (Figure 4.6). The effect of miR-579 and miR-561 was abolished when the corresponding microRNA (miR-579 and miR-561) response elements (MREs) were deleted or mutated in the 3'UTR of *HSD11B1* mRNA (Figure 4.8 and 4.9). These data indicated that the predicted MREs are critical for the direct and specific binding of miR-579 and miR-561 to the *HSD11B1* mRNA. Though luciferase assays could be used to demonstrate physical interaction between miRNA and mRNA, it's not available to directly prove it by using this system. To investigate the regulation of endogenous human 11 β -HSD1 expression by miR-579 and miR-561, A549 and HepG2 cell lines were used, which are known to express wild-type 11 β -HSD1. Normally, the level of endogenous 11 β -HSD1 is very low in A549 and HepG2 cell lines (Staab *et al.*, 2011) and it is very hard to detect 11 β -HSD1 by Western blot. *HSD11B1* mRNA was increased after induction with dexamethasone (Figure 4.14) and 11 β -HSD1 was increased after induction with dexamethasone proved by dual-luciferase assay system (Figure 4.17). Therefore, it might be possible to detect 11 β -HSD1 after induction with dexamethasone. However, Western blot results were very disappointing (Figure 4.20), 11 β -HSD1 was undetected using microsomes and total cell proteins from A549 and HepG2 cells, while 11 β -HSD1 was detected using human liver microsomes as positive control. In addition, the homogenous time-resolved fluorescence (HTRF) assay was also used for the detection of cortisol activity. This method could be used to prove 11 β -HSD1 activity indirectly.

Unfortunately, HTRF assay failed to detect the cortisol activity in microsomes from A549 and HepG2 cells (data not shown). In other words, it failed to detect endogenous 11 β -HSD1 expression in A549 and HepG2 cells using Western blot and HTRF assay. The main reason is low expression of 11 β -HSD1 in A549 and HepG2 cells (Staab *et al.*, 2011).

5.3 Mechanism of miRNA-mediated suppression: mRNA degradation or translational repression

MiRNAs can downregulate gene expression by either of two posttranscriptional mechanisms: mRNA degradation or translational repression. In plants, miRNAs complement with corresponding mRNA targets precisely, resulting in cleavage and destruction of the target mRNAs. In animals, complementarity of miRNAs and target mRNAs is generally imperfect (Lai, 2004), but partial complementarity is sufficient to trigger target mRNA degradation (Bagga *et al.*, 2005; Du *et al.*, 2005, Lim *et al.*, 2005) or translational repression. In animals, some miRNAs, such as miR-196 inhibits *HOXB8* expression by cleavage of *HOXB8* mRNA in mouse embryos (Yekta *et al.*, 2004). However, translational repression seems to be the key approach in animals (Bartel, 2004). In this study, miR-561 and miR-579 bound to the 3'UTR of *HSD11B1* mRNA with imperfect complementarity (Figure 4.7). A comparison of firefly (reporter) and *Renilla* (control) luciferase mRNA levels with the corresponding luciferase activities (Figures 4.11 and 4.6) demonstrated that the regulatory mechanism is mainly translational repression-based, which is the main mechanism for metazoan miRNAs (Bartel, 2004). Furthermore, the levels of endogenous *HSB11B1* mRNA are not affected by hsa-miR-561 and hsa-miR-579 (Figure 4.12). Collectively, the results show that the mechanism of miRNA-mediated suppression of *HSD11B1* expression is based on translational repression (Figure 5.2).

Up to date, miR-579 has been mentioned very little in the literature. One study by EI Gazzar *et al.* identified that miR-579 binds to the 3'UTR of TNF α . Expression profiling revealed that miR-221, miR-579, and miR-125b were selectively induced in LPS-tolerant cells, and miR-221 accelerates TNF α mRNA degradation, whereas miR-579 and miR-125b block TNF α translation (EI Gazzar *et al.*, 2010). Thus, the mechanism of miR-579-mediated suppression of TNF α expression is the same as that in *HSD11B1* expression: translational repression. For miR-561, there is no related report its downregulation of gene expression.

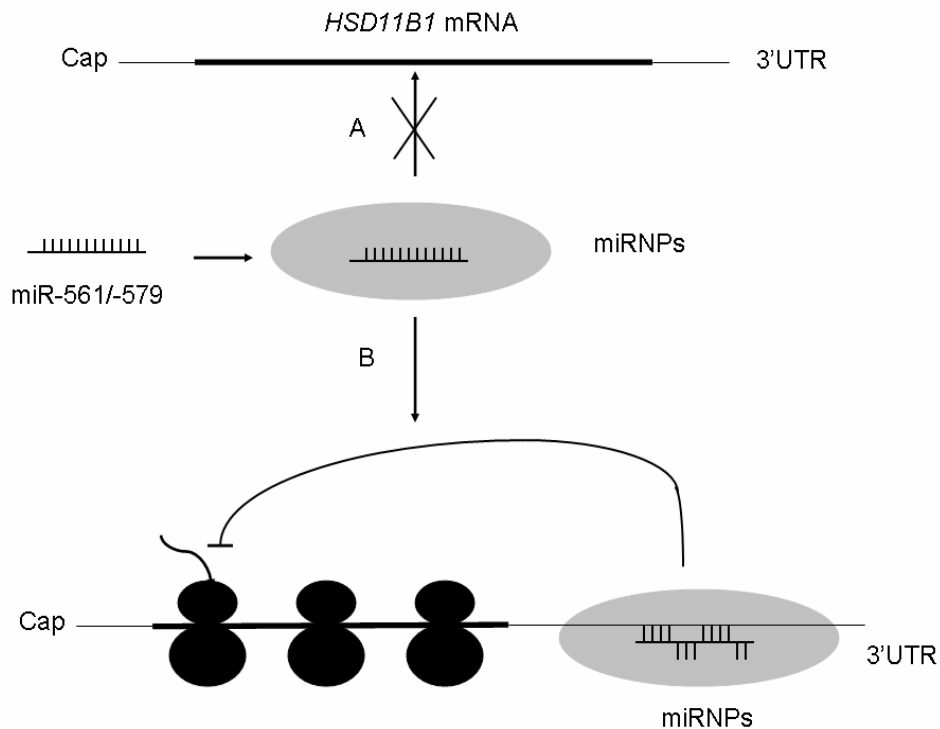


Figure 5.2 Mechanism of miR-561/-579-mediated suppression in *HSD11B1* expression.

A: mRNA degradation B: translational repression. Repression of *HSD11B1* expression by miR-561 and -579 occurs at the translational level, but not at the transcriptional level.

In the introduction section, it has been mentioned that miRNAs can repress protein expression in all steps of mRNA translation, including inhibition of translational initiation, inhibition of translational elongation, premature termination of translation (like ribosome drop-off) or proteolysis (degradation of nascent peptide) (Figure 1.6). In this study, the mechanism of miR-579 and miR-561-mediated downregulation of *HSD11B1* expression was demonstrated to be translational repression rather than mRNA degradation, but it is still unknown which step of 11 β -HSD1 translation is controlled by miRNAs.

5.4 Glucocorticoids versus miRNAs for regulation of *HSD11B1* expression

Glucocorticoids (GCs) are a class of steroid hormones that are secreted by the adrenal cortex and that are regulated by adrenocorticotrophic hormone (ACTH) largely under the control of the hypothalamic-pituitary-adrenal axis. GCs have many diverse effects, including potentially harmful side effects. Chronic glucocorticoids excess causes Cushing's syndrome, obesity, type 2 diabetes, insulin resistance, dyslipidemia, hypertension, heart disease and memory

Discussion

impairments (Orth, 1995; Wamil and Seckl, 2007). Glucocorticoids themselves potently increased *HSD11B1* expression in many cells, providing a potential feed-forward system to pathology. Glucocorticoids such as dexamethasone and cortisol are important regulators of *HSD11B1* expression in human lung and liver (Yang *et al.*, 2009). *HSD11B1* mRNA could be induced by glucocorticoids *in vivo* (Yang *et al.*, 1994; Hundertmark *et al.*, 1994; Jamieson *et al.*, 1999; Michailidou *et al.*, 2007), although the regulation is tissue-specific and complex. Most regulators of *HSD11B1* expression are likely to act indirectly, and the only direct regulators of *HSD11B1* transcription described to date comprise members of the CCAAT/enhancer binding protein (C/EBP) family of transcription factors (Williams *et al.*, 2007; Bruley *et al.*, 2006). CCAAT/enhancer binding proteins (C/EBPs) are a family of transcription factors, which promote the expression of certain genes through interaction with their promoter. *HSD11B1* is transcribed from two distinct promoters, the distal promoter P1 or the proximal promoter P2. Transcription from Promoter P2 in liver, brain, and adipose tissue is predominant and dependent on the transcription factor C/EBP α (Williams *et al.*, 2007; Bruley *et al.*, 2006). Transcription from Promoter P1 is C/EBP α independent (Bruley *et al.*, 2006). Sai *et al.* have investigated the molecular mechanisms. They proved that glucocorticoids regulate transcription of *HSD11B1* via promoter P2 and exploit an A549 cell model system in which endogenous *HSD11B1* is expressed and induced by dexamethasone (Sai *et al.*, 2008). In this model, glucocorticoid induction of *HSD11B1* expression is indirect and requires CCAAT/enhancer-binding protein (C/EBP). The glucocorticoid-response region is located between -196 and -88 with respect to the transcription start site of *HSD11B1*, which contains two binding sites for C/EBP transcription factors. These sites are essential for the glucocorticoid response and C/EBP binding (Figure 5.3; Sai *et al.*, 2008).

In the present study, the results show that *HSD11B1* expression on the transcriptional level was induced by glucocorticoids (Figure 4.14). However, the miRNA suppression occurs on the translational level. Mature miRNA is assembled into a microribonucleoprotein (miRNP), which binds to the 3'UTR of *HSD11B1* mRNA, leading to repression of protein synthesis (Figure 5.3). Due to these different regulatory mechanisms exerted by glucocorticoids and miRNAs in *HSD11B1* expression, can be controlled at the transcriptional and translational level, respectively. Therefore, it is possible that miR-579 can still inhibit *HSD11B1* expression after induction with glucocorticoids proved by dual luciferase assay system (Figure 4.18A and B). Moreover, glucocorticoids induction of *HSD11B1* expression is so strong that the repression by miRNA is relatively negligible, in the case of hsa-miR-561

(Figure 4.18C and D). In contrast, hsa-miR-579 is a more potent repressor than hsa-miR-561, and repression of *HSD11B1* expression could be detected after glucocorticoids induction (Figure 4.18A and B). Therefore, miRNAs, to some extent, could resist the effect of *HSD11B1* expression by glucocorticoids, based on this mechanism, miRNAs may be a promising 11 β -HSD1 inhibitor for therapeutic diseases in the future.

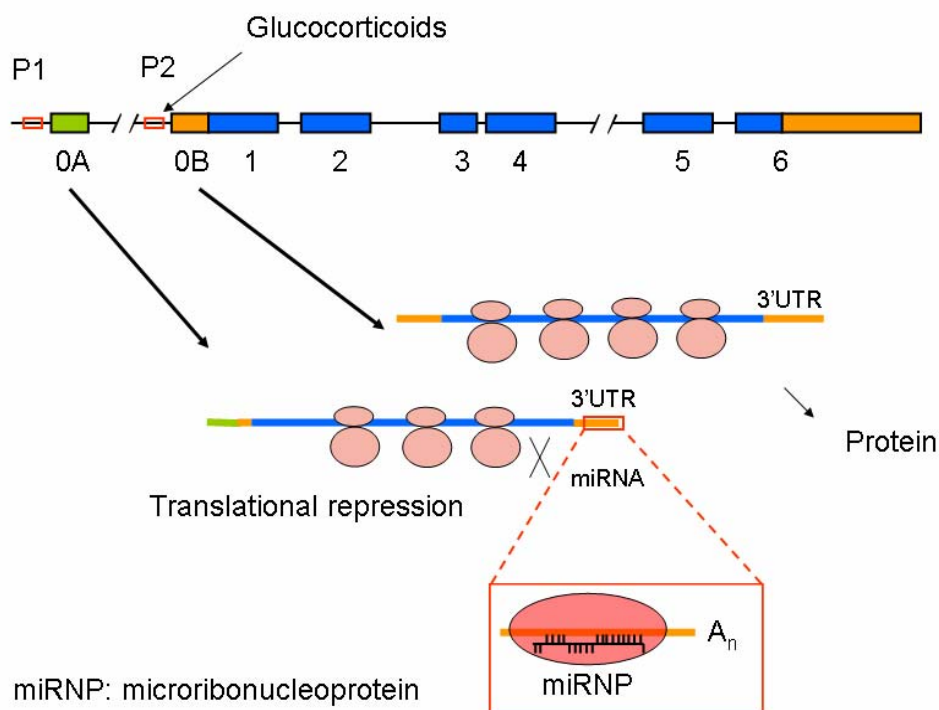


Figure 5.3 Regulation of *HSD11B1* expression by glucocorticoids and miRNAs. After binding at the promoter P2, GCs promote the transcription of *HSD11B1*, while translation of *HSD11B1* mRNA can be inhibited by miRNAs. P1 and P2 represent Promoter 1 and 2 of *HSD11B1*, respectively. 0A, 0B, 1~6 represent exons.

5.5 The regulation of *HSD11B1* expression

The regulation of *HSD11B1* expression is controlled by two distinct promoters, namely distal promoter P1 and proximal promoter P2, an aspect which to date has been studied very little. However, studies in the mouse have shown that both promoters are active in liver, lung, adipose tissue and brain (Bruley *et al.*, 2006). Currently, the human *HSD11B1* promoter has not yet been characterized in detail. Most of research groups mainly focused on studying for human *HSD11B1* promoter P2, little for *HSD11B1* promoter P1. For instance, Williams *et al.*

Discussion

(2000) demonstrated that C/EBP α (CCAAT/enhancer binding protein) is a potent activator of hepatic transcription of *HSD11B1* in hepatoma cells, and mice deficient in C/EBP α have reduced hepatic *HSD11B1* expression. In contrast, C/EBP β is a relatively weak activator for *HSD11B1* expression. They also showed that *HSD11B1* promoter (proximal promoter P2; between -812 and +76) contains 10 C/EBP binding sites, and mutation of the promoter proximal sites decreases the C/EBP inducibility (Williams *et al.* 2000). To characterize some mechanisms which control the expression of the human *HSD11B1* in preadipocytes, Gout *et al.* (2006) demonstrated that two members of the C/EBP family, C/EBP α and C/EBP β are required for the basal transcriptional activity of *HSD11B1* in 3T3-L1 preadipocyte cells. This effect depends on C/EBP binding sites. Two putative C/EBP binding sites are located in a region of the promoter between -48 and -178 and relatively conserved among species, human, baboon, rat and mouse. Indeed, mutation of C/EBP binding site led to a significant decrease in basal *HSD11B1* promoter (proximal promoter P2) activity. A differential regulation of the human *HSD11B1* promoter depending on the cell type was observed. Promoter fragments were analyzed in human HepG2 cells and undifferentiated and differentiated murine 3T3-L1 cells. A strong repressor of the basal promoter activity was only found between -85 and -172 in HepG2 cells, while an additional repressor appeared to be active between -342 and -823 in human HepG2 cells and undifferentiated and differentiated murine 3T3-L1 cells (Andres *et al.*, 2007). Recently, Staab *et al.* (2011) demonstrated that the distal promoter P1 (*HSD11B1*-Promoter P1) predominated in the human tumor cell lines A431 and HT-29 and contributed significantly to overall *HSD11B1* expression in human lung (Staab *et al.*, 2011). The proximal promoter P2 (*HSD11B1*-Promoter P2) predominated in most tissues and cell lines assessed, including human liver, human lung, human subcutaneous adipose tissue, and the cell lines A549, Caco-2, C2C12 and 3T3-L1 (Staab *et al.*, 2011).

In this study, glucocorticoids (cortisol and dexamethasone) increased *HSD11B1* mRNA transcription via both distal promoter P1 and proximal promoter P2, but promoter P2 predominated in A549 cells (Figure 4.14). To analyze the promoter activity, the two fragments of *HSD11B1*-promoter, distal promoter P1 (2.173 bp) and proximal promoter P2 (2506 bp), were cloned into plasmids of dual-luciferase assay system. The result showed that 11 β -HSD1 expression in A549 cells is significantly increased via promoter P2 after induction with cortisol and dexamethasone, but not significantly changed via promoter P1 (Figure 4.17). Consistent with the results reported by Sai *et al.*, they demonstrated that the promoter P2, but not the promoter P1, of *HSD11B1* is more important in A549 cells. Dexamethasone increased

Discussion

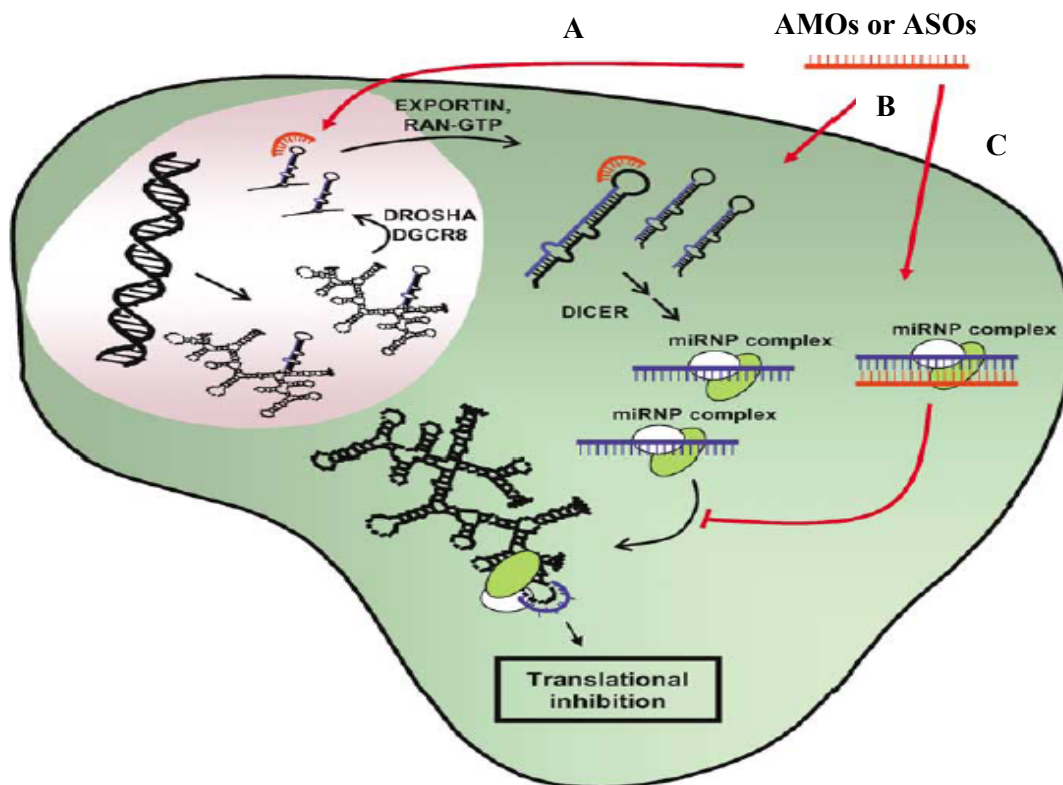
activity of a promoter P2-reporter construct only. Moreover, they found that the region between -196 and -124 is essential for glucocorticoid induction of *HSD11B1* promoter P2 (Sai *et al.*, 2008). Furthermore, more regulatory factors were detected using dual-luciferase assay system in A549 cells. However, no promoter activity is shown (Figure 4.19). It is possible reason that both of fragments of Promoter 1 and Promoter 2 do not contain the related binding sites of the regulatory factors.

To date, it has been reported that many regulatory factors are involved in the regulation of *HSD11B1* expression, including some proinflammatory cytokines (TNF- α and IL-1 β), growth hormone, leptin, insulin, glucocorticoids (cortisol and dexamethasone), CCATT/enhancer binding protein (C/EBP), peroxisome proliferator-activated receptor (PPAR) agonists, sex hormones, thyroid hormone and other nuclear receptors (Table 1.3). The present study is the first report that miRNAs act as potential novel regulators of *HSD11B1* expression.

The regulation of *HSD11B1* expression occurs in a highly tissue-specific manner (Tomlinson *et al.*, 2004). For example, several studies have demonstrated that TNF- α increases 11 β -HSD1 mRNA transcription and activity of this enzyme in various cell models, such as human osteoblasts, adipose stromal cells, adipocytes and hepato cellular carcinoma cells (Cooper *et al.*, 2001; Tomlinson *et al.*, 2001; Friedberg *et al.*, 2003; Iwasaki *et al.*, 2008), but not in human monocytes and hepatocytes (Thieringer *et al.*, 2001; Tomlinson *et al.*, 2001). Leptin treatment of ob/ob mice markedly increased hepatic 11 β -HSD1 activity and mRNA transcription (Liu *et al.*, 2003). Leptin causes a borderline significant increase in 11 β -HSD1 activity in omental adipose stromal cells, but not in human hepatocytes (Tomlinson *et al.*, 2001). Insulin inhibits 11 β -HSD1 activity in primary cultures of rat hepatocytes (Liu *et al.*, 1996) and 3T3-L1 cells (Napolitano *et al.*, 1998), but not changes 11 β -HSD1 activity in human adipose stromal cells (Bujaska *et al.*, 1999). Retinoic acid reduces glucocorticoid sensitivity in C2C12 myotubes by decreasing 11 β -hydroxysteroid dehydrogenase type 1 and glucocorticoid receptor activities (Aubry and Odermatt 2009). Human monocyte expression of 11 β -HSD1 is induced by Vitamin D₃ (Thieringer *et al.*, 2001). Based on this kind of highly tissue-specific manner, it might be explained that TNF- α , Leptin, insulin and so on, did not influence activity of 11 β -HSD1 promoter, by absence of relative factors which react with regulatory factors in lung cells (A549 cells, Figure 4.19). However, the underlying mechanism is still unknown.

5.6 The presence of the studied miRNAs in human liver cells

Studies have reported that anti-microRNA oligonucleotides (AMOs) or antisense oligonucleotides (ASOs) have been developed to inhibit miRNAs in variety of culture cells or organisms (Davis *et al.*, 2006; Esau, 2008). For instance, AMOs have been used successfully to downregulate miR-21 expression in A549 cells (Fei *et al.*, 2008) and inhibit the liver-specific miR-122 in mice (Esau *et al.*, 2006; Krutzfeldt *et al.*, 2005). As mentioned in the introduction section, the biogenesis of miRNAs is a multistep process (as shown in Figure 1.4). Therefore, multiple steps could be targeted with AMOs for inhibition of miRNA production or function (Weiler *et al.*, 2006). The major mechanism for AMOs is believed to be the targeted degradation of the pri-miRNA, pre-miRNA, and mature miRNA. Therefore, AMOs or ASOs interference with the role of miRNA are summarized in three possible pathways (Figure 5.4, Weiler *et al.*, 2006). Firstly, targeted degradation of the pri-miRNA transcript in the nucleus with AMOs may be feasible, and could be advantageous for inhibiting production of miRNA from a pri-miRNA transcript. Secondly, by pathway B, targeting the pre-miRNA hairpin with AMOs is also theoretically possible. The last, the most straightforward and apparently most effective AMOs tested so far are complementary to the mature miRNA, designed to block its function in miRNP complex. Targeting of mature miRNAs with such AMOs has been reported by many investigators in a variety of cultured cells and organisms (Hutvagner *et al.*, 2004; Davis *et al.*, 2006; Esau, 2008).



Discussion

Figure 5.4 Interference with the miRNA pathway using synthetic oligonucleotides.

Inhibition of miRNA activity may be achieved by introducing anti-miRNA oligonucleotides (AMOs) or antisense oligonucleotides (ASOs) complementary to the pri-miRNA (primary-miRNA), the pre-miRNA (precursor-miRNA) or the mature miRNA. A, B and C represent via pri-miRNA, pre-miRNA and mature miRNA pathways, respectively.

In an initial effort to assess the presence of hsa-miR-579 and hsa-miR-561 in hepatocytes, AMOs (AMO-579 and AMO-561) are designed to target the mature miR-579 and miR-561 in HepG2 cells. These results demonstrated that AMO-579 and AMO-561 not only inhibit the role of exogenous miR-579 and miR-561, but also block the role of endogenous miR-579 and miR-561 (Figure 4.21). This is a strong indication of presence of endogenous hsa-miR-579 and -561 in HepG2 cells, a finding which is in agreement with web-based tissue profiling using the smiRNadb miRNA expression atlas (Figure 4.1, www.mirz.unibas.ch, Hausser *et al.*, 2009; Landgraf *et al.*, 2007). In this work, the dual-luciferase assay system and AMOs were used to detect interesting miRNAs, the advantage of this method is rapidly and easily. Meanwhile, AMOs are a powerful tool for uncovering new areas of miRNA biology, with the gradual deepening of research, AMOs inhibition of miRNA function displays a potential therapeutic approach for miRNA therapy of human diseases.

Normally, the most straightforward RNA detection method is northern blot analysis, which is a widely used method for RNA analyses because it is generally a readily available technology for laboratories. To verify the presence of miR-561 and miR-579 in hepatocytes and HepG2 cells, the experiment was performed by Northern blot. 20 ng of positive control (DNA oligonucleotides) showed a strong signal. However, we could not find any signal for miR-561 or miR-579 with 10 µg of total RNA (Figure 4.22). Two reasons have to be considered: miRNAs are short, average about 21 nucleotides in length, so miRNAs are more difficult to detect than large RNA; On the other hand, a DNA oligonucleotide probe has been used in this experiment, and traditional DNA oligonucleotide probe has a poor sensitivity to complement to target miRNA, which is especially pronounced that investigated miRNAs are at a low abundance.

Although Northern blot failed to detect the expected miRNAs in hepatocytes, another method with higher sensitivity, RT-PCR, was used to prove the presence of miRNAs. This approach requires small amounts of starting material and can provide accurate results. Using specific

primers (designed and obtained by Ambion GmbH), both miR-561 and miR-579 are successfully amplified in both human hepatocytes and HepG2 cells (Figure 4.24). Previously, miR-579 has been detected in HepG2 cells and hepatocytes (www.mirz.unibas.ch, Hausser *et al.*, 2009; Landgraf *et al.*, 2007, Figure 4.1). Moreover, miR-561 is firstly detected in normal hepatocytes and HepG2 cells.

5.7 Regulatory role of microRNAs in liver

In obese patients, *HSD11B1* expression is increased in adipose tissue, but typically decreased in liver, and the underlying tissue-specific mechanisms are largely unknown (Livingstone *et al.*, 2000). As miRNA expression is highly tissue-specific manner and regulation by miRNAs is predominantly negative. In this study, two miRNAs, miR-561 and miR-579, have been identified to downregulate *HSD11B1* expression. As shown in this study, miR-561 and miR-579 were detected from human hepatocytes and HepG2 cells. This may explain the mechanism by which *HSD11B1* expression is downregulated in liver tissue of obese patients. Up to date, we know little about the roles of miR-561 and miR-579, but it is quite sure that many new and unanticipated roles of miRNAs in the control of normal and abnormal liver functions are awaiting discovery.

At the beginning, miR-561 or miR-579 transcription was expected to occur in hepatocytes from normal, overweight and obese people. Because the hepatocyte samples (from normal, overweight and obese people) were not easily obtained for this experiment, in each group there were only two different samples. In fact, the sample numbers were not sufficient. The semi-quantitative RT-PCR results showed that miR-561 transcriptions were at similar levels in hepatocytes with different BMI (Figure 4.25) and miR-579 transcriptions were significantly lower in both female and male obese people than in the corresponding female and male samples of normal weight people (Figure 4.25). To get more convincing results, the sample numbers should be expanded. Furthermore, the size of miRNA is too short and it is impossible to detect all miRNAs in total RNA isolated from frozen hepatocytes. Therefore, these reasons should be considered as well.

So far, many studies have uncovered profound and unexpected roles for miRNAs, in the control of diverse aspects of hepatic function and dysfunction, including hepatocyte growth, metabolism, stress response, liver cancer, viral infection, immunity, gene expression, and maintenance of hepatic phenotype (Krutzfeld and Stoffel, 2006; Girard *et al.*, 2008; Lu and

Liston, 2009). In hepatocellular carcinoma (HCC), miRNA dysregulation plays a key role in mediating the pathogenicity of several etiologic risk factors and they promote a number of cancer-inducing signaling pathways (Law and Wong, 2011). Moreover, another study has also demonstrated its potential value in the clinical management of HCC patients as some miRNAs may be used as prognostic or diagnostic markers (Girard *et al.*, 2008). Many miRNAs such as miR-21, miR-34a, miR-106a, miR-223, and miR-224, are upregulated in hepatocellular carcinoma (HCC) compared to that in benign hepatocellular tumors such as adenomas or focal nodular hyperplasia (Meng *et al.*, 2007; Wong *et al.*, 2008). Many other miRNAs have been noted to be decreased in HCC compared to non-tumoral tissue, such as miR-122a, miR-145, and miR-199a, miR-422b (Kutay *et al.*, 2006; Meng *et al.*, 2007; Wong *et al.*, 2008; Varnholt *et al.*, 2008; Gramantieri *et al.*, 2007). Study by Li *et al.* found that miR-183 was up-regulated in HCC tumor tissue. Moreover, they validated that miR-183 could repress the programmed cell death 4 (PDCD4) expression and analyzed its functions in human HCC cells (Li *et al.*, 2010). Furthermore, miR-122 and miR-152 have been reported in modulating the response to hepatitis C virus infection (Kerr *et al.*, 2011; Girard *et al.*, 2008).

5.8 Pathway Enrichment Analysis

In efforts to place the repression of *HSD11B1* expression by the identified miRNAs in a broader context of molecular networks, we searched for overrepresented pathways among all potential targets of hsa-miR-561 and -579. Several enriched pathways were found that have previously been associated with metabolic disease and/or glucocorticoid signalling. A striking result was the finding of one signalling pathways for nutrient metabolism, the insulin signalling pathway, for both miRNAs. As to the insulin signalling pathway, this finding raises the possibility that hepatic downregulation of *HSD11B1* expression might occur in the context of miRNA-based downregulation of multiple targets involved in insulin signalling, ultimately leading to the development of insulin resistance.

Further overrepresented pathways with linkage to glucocorticoid metabolism are long-term potentiation, neurodegenerative disease, and long-term depression. Neuronal vulnerability, depression and age-associated cognitive impairment correlate with elevated glucocorticoid levels (Wamil *et al.*, 2007; Poor *et al.*, 2004; Rajan *et al.*, 1996; Ajilore *et al.*, 1999). Furthermore, it has been shown that 11 β -HSD1 levels increase during aging and cause memory impairment (Holmes *et al.*, 2010). Consistently, 11 β -HSD1 knockout mice show less learning impairment as well as decreased corticosterone levels in the hippocampus coming

Discussion

along with enhanced long-term potentiation (Yau *et al.*, 2001; Yau *et al.*, 2007). Finally, a rare single nucleotide polymorphism in the 5'UTR of *HSD11B1* associates with increased risk for Alzheimer's disease (de Quervain *et al.*, 2004). As to the remaining enriched pathways, no obvious connections with 11 β -HSD1 and/or glucocorticoid metabolism/signalling have been reported to date.

Hsa-miR-561 is located in intron 1 of *GULP1* (Table 5.1). Together with its host gene *GULP1*, intronic hsa-miR-561 is overexpressed in multiple myeloma primary tumors (Ronchetti *et al.*, 2008), but has not been mentioned in any other context to date. Interestingly, *GULP1*, which encodes a protein that plays a role in the engulfment of apoptotic cells as well as in cellular glycosphingolipid and cholesterol transport, is downregulated by activated glucocorticoid receptor α (Lu *et al.*, 2007). As host genes and intronic miRNAs are typically co-regulated (Baskerville *et al.*, 2005), it can be speculated that downregulation of hsa-miR-561 in response to glucocorticoids might contribute to the fine-tuning of glucocorticoid-induced expression of *HSD11B1*.

Neither hsa-miR-561 nor hsa-miR-579 has so far been mentioned in the context of obesity and diabetes. However, as all studies on differential miRNA transcription in this regard have been performed with rodent model systems (Esau *et al.*, 2004; He *et al.*, 2007; Lovis *et al.*, 2008; Herrera *et al.*, 2009; Herrera *et al.*, 2010). A search in miRBase (<http://www.mirbase.org/>) reveals a miRNA count of 940 for *Homo sapiens* in contrast to 590 in *Mus musculus* and 326 in *Rattus norvegicus*, and the rodent entries include neither miR-561 nor miR-579. Considering their relatively well-conserved MREs in the *HSD11B1* mRNA (Table 5.1) and 3'UTRs of other genes as found in the pathway enrichment analysis by DIANA mirPath (Table 4.5), it is nevertheless plausible that both miRNAs can be found in other mammalian species. However, as there is no experimental evidence for the existence of these miRNAs in rodents yet, they are not included on miRNA microarrays commonly used for their detection (Esau *et al.*, 2004; He *et al.*, 2007; Lovis *et al.*, 2008; Herrera *et al.*, 2009; Herrera *et al.*, 2010).

Discussion

Table 5.1 Compiled information on the here described miRNAs binding to the 3'UTR of *HSD11B1* mRNA.

hsa-miR	Genomic location ¹	Position of MRE seed in <i>HSD11B1</i> 3'UTR ²	3'-UTR MRE conserved in ³	miRNA expression in ⁴	regulation in disease or other processes ⁵
-561	Intron 1 of <i>GULP1</i> ⁶	325-331	Chimpanzee, Rhesus, Horse, Rabbit, Cow, Macaque, Armadillo, Elephant	human adrenocarcinoma cell line SW13, human embryonic kidney cell line HEK293, human multiple myeloma cell lines (Ronchetti <i>et al.</i> , 2008)	↑ multiple myeloma cell lines (Ronchetti <i>et al.</i> , 2008)
-579	Intron 11 of <i>ZFR</i> ⁷	400-406	Chimpanzee, Mouse, Rat, Guinea pig, Rabbit	human hepatoma cell line HepG2 (see Figure 4.1), human teratocarcinoma cell line NT2, human fibroblasts (Maes <i>et al.</i> , 2008), human acute monocytic leukemia cell line THP-1 (EI Gazzar <i>et al.</i> , 2010)	↓ irradiation (Maes <i>et al.</i> , 2008) negatively regulates expression of TNT- α (EI Gazzar <i>et al.</i> , 2010)

¹ according to miRBase (<http://www.mirbase.org/>), (Griffiths-Jones, 2004; Griffiths-Jones *et al.*, 2006; Griffiths-Jones *et al.*, 2008)

² according to TargetScan (<http://www.targetscan.org/>), Lewis *et al.*, 2003; Lewis *et al.*, 2005; Liu *et al.*, 2003; Grimson *et al.*, 2007)

³ compiled from the results by TargetScan (<http://www.targetscan.org/>), Lewis *et al.*, 2003; Lewis *et al.*, 2005; Liu *et al.*, 2003; Grimson *et al.*, 2007) and by DIANA micro-T (<http://diana.cslab.ece.ntua.gr/microT>), Maragkakis *et al.*, 2009)

⁴ according to the smiRNAdb miRNA expression atlas (<http://www.mirz.unibas.ch>), Landgraf *et al.*, 2007; Hausser *et al.*, 2009) and other references as cited

⁵ according to the human microRNA disease database (HMDD, <http://cmbi.bjmu.edu.cn/hmdd>), Lu *et al.*, 2008) and the miR2 Disease Base (<http://www.mir2disease.org/>)

⁶ GULP1: PTB domain-containing engulfment adapter protein 1, modulates cellular glycosphingolipid and cholesterol transport; downregulated by activated GR α

⁷ ZFR: Zinc finger RNA-binding protein, involved in postimplantation and gastrulation stages of development

5.9 Outlook

In this work, two human miRNAs, hsa-miR-561 and hsa-miR-579, were identified as potential novel regulators of *HSD11B1* expression. Evidence from the literature and experiments, as *e.g.* the intronic location of hsa-miR-561 in a glucocorticoid-responsive gene, and both hsa-miR-561 and hsa-miR-579 have been detected in hepatocytes, as well as target miRNA-enriched pathways strengthen their potential role in pathological conditions associated with deregulated glucocorticoid metabolism/signalling. Furthermore, the obtained results raise the possibility that regulation of *HSD11B1* expression in obesity, type 2 diabetes, and cognitive impairment might occur in a broader context of miRNA-based downregulation of entire pathways. However, the relative contribution of these miRNAs to overall regulation of *HSD11B1* remains unclear. Nevertheless, the obtained results encourage the in depth-study of the miRNAs identified in the context of the aetiology of the metabolic syndrome and neuronal disorders in the future work.

6 References

- Abdallah BM, Beck-Nielsen H and Gaster M 2005 Increased expression of 11-beta hydroxysteroid dehydrogenase type 1 in type 2 diabetic myotubes. *Eur J Clin Invest* 35: 627-634.
- Ajilore OA and Sapolsky RM 1999 In vivo characterization of 11 β -hydroxysteroid dehydrogenase in rat hippocampus using glucocorticoid neuroendangerment as an endpoint. *Neuroendocrinology* 69: 138-144.
- Alfaidy N, Xiong ZG, Myatt L, Lye SJ, MacDonald JF and Challis JR 2001 Prostaglandin F $_{2\alpha}$ potentiates cortisol production by stimulating 11 β -hydroxysteroid dehydrogenase 1: a novel feedback loop that may contribute to human labor. *J Clin Endocrinol Metab* 86: 5585-5592.
- Ambros V 2003 MicroRNA pathways in flies and worms: Growth, death, fat, stress and timing. *Cell* 113: 673-676.
- Amelung D, Huebner HJ, Roka L and Meyerheim G 1953 Conversion of cortisone compound F. *J Clin Endocrinol Metab* 13: 1125-1129.
- Andersen DC, Jensen CH, Schneider M 2010 MicroRNA-15a fine-tunes the level of Delta-like 1 homolog (DLK1) in proliferating 3T3-L1 preadipocytes. *Exp Cell Res* 316: 1681-1691.
- Andres J, Mai K, Mohlig M, Weickert MO, Bumke-Vogt C, Diederich S, Pfeiffer A, Bahr V and Spranger J 2007 *Archives of Physiology and Biochemistry* 113: 110-115.
- Andrews RC, Herlihy O, Livingstone DE, Andrew R and Walker BR 2002 Abnormal cortisol metabolism and tissue sensitivity to cortisol in patients with glucose intolerance. *J Clin Endocrinol Metab* 87: 5587-93.
- Andrews RC, Rooyackers O and Walker BR 2003 Effects of the 11 β -hydroxysteroid dehydrogenase inhibitor carbenoxolone on insulin sensitivity in men with type 2 diabetes. *J Clin Endocrinol Metab* 88: 285-291.
- Arcuri F, Battistini S, Hausknecht V, Cintorno M, Lockwood CJ and Schatz F 1997 Human endometrial decidual cell-associated 11 β -hydroxysteroid dehydrogenase expression: its potential role in implantation. *Early Pregnancy* 3: 259-264.
- Aubry EM and Odermatt A 2009 Retinoic acid reduces glucocorticoid sensitivity in C2C12 myotubes by decreasing 11 β -hydroxysteroid dehydrogenase type 1 and glucocorticoid receptor activities. *Endocrinology* 150(6): 2700-2708.
- Bagga S, Bracht J, Hunter S, Massirer K, Holtz J, Eachus R and Pasguenlli AE 2005 Regulation by let-7 and lin-4 miRNAs results in target mRNA degradation. *Cell* 122: 553-563.
- Balasubramanyam M, Aravind S, Gokulakrishnan K, Prabu P, Sathishkumar C, Ranjani H and Mohan V 2011 Impaired miR-146a expression links subclinical inflammation and insulin resistance in type 2 diabetes. *Mol Cell Biochem* 351: 197-205.

References

- Bartel DP 2004 MicroRNAs: genomics, biogenesis, mechanism, and function. *Cell* 116: 281-297.
- Bartel DP 2009 MicroRNAs: target recognition and regulatory functions. *Cell* 136: 215-233.
- Baskerville S and Bartel DP 2005 Microarray profiling of microRNAs reveals frequent coexpression with neighboring miRNAs and host genes. *RNA* 11: 241-247.
- Bays HE, Chapman RH and Grandy S 2007 The relationship of body mass index to diabetes mellitus, hypertension and dyslipidaemia: comparison of data from two national surveys. *Int J Clin Pract* 61: 737-747.
- Berezikov E, Guryev V, van de Belt J, Wienholds E, Plasterk RH, and Cuppen E 2005 Phylogenetic shadowing and computational identification of human microRNA genes. *Cell* 120: 21-24.
- Berger J, Tanen M, Elbrecht A, Hermanowski-Vosatka A, Moller DE, Wright SD and Thieringer R 2001 Peroxisome proliferator-activated receptor- γ ligands inhibit adipocyte 11 β -hydroxysteroid dehydrogenase type 1 expression and activity. *J Biol Chem* 276: 12629-12635.
- Betel D, Wilson M, Gabow A, Marks DS and Sander C 2008 The microRNA.org resource: targets and expression. *Nucleic Acids Res.* 36: D149-153.
- Blum A, Martin HJ and Maser E 2000 Human 11 β -Hydroxysteroid dehydrogenase type 1 is enzymatically active in its nonglycosylated form. *Biochem Biophys Res Commun* 276: 428-434.
- Blum A and Maser E 2003 Enzymology and molecular biology of glucocorticoid metabolism in humans. *Prog Nucleic Acid Res Mol Biol* 75: 173-216.
- Brereton PS, van Driel RR, Suhaimi F, Koyama K, Dilley R and Krozowski Z 2001 Light and electron microscopy localization of the 11 β -hydroxysteroid dehydrogenase type 1 enzyme in the rat. *Endocrinology* 142: 1644-1651.
- Brochu M, Tchernof A, Dionne IJ, Sites CK, Eltabbakh GH, Sims EA and Poehlman ET 2001 What are the physical characteristics associated with a normal metabolic profile despite a high level of obesity in postmenopausal women? *J Clin Endocrinol Metab* 86: 1020-1025.
- Bruley C, Lyons V, Worsley AG, Wilde MD, Darlington GD, Morton NM, Seckl JR and Chapman KE 2006 A novel promoter for the 11 β -hydroxysteroid dehydrogenase type 1 gene is active in lung and is C/EBP α independent. *Endocrinology* 147: 2879-2885.
- Bujaska IJ, Kumar S and Stewart PM 1997 Does central obesity reflect ‘‘Cushing’s disease of the omentum’’? *Lancet* 349: 1210-1213.
- Bujaska IJ, Kumar S, Hewison M and Stewart PM 1999 Differentiation of adipose stromal cells: the roles of glucocorticoids and 11 β -hydroxysteroid dehydrogenase. *Endocrinology* 140: 3188-3196.

References

- Burton PJ, Krozowski ZS and Waddell BJ 1998 Immunolocalization of 11 β -hydroxysteroid dehydrogenase types 1 and 2 in rat uterus: variation across the estrous cycle and regulation by estrogen and progesterone. *Endocrinology* 139: 376-382.
- Bushati N and Cohen SM 2007 microRNA functions. *Annu Rev Cell Dev Biol* 23: 175-205.
- Cai TQ, Wong B, Mundt SS, Thiernger R, Wright SD and Hermanowski-Vosatka A 2001 Induction of 11 beta-hydroxysteroid dehydrogenase type 1 but not-2 in human aortic smooth muscle cells by inflammatory stimuli. *J Steroid Biochem Mol Biol* 77(2-3): 117-122.
- Care A, Catalucci D, Felicetti F, Bonci D, Addario A and Condorelli G 2007 MicroRNA-133 controls cardiac hypertrophy. *Nat Med* 13: 613-618.
- Castello R, Schwarting R, Muller C and Hierholzer K 1989 Immunohistochemical localization of 11-hydroxysteroid dehydrogenase in rat kidney with monoclonal antibody. *Renal Physiol Biochem* 12: 320-327.
- Chen JF, Mandel EM, Thomson JM, Wu Q, Callis TE, Hammond SM, Conlon FL and Wang DZ 2006 The role of microRNA-1 and microRNA-133 in skeletal muscle proliferation and differentiation. *Nat Genet* 38: 228-233.
- Chendrimada TP, Gregory RI, Kumaraswamy E, Norman J, Cooch NM, Nishikura K and Shiekhattar R 2005 TRBP recruits the Dicer complex to Ago2 for microRNAs processing and gene silencing. *Nature* 436: 740-744.
- Chendrimada TP, Finn KJ, Ji X, Baillat D, Gregory RI, Liebhaber SA, Pasquinelli AE and Shiekhattar R 2007 MicroRNA silencing through RISC recruitment of eIF6. *Nature* 447: 823-828.
- Chu JW, Matthias DF, Belanoff J, Schatzberg A, Hoffman AR and Feldman D 2001 Successful long-term treatment of refractory Cushing's diseases with high-dose mifepristone. *J Clin Endocrinol Metab* 86: 3568-3573.
- Cooper MS, Walker EA, Bland R, Fraser WD, Hewison M and Stewart PM 2000 Expression and functional consequences of 11 β -hydroxysteroid dehydrogenase activity in human bone. *Bone* 27: 375-381.
- Cooper MS, Bujalska I, Rabbitt E, Walker EA, Bland R, Sheppard MC, Hewison M and Stewart PM 2001 Modulation of 11 β -hydroxysteroid dehydrogenase isozymes by proinflammatory cytokines in osteoblasts: an autocrine switch from glucocorticoid inactivation to activation. *J Bone Miner Res* 16: 1037-1044.
- Cooper MS, Rabbitt EH, Goddard PE, Bartlett WA and Stewart PM 2002 Osteoblastic 11 β -hydroxysteroid dehydrogenase type 1 activity increases with age and glucocorticoid exposure. *J Bone Miner Res* 17: 979-986.
- Cortes-Sempere M and Ibanez de Caceres I 2011 MicroRNA as novel epigenetic biomarkers for human cancer. *Clin Transl Oncol* 13: 357-362.

References

- Davani B, Khan A, Hult M, Martensson E, Okret S, Efendic S, Jornvall H and Oppermann UC 2000 Type 1 11 β -hydroxysteroid dehydrogenase mediates glucocorticoid activation and insulin release in pancreatic islets. *J Biol Chem* 275: 34841-34844.
- Davis S, Lollo B, Freier S and Esau C 2006 Improved targeting of miRNA with antisense oligonucleotides. *Nucleic Acids Res.* 34: 2294-2304.
- DeFronzo RA and Ferrannini E 1991 Insulin resistance. A multifaceted syndrome responsible for NIDDM, obesity, hypertension, dyslipidemia, and atherosclerotic cardiovascular disease. *Diabetes Care* 14: 173-194.
- Draper N, Echwald SM, Lavery GG, Walker EA, Fraser R, Davies E, Sorensen TI, Astrup A, Adamski J, Hewison M, Connell JM, Pedersen O and Stewart PM 2002 Association studies between microsatellite markers within the gene encoding human 11 β -hydroxysteroid dehydrogenase type 1 and body mass index, waist to hip ratio, and glucocorticoid metabolism. *J Clin Endocrinol Metab* 87: 4984-4990.
- Draper N and Stewart PM 2005 11 β -Hydroxysteroid dehydrogenase and the pre-receptor regulation of corticosteroid hormone action. *Endocrinology* 186: 251-271.
- Du T and Zamore PD 2005 microPrimer: the biogenesis and function of microRNA. *Development* 132: 4645-4652.
- Duplomb L, Lee Y, Wang MY, Park BH, Takaishi K, Agarwal Ak and Unger RH 2004 Increased expression and activity of 11 beta-HSD1 in diabetic islets and prevention with troglitazone. *Biochem Biophys Res Commun* 313: 594-599.
- Edward CR, Stewart PM, Burt D, Brett L, McIntyre MA, Sutanto WS, de Kloet ER and Monder C 1988 Localisation of 11 beta-hydroxysteroid dehydrogenase-tissue specific protector of the mineralocorticoid receptor. *Lancet* 2: 986-989.
- EI Gazzar M and McCall CE 2010 MicroRNAs distinguish translational from transcriptional silencing during endotoxin tolerance. *J Biol Chem* 285: 20940-20951.
- EI Ouamari A, Baroukh N, Martens GA, Lebrun P, Pipeleers D and van Obberghen E 2008 miR-375 targets 3'-phosphoinositide-dependent protein kinase-1 and regulates glucose-induced biological responses in pancreatic β -cells. *Diabetes* 57: 2708-2717.
- Esau C, Kang X, Peralta E, Hanson EG, Ravichandran LV, Sun Y, Koo S, Perera RJ, Jain R, Dean NM, Freier SM, Bennett CF, Lollo B and Griffey 2004 MicroRNA-143 regulates adipocyte differentiation. *J Biol Chem* 279: 52361-52365.
- Esau CC 2008 Inhibition of microRNA with antisense oligonucleotides. *Methods* 44: 55-60.
- Escher G, Galli I, Vishwanath BS, Frey BM and Frey FJ 1997 Tumor Necrosis Factor α and interleukin 1 β enhance the cortisone/cortisol shuttle. *J Exp Med* 186: 189-198.
- Esquela-Kerscher A and Slack FJ 2006 Oncomirs-microRNAs with a role in cancer. *Nat Rev Cancer* 6: 259-269.

References

- Eulatio A, Huntzinger E and Izaurralde E 2008 Getting to the root of miRNA-mediated gene silencing. *Cell* 132: 9-14.
- Evagelatou M, Peterson SL and Cooke BA 1997 Leukocytes modulate 11 β -hydroxysteroid dehydrogenase (11 β -HSD) activity in human granulosa-lutein cell cultures. *Mol Cell Endocrinol* 133: 81-88.
- Felber JP and Golay A 2002 Pathway from obesity to diabetes. *Int J Obes Relat Metab Disorder* 26: S39-45.
- Fei J, Lan F, Guo M, LI Y and Liu Y 2008 Inhibitory effects of anti-miRNA oligonucleotides (AMOs) on A549 cell growth. *J Drug Target* 16: 688-693.
- Feig PU, Shah S, Hermanowski-Vosatka A, Plotkin D, Springer MS, Donahue S, Thach C, Klein EJ, Lai E and Kaufman KD 2011 Diabetes *Obes Metab* 13: 498-504.
- Ferland-McCollough D, Ozanne SE, Siddle K, Willis AE and Bushell M 2010 The involvement of microRNAs in type 2 diabetes. *Biochem Soc Trans* 38: 1565-1570.
- Filipowicz W, Bhattacharyya SN and Sonenberg N 2008 Mechanisms of post-transcriptional regulation by microRNAs: are the answers in sight? *Nature* 9: 102-14.
- Friedberg M, Zoumakis E, Hiroi N, Bader T, Chrousos GP and Hochberg Z 2003 Modulation of 11beta-hydroxysteroid dehydrogenase type 1 in mature human subcutaneous adipocytes by hypothalamic messengers. *J Clin Endocrinol Metab* 88: 385-393.
- Gallagher IJ, Scheele C, Keller P, Nielsen AR, Remenyi J, Fischer CP, Roder K, Babraj J, Wahlestedt C, Hutvagner G, Pedersen BK and Timmons JA 2010 Integration of microRNA changes in vivo identifies novel molecular features of muscle insulin resistance in type 2 diabetes. *Genome Med* 2: 9.
- Gerin I, Bommer GT, McCoin CS, Sousa KM, Krishnan V and MacDougald OA 2010 Roles for miRNA-378/378* in adipocyte gene expression and lipogenesis. *Am J Physiol Endocrinol Metab* 299: E198-206.
- Gettys TW, Watson PM, Taylor IL and Collins S 1997 RU-486 ameliorates diabetes but does not correct deficient beta-adrenergic signaling in adipocytes from mature C57BL/6J-ob/ob mice. *Int J Obes Relat Metab Disord* 21: 865-373.
- Giraldez AJ, Mishima Y, Rihel J, Grocock RJ, Van Dongen S, Inoue K, Enright AJ and Schier AF 2006 Zebrafish MiR-430 promotes deadenylation and clearance of maternal mRNAs. *Science* 312: 75-79.
- Girard M, Jacquemin E, Munnich A, Lyonnet S and Henrion-Caude A 2008 miR-122, a paradigm for the role of microRNAs in the liver. *J Hepatol* 48: 648-656.
- Gottfried-Blackmore A, Sierra A, McEwen BS, Ge R and Bulloch K 2010 Microglia express functional 11 beta-hydroxysteroid dehydrogenase type 1. *Glia* 58: 1257-1266.
- Gout J, Tirard J, Thevenon C, Riou JP, Begeot M and Naville D 2006 CCAAT/enhancer-binding protein (C/EBPs) regulate the basal and cAMP-induced transcription of the

References

- human 11 β -hydroxysteroid dehydrogenase encoding gene in adipose cells. *Biochimie* 88: 1115-1124.
- Grammantièri L, Ferracin M, Fornari F, Veronese A, Sabbioni S, Liu CG, Calin GA, Giovannini C, Ferrazzi E and Grazi GL 2007 Cyclin G1 is a target of miR-122a, a microRNA frequently down-regulated in human hepatocellular carcinoma. *Cancer Res* 67: 6092-6099.
- Griffiths-Jones S 2004 The microRNA Registry *Nucleic Acids Res* 32: D109-111.
- Griffiths-Jones S, Grocock RJ, van Dongen S, Bateman A and Enright AJ 2006 miRBase: microRNA sequences, targets and gene nomenclature. *Nucleic Acids Res.* 34: D140-144.
- Griffiths-Jones S, Saini HK, van Dongen S and Enright AJ 2008 miRBase: tools for microRNA genomics. *Nucleic Acids Res.* 36: D154-158.
- Grimson A, Farh KK, Johnston WK, Garrett-Engele P, Lim LP and Bartel DP 2007 MicroRNA targeting specificity in mammals: determinants beyond seed pairing. *Mol Cell* 27: 91-105.
- Gupta S, Alfaidy N, Holloway AC, Whittle WL, Lye SJ, Gibb W and Challis JR 2003 Effects of cortisol and oestradiol on hepatic 11 β -hydroxysteroid dehydrogenase type 1 and glucocorticoid receptor proteins in late-gestation sheep fetus. *J Endocrinol* 176: 175-184.
- Hammami MM and Siiteri PK 1991 Regulation of 11 β -hydroxysteroid dehydrogenase activity in human skin fibroblasts: enzymatic modulation of glucocorticoid action. *J Clin Endocrinol Metab* 73: 326-334.
- Han J, Lee Y, Yeom KH, Nam JW, Heo I, Rhee JK, Sohn SY, Cho Y, Zhang BT and Kim VN 2006 Molecular basis for the recognition of primary microRNAs by the Drosha-DGCR8 complex. *Cell* 125: 887-901.
- Handoko K, Yang K, Strutt B, Khalil W and Killinger D 2000 Insulin attenuates the stimulatory effects of tumor necrosis factor alpha on 11beta-hydroxysteroid dehydrogenase type 1 in human adipose stromal cells. *J Steroid Biochem Mol Biol* 72: 163-168.
- Hardy RS, Filer A, Cooper MS, Parsonage G, Raza K, Hardie DL, Rabbitt EH, Stewart PM, Buckley CD and Hewison M 2006 Differential expression, function and response to inflammatory stimuli of 11beta-hydroxysteroid dehydrogenase type 1 in human fibroblasts: a mechanism for tissue-specific regulation of inflammation. *Arthritis Res Ther* 8(4): R108.
- Hausser J, Berninger P, Rodak C, Jantscher Y, Wirth S and Zavolan M 2009 Mirz: an integrated microRNA expression atlas and target prediction resource. *Nucleic Acids Res* 37: W266-272.

References

- He A, Zhu L, Gupta N, Chang Y and Fang F 2007 Overexpression of micro ribonucleic acid 29, highly up-regulated in diabetic rats, leads to insulin resistance in 3T3-L1 adipocytes. *Mol Endocrinol* 21: 2785-2794.
- Heneghan HM, Miller N, McAnena OJ, O'Brien T and Kerin MJ 2011 Differential miRNA expression in omental adipose tissue and in the circulation of obese patients identified novel metabolic biomarkers. *J Clin Endocrinol Metab* 96: E846-850.
- Hennebold JD, Ryu SY, Mu HH, Galbraith A and Daynes RA 1996 11 β -Hydroxysteroid dehydrogenase modulation of glucocorticoid activities in lymphoid organs. *Am J Physiol* 270: R1296-R1306.
- Hermanowski-Vosatka A, Gerhold D, Mundt SS, Loving VA, Lu M, Chen Y, Elbrecht A, Wu M, Doebber T, Kelly L, Milot D, Guo Q, Wang PR, Ippolito M, Chao YS, Wright SD and Thieringer R 2000 PPAR α agonists reduce 11 β -hydroxysteroid dehydrogenase type 1 in the liver. *Biochem Biophys Res Commun* 279: 330-336.
- Hermanowski-Vosatka A, Balkovec JM, Cheng K and Thieringer R 2005 11 β -HSD1 inhibition ameliorates metabolic syndrome and prevents progression of atherosclerosis in mice. *J Exp Med* 202: 517-527.
- Herrera BM, Lockstone HE, Taylor JM, Wills QF, Kaisaki PJ, Barrett A, Camps C, Fernandez C, Ragoussis J, Gauguier D, McCarthy MI and Lindgren CM 2009 MicroRNA-125a is over-expressed in insulin target tissues in a spontaneous rat model of Type 2 Diabetes. *BMC Medical Genomics* 2: 54.
- Herrera BM, Lockstone HE, Taylor JM, Ria M, Barrett A, Collins S, Kaisaki P, Argoud K, Fernandez C, Travers ME, Grew JP, Randall JC, Gloyn AL, Gauguier D, McCarthy MI, and Lindgren CM 2010 Global microRNA expression profiles in insulin target tissues in a spontaneous rat model of type 2 diabetes. *Diabetologia* 53: 1099-1109.
- Ho CK, Tetsuka M and Hillier SG 1999 Regulation of 11 β -hydroxysteroid dehydrogenase isoforms and glucocorticoid receptor gene expression in the rat uterus. *J Endocrinol* 163: 425-431.
- Holmes MC, Carter RN, Noble J, Chitnis S, Dutia A, Paterson JM, Mullins JJ, Seckl JR and Yau JL 2010 11 β -hydroxysteroid dehydrogenase type 1 expression is increased in the aged mouse hippocampus and parietal cortex and causes memory impairments. *J Neurosci* 30: 6916-6920.
- Hou W, Tian Q, Zheng J and Bohkovsky HL 2010 MicroRNA-196 represses Bach1 protein and hepatitis C virus gene expression in human hepatoma cells expressing hepatitis C viral proteins. *Hepatology* 51: 1494-1504.
- Hu A, Fatma S, Cao J, Grunstein JS, Nino G, Grumbach Y and Grunstein MM 2009 Th2 cytokine-induced upregulation of 11 β -hydroxysteroid dehydrogenase-1 facilitates glucocorticoid suppression of proasthmatic airway smooth muscle function. *Am J Physiol Lung Cell Mol Physiol* 296: L790-803.
- Huang B, Qin W, Zhao B, Shi Y, Yao C, Li J, Xiao H and Jin Y 2009 MicroRNA expression profiling in diabetic GK rat model. *Acta Biochim Biophys Sin* 41: 472-477.

References

- Huang Y, Li X, Lin H, Chu Y, Chen B, Lian Q and Ge RS 2010 Regulation of 11 beta-hydroxysteroid dehydrogenase type 1 and 2 by IGF-1 in mice. *Biochem Biophys Res Commun* 391: 1752-1756.
- Hughes KA, Webster SP and Walker BR 2008 11-Beta hydroxysteroid dehydrogenase type 1 (11beta-HSD1) inhibitors in type 2 diabetes mellitus and obesity. *Expert Opin Investing Drugs* 17: 481-496.
- Hundertmark S, Ragosch V, Schein B, Buhler H, Lorenz U, Fromm M and Weitzel HK 1994 Gestational age dependence of 11 β -hydroxysteroid dehydrogenase and its relationship to the enzymes of phosphatidylcholine synthesis in lung and liver of fetal rat. *Biochim Biophys Acta* 1210: 348-354.
- Hutvagner G, Simard MJ, Mello CC and Zamore PD 2004 Sequence-specific inhibition of small RNA function. *PLoS Biol* 2: E98.
- Iwasaki Y, Takayasu S, Nishiyama M, Tsuqita M, Taquchi T, Asai M, Yoshida M, Kambayashi M and Hashimoto K 2008 Is the metabolic syndrome an intracellular Cushing state? Effects of multiple humoral factors on the transcriptional activity of the hepatic glucocorticoid-activating enzyme (11beta-hydroxysteroid dehydrogenase type 1) gene. *Mol Cell Endocrinol* 285: 10-18.
- Jamieson PM, Chapman KE and Seckl JR 1999 Tissue- and temporal-specific regulation of 11 β -hydroxysteroid dehydrogenase type 1 by glucocorticoids in vivo. *J Steroid Biochem Mol Biol* 68: 245-250.
- Jellinck PH, Pavlides C, Sakai RR and McEwen BS 1999 11 β -Hydroxysteroid dehydrogenase functions reversibly as an oxidoreductase in the rat hippocampus in vivo. *J Steroid Biochem Mol Biol* 71: 139-144.
- Jennewein C, von Knethen A, Schmid T and Brüne B 2010 MicroRNA-27b contributes to lipopolysaccharide-mediated peroxisome proliferators-activated receptor γ (PPAR γ) mRNA destabilization. *J Biol Chem* 285: 11846-11853.
- Jones-Rhoades MW, Bartel DP and Bartel B 2006 MicroRNAs and their regulatory in plants. *Annu Rev Plant Biol* 57: 19-53.
- Kajimoto K, Naraba H and Iwai N 2006 MicroRNA and 3T3-L1 pre-adipocyte differentiation RNA 12: 1626-1632.
- Karbiener M, Fischer C, Nowitsch S, Opriessnig P, Papak C, Ailhaud G, Dani C, Amri EZ and Scheideler M 2009 microRNA miR-27b impairs human adipocyte differentiation and targets PPARgamma. *Biochem Biophys Res Commun* 390: 247-251.
- Karolina DS, Armugam A, Tavintharan S, Wong MT, Lim SC, Sum CF and Jeyaseelan K 2011 MicroRNA 144 impairs insulin signaling by inhibiting the expression of insulin receptor substrate 1 in type 2 diabetes mellitus. *PLoS One* 6: e22839.

References

- Keller P, Gburcik V, Petrovic N, Gallagher IJ, Hedergaard J, Cannon B and Timmons JA 2011 Gene-Chip studies of adipogenesis-regulated microRNAs in mouse primary adipocytes and human obesity. *BMC Endocr Disord* 11: 7.
- Kennell JA, Gerin I, MacDougald OA and Cadigan KM 2008 The microRNAs miR-8 is a conserved negative regulator of Wnt signaling. *Proc Natl Acad Sci USA* 105: 15417-15422.
- Kerr TA, Korenblat KM and Davidson NO 2011 MicroRNAs and liver disease. *Transl Res* 157: 241-252.
- Kim SY, Kim YA, Lee HW, Son YH, Lee GY, Lee JW, Lee YS and Kim JB 2010 miR-27a is a negative regulator of adipocyte differentiation via suppressing PPARgamma expression. *Biochem Biophys Res Commun* 392: 323-328.
- Kim YJ, Hwang SJ, Bae YC and Jung JS 2009 MiR-21 regulates adipogenic differentiation through the modulation of TGF-beta signaling in mesenchymal stem cells derived from human adipose tissue. *Stem Cells* 27: 3093-3102.
- Kinoshita M, Ono K, Horie T, Nagao K, Nishi H, Kuwabara Y, Takanabe-Mori R, Hasegawa K, Kita T and Kimura T 2010 Regulation of adipocyte differentiation by activation of serotonin (5-HT) receptors 5-HT_{2A}R and 5-HT_{2C}R and involved of microRNA-448-mediated repression of KLF5. *Mol Endocrinol* 24: 1978-1987.
- Kiriakidou M, Tan GS, Lamprinakı S, Nelson PT and Mourelatos Z 2007 An mRNA m7G Cap Binding-like Motif within Human Ago2 Represses Translation. *Cell* 129: 1141-1151.
- Klötting N, Berthold S, Kovacs P, Schön MR, Fasshauer M, Ruschke K, Stumvoll M and Blüher M 2009 MicroRNA expression in human omental and subcutaneous adipose tissue. *PLoS ONE* 4: e4699.
- Kolonin MG, Saha PK, Chan L, Pasgualini R and Arap W 2004 Reversal of obesity by targeted ablation of adipose tissue. *Nat Med* 10: 625-632.
- Korbonits M, Bujalska I, Shimojo M, Nobes J, Jordan S, Grossman AB and Stewart PM 2001 Expression of 11 β -hydroxysteroid dehydrogenase isoenzymes in the human pituitary: induction of the type 2 enzyme in corticotropinomas and other pituitary tumors. *J Clin Endocrinol Metab* 86: 2728-2733.
- Krutzfeldt J and Stoffel M 2006 MicroRNAs: a new class of regulatory genes affecting metabolism. *Cell Metab* 4: 9-12.
- Kutay H, Bai S, Datta J, Motiwala T, Pogribny I, Frankel W, Jacob ST and Ghoshal K 2006 Downregulation of miR-122 in the rodent and human hepatocellular carcinomas. *J Cell Biochem* 99: 671-678.
- Lai EC 2004 Predicting and validating microRNA targets. *Genome Biol* 5: 1151-1156.
- Landgraf P, Rusu M, Sheridan R, Sewer A, Iovino N, Aravin A, Pfeffer S, Rice A, Kamphorst AO, Landthaler M, Lin C, Socci ND, Hermida L, Fulci V, Chiaretti S, Foa R, Schliwka

References

- J, Fuchs U, Novosel A, Müller RU, Schermer B, Bissels U, Inman J, Phan Q, Chien M, Weir DB, Choksi R, De Vita G, Frezzetti D, Trompeter HI, Hornung V, Teng G, Hartmann G, Palkovits M, Di Lauro R, Wernet P, Macino G, Rogler CE, Nagle JW, Ju J, Papavasiliou FN, Benzing T, Lichter P, Tam W, Brownstein MJ, Bosio A, Borkhardt A, Russo JJ, Sander C, Zavolan M and Tuschl T 2007 A mammalian microRNA expression atlas based on small RNA library sequencing. *Cell* 129: 1401-1414.
- Laplante M, Sell H, MacNaul KL, Richard D, Berger JP and Deshaies Y 2003 PPAR γ activation mediates adipose depot-specific effects on gene expression and lipoprotein lipase activity: mechanism for modulation of postprandial lipemia and differential adipose accretion. *Diabetes* 52: 292-299.
- Law PT and Wong N 2011 Emerging roles of microRNA in the intercellular signaling networks of hepatocellular carcinoma. *J Gastroenterol Hepatol* 26: 437-449.
- Le MT, Teh C, Shyh-Chang N, Xie H, Zhou B, Korzh V, Lodish HF and Lim B 2009 MicroRNA-125b is a novel negative regulator of p53. *Genes Dev* 23: 862-876.
- Lean ME, Han TS and Seidell JC 1998 Impairment of health and quality of life in people with large waist circumference. *Lancet* 351: 853-856.
- Leckie CM, Welberg LA and Seckl JR 1998 11 β -Hydroxysteroid dehydrogenase is a predominant reductase in intact rat Leydig cells. *J Endocrinol* 159: 233-238.
- Lee HY, Acosta TJ Skarzynski DJ and Okuda K 2009 Prostaglandin F $_{2\alpha}$ stimulates 11 β -hydroxysteroid dehydrogenase 1 enzyme bioactivity and protein expression in bovine endometrial stromal cells. *Biol Reprod* 80: 657-664.
- Lee RC, Feinbaum RL and Ambros V 1993 The *C. elegans* heterochronic gene *lin-4* encodes small RNAs with antisense complementarity to *lin-14*. *Cell* 75: 843-854.
- Lewis BP, Shih IH, Jones-Rhoades MW, Bartel DP and Burge CB 2003 Prediction of mammalian microRNA targets. *Cell* 115: 787-798.
- Lewis BP, Burge CB and Bartel DP 2005 Conserved seed pairing, often flanked by adenosines, indicates that thousands of human genes are microRNA targets. *Cell* 120: 15-20.
- Li J, Fu H, Xu C, Tie Y, Xing R, Zhu J, Qin Y, Sun Z and Zheng X 2010 miR-183 inhibits TGF-beta1-induced apoptosis by downregulation of PDCD4 expression in human hepatocellular carcinoma cells. *BMC Cancer* 10: 354.
- Li QJ, Chau J, Ebert PJ, Sylvester G, Min H, Liu G, Braich R, Manoharan M, Soutschek J, Share P, Klein LO, Davis MM and Chen CZ 2007 miR-181a is an intrinsic modulator of T cell sensitivity and selection. *Cell* 129:147-161.
- Lim LP, Lau NC, Garrett-Engele P, Grimson A, Schelter JM, Castle J, Bartel DP, Linsley PS and Johnson JM 2005 Microarray analysis shows that some microRNAs downregulate large numbers of target mRNAs. *Nature* 433: 769-773.

References

- Lin PY and Yang PC 2011 Circulating miRNA signature for early diagnosis of lung cancer. *EMBO Mol Med* 8: 436-437.
- Lin Q, Gao Z, Alarcon RM, Ye J and Yun Z 2009 A role of miR-27 in the regulation of adipogenesis. *FEBS J* 276: 2348-2358.
- Ling HY, Ou HS, Feng SD, Zhang XY, Tuo QH, Chen LX, Zhu BY, Gao ZP, Tang CK, Yin WD, Zhang L and Liao DF 2009 Changes in microRNA profile and effects of miR-320 in insulin-resistant 3T3-L1 adipocytes. *Clin Exp Pharmacol Physiol* 9: e32-39.
- Liu J, Wang L, Zhang A, Di W, Zhang X, Wu L, Yu J, Zha J, Lv S, Cheng P, Hu M, Li Y, Qi H, Ding G and Zhong Y 2011 Adipose tissue-targeted 11 β -hydroxysteroid dehydrogenase type 1 inhibitor protects against diet-induced obesity. *Endocr J* 58: 199-299.
- Liu Y, Nakagawa Y, Wang Y, Li R, Li X, Ohzeki T and Friedman TC 2003 Leptin activation of corticosterone production in hepatocytes may contribute to the reversal of obesity and hyperglycemia in leptin-deficient ob/ob mice. *Diabetes* 52: 1409-1416.
- Liu YJ, Nakagawa Y, Nasuda K, Saequsa H and Iqarashi Y 1996 Effect of growth hormone, insulin and dexamethasone on 11 β -hydroxysteroid dehydrogenase activity on a primary culture of rat hepatocytes. *Life Sci* 59: 227-234.
- Liu YJ, Nakagawa Y, Wang Y, Li R, Li X, Ohzeki T and Friedman TC 2003 Leptin activation of corticosterone production in hepatocytes may contribute to the reversal of obesity and hyperglycemia in leptin-deficient ob/ob mice. *Diabetes* 52: 1409-1416.
- Livingstone DE, Jones GC, Smith K, Jamieson PM, Andrew R, Kenyon CJ and Walker BR 2000 Understanding the role of glucocorticoids in obesity: tissue-specific alterations of corticosterone metabolism in obese Zucker rats. *Endocrinology* 141: 560-563.
- Livingstone DEW and Walker BR 2003 Is 11 β -hydroxysteroid dehydrogenase type 1 a therapeutic target? Effects of carbenoxolone in lean and obese Zucker rats. *J Pharmacol Exp Ther* 305: 167-172.
- Lovis P, Roggli E, Laybutt DR, Gattesco S, Yang JY, Widmann C, Abderrahmani A and Regazzi R 2008 Alterations in microRNA expression contribute to fatty acid-induced pancreatic beta-cell dysfunction. *Diabetes* 57: 2728-2736.
- Low SC, Assaad SN, Rajan V, Chapman KE, Edwards CR and Seckl JR 1993 Regulation of 11 β -hydroxysteroid dehydrogenase by sex steroids in vivo: further evidence for the existence of a second dehydrogenase in rat kidney. *J Endocrinol* 139: 27-35.
- Low SC, Chapman KE, Edwards CR, Wells T, Robinson IC and Seckl JR 1994 Sexual dimorphism of hepatic 11 β -hydroxysteroid dehydrogenase in the rat: the role of growth hormone patterns. *J Endocrinol* 143: 541-548.
- Lu LF and Liston A 2009 MicroRNA in the immune system, microRNA as an immune system. *Immunology* 127: 291-298.

References

- Lu M, Zhang Q, Deng M, Miao J, Guo Y, Gao W and Cui Q 2008 An analysis of human microRNA and disease association. *PLoS One* 3: e3420.
- Lu NZ, Collins JB, Grissom SF and Cidlowski JA 2007 Selective regulation of bone cell apoptosis by translational isoforms of the glucocorticoid receptor. *Mol Cell Biol* 20: 7143-7160.
- Lund E, Guttinger S, Calado A, Dahlberg JE and Kutay U 2004 Nuclear export of microRNAs precursors. *Science* 303: 95-98.
- Ma XH, Wu WX and Nathanielsz PW 2003 Gestation-related and betamethasone-induced changes in 11 β -hydroxysteroid dehydrogenase types 1 and 2 in the baboon placenta. *Am J Obstet Gynecol* 188: 13-21.
- Maes OC, An J, Sarojini H, Wu H and Wang E 2008 Changes in MicroRNA expression patterns in human fibroblasts after low-LET radiation. *J Cell Biochem* 105: 824-834.
- Maser E, Völker B and Friebertshäuser J 2002 11 β -Hydroxysteroid dehydrogenase types 1 from human liver: dimerization and enzyme cooperativity support its postulated roles as glucocorticoid reductase. *Biochemistry* 41: 2459-2465.
- Maragkakis M, Alexiou P, Papadopoulos GL, Reczko M, Dalamagas T, Giannopoulos G, Goumas G, Koukis E, Kourtis K, Simossis VA, Sethupathy P, Vergoulis T, Koziris N, Sellis T, Tsanakas P and Hatzigeorgiou AG 2009 Accurate microRNA target prediction correlates with protein repression levels. *BMC Bioinformatics* 10: 295.
- Maragkakis M, Reczko M, Simossis VA, Alexiou P, Papadopoulos GL, Dalamagas T, Giannopoulos G, Goumas G, Koukis E, Kourtis K, Vergoulis T, Koziris N, Sellis T, Tsanakas P and Hatzigeorgiou AG 2009 DIANA-microT web server: elucidating microRNA functions through target prediction. *Nucleic Acids Res.* 37: W273-276.
- Martens-Uzunova ES, Jalava SE, Dits NF, van Leenders GJ, Moller S, Trapman J, Bangma GH, Litman T, Visakorpi T and Jenster G 2011 Diagnostic and prognostic signatures from the small non-coding RNA transcriptome in prostate cancer. *Oncogene* (Epub ahead of print).
- Martinelli R, Nardelli C, Pilone V, Buonomo T, Liquori R, Castano I, Buono P, Masone S, Persico G, Forestieri P, Pastore L and Sacchetti L 2010 miR-519d overexpression is associated with human obesity. *Obesity* 18: 2170-2176.
- Masuzaki H, Paterson J, Shinyama H, Morton NM, Mullins JJ, Seckl JR and Flier JS 2001 A transgenic model of visceral obesity and the metabolic syndrome. *Science* 294: 2166-2170.
- McGregor RA and Choi MS 2011 microRNAs in the regulation of adipogenesis and obesity. *Curr Mol Med* 11: 304-316.
- Meng F, Henson R, Wehbe-Janek H, Ghoshal K, Jacob ST and Patel T 2007 MicroRNA-21 regulates expression of the PTEN tumor suppressor gene in human hepatocellular cancer. *Gastroenterology* 133: 647-658.

References

- Michael AE, Evagelatou M, Norgate DP, Clarke RJ, Antoniw JW, Stedman BA, Brennan A, Welsby R, Bujalska I, Stewart PM and Cook BA 1993 Direct inhibition of ovarian steroidogenesis by cortisol and the modulatory role of 11 β -hydroxysteroid dehydrogenase. *Clin Endocrinol (Oxf)* 38: 641-644.
- Michailidou Z, Coll AP, Kenyon CJ, Morton NM, O'Rahilly S, Seckl JR and Chapman KE 2007 Peripheral mechanisms contributing to the glucocorticoid hypersensitivity in proopiomelanocortin null mice treatment with corticosterone. *J Endocrinol* 194: 161-170.
- Moisan MP, Seckl JR and Edwards CRW 1990 11 β -Hydroxysteroid dehydrogenase bioactivity and messenger RNA expression in rat forebrain: localization in hypothalamus, hippocampus, and cortex. *Endocrinology* 127: 1450-1455.
- Moore JS, Monson JP, Kaltsas G, Putignano P, Wood PJ, Sheppard MC, Besser GM, Taylor NF and Stewart PM 1999 Modulation of 11 β -hydroxysteroid dehydrogenase isozymes by growth hormone and insulin-like growth factor: in vivo and in vitro studies. *J Clin Endocrinol Metab* 84(11): 4172-4177.
- Morris KL and Zemel MB 2005 1, 25-dihydroxyvitamin D₃ modulation of adipocyte glucocorticoid function. *Obes Res* 13: 670-677.
- Nakanishi N, Nakagawa Y, Tokushige N, Aoki N, Matsuzaka Z, Ishii K, Yahagi N, Kobayashi K, Yatoh S, Takahashi A, Suzuki H, Urayama O, Yamada N and Shimano 2009 The up-regulation of microRNA-335 is associated with lipid metabolism in liver and white adipose tissue of genetically obese mice. *Biochem Biophys Res Commun* 385: 492-496.
- Nakano S, Inada Y, Masuzaki H, Tanaka T, Yasue S, Ishii T, Arai N, Ebihara K, Hosoda K, Maruyama K, Yamazaki Y, Shibata N and Nakao K 2007 Bezafibrate regulates the expression and enzyme activity of 11 β -hydroxysteroid dehydrogenase type 1 in murine adipose tissue and 3T3-L1 adipocytes. *Am J Physiol Endocrinol Metab* 292: E1213-1222.
- Napolitano A, Voice MW, Edwards CR, Seckl JR and Chapman KE 1998 11 beta-hydroxysteroid dehydrogenase 1 in adipocytes: expression is differentiation-dependent and hormonally regulated. *J Steroid Biochem Mol Biol* 64: 251-260.
- Nielsen CB, Shomron N, Sandberg R, Hornstein E, Kitzman J and Burge CB 2007 Determinants of targeting by endogenous and exogenous microRNAs and siRNAs. *RNA* 13: 1894-1910.
- Nissen SE and Wolski K 2007 Effect of rosiglitazone on the risk of myocardial infarction and death from cardiovascular causes. *N Engl J Med* 356: 2457-2471.
- Nottrott S, Simard MJ and Richter JD 2006 Human let-7a miRNA blocks protein production on actively translating polyribosomes. *Nat Struct Mol Biol* 13: 1108-1114.
- Nuotio-Antar AM, Hachey D and Hasty AH 2007 Carbenoxolone treatment attenuates symptoms of metabolic syndrome and atherogenesis in obese, hyperlipidemic mice. *Am J Physiol Endocrinol Metab* 293: E517-528.

References

- Nwe KH, Hamid A, Morat PB and Khalid BA 2000 Differential regulation of the oxidative 11 β -hydroxysteroid dehydrogenase activity in testis and liver. *Steroids* 65: 40-45.
- Ortega FJ, Moreno-Navarrete JM, Pardo G, Sabater M, Hummel M, Ferrer A, Rodriguez-Hermosa JI, Ruiz B, Ricart W, Peral B and Fernandez-Real JM 2010 MiRNA expression profile of human subcutaneous adipose and during adipocyte differentiation. *PLoS ONE* 5: e9022.
- Orth DN 1995 Cushing's syndrome. *N Engl J Med* 332: 791-803.
- Oskowitz A, Lu J, Penforis P, Ylostalo J, McBride J, Flemington EK, Prockop DJ and Pochampally R 2008 Human multipotent stromal cells from bone marrow and microRNA: Regulation of differentiation and leukemia inhibitory factor expression. *Proc Natl Acad Sci USA* 105: 18372-18377.
- Papadopoulos GL, Alexiou P, Maragkakis M, Reczko M and Hatzigeorgiou AG 2009 DIANA-mirPath: Integrating human and mouse microRNAs in pathways. *Bioinformatics* 25: 1991-1993.
- Pepe GJ, Brurch MG and Albrecht ED 1999 Expression of 11 β -hydroxysteroid dehydrogenase types 1 and 2 proteins in human and baboon placental syncytiotrophoblast. *Placenta* 20: 575-582.
- Petersen CP, Bordeleau ME, Pelletier J and Sharp PA 2006 Short RNAs repress translation after initiation in mammalian cells. *Mol Cell* 21: 533-542.
- Poor V, Juricskay S, Gati A, Osvath P and Tenyi T 2004 Urinary steroid metabolites and 11 β -hydroxysteroid dehydrogenase activity in patients with unipolar recurrent major depression. *J Affect Disord* 81: 55-59.
- Poy MN, Hausser J, Trajkovski M, Braun M, Collins S, Rorsman P, Zavolan M and Stoffel M 2009 miR-375 maintains normal pancreatic α - and β -cell mass. *Proc Natl Acad Sci USA* 106: 5813-5818.
- de Quervain DJ, Poirier R, Wollmer MA, Grimaldi LM, Tsolaki M, Streffer JR, Hock C, Nitsch RM, Mohajeri MH and Papassotiropoulos A 2004 Glucocorticoid-related genetic susceptibility for Alzheimer's disease. *Hum Mol Genet* 13: 47-52.
- Qin L, Chen Y, Niu Y, Chen W, Wang Q, Xiao S, Li A, Xie Y, Li J, Zhao X, He Z and Mo D 2010 A deep investigation into the adipogenesis mechanism: profile of microRNAs regulating adipogenesis by modulating the canonical Wnt/beta-catenin signaling pathway. *BMC Genomics* 11: 320.
- Rajan V, Edwards CR and Seckl JR 1996 11 β -Hydroxysteroid dehydrogenase in cultured hippocampal cells reactivates inert 11-dehydrocorticosterone, potentiating neurotoxicity. *J Neurosci* 16: 65-70.
- Rask E, Olsson T, Soderberg S, Andrew R, Livingstone DE, Johnson O and Walker BR 2001 Tissue-specific dysregulation of cortisol metabolism in human obesity. *J Clin Endocrinol Metab* 86: 1418-1421.

References

- Rauz S, Walker EA, Shackleton CH, Hewison M, Murray PI and Stewart PM 2001 Expression and putative role of 11 β -hydroxysteroid dehydrogenase isozymes within the human eye. *Invest Ophthalmol Vis Sci* 42: 2037-2042.
- Reinhart BJ, Slack FJ, Basson M, Pasquinelli AE, Bettinger JC, RouqvieAE, Horvitz HR and Ruvkun G 2000 The 21-nucleotide let-7 RNA regulates developmental timing in *Caenorhabditis elegans*. *Nature* 403: 901-906.
- Rhoades MW, Reinhart BJ, Lim LP, Burge CB, Bartel B and Bartel DP 2002 Prediction of plant microRNA targets. *Cell* 110: 513-520.
- Ricketts ML, Verhaeg JM, Bujalska I, Howie AJ, Rainey WE and Stewart PM 1998 Immunohistochemical localization of type 1 11 β -hydroxysteroid dehydrogenase in human tissues. *J Clin Endocrinol Metab* 83: 1325-1335.
- Rogler CE, Levoci L, Ader T, Massimi A, Tchaikovskaya T, Norel R and Rogler LE 2009 MicroRNA-23b cluster microRNAs regulate transforming growth factor-beta/bone morphogenetic protein signaling and liver stem cell differentiation by targeting Smads. *Hepatology* 50: 575-584.
- Ronchetti D, Lionetti M, Mosca L, Agnelli L, Andronache A, Fabris S, Deliliers GL and Neri A 2008 An integrative genomic approach reveals coordinated expression of intronic miR-335, miR-342, and miR-561 with deregulated host genes in multiple myeloma. *BMC Med Genomics* 1: 37.
- Rosen ED and MacDougald OA 2006 Adipocyte differentiation from the inside out. *Nat Rev Mol Cell Biol* 7: 885-896.
- Rundle SE, Funder JW, Laskhmi V and Monder C 1989 The intrarenal localization of mineralocorticoid receptors and 11 beta-dehydrogenase: immunocytochemical studies. *Endocrinology* 125: 1700-1704.
- Sakamuri SS, Ananthmakula P, Nappan Veetil G and Ayyalasomayajula V 2011 Vitamin A decreases pre-receptor amplification of glucocorticoids in obesity: study on the effect of vitamin A on 11 beta-hydroxysteroid dehydrogenase type 1 activity in liver and visceral fat of WNIN/Ob obese Rats. *Nutr J* 10: 70.
- Sankar BR, Maran RR, Sudha S, Govindarajulu P and Balasubramanian K 2000 Chronic corticosterone treatment impairs Leydig cell 11 β -hydroxysteroid dehydrogenase activity and LH-stimulated testosterone production. *Horm Metab Res* 32: 142-146.
- Schratt GM, Tuebing F, Nigh EA, Kane CG, Sabatini ME, Kiebler M and Greenberg 2006 A brain-specific microRNA regulates dendritic spine development. *Nature* 439: 283-289.
- Seckl JR and Walker BR 2001 Minireview: 11beta-hydroxysteroid dehydrogenase type 1- a tissue-specific amplifier of glucocorticoid action. *Endocrinology* 142: 1371-1376.
- Sheppard KE and Autelitano DJ 2002 11 β -Hydroxysteroid dehydrogenase 1 transforms 11-dehydrocorticosterone into transcriptionally active glucocorticoid in neonatal rat heart. *Endocrinology* 143: 198-204.

References

- Smith MP, Keay SD, Hall L, Harlow CR and Jenkins JM 1997 The detection and confirmation of 11 β -hydroxysteroid dehydrogenase type 1 transcripts in human luteinized granulosa cells using RT-PCR and plasmid pUC18. *Mol Hum Reprod* 3: 651-654.
- Sorensen B, Winn M, Rohde J, Shuai Q, Wang J, Fung S, Monzon K, Chiou W, Stolarik D, Imade H, Pan L, Deng X, Chovan L, Longenecker K, Judge R, Qin W, Brune M, Camp H, Frevert EU, Jacobson P and Link JT 2007 Adamantane sulfone and sulfonamide 11-beta-HSD1 inhibitors. *Bioorg Med Chem Lett* 17: 527-532.
- Srivastava RA 2009 Fenofibrate ameliorates diabetic and dyslipidemic profiles in KKAY mice partly via down-regulation of 11 β -HSD1, PEPCK and DGAT2. Comparison of PPAR α , PPAR γ , and liver x receptor agonists. *Eur J Pharmacol* 607: 258-263.
- Staab CA and Maser E 2010 11beta-hydroxysteroid dehydrogenase type 1 is an important regulator at the interface of obesity and inflammation. *J Steroid Biochem Mol Biol* 119: 56-72.
- Staab CA, Stegk JP, Haenisch S, Neiß E, Köbsch K, Ebert B, Cascorbi I and Maser E 2011 Analysis of alternative promoter usage in expression of HSD11B1 including the development of a transcript-specific quantitative real-time PCR method. *Chem Biol Interact* 191: 104-112.
- Stewart PM, Boulton A, Kumar S, Clark PM and Shackleton CH 1999 Cortisol metabolism in human obesity: impaired cortisone to cortisol conversion in subjects with central adiposity. *J Clin Endocrinol Metab* 84: 1022-1027.
- Stokes J, Noble J, Brett L, Phillips C, Seckl JR O'Brien C and Andrew R 2000 Distribution of glucocorticoid and mineralocorticoid receptors and 11 β -hydroxysteroid dehydrogenase in human and rat ocular tissues. *Invest Ophthalmol Vis Sci* 41: 1629-1638.
- Stulnig TM, Oppermann U, Steffensen KR, Schuster GU and Gustafsson JA 2002 Liver X receptors downregulate 11beta-hydroxysteroid dehydrogenase type 1 expression and activity. *Diabetes* 51(8): 2426-2433.
- Stulnig TM and Waldhausl W 2004 11 β -hydroxysteroid dehydrogenase types 1 in obesity and type 2 diabetes. *Diabetologia* 47: 1-11.
- Su X, Vicker N, Lawrence H, Smith A, Purohit A, Reed MJ and Potter BV 2007 Inhibition of human and rat 11 β -hydroxysteroid dehydrogenase type 1 by 18-beta-glycyrrhetic acid derivatives. *J Steroid Biochem Mol Biol* 104: 312-320.
- Sun F, Wang J, Pan Q, Yu Y, Zhang Y, Wan Y, Wang J, Li X and Hong A 2009 Characterization of function and regulation of miR-24-1 and miR-31. *Biochem Biophys Res Commun* 380: 660-665.
- Sun K, Yang K and Challis JR 1997 Differential expression of 11 β -hydroxysteroid dehydrogenase types 1 and 2 in human placenta and fetal membranes. *J Clin Endocrinol Metab* 82: 300-305.

References

- Sun T, Fu M, Bookout AL, Kliewer SA and Mangelsdorf DJ 2009 MicroRNA let-7 regulates 3T3-L1 Adipogenesis. *Mol Endocrinol* 23: 925-931.
- Takanabe R, Ono K, Abe Y, Takaya T, Horie T, Wada H, Kita T, Satoh N, Shimatsu A and Hasegawa K 2008 Up-regulated expression of microRNA-143 in association with obesity in adipose tissue of mice fed high-fat diet. *Biochem Biophys Res Commun* 376: 728-732.
- Tang G, Reinhart BJ, Bartel DP and Zamore PD 2003 A biochemical framework for RNA silencing in Plants. *Genes Dev* 17: 49-63.
- Tang YF, Zhang Y, Li XY, Li C, Tian W and Liu L 2009 Expression of miR-31, miR-125b-5p, and miR-326 in the adipogenic differentiation process of adipose-derived stem cells. *OMICS* 13: 331-336.
- Tannin GM, Agarwal AK, Monder C, New MI and White PC 1991 The human gene for 11 β -hydroxysteroid dehydrogenase. Structure, tissue distribution, and chromosomal localization. *J Biol Chem* 266: 16653-16658.
- Terakado M, Kumagami H and Takahashi H 2011 Distribution of glucocorticoid receptors and 11 beta-hydroxysteroid dehydrogenase isoforms in the rat inner ear. *Hear Res* (Epub ahead of print).
- Tetsuka M, Haines LC, Milne M, Simpson GE and Hillier SG 1999 Regulation of 11 β -hydroxysteroid dehydrogenase type 1 gene expression by LH and interleukin-1 β in cultured rat granulosa cells. *J Endocrinol* 163: 417-423.
- Thieringer R, Le Grand CB, Carbin L, Cai TQ, Wong B, Wright SD, and Hermanowski-Vosatka A 2001 11 β -Hydroxysteroid dehydrogenase type 1 is induced in human monocytes upon differentiation to macrophages. *J Immunol* 167: 30-35.
- Thompson A, Han VK and Yang K 2002 Spatial and temporal patterns of expression of 11 β -hydroxysteroid dehydrogenase types 1 and 2 messenger RNA and glucocorticoid receptor protein in the murine placenta and uterus during late pregnancy. *Bio Reprod* 67: 1708-1718.
- Tiganescu A, Walker EA, Hardy RS, Mayes AE and Stewart PH 2011 Localization, age- and site-dependent expression, and regulation of 11 beta-hydroxysteroid dehydrogenase type 1 in Skin. *J Invest Dermatol* 131: 30-36.
- Tiosano D, Eisentein I, Militianu D, Chrousos GP and Hochberg Z 2003 11 beta-Hydroxysteroid dehydrogenase activity in hypothalamic obesity. *J Clin Endocrinol Metab* 88: 379-384.
- Tiwari A 2010 INCB-13739, 11 β -hydroxysteroid dehydrogenase type 1 inhibitor for the treatment of type 2 diabetes. *Drugs* 13: 266-275.
- Tomlinson JW and Stewart PM 2001a Cortisol metabolism and the role of 11beta-hydroxysteroid dehydrogenase. *Best Pract Res Clin Endocrinol Metab* 15: 61-78.

References

- Tomlinson JW, Moore J, Cooper MS, Bujalska I, Shahmanesh M, Burt C, Strain A, Hewison M and Stewart PM 2001 Regulation of expression of 11 beta-hydroxysteroid dehydrogenase type 1 in adipose tissue: tissue-specific induction by cytokines. *Endocrinology* 142: 1982-1989.
- Tomlinson JW, Walker EA, Bujalska IJ, Draper N, Lavery GG, Cooper MS, Hewison M and Stewart PM 2004 11beta-Hydroxysteroid dehydrogenase type 1: a tissue-specific regulator of glucocorticoid response. *Endocrine Rev* 25(5): 831-866.
- Tomlinson JW, Sherlock M, Hughes B, Hughes SV, Kilvington F, Bartlett W, Courtney R, Rejto P, Carley W and Stewart PM 2007 Inhibitor of 11 β -hydroxysteroid dehydrogenase type 1 activity in vivo limits glucocorticoid exposure to human adipose tissue and decreases lipolysis. *J Clin Endocrinol Metab* 92: 857-864.
- Trajkovski M, Hausser J, Soutschek J, Bhat B, Akin A, Zavolan M, Heim MH and Stoffel M 2011 MicroRNAs 103 and 107 regulate insulin sensitivity. *2011 Nature* 474: 649-653.
- Tsigelny I and Baker ME 1995 Structures important in mammalian 11beta- and 17beta-hydroxysteroid dehydrogenases. *J Steroid Biochem Mol Biol* 55: 589-600.
- Tsuqita M, Iwasaki Y, Nishiyama M, Taquchi T, Shinahara M, Taniuchi Y, Kambayashi M, Terada Y and Hashimoto K 2008 Differential regulation of 11 beta-hydroxysteroid dehydrogenase type -1 and -2 gene transcription by proinflammatory cytokines in vascular smooth muscle cells. *Life Sci* 83: 426-432.
- Vallejo AN, Pogulis RJ and Pease LR 1994 In vitro synthesis of novel genes: mutagenesis and recombination by PCR. *PCR Methods Appl* 4: S123-130.
- Valsamakis G, Anwar A, Tomlinson JW, Shackleton CH, McTernan PG, Chetty R, Wood PJ, Banerjee AK, Holder G, Barnett AH, Stewart PM and Kumar S 2004 11 β -Hydroxysteroid dehydrogenase type 1 activity in lean and obese males with type 2 diabetes mellitus. *J Clin Endocrinol Metab* 89: 4755-4761.
- Varnholt H, Drebber U, Schulze F, Wedemeyer I, Schirmacher P, Dienes HP and Odenthal M 2008 MicroRNA gene expression profile of hepatitis C virus-associated hepatocellular carcinoma. *Hepatology* 47: 1223-1232.
- Verspohl EJ 2009 Novel therapeutics for type 2 diabetes: incretin hormone mimetics (glucagons-like peptide-1 receptor agonists) and dipeptidyl peptidase-4 inhibitors. *Pharmacol Ther* 124: 113-138.
- Voice MW, Seckl JR, Edwards CR and Chapman KE 1996 11 β -hydroxysteroid dehydrogenase type 1 expression in 2S FAZA hepatoma cells is hormonally regulated: a model system for the study of the hepatic glucocorticoid metabolism. *Biochem J* 317: 621-625.
- Waddell BJ, Hisheh S, Krozowski ZS and Burton PJ 2003 Localization of 11 β -hydroxysteroid dehydrogenase types 1 and 2 in the male reproductive tract. *Endocrinology* 144: 3101-3106.

References

- Walker BR, Campbell JC, Williams BC and Edwards CR 1992 Tissue-specific distribution of the NAD (+)-dependent isoform of 11 beta-hydroxysteroid dehydrogenase. *Endocrinology* 131: 970-972.
- Wamil M and Seckl JR 2007 Inhibition of 11 β -hydroxysteroid dehydrogenase type 1 as a promising therapeutic target. *Drug Discovery Today* 12: 504-520.
- Wan ZK, Chenail E, Li HQ, Kendall C, Wang Y, Gingras S, Xiang J, Masefski WW, Mansour TS, Saiah E 2011 Synthesis of potent and orally efficacious 11beta-hydroxysteroid dehydrogenase type 1 inhibitor HSD-016. *J Org Chem* (Epub ahead of print).
- Wang Q, Li YC, Wang J, Kong J, Qi Y, Quigg RJ and Li X 2008 miR-17/92 cluster accelerates adipocyte differentiation by negatively regulating tumor-suppressor Rb2/p130. *Proc Natl Acad Sci USA* 105: 2889-2894.
- Weiler J, Hunziker J and Hall J 2006 Anti-miRNA oligonucleotides (AMOs): ammunition to target miRNAs implicated in human disease? *Gene Therapy* 13: 496-502.
- Whorwood CB, Sheppard MC and Stewart PM 1993 Tissue specific effects of thyroid hormone on 11 β -hydroxysteroid dehydrogenase gene expression. *J Steroid Biochem Mol Biol* 46: 539-547.
- Whorwood CB, Ricketts ML and Stewart PM 1994 Epithelial cell localization of type 2 11 β -hydroxysteroid dehydrogenase in rat and human colon. *Endocrinology* 135: 2533-2541.
- Whorwood CB, Mason JJ, Ricketts ML, Howie AJ and Stewart PM 1995 Detection of human 11 β -hydroxysteroid dehydrogenase isoforms using reverse transcriptase polymerase chain reaction and localization of the type 2 isoform to renal collecting ducts. *Mol Cell Endocrinol* 110: R7-R12.
- Whorwood CB, Donovan SJ, Flanagan D, Phillips DI and Byrne CD 2002 Increased glucocorticoid receptor expression in human skeletal muscle cells may contribute to the pathogenesis of the metabolic syndrome. *Diabetes* 51: 1066-1075.
- Williams LJ, Lyons V, MacLeod I, Rajan V, Darlington GJ, Poli V, Seckl JR and Chapman KE 2000 C/EBP regulates hepatic transcription of 11 beta-hydroxysteroid dehydrogenase type 1. A novel mechanism for cross-talk between the C/EBP and glucocorticoid signaling pathways. *J Biol Chem* 275: 30232-30239.
- Wolkowitz OM, Reus VI, Chan T, Manfredi F, Raum W, Johnson R and Canick J 1999 Antigluco-corticoid treatment of depression: double-blind ketoconazole. *Biol Psych* 45: 1070-1074.
- Wong QW, Lung RW, Law PT, Lai PB, Chan KY, To KF and Wong N 2008 MicroRNA-223 is commonly repressed in hepatocellular carcinoma and potentiates expression of Stathmin 1. *Gastroenterology* 135: 257-269.
- Xiang J, Ipek M, Suri V, Tam M, Xing Y, Huang N, Zhang Y, Tobin J, Mansour TS and McKew J 2007 Beta-keto sulfones as inhibitors of 11-beta-hydroxysteroid dehydrogenase type 1 and the mechanism of action. *Bioorg Med Chem* 15: 4396-4405.

References

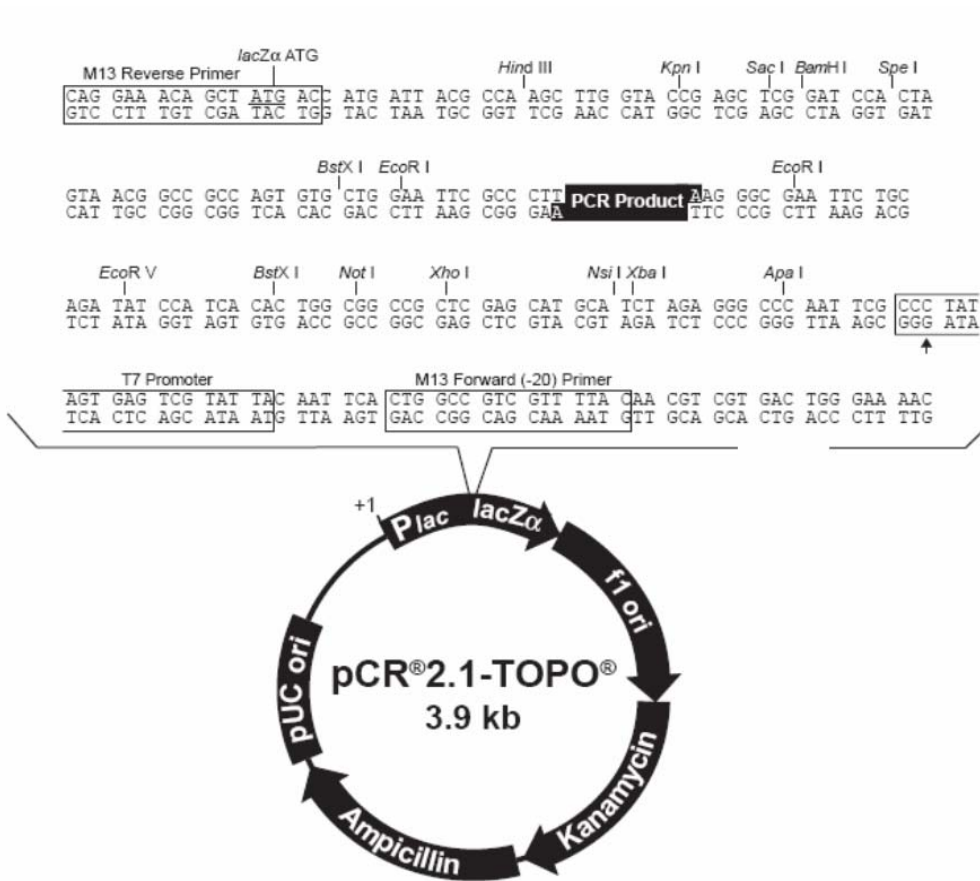
- Xie H, Lim B and Lodish HF 2009 MicroRNAs induced during adipogenesis that accelerate fat cell development are downregulated in obesity. *Diabetes* 58: 1050-1057.
- Yang K, Berdusco E and Challis J 1994 Opposite effects of glucocorticoid on hepatic 11 β -hydroxysteroid dehydrogenase mRNA and activity in fetal and adult sheep. *J Endocrinol* 143: 121-126.
- Yang Z, Zhu P, Guo C, Zhu X and Sun k 2009 Expression of 11 β -hydroxysteroid dehydrogenase type 1 in human fetal lung and regulation of its expression by interleukin-1 β and cortisol. *J Clin Endocrinol Metab* 94: 306-313.
- Yang Z, Bian C, Zhou H, Huang S, Wang S, Liao L and Zhao RC 2011 MicroRNA hsa-miR-138 inhibits adipogenic differentiation of human adipose tissue-derived mesenchymal stem cells through adenovirus EID-1. *Stem Cells and Development* 20: 259-267.
- Yau JL, Noble J, Kenyon CJ, Hibberd C, Kotelevtsev Y, Mullins JJ and Seckl JR 2001 Lack of tissue glucocorticoid reactivation in 11 β -hydroxysteroid dehydrogenase type 1 knockout mice ameliorates age-related learning impairments. *Proc Natl Acad Sci USA* 98: 4716-4721.
- Yau JL, McNair KM, Noble J, Brownstein D, Hibberd C, Morton N, Mullins JJ, Morris RG, Cobb S and Seckl JR 2007 Enhanced hippocampal long-term potentiation and spatial learning in aged 11 β -hydroxysteroid dehydrogenase type 1 knock-out mice. *J Neurosci* 27: 10487-10496.
- Yekta S, Shih IH and Bartel DP 2004 MicroRNA-directed cleavage of HOXB8 mRNA. *Science* 304, 594-596.
- Yi R, Qin Y, Macara IG and Cullen BR 2003 Exportin-5 mediates the nuclear export of pre-microRNAs and short hairpin RNAs. *Genes Dev* 17: 3011-3016.
- Yudt MR and Cidlowski 2002 The glucocorticoid receptor: coding a diversity of proteins and responses through a single gene. *Mol Endocrinol* 16: 1719-1726.
- Yue J and Tigy G 2006 MicroRNA trafficking and human cancer. *Cancer Biol Ther* 5: 573-578.
- Zampetaki A, Kiechl S, Drozdov I, Willeit P, Mayr U, Prokopi M, Mayr A, Weger S, Oberhollenzer F, Bonora E, Shah A, Willeit J and Mayr M 2010 Plasma microRNA profiling reveals loss of endothelial miR-126 and other microRNAs in type 2 diabetes. *Circ Res* 107: 810-817.
- Zhao E, Keller MP, Rabaglia ME, Oler AT, Stapleton DS, Schueler KL, Neto EC, Moon JY, Wang P, Wang IM, Lum PY, Ivanovska I and Attie AD 2009 Obesity and genetics regulate microRNAs in islets, liver, and adipose of diabetic mice. *Mamm Genome* 20: 476-485.

7 Appendix

7.1 Plasmid maps

7.1.1 pCR2.1-TOPO

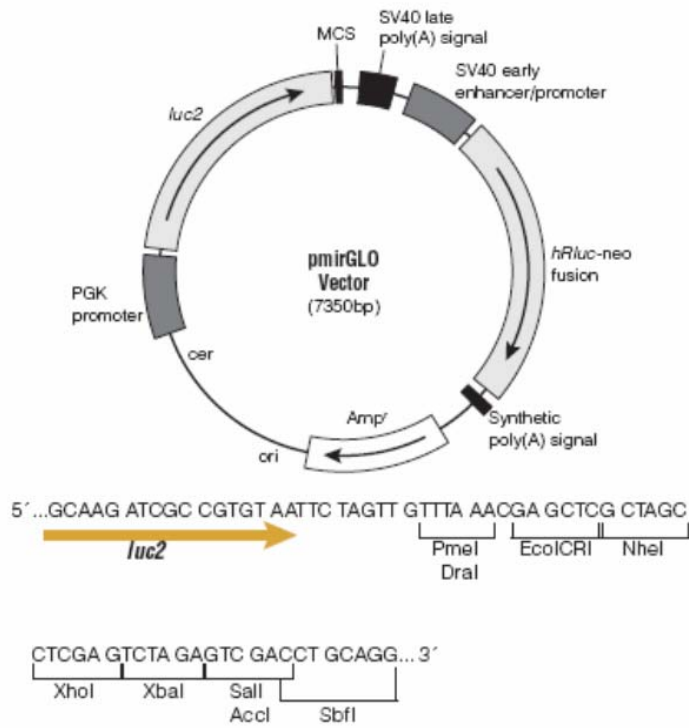
The map below shows the features of pCR2.1-TOPO and the sequence surrounding the TOPO Cloning sites. Restriction sites are labeled to indicate the actual cleavage site. The vector is used for the direct insertion of *Taq* polymerase-amplified PCR products.



Appendix

7.1.2 pmir-GLO

The pmir-GLO dual-luciferase miRNA target expression vector is designed to quantitatively evaluate microRNAs (miRNA) activity by the insertion of miRNA target sequence on the downstream of the firefly luciferase gene (*luc2*). Firefly luciferase is the primary reporter gene; decrease of firefly luciferase expression indicates the binding of endogenous or introduced miRNAs to the cloned miRNA target sequence. The pmir-GLO vector, firefly luciferase (*luc2*) is used as the primary reporter to monitor mRNA regulation, and *Renilla* luciferase (*hRluc-neo*) is acting as a control reporter for normalization and selection.



7.2 Sequences

7.2.1 *HSD11B1*-3'UTR

Nucleotide sequence of *HSD11B1*-3'UTR including relevant restriction sites:

CTCGAG

*Xho*I

```

1  GAACTCCCTG AGGGCTGGGC ATGCTGAGGG ATTTTGGGAC TGTTCTGTCT
51  CATGTTTATC TGAGCTCTTA TCTATGAAGA CATCTTCCCA GAGTGTCCCC
101 AGAGACATGC AAGTCATGGG TCACACCTGA CAAATGGAAG GAGTTCCTCT
151 AACATTTGCA AAATGGAAAT GTAATAATAA TGAATGTCAT GCACCGCTGC
201 AGCCAGCAGT TGTA AAAATTG TTAGTAAACA TAGGTATAAT TACCAGATAG
251 TTATATTA AA TTTATATCTT ATATATAATA ATATGTGATG ATTAATACAA
301 TATTAATTAT AATAAAGGTC ACATAAACTT TATAAATTCA TAACTGGTAG
351 CTATAACTTG AGCTTATTCA GGATGGTTTC TTTAAAACCA TAAACTGTAC
401 AAATGAAATT TTTCAATATT TGTTTCTTA CAGCTG

```

*Sal*I

7.2.2 *HSD11B1*-Promoter 1

Nucleotide sequence of *HSD11B1*-Promoter 1 including relevant restriction sites:

CCCGGG

*Xma*I

```

1  GCCCAGAAAA ATTAGGAGAC AAAGCCCAA AGAGGCAATA GTCAGCTTCT
51  TTCATTGGTA AGCTAAGGCT TCAAAATAAA ATTTTAACTT GAGAATGGTC
101 TCTCTCAAAG ACTCTGATAC CACCTAAAAC CTACCCTCCT TTCATTTCTC
151 TTTCTACTCA GCTTTACCTG ACCTTCAACA TGAGACAACC GTTTCTTCTA
201 AGTTTTCTCT GAAAAAGAGT AATCACATTG TAAAACCTGCT AAACCAGAGG
251 GGAGCCCTAA AAAGCTGAAT TTAAACCCTG GCCTGGAGCA AAATTA AAAG
301 TTATCATGAA AGATTTTCCT AAGCCTCAGG GGTGGTTGAG CAGAAATTAG
351 TTAACAATTC AGGATTTTAT TAGGTACTTA TTGTTCTGGA TTAAACATCT
401 GTACCAAATG ATTCAGTTAA TTGTTAGTCC ATCCAATAGA GAAAAAAAT
451 TATAAGCAGC AGGGTAAGAA AAAAATTAAA TAACTCAGTT GTGCAAATG
501 AAAAACAAAC GCCTTAAGTG GACAAGAAAA ACCTTGAAAA TCCAGTACAA

```

Appendix

551 AAAGCAATTT CAAAAAATC TTTCTTTTAA AAGTATGTTA GACAAAGATT
601 AAAAATTGTA AACTAAATGA AAATGAAAAG AGACTTCAGA AAACTTTCAA
651 AGAGCATTCT GGAGTACACT CAACAGCTGA AATAAAAGAA ACATTGTCTT
701 TATTTTTTTC TATTAAAGGG CTCAAATATG AATTCAGAGA TTTAATGAGA
751 AAAAAGTAAT TGAAATATGA AACTGACAGC TTAGAAAATA TCCAATACAT
801 AGCTAGATAT TTTAGAGAG CTCTAGAAAG TAAATAAGCT AGAAATCAAT
851 AGAACGTATG GTTCTCTACA TAAAAAACT TGCCCCGAAA TAAAAACAAA
901 GCCAAAAGT CTTCTATTTT CTAAGAATTG GGAACATATA GAGAGGGGTA
951 CTTGTAGATA TTGCAAGCAA AAGTGTCATT CAAAGAACCA ATGTTCCACA
1001 TTGGCTAAGT AACAGAAAGA TGAATTTGAC AAATCTGTCT AATGGTGTTC
1051 CTCAAAGGA GACATTAGTA CCCAACAATT ACAGTCCTTC CTCGGAGTTT
1101 GTGTCCCCAA ATCTCAGAGG GGCCAGTCGC TATACTCTCC ATCAGGGCAT
1151 AGCTACATCT AGCATGGCTT ACCACTCTAT CCCAGCCTC TAGCCCAGTG
1201 CCTAGCATAG AGTAGATGCT TATTAGATAT CTGTTGAACA AATGAAGAAA
1251 TAGAGGAAGA AAGTACATTT TTGTTTTGAC ATGCTGTAGT CCCTTCCTTA
1301 GTCCAGAGAT CACAAACCTC TGAATTGGGA TGTGACTCTC TCTGTCATTA
1351 ATCGGCAAGA ATCATGGTAG AATTATTGTC CCTACTTACG GATTCTCTTT
1401 CCCTTATACA TCCCATTGCA GATTCCTGTC TTCCCTTTAC ATCCACTCCA
1451 ACATCAGCTG ATGCAGTCAC TAAAATGGTT TATAAGTCAC ATATGAGATT
1501 CCCTAAGGAG TTTATAATTG AGAAATGTGT GGACACACAG GCCTCACAGA
1551 ATGCACTGGA TCACTAGAGT CTCTCCTGGT GAAAAGGGAA AACCTGCCCA
1601 AATCCAGTTT TTGTTTCAGT AACTTCCTTT GAGACAAAGT CAGGAATCTG
1651 AGAGTAAGCA CCTGCTAAGG GTGGGACAGG GGCTCTGTCT GGTATGCCTC
1701 TCCCATGTTA AGAGCTAACA ATAGTAATGG ATAAGTCTCC AGGGCAACCA
1751 GGACCACTTC CAAGCATTC TGTCTTGGGC TGCCTCGAGG GCTCCTCTGT
1801 CCTTTGGGGA GACTGATTG ATGCCTGATG CCCAGAACTG GCCCACTCTG
1851 GCTTCTCTTT GGAGCTGTCT CTGCAGGCGC CTTCTGGCTG CCAGCTCGGT
1901 CCTAGCATAA GGGACTTCTT CCTTGGCCTG GGTTTCACCT TCTTGTATCA
1951 GGTGGCAGAC CAGCTGGTTT CAGTCCAAA TCAGGTCTTC TGACTCCTCC
2001 CAGAAACCAA CCAACTTCTG AGCAGGAAAT CCTGCCCTC CCCAAAGAGT
2051 GGGAAACCGC AAAGGAAGAG AGAGATGAAA CAGAAGGAAA GGCAGAGGAG
2101 GAGGGAGAGA GAGAGAAGAG AAGAAAAGA AAAAAGAACA TCAATAAAAA

Appendix

2151 GAAGTCAGAT TTGTTGAAA TCT CCCGGG

*Xma*I

7.2.3 *HSD11B1*-Promoter 2

Nucleotide sequence of *HSD11B1*-Promoter 2 including relevant restriction sites:

CCCGGG

*Xma*I

1 GAGAACCAGC CATGTAAATA TGGACACAAA GTGGATTAGA TGTTTATTAT
51 ATAATATGGT CAAAGTGTGG TCCCCATGGG TCTCTGAGAC CCTCTTGAAG
101 GGTGAAAGG TCAAACTAT TTTCATAATT AACTAAGAC ATTACCTGAC
151 TTTTCCAGAG GCTACAGGAT GTATGCTAAT GCCACTGCCC TGAATGCTAA
201 TGGAATGTAT GCTTATGTAT TCTTGAGCTT TAGAAAAAAA TCCTCAGTCT
251 TAATTTCTAA TGCATAAATT GCAATAGCAA TATCAATAGG TAAAACCTAC
301 ACAGGCAAAA GTTCTTTGAG GTCCTTGGA ATTATTAAGA GTATACAAGG
351 GTCCTGAGAC CAAAATTTG AGAACTGGTA AGATTTAATG CATCAACTAC
401 CATTACACAG TGTCCTTGTT TCTCATCAAT GCATTTTATA TAGCAATTAT
451 TTTATCTAAT CCCATGAAAC TCACTTTATT GGATGCTTTT GCCATATCCT
501 TATTTTCTAG CATCGTAGCT ATTAGGTCAT CTAATTATTA ATCTGTTTGT
551 GTCCTTGGGT TTAAATGTGT CTTTGTAGGC CACACAATGT TGGACTTCAT
601 TTTTAAATGG AGCCAACAAT CAGCAATTGT TAATGCATTT GCTTTGTGTT
651 CTATTACTCT GCAGTTTATC TTACTCATTG TTATTTTGC TTTCTTTAAA
701 TTTATGTTTT CTTAATGGAC TTTAAAATTC TTTATTTATT TTTTATGTCA
751 GACAATAAAC ATCCCTAGTC TGCCCATCTT TCTATCATTT CAACATCATC
801 ATATTTCAA ATAACCTTTC ATTGTTTCCT ATAATTTTAC TATTAATAGT
851 ATAGGATTAA GAAAATAAAC CTTATCTGGG TTCTGGCTGG CACTGCCTTC
901 CCTCTAGGGA TGAAAATGGA GTGTAGTCTG TAATATATCC TGGTATCATA
951 AATATATTTA TAAAATTATA CAAATGTAGC TTGCAGTTCT AAAGGCATGT
1001 AATCTAATTT TTAATTGAAT TTTATCTTTT TTCTCTTTT GTCTTCATA
1051 GACCTCGAGC TCTGTCTAGC CCTCAACTGT TCTCAAATCT CCATTGTTTT
1101 CTACAAGTGA CCCTCACAGC TGTGGGCCTT TGTTGACAAA TTGTTTCATC
1151 TCCTCTGGGT CTTAAATTAT TTTCTCTTAC TCTAAAGTGA AAATTTGATG

Appendix

1201 AATGTTTCCA GATACTGCAC TTGGAATCAT AACTTAATTT CCCTTAACCT
1251 TGTGTAAATT CTGTCCCCC ACTACTCCCA ACTCCTATCC CTCCTCCAAA
1301 GCACTGATAC TTATTATCAC ATTTAAATTT TTTCCCCGCT CTA CTACTGATAA
1351 CTTACAGAAT GCAGGACTGC ATTGTGATGG GGTAATTTCC ATGAGTTGAT
1401 TGGTTGGTTT TGAGTTGAAA AACTTAACAA TGATACATCT TAAATTCTTT
1451 CTTTGAGGAT TATTCCTTAA TGAATTCGTG CTACGGACAT ACTGAGGTGG
1501 TTATTTTTAT ATTTCCCTGA TAATAAATTC TAAATTGCTA AGGGTTTCTT
1551 ACCACCCTCG TCCTTTTACT GTTACTAGAT CTATTTTTAG CTGGTGTGGG
1601 CGTCCCAGC TAGTTTCACT TGCCTAATGC TAGTTCTTTT TTCTTCTACA
1651 TCAGGTGCGC TCTTCCTAGC ATCTTCTCCA TGTTTCTTGT TGCTCTACAG
1701 CATTTACAAG ACCCAGTTTA ATAGTTTAGT GCCTTTTTTG TCACTCATT
1751 TTTCTTCTTT GTTCTCTGTT AAAATAATAA GTGTATGATC CATTGCACCT
1801 GCCTTAGAGT CTTGAACCAG TCTTGGATTT CCCGCCATCT GGGTCTGGC
1851 TGGCTTGCAA TTTCTCCTTT GATGTTGTAA TACTTTTTCA TTGAACTTGA
1901 GTGTGGGGCT TATAGAGCTT CTTTGCTTTC ATTATTTTTT CCCAAAATGT
1951 GCACATTTTT TTTCTTAAGC TTATTTTGCT GTTTTGTGCT GTTATTTTTA
2001 ATTGCTTCCC ACTGGGTGGG GGGGTAGGGG GACTGAGAGT GAGATTTGGC
2051 TTGAGTTTGG CTCTCTTTGC TATTACTCAC ATTTCCCCC AGAAGCCCTA
2101 CATGCACTCC TCTCTCTCTG TCTTTGACAA ATTACTTTTG AAAGATCATT
2151 GATCCCTGGC GTAAATGGTG TTAAGAGTAA GATGGACTCG GGTAGGGATG
2201 CTCAGGAATC CAGTCCTGTA CAGTCATGAG CTTGGCCATC TGGAAGTCTC
2251 CTCTTGCTCA ATGAAATGGA GTAAACATTG TCCATTATGA AATCCACCAC
2301 ACAGGCTGCC AGGGACGAAT GGGATCCCAC CCAAAGCCAA TCGTGCTCT
2351 GACAGGGAAA TTGGCTAGCA CTGCCTGAGA CTA CTACTCCAGC CTCCCCGTC
2401 CCTGATGTCA CAATTCAGAG GCTGCTGCCT GCTTAGGAGG TTGTAGAAAG
2451 CTCTGTAGGT TCTCTCTGTG TGTCTTACAG GAGTCTTCAG GCCAGCTCCC
2501 TGTCGG CCCGGG

*Xma*I

7.3 Supplement data

Table 1 (Figure 4.4)

Ratio (DNA/Lipofectamine)						average \pm SD
1: 0.5	Firefly (RLU)	74157	82479	90053	82230 \pm 7950.93	
	Renilla (RLU)	15326	18327	15013	16222 \pm 1829.69	
	Ratio (F/R)	4.84	4.50	6.00	5.11 \pm 0.79	
1: 1	Firefly (RLU)	142895	167184	187583	165887 \pm 22372.20	
	Renilla (RLU)	27201	30175	35654	31010 \pm 4287.92	
	Ratio (F/R)	5.25	5.54	5.26	5.35 \pm 0.16	
1: 2	Firefly (RLU)	376870	428718	458806	421465 \pm 41446.78	
	Renilla (RLU)	80257	84526	93657	86146.67 \pm 6845.43	
	Ratio (F/R)	4.70	5.07	4.90	4.89 \pm 0.19	
1: 3	Firefly (RLU)	646552	689104	733943	689866 \pm 43700.49	
	Renilla (RLU)	138546	125864	143698	136036 \pm 9178.12	
	Ratio (F/R)	4.67	5.47	5.11	5.08 \pm 0.40	
1: 5	Firefly (RLU)	437452	391625	445084	424720 \pm 28914.32	
	Renilla (RLU)	78241	89654	84215	84036 \pm 5708.59	
	Ratio (F/R)	5.59	4.37	5.29	5.08 \pm 0.64	

Note: F and R represent Firefly and Renilla.

Appendix

Table 2 (Figure 4.5)

Ratio (DNA/Lipofectamine)		average \pm SD			
1: 0.5	Firefly (RLU)	45750	61486	59710	55649 \pm 8618.37
	Renilla (RLU)	26593	31231	28480	28768 \pm 2332.37
	Ratio (F/R)	1.72	1.97	2.10	1.93 \pm 0.19
1: 1	Firefly (RLU)	154571	155997	114844	141804 \pm 23358.93
	Renilla (RLU)	77159	74553	65804	72505 \pm 5948.00
	Ratio (F/R)	2.00	2.09	1.75	1.95 \pm 0.18
1: 2	Firefly (RLU)	376221	343759	334621	351534 \pm 21862.62
	Renilla (RLU)	171049	181581	177924	176851 \pm 5347.31
	Ratio (F/R)	2.20	1.89	1.88	1.99 \pm 0.18
1: 3	Firefly (RLU)	289088	386458	307344	327630 \pm 51757.81
	Renilla (RLU)	153133	178129	157982	163081 \pm 13255.28
	Ratio (F/R)	1.89	2.17	1.95	2.00 \pm 0.15
1: 5	Firefly (RLU)	245492	215857	184429	215259 \pm 30535.89
	Renilla (RLU)	109026	125384	108228	114213 \pm 9682.88
	Ratio (F/R)	2.25	1.72	1.70	1.89 \pm 0.31

Note: F and R represent Firefly and Renilla.

Appendix

Table 3 (Figure 4.6)

		Relative luciferase activity (%)						
		n=1 average \pm SD (n=3)*						
		(Figure 4.6A)						
no miRNA	Firefly (RLU)	29267	32552	44423	42327	31768		
	Renilla (RLU)	5345	6215	8634	8464	6554		
	Ratio (F/R)	5.48	5.24	5.15	5.00	4.85	100	100 \pm 3.26
negative control	Firefly (RLU)	13820	12657	14282	14087	14127		
	Renilla (RLU)	3105	2378	2845	2603	2709		
	Ratio (F/R)	4.45	5.32	5.02	5.41	5.21	98.89	98.02 \pm 11.88
miR-561	Firefly (RLU)	8956	9653	8697	9218	9475		
	Renilla (RLU)	2305	2623	2507	2403	2825		
	Ratio (F/R)	3.89	3.68	3.47	3.84	3.35	70.90	72.28 \pm 6.69
miR-579	Firefly (RLU)	7015	6826	6932	6038	6398		
	Renilla (RLU)	2628	2417	2098	1925	1764		
	Ratio (F/R)	2.67	2.82	3.30	3.14	3.63	60.53	57.34 \pm 4.04
miR-181b	Firefly (RLU)	13026	12036	13102	12761	10019		
	Renilla (RLU)	3125	2735	3630	2105	1996		
	Ratio (F/R)	4.17	4.40	3.61	6.06	5.02	90.48	87.61 \pm 4.98
miR-340	Firefly (RLU)	6863	6674	5454	6458	6455		
	Renilla (RLU)	2063	1877	1539	1827	2683		
	Ratio (F/R)	3.33	3.56	3.54	3.53	2.41	63.67	56.57 \pm 2.58

n=2 and n=3 are not shown.

Note: F and R represent Firefly and Renilla.

Appendix

		Relative luciferase activity (%)						n=1 average \pm SD (n=3)* (Figure 4.6B)	
no miRNA	Firefly (RLU)	8032	11527	11030	10085	8904			
	Renilla (RLU)	3595	4928	5308	5325	5515			
	Ratio (F/R)	2.23	2.34	2.08	1.89	1.61	100	100 \pm 4.52	
negative control	Firefly (RLU)	8979	11091	15226	15883	14589			
	Renilla (RLU)	4728	5437	8346	7517	6456			
	Ratio (F/R)	1.90	2.04	1.82	2.11	2.26	99.77	96.32 \pm 7.46	
miR-561	Firefly (RLU)	7356	6229	6396	6969	6436			
	Renilla (RLU)	5409	4456	4014	4607	4997			
	Ratio (F/R)	1.36	1.40	1.59	1.51	1.29	70.40	77.74 \pm 11.07	
miR-579	Firefly (RLU)	2730	2199	3856	2287	2508			
	Renilla (RLU)	2281	2093	3546	2185	2004			
	Ratio (F/R)	1.20	1.05	1.09	1.05	1.25	55.45	59.73 \pm 3.29	
miR-181b	Firefly (RLU)	8265	6544	7912	5583	9337			
	Renilla (RLU)	4597	2993	4573	2809	4518			
	Ratio (F/R)	1.80	2.19	1.73	1.99	2.07	96.15	92.70 \pm 13.12	
miR-340	Firefly (RLU)	6166	5428	4300	3754	6365			
	Renilla (RLU)	5074	4954	3622	2239	5363			
	Ratio (F/R)	1.22	1.10	1.19	1.68	1.19	62.62	60.15 \pm 15.06	

n=2 and n=3 are not shown.

Note: F and R represent Firefly and Renilla.

Appendix

Table 4 (Figure 4.8)

		Relative luciferase activity (%)						
		n=1 average \pm SD (n=3)*						
		(Figure 4.8A)						
UTR, WT	Firefly (RLU)	36602	33074	33509	36953	40859		
	Renilla (RLU)	3365	3968	3793	3369	3455		
	Ratio (F/R)	10.88	8.34	8.83	10.97	11.83	100	100 \pm 4.69
UTR, WT + miR-561	Firefly (RLU)	13397	12650	9569	8840	9672		
	Renilla (RLU)	1817	1721	1253	1281	1013		
	Ratio (F/R)	7.37	7.35	7.64	6.90	9.55	76.33	78.91 \pm 1.74
561-del	Firefly (RLU)	96590	88866	84949	53948	59675		
	Renilla (RLU)	9121	9767	7778	5674	6103		
	Ratio (F/R)	10.59	9.10	10.92	9.51	9.78	100	100 \pm 7.42
561-del + miR-561	Firefly (RLU)	38876	31450	27758	28834	26800		
	Renilla (RLU)	3757	3102	2281	3049	2292		
	Ratio (F/R)	10.35	10.14	12.17	9.46	11.69	107.83	106.29 \pm 6.99
561-mut	Firefly (RLU)	122023	141200	132882	112010	120372		
	Renilla (RLU)	11793	14512	12331	10903	12825		
	Ratio (F/R)	10.35	9.73	10.78	10.27	9.39	100	100 \pm 5.91
561-mut + miR-561	Firefly (RLU)	67171	56991	57909	53414	61990		
	Renilla (RLU)	6764	5429	5717	5468	7576		
	Ratio (F/R)	9.93	10.50	10.13	9.77	8.18	96.03	96.24 \pm 1.39

n=2 and n=3 are not shown.

Note: F and R represent Firefly and Renilla.

Appendix

		Relative luciferase activity (%)						
		n=1 average \pm SD (n=3)*						
		(Figure 4.8B)						
UTR, WT	Firefly (RLU)	30954	38393	28572	44908	39541		
	Renilla (RLU)	3243	3598	2897	4576	4063		
	Ratio (F/R)	9.54	10.67	9.86	9.81	9.73	100	100 \pm 5.36
UTR, WT + miR-579	Firefly (RLU)	5416	7715	11074	10388	11046		
	Renilla (RLU)	1039	1247	1770	1641	1874		
	Ratio (F/R)	5.21	6.19	6.26	6.33	5.89	60.21	57.93 \pm 8.25
579-del	Firefly (RLU)	90968	86902	80265	107027	89725		
	Renilla (RLU)	8079	8602	7424	8176	9060		
	Ratio (F/R)	11.26	10.10	10.81	13.09	9.90	100	100 \pm 2.69
579-del + miR-579	Firefly (RLU)	40453	43805	37615	40932	45383		
	Renilla (RLU)	3853	3585	3395	3866	3948		
	Ratio (F/R)	10.50	12.22	11.08	10.59	11.50	101.29	105.98 \pm 6.69
579-mut	Firefly (RLU)	133394	116429	100704	118749	104513		
	Renilla (RLU)	12627	11666	9037	9931	9400		
	Ratio (F/R)	10.56	9.98	11.14	11.96	11.12	100	100 \pm 8.26
579-mut + miR-579	Firefly (RLU)	62339	56523	46612	51807	56134		
	Renilla (RLU)	5428	4972	4830	5362	4834		
	Ratio (F/R)	11.48	11.37	9.65	9.66	11.61	98.20	100.78 \pm 3.30

n=2 and n=3 are not shown.

Note: F and R represent Firefly and Renilla.

Appendix

		Relative luciferase activity (%)						
		n=1 average \pm SD (n=3)*						
		(Figure 4.8C)						
UTR, WT	Firefly (RLU)	35812	33460	25750	25438	28241		
	Renilla (RLU)	3482	3017	2890	2428	2625		
	Ratio (F/R)	10.28	11.09	8.91	10.48	10.76	100	100 \pm 7.32
UTR, WT + miR-340	Firefly (RLU)	6863	6674	5454	6458	6455		
	Renilla (RLU)	1056	1277	1078	1127	1036		
	Ratio (F/R)	6.50	5.23	5.06	5.73	6.23	55.79	56.57 \pm 2.58
340-del	Firefly (RLU)	63194	47407	60647	48888	34429		
	Renilla (RLU)	5279	4245	4706	4588	2853		
	Ratio (F/R)	11.97	11.17	12.89	10.66	12.07	100	100 \pm 3.67
340-del + miR-340	Firefly (RLU)	12499	16751	11508	9532	12999		
	Renilla (RLU)	1292	1497	944	1054	1102		
	Ratio (F/R)	9.67	11.19	12.19	9.04	11.80	91.74	86.22 \pm 6.32
340-mut	Firefly (RLU)	28185	20701	21438	16782	16741		
	Renilla (RLU)	2820	1711	2324	1343	1624		
	Ratio (F/R)	9.99	12.10	9.22	12.50	10.31	100	100 \pm 4.17
340-mut + miR-340	Firefly (RLU)	11510	9377	9839	9208	8481		
	Renilla (RLU)	1270	1007	1188	1217	921		
	Ratio (F/R)	9.06	9.31	8.28	7.57	9.21	80.25	75.33 \pm 9.69

n=2 and n=3 are not shown.

Note: F and R represent Firefly and Renilla.

Appendix

Table 5 (Figure 4.9)

							Relative luciferase activity (%)	
							n=1	average \pm SD (n=3)*
							(Figure 4.9A)	
UTR, WT	Firefly (RLU)	4567	2163	2277	2999	3017		
	Renilla (RLU)	1571	920	1032	1204	1382		
	Ratio (F/R)	2.91	2.35	2.21	2.49	2.18	100	100 \pm 9.12
UTR, WT + miR-561	Firefly (RLU)	2852	3537	4375	2283	4507		
	Renilla (RLU)	1504	1768	2496	1192	2229		
	Ratio (F/R)	1.90	2.00	1.75	1.92	2.02	78.98	83.11 \pm 6.11
561-del	Firefly (RLU)	4610	5394	7116	5060	3243		
	Renilla (RLU)	2505	2122	2503	1770	1359		
	Ratio (F/R)	1.84	2.54	2.84	2.86	2.39	100	100 \pm 4.36
561-del + miR-561	Firefly (RLU)	5745	6568	5670	6881	4845		
	Renilla (RLU)	1876	3423	1876	2193	1910		
	Ratio (F/R)	3.06	1.92	3.02	3.14	2.54	109.68	112.85 \pm 33.01
561-mut	Firefly (RLU)	4595	4726	3025	3493	2693		
	Renilla (RLU)	1797	1910	1379	1373	1016		
	Ratio (F/R)	2.56	2.47	2.19	2.54	2.65	100	100 \pm 5.17
561-mut + miR-561	Firefly (RLU)	5387	3709	6357	5142	3314		
	Renilla (RLU)	2648	1508	1912	2432	1384		
	Ratio (F/R)	2.03	2.46	3.32	2.11	2.39	99.26	92.08 \pm 8.26

n=2 and n=3 are not shown.

Note: F and R represent Firefly and Renilla.

Appendix

								Relative luciferase activity (%)	
								n=1	average \pm SD (n=3)*
								(Figure 4.9B)	
UTR, WT	Firefly (RLU)	6436	5076	3688	2621	2339			
	Renilla (RLU)	2506	1988	1926	1312	1119			
	Ratio (F/R)	2.57	2.55	1.91	2.00	2.09	100	100 \pm 7.64	
UTR, WT + miR-579	Firefly (RLU)	1761	1634	1937	1365	1875			
	Renilla (RLU)	1436	1383	1648	1345	1019			
	Ratio (F/R)	1.23	1.18	1.18	1.01	1.84	57.87	60.64 \pm 10.80	
579-del	Firefly (RLU)	2395	2423	1387	2542	2463			
	Renilla (RLU)	1194	1206	821	1061	1032			
	Ratio (F/R)	2.01	2.01	1.69	2.40	2.39	100	100 \pm 5.27	
579-del + miR-579	Firefly (RLU)	2857	3597	2840	2963	3453			
	Renilla (RLU)	1422	1867	1271	1057	1623			
	Ratio (F/R)	2.01	1.93	2.23	2.80	2.13	105.86	103.12 \pm 23.57	
579-mut	Firefly (RLU)	5387	3709	6357	5142	3314			
	Renilla (RLU)	2648	1508	3912	2432	1384			
	Ratio (F/R)	2.03	2.46	1.62	2.11	2.39	100	100 \pm 9.04	
579-mut + miR-579	Firefly (RLU)	2472	3028	1928	1693	3542			
	Renilla (RLU)	1420	1346	961	771	1879			
	Ratio (F/R)	1.74	2.25	2.01	2.20	1.89	94.82	96.62 \pm 17.62	

n=2 and n=3 are not shown.

Note: F and R represent Firefly and Renilla.

Appendix

								Relative luciferase activity (%)	
								n=1	average \pm SD (n=3)*
								(Figure 4.9C)	
UTR, WT	Firefly (RLU)	4084	4460	4683	4933	4380			
	Renilla (RLU)	1719	1999	1919	2140	1963			
	Ratio (F/R)	2.38	2.23	2.44	2.31	2.23	100	100 \pm 3.27	
UTR, WT + miR-340	Firefly (RLU)	2111	2404	1875	1924	1698			
	Renilla (RLU)	1789	1928	1297	1391	1154			
	Ratio (F/R)	1.18	1.25	1.45	1.38	1.47	58.07	60.01 \pm 10.88	
340-del	Firefly (RLU)	6880	7041	10255	8711	7910			
	Renilla (RLU)	3398	3324	4651	3565	3369			
	Ratio (F/R)	2.02	2.12	2.20	2.44	2.35	100	100 \pm 5.89	
340-del + miR-340	Firefly (RLU)	5415	4588	4968	4906	3975			
	Renilla (RLU)	2974	2209	2521	2386	2069			
	Ratio (F/R)	1.82	2.08	1.97	2.06	1.92	88.39	85.93 \pm 6.14	
340-mut	Firefly (RLU)	6491	6982	6552	6742	6644			
	Renilla (RLU)	3365	3440	2837	3244	2854			
	Ratio (F/R)	1.93	2.03	2.31	2.08	2.33	100	100 \pm 8.14	
340-mut + miR-340	Firefly (RLU)	3548	3508	3281	2874	3044			
	Renilla (RLU)	2002	2221	1741	2213	1740			
	Ratio (F/R)	1.77	1.58	1.88	1.30	1.75	77.61	74.31 \pm 1.37	

n=2 and n=3 are not shown.

Note: F and R represent Firefly and Renilla.

Appendix

Table 6 (Figure 4.10)

								Relative luciferase activity (%)	
								n=1	average \pm SD (n=3)*
								(Figure 4.10A)	
pmir-GLO	Firefly (RLU)	8421	9014	9672	9115	10372			
	Renilla (RLU)	5455	4833	5862	5808	6641			
	Ratio (F/R)	1.54	1.87	1.65	1.57	1.56	100	100 \pm 3.25	
pmir-UTR	Firefly (RLU)	6370	7310	7477	7552	7732			
	Renilla (RLU)	4404	4962	4638	4554	5121			
	Ratio (F/R)	1.45	1.47	1.61	1.66	1.51	94.01	95.47 \pm 6.23	
pmir-GLO + miR-561	Firefly (RLU)	8547	8230	9566	8191	9304			
	Renilla (RLU)	5345	4923	5463	5744	5735			
	Ratio (F/R)	1.60	1.67	1.75	1.43	1.62	98.54	95.18 \pm 5.08	
pmir-UTR + miR-561	Firefly (RLU)	3504	3673	3691	3744	3502			
	Renilla (RLU)	2758	3092	3496	3084	2923			
	Ratio (F/R)	1.27	1.19	1.06	1.21	1.20	72.36	68.08 \pm 4.52	

								Relative luciferase activity (%)	
								n=1	average \pm SD (n=3)*
								(Figure 4.10B)	
pmir-GLO	Firefly (RLU)	10635	10444	9589	9401	10168			
	Renilla (RLU)	5358	5178	5314	5219	5137			
	Ratio (F/R)	1.98	2.02	1.80	1.80	1.98	100	100 \pm 3.25	
pmir-UTR	Firefly (RLU)	5713	7885	3613	5224	4961			
	Renilla (RLU)	3062	4106	1821	2627	2853			
	Ratio (F/R)	1.87	1.92	1.98	1.99	1.74	99.07	99.41 \pm 5.03	
pmir-GLO + miR-579	Firefly (RLU)	8420	10259	10176	9183	9213			
	Renilla (RLU)	4214	5180	5898	5110	5196			
	Ratio (F/R)	2.00	1.98	1.73	1.80	1.77	96.74	98.68 \pm 5.91	
pmir-UTR + miR-579	Firefly (RLU)	1590	2360	2660	2625	2630			
	Renilla (RLU)	1362	1953	2303	2484	2340			
	Ratio (F/R)	1.17	1.21	1.16	1.06	1.12	59.58	55.15 \pm 6.79	

Appendix

		Relative luciferase activity (%)						
		n=1 average \pm SD (n=3)*						
		(Figure 4.10C)						
pmir-GLO	Firefly (RLU)	11421	13144	9672	9511	10372		
	Renilla (RLU)	6453	7833	6162	5808	6641		
	Ratio (F/R)	1.77	1.68	1.57	1.64	1.56	100	100 \pm 4.99
pmir-UTR	Firefly (RLU)	6370	8310	7477	8552	9732		
	Renilla (RLU)	4404	5262	4638	5154	6121		
	Ratio (F/R)	1.45	1.58	1.61	1.66	1.59	95.99	95.47 \pm 6.23
pmir-GLO + miR-340	Firefly (RLU)	8925	7585	8711	8431	8825		
	Renilla (RLU)	6748	5925	6317	5938	6453		
	Ratio (F/R)	1.32	1.28	1.38	1.42	1.37	82.38	78.45 \pm 4.38
pmir-UTR + miR-340	Firefly (RLU)	4321	5263	4574	3973	5042		
	Renilla (RLU)	4549	5071	4792	5312	5307		
	Ratio (F/R)	0.95	1.04	0.95	0.75	0.95	56.47	53.89 \pm 3.85

n=2 and n=3 are not shown.

Note: F and R represent Firefly and Renilla.

Appendix

Table 7 (Figure 4.17)

		Relative luciferase activity (%)						
							n=1	average \pm SD (n=3)*
Pmir-P1	Firefly (RLU)	565	365	560	628	745		
	Renilla (RLU)	3052	2305	2584	2768	2632		
	Ratio (F/R)	0.19	0.16	0.22	0.23	0.28	100	100 \pm 8.36
Pmir-P1 + Dexmethasone	Firefly (RLU)	901	871	982	805	765		
	Renilla (RLU)	4156	4212	5005	3921	3400		
	Ratio (F/R)	0.22	0.21	0.20	0.21	0.23	98.13	96.85 \pm 2.94
Pmir-P1 + Cortisol	Firefly (RLU)	699	584	756	852	862		
	Renilla (RLU)	3658	2904	3773	3944	4066		
	Ratio (F/R)	0.19	0.20	0.20	0.22	0.21	95.37	93.43 \pm 4.96
Pmir-P2	Firefly (RLU)	675	950	764	752	756		
	Renilla (RLU)	2287	2778	2506	2871	3578		
	Ratio (F/R)	0.30	0.34	0.30	0.26	0.21	100	100 \pm 5.23
Pmir-P2 + Dexmethasone	Firefly (RLU)	1784	1534	1687	1619	1894		
	Renilla (RLU)	4319	4094	4245	4410	3930		
	Ratio (F/R)	0.41	0.37	0.40	0.37	0.48	143.74	140.71 \pm 6.36
Pmir-P2 + Cortisol	Firefly (RLU)	1454	1408	1551	2336	1626		
	Renilla (RLU)	4360	3071	3672	5084	3905		
	Ratio (F/R)	0.33	0.46	0.42	0.46	0.42	147.70	143.58 \pm 3.55

n=2 and n=3 are not shown.

Note: F and R represent Firefly and Renilla.

Appendix

Table 8 (Figure 4.18)

		Relative luciferase activity (%)						
							n=1	average ± SD (n=3)*
							(Figure 4.18A)	
Control	Firefly (RLU)	796	714	838	735	703		
	Renilla (RLU)	3728	3148	3474	3289	2922		
	Ratio (F/R)	0.21	0.23	0.24	0.22	0.24	100	100 ± 7.64
miR-579	Firefly (RLU)	221	311	461	463	382		
	Renilla (RLU)	1983	2841	3543	3200	2201		
	Ratio (F/R)	0.11	0.11	0.13	0.14	0.17	58.42	54.62 ± 6.36
Dex	Firefly (RLU)	1965	2421	3229	2391	3518		
	Renilla (RLU)	5571	7136	8947	6435	8864		
	Ratio (F/R)	0.35	0.34	0.36	0.37	0.40	158.98	159.13 ± 8.53
miR-579/Dex	Firefly (RLU)	1513	1386	1455	1606	1959		
	Renilla (RLU)	5841	6561	6147	7108	7071		
	Ratio (F/R)	0.26	0.211	0.24	0.23	0.28	105.62	108.09 ± 9.92

		Relative luciferase activity (%)						
							n=1	average ± SD (n=3)*
							(Figure 4.18B)	
Control	Firefly (RLU)	888	728	955	918	892		
	Renilla (RLU)	3499	2727	2969	2584	3833		
	Ratio (F/R)	0.25	0.27	0.32	0.36	0.23	100	100 ± 8.31
miR-579	Firefly (RLU)	434	509	525	512	408		
	Renilla (RLU)	2669	3534	3084	3479	2110		
	Ratio (F/R)	0.16	0.14	0.17	0.15	0.19	57.15	56.49 ± 10.21
Cortisol	Firefly (RLU)	1858	1740	1969	2013	2045		
	Renilla (RLU)	4587	4296	4473	4466	4502		
	Ratio (F/R)	0.41	0.41	0.44	0.45	0.45	150.68	148.95 ± 13.75
miR-579/Cortisol	Firefly (RLU)	1182	1833	1176	1551	1775		
	Renilla (RLU)	4333	5421	4506	4832	6557		
	Ratio (F/R)	0.27	0.34	0.26	0.32	0.27	102.32	105.46 ± 6.39

Appendix

		Relative luciferase activity (%)						
		n=1 average ± SD (n=3)*						
		(Figure 4.18C)						
Control	Firefly (RLU)	1410	1867	2371	2414	2203		
	Renilla (RLU)	6713	8340	8473	8202	8032		
	Ratio (F/R)	0.21	0.22	0.28	0.29	0.27	100	100 ± 4.26
miR-561	Firefly (RLU)	1074	1597	1078	1358	1931		
	Renilla (RLU)	5101	7860	6659	6888	8991		
	Ratio (F/R)	0.21	0.20	0.16	0.20	0.21	77.01	74.66 ± 4.03
Dex	Firefly (RLU)	4998	4374	4526	5739	5771		
	Renilla (RLU)	12133	11902	12019	13748	14299		
	Ratio (F/R)	0.41	0.37	0.38	0.42	0.40	154.18	158.40 ± 13.02
miR-561/Dex	Firefly (RLU)	3352	4247	4846	5310	4604		
	Renilla (RLU)	9138	12231	11994	13202	12799		
	Ratio (F/R)	0.37	0.35	0.40	0.40	0.36	146.61	143.34 ± 10.46

		Relative luciferase activity (%)						
		n=1 average ± SD (n=3)*						
		(Figure 4.18D)						
Control	Firefly (RLU)	1240	1548	1657	1390	1459		
	Renilla (RLU)	4655	5603	5777	4399	4205		
	Ratio (F/R)	0.27	0.28	0.29	0.32	0.35	100	100 ± 9.36
miR-561	Firefly (RLU)	702	671	709	682	763		
	Renilla (RLU)	2875	3034	3110	2748	3312		
	Ratio (F/R)	0.24	0.22	0.23	0.25	0.23	78.52	77.99 ± 10.35
Cortisol	Firefly (RLU)	4785	4333	5294	3603	4816		
	Renilla (RLU)	9899	9958	9553	8599	9447		
	Ratio (F/R)	0.48	0.44	0.55	0.42	0.51	160.91	156.28 ± 7.11
miR-561/Cortisol	Firefly (RLU)	3942	4002	4892	3857	3913		
	Renilla (RLU)	8679	9097	10750	9011	9027		
	Ratio (F/R)	0.45	0.44	0.46	0.43	0.43	148.13	145.67 ± 14.76

n=2 and n=3 are not shown. Note: F and R represent Firefly and Renilla.

Appendix

Table 9 (Figure 4.19)

							Relative luciferase activity (%)	
							n=1	average \pm SD (n=3)*
							(Figure 4.19A)	
Control	Firefly (RLU)	960	935	1034	831	901		
	Renilla (RLU)	5519	5846	5749	5157	5205		
	Ratio (F/R)	0.17	0.16	0.18	0.16	0.17	100	100 \pm 3.57
TNFalpha	Firefly (RLU)	939	1078	1041	981	983		
	Renilla (RLU)	5038	6609	6074	5885	5991		
	Ratio (F/R)	0.19	0.16	0.17	0.17	0.16	100.43	108.21 \pm 7.62
Insulin	Firefly (RLU)	871	809	1011	907	1102		
	Renilla (RLU)	5593	5474	6089	5622	6593		
	Ratio (F/R)	0.16	0.15	0.17	0.16	0.17	94.11	96.34 \pm 10.74
Leptin	Firefly (RLU)	794	908	1096	932	933		
	Renilla (RLU)	4922	5083	6524	5170	5077		
	Ratio (F/R)	0.16	0.18	0.17	0.18	0.18	102.83	102.33 \pm 5.72
Resistin	Firefly (RLU)	837	1072	803	1096	948		
	Renilla (RLU)	5405	6172	5088	6284	5124		
	Ratio (F/R)	0.15	0.17	0.16	0.17	0.19	99.74	106.67 \pm 8.63
Adiponectin	Firefly (RLU)	846	948	824	873	855		
	Renilla (RLU)	5314	5350	4676	5217	4925		
	Ratio (F/R)	0.16	0.18	0.18	0.17	0.17	100.66	99.01 \pm 7.78

n=2 and n=3 are not shown.

Note: F and R represent Firefly and Renilla.

Appendix

								Relative luciferase activity (%)	
								n=1	average \pm SD (n=3)*
								(Figure 4.19B)	
Control	Firefly (RLU)	996	865	792	1001	779			
	Renilla (RLU)	5069	5086	4269	4661	4195			
	Ratio (F/R)	0.20	0.17	0.19	0.21	0.19	100	100 \pm 5.06	
Retinoic acid	Firefly (RLU)	846	961	971	899	867			
	Renilla (RLU)	4308	4806	5148	5151	5031			
	Ratio (F/R)	0.20	0.20	0.19	0.17	0.17	97.82	95.33 \pm 7.49	
WY14643	Firefly (RLU)	810	916	720	797	985			
	Renilla (RLU)	4653	5397	4070	4413	5488			
	Ratio (F/R)	0.17	0.17	0.18	0.18	0.18	92.47	94.17 \pm 9.61	
Vitamin D3	Firefly (RLU)	966	809	903	1069	982			
	Renilla (RLU)	5061	4093	5094	4978	4529			
	Ratio (F/R)	0.19	0.20	0.18	0.21	0.22	104.71	106.04 \pm 11.66	
Ciglitazone	Firefly (RLU)	731	730	759	1145	910			
	Renilla (RLU)	4228	3710	4424	5350	4017			
	Ratio (F/R)	0.17	0.20	0.17	0.21	0.23	103.07	99.47 \pm 5.77	
Trichostatin A	Firefly (RLU)	904	867	767	914	995			
	Renilla (RLU)	4154	4741	4617	5347	4845			
	Ratio (F/R)	0.22	0.18	0.17	0.17	0.21	98.99	95.74 \pm 14.76	
Estradiol	Firefly (RLU)	917	1083	1079	916	1085			
	Renilla (RLU)	4226	5862	4784	4574	5842			
	Ratio (F/R)	0.22	0.18	0.23	0.20	0.19	106.37	104.69 \pm 6.43	

n=2 and n=3 are not shown.

Note: F and R represent Firefly and Renilla.

Appendix

								Relative luciferase activity (%)	
								n=1	average \pm SD (n=3)*
								(Figure 4.19C)	
Control	Firefly (RLU)	733	1063	1012	636	851			
	Renilla (RLU)	5050	6710	6907	5016	6492			
	Ratio (F/R)	0.15	0.16	0.15	0.13	0.13	100	100 \pm 6.02	
TNFalpha	Firefly (RLU)	1024	820	1011	863	1070			
	Renilla (RLU)	6393	6429	6289	6286	7314			
	Ratio (F/R)	0.16	0.13	0.16	0.14	0.15	103.40	110.13 \pm 8.72	
Insulin	Firefly (RLU)	1016	951	1156	1102	1055			
	Renilla (RLU)	6372	7427	7627	6846	7702			
	Ratio (F/R)	0.16	0.13	0.15	0.16	0.14	104.10	93.33 \pm 12.97	
Leptin	Firefly (RLU)	696	883	1117	900	969			
	Renilla (RLU)	5685	6576	7307	5942	6952			
	Ratio (F/R)	0.12	0.13	0.15	0.15	0.14	98.93	108.22 \pm 6.43	
Resistin	Firefly (RLU)	692	629	929	848	750			
	Renilla (RLU)	5042	5087	7024	6389	5258			
	Ratio (F/R)	0.14	0.12	0.13	0.13	0.14	94.43	99.45 \pm 8.87	
Adiponectin	Firefly (RLU)	800	831	887	930	585			
	Renilla (RLU)	5718	5814	5815	6429	4278			
	Ratio (F/R)	0.14	0.14	0.15	0.14	0.14	101.24	103.67 \pm 4.95	

n=2 and n=3 are not shown.

Note: F and R represent Firefly and Renilla.

Appendix

		Relative luciferase activity (%)						n=1 average \pm SD (n=3)*	
								(Figure 4.19D)	
Control	Firefly (RLU)	865	965	960	928	1045			
	Renilla (RLU)	4552	4305	4584	4768	4632			
	Ratio (F/R)	0.19	0.22	0.21	0.19	0.23	100	100 \pm 8.23	
Retinoic acid	Firefly (RLU)	977	828	1033	865	1175			
	Renilla (RLU)	4889	4303	5298	4734	5341			
	Ratio (F/R)	0.20	0.19	0.19	0.18	0.22	94.84	92.65 \pm 11.84	
WY14643	Firefly (RLU)	1016	998	897	1096	938			
	Renilla (RLU)	5061	4683	5084	5235	5271			
	Ratio (F/R)	0.20	0.21	0.18	0.21	0.18	93.66	96.58 \pm 6.87	
Vitamin D3	Firefly (RLU)	928	1122	979	925	1008			
	Renilla (RLU)	4219	5149	4563	4486	4235			
	Ratio (F/R)	0.22	0.22	0.21	0.21	0.24	105.06	107.34 \pm 9.68	
Ciglitazone	Firefly (RLU)	1074	977	1248	981	914			
	Renilla (RLU)	5044	4584	5129	4830	3758			
	Ratio (F/R)	0.21	0.21	0.24	0.20	0.24	106.88	105.39 \pm 5.86	
Trichostatin A	Firefly (RLU)	924	1232	1068	958	1290			
	Renilla (RLU)	4569	5763	5260	5629	5500			
	Ratio (F/R)	0.20	0.21	0.20	0.17	0.23	98.08	96.47 \pm 8.76	
Estradiol	Firefly (RLU)	1128	954	1062	924	1028			
	Renilla (RLU)	4951	5009	4330	4383	5550			
	Ratio (F/R)	0.23	0.19	0.25	0.21	0.19	101.51	104.33 \pm 5.64	

n=2 and n=3 are not shown.

Note: F and R represent Firefly and Renilla.

Appendix

Table 10 (Figure 4.21)

								Relative luciferase activity (%)	
								n=1	average \pm SD (n=3)*
								(Figure 4.21A)	
Control	Firefly (RLU)	11532	10776	13521	9355	13768			
	Renilla (RLU)	2540	2066	2429	2176	3119			
	Ratio (F/R)	4.54	5.22	5.57	4.30	4.41	100	100 \pm 14.92	
miR-579	Firefly (RLU)	4179	4291	4687	5151	3251			
	Renilla (RLU)	1423	1554	1412	1590	1534			
	Ratio (F/R)	2.94	2.76	3.32	3.24	2.12	59.81	57.53 \pm 10.03	
miR-579 /AMO-579	Firefly (RLU)	5016	6673	6564	6190	6829			
	Renilla (RLU)	1234	1430	1584	1401	1553			
	Ratio (F/R)	4.06	4.67	4.14	4.39	4.40	90.13	90.00 \pm 13.29	
AMO-579	Firefly (RLU)	7097	8352	7787	6968	7514			
	Renilla (RLU)	1283	1347	1280	1330	1419			
	Ratio (F/R)	5.53	6.20	6.08	5.24	5.30	117.95	121.69 \pm 8.25	
DNA-579	Firefly (RLU)	7852	11355	8842	8843	7656			
	Renilla (RLU)	1870	2332	1862	1893	1575			
	Ratio (F/R)	4.20	4.87	4.75	4.67	4.86	97.14	99.43 \pm 15.40	

n=2 and n=3 are not shown.

Note: F and R represent Firefly and Renilla.

Appendix

		Relative luciferase activity (%)						
							n=1	average \pm SD (n=3)*
							(Figure 4.21B)	
Control	Firefly (RLU)	48303	55435	61226	33861	59928		
	Renilla (RLU)	7979	8008	8717	6827	8593		
	Ratio (F/R)	6.05	6.92	7.02	4.96	6.97	100	100 \pm 5.71
miR-561	Firefly (RLU)	18129	8733	13463	17573	14702		
	Renilla (RLU)	3870	1798	2729	3358	3296		
	Ratio (F/R)	4.68	4.86	4.93	5.23	4.46	75.68	75.57 \pm 4.59
miR-561 /AMO-561	Firefly (RLU)	14083	14727	15274	13583	14149		
	Renilla (RLU)	2383	2689	2332	2243	2560		
	Ratio (F/R)	5.91	5.48	6.55	6.06	5.53	92.44	95.46 \pm 5.53
AMO-561	Firefly (RLU)	46106	47122	42466	40306	39517		
	Renilla (RLU)	6074	6593	5580	5436	5040		
	Ratio (F/R)	7.59	7.15	7.61	7.41	7.84	117.75	120.87 \pm 5.53
DNA-561	Firefly (RLU)	28705	20276	29041	17458	35180		
	Renilla (RLU)	4517	3565	4230	3373	5104		
	Ratio (F/R)	6.35	5.69	6.87	5.18	6.89	97.00	104.99 \pm 4.34

n=2 and n=3 are not shown.

Note: F and R represent Firefly and Renilla.

Figure 1
(Figure 4.11)

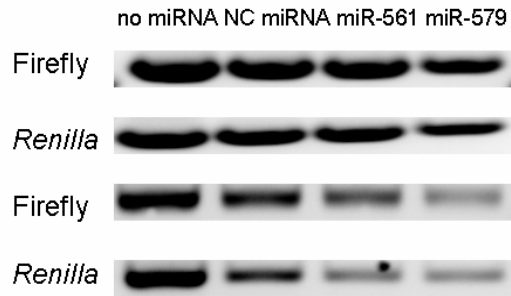
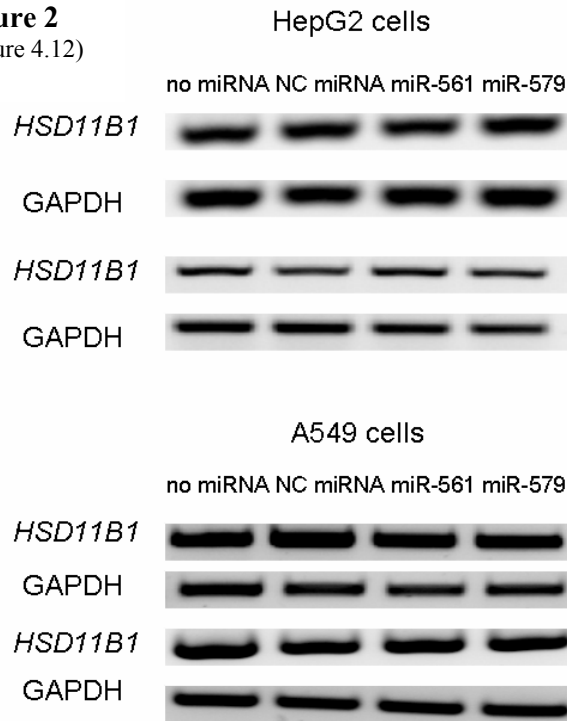


Figure 2
(Figure 4.12)



Appendix

Figure 3
(Figure 4.14)

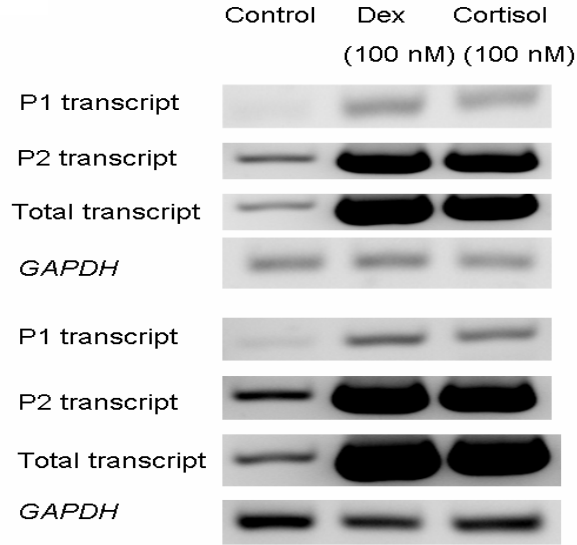


Figure 4
(Figure 4.20)

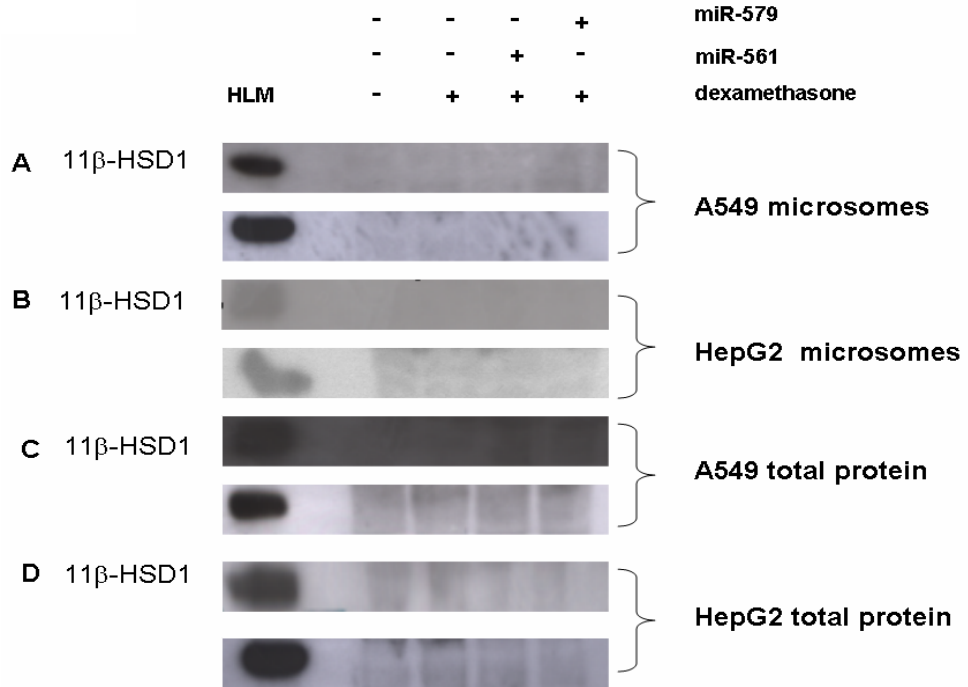


Figure 5
(Figure 4.22)

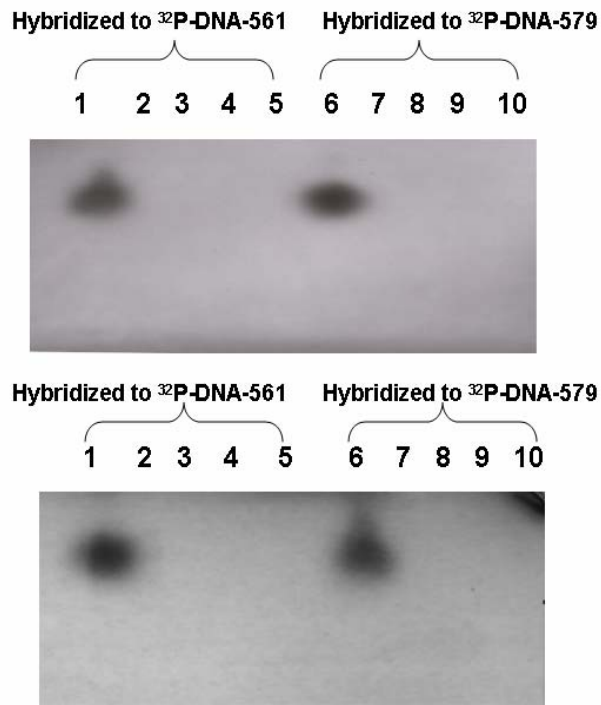


Figure 6
(Figure 4.24)

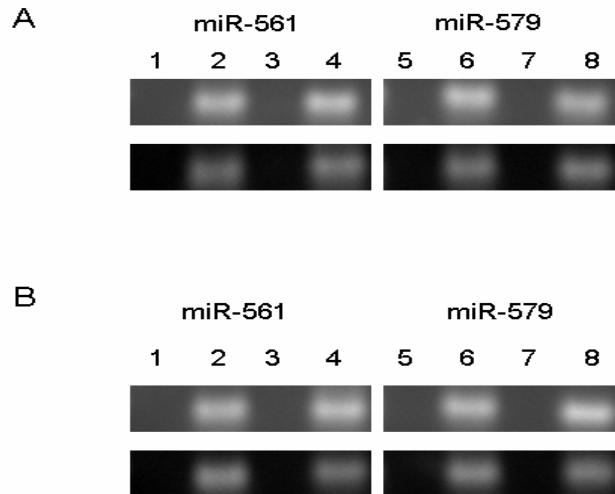
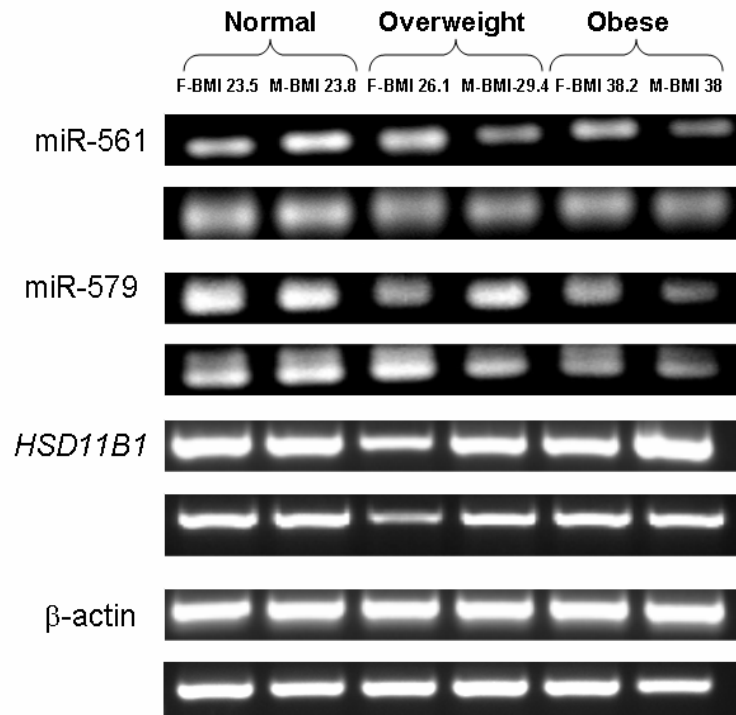


Figure 7
(Figure 4.25)



Acknowledgements

This dissertation summarized three years of my work in the field of 11 β -hydroxysteroid dehydrogenase type 1 in the Institute of Toxicology and Pharmacology for Natural Scientists, University Medical School Schleswig-Holstein, Campus Kiel.

During my PhD, I had a pleasant experience and lots of support from many different people, all of whom deserve my gratitude. First of all, I would like to thank my supervisors Prof. Dr. Edmund Maser and Dr. Claudia Staab for giving me the opportunity to work on an inspiring subject with all the scientific freedom and support one could wish for.

The discussion with my colleagues contributed to a big extent to the progress of this work. Their helpfulness and collaboration as well as the good working atmosphere always remain in my mind. Especially thanks should be given to Dr. Claudia Staab who translated the summary of the thesis to German, and always patiently corrected my thesis for several times; I would like to thank Dr. Guangming Xiong for his helpfulness in this work; I would also like to thank everybody in our institute for their help.

My utmost gratitude goes to China Scholarship Council for funding me studying in Kiel for three years.

Finally, I am most grateful for the support of my family for all the support they have given me over the years.

Kiel, 2011

Yanyan Han

Curriculum vitae

Name: Yanyan Han

Gender: Female

Date of birth: May 4th, 1984

Place of birth: Heilongjiang, People Republic of China

Nationality: Chinese

Email: hanyanyan1984@126.com

Language: Chinese, English

- 01.2009-Present PhD student, Institute of Toxicology and Pharmacology for Natural Scientists University Medical School Schleswig-Holstein Campus Kiel, Germany
Director: Prof. Dr. Edmund Maser
- 09.2007-06.2009 Master of Theoretical Veterinary Medicine, Jilin University, Changchun, P. R. China
09. 2003-06. 2007 Bachelor of Veterinary Medicine, Heilongjiang Baiyi Agricultural University, Daqing, P. R. China
- 09.2000-06.2003 High school, Mishan, Heilongjiang, P. R. China

Publication

Yanyan Han, Claudia A Staab-Weijnitz, Guangming Xiong and Edmund Maser Identification of microRNAs as a potential novel regulatory mechanism in *HSD11B1* expression (to be submitted)

Deguang Song, Wanju Zhu, Zhanfeng Wang, Wenqi He, **Yanyan Han**, Huijun Lu and Feng Gao Ultrastructural changes of calf primary culture oral mucosa cells inoculated with vesicular stomatitis virus. Chinese Journal of Veterinary Science 2008 (28): 8.

Erklärung

Eidesstattliche Erklärung:

Hiermit erkläre ich an Eides statt, dass ich die vorgelegte Dissertation mit dem Titel „Identification of microRNAs as potential novel regulators of *HSD11B1* expression“ selbständig und ohne unerlaubte Hilfe angefertigt habe und dass ich die Arbeit noch keinem anderen Fachbereich bzw. noch keiner anderen Fakultät vorgelegt habe.

Kiel, 2011

(Yanyan Han)